CHAPTER 1:

Introduction and Literature Review

1.1. General Introduction

Patients afflicted with Sanfilippo syndrome (or mucopolysaccharidosis (MPS) types IIIA, B, C or D) display a severe and progressive neurological decline with behavioural changes such as regression in development, mental retardation, increased aggression and sleep problems. For MPS IIIA, these symptoms are the result of a deficiency of lysosomal sulphamidase (NS) enzyme activity. The somatic pathology of several lysosomal storage disorders (LSD) has been resolved using bone marrow transplantation (BMT), cord blood transplantation or by regular intravenous infusions of recombinantly-produced lysosomal enzyme (enzyme replacement therapy, ERT) (Neufeld and Muenzer, 2001; Martin *et al*, 2006). However, BMT does not alter the disease progression of Sanfilippo patients (Hoogerbrugge *et al*, 1995; Shapiro *et al*, 1995), requires a suitable marrow donor and is associated with significant mortality and morbidity, and peripherally-delivered ERT is insufficient to effectively ameliorate the central nervous system (CNS) deficits at the doses currently employed. Consequently, a safe and more effective therapy is required for treating the neurodegeneration observed in approximately two-thirds of LSD. This study will focus on MPS IIIA as a model of neurological LSD due to the availability of a well-characterised naturally-occurring animal model, the MPS IIIA mouse, which closely parallels the human condition.

Preliminary studies conducted in MPS IIIA mice have provided "proof of concept" that if recombinant human NS (rhNS) can be delivered to the CNS, it is able to correct metabolic, enzymatic and behavioural deficits (Gliddon and Hopwood, 2004; Savas *et al*, 2004; Hemsley *et al*, 2007). However, if a continuous supply of NS is not maintained within the brain, the heparan sulphate (HS) storage re-accumulates (Savas *et al*, 2004). Therefore, this study was designed to evaluate the safety and therapeutic efficacy of a gene therapy viral vector, canine adenovirus serotype II (CAV-2), as a means of generating active rhNS on a long-term basis in the MPS IIIA mouse CNS.

This literature review will introduce the lysosome, lysosomal enzymes and LSD, and will detail the biochemistry, clinical pathology and diagnosis of MPS IIIA. The experimental

therapies that are under evaluation for neurological LSD will be overviewed, with a particular focus on gene therapy. The similarities and differences between human and CAV-2 vectors will also be discussed.

1.2. The Lysosome and the Biosynthesis and Processing of Lysosomal Enzymes

The Lysosome

The lysosome was first described in 1955 after tissue fractionation studies found that the distribution of several hydrolytic enzymes co-localised within the same granular compartment (De Duve *et al*, 1955). Lysosomes are acidic, hydrolase-rich, membrane-bound organelles involved in the step-wise degradation of large macromolecules into monomeric components which can be recycled by other biosynthetic pathways or eliminated from the cell. The macromolecules targeted for degradation enter the cell via receptor-mediated endocytosis, phagocytosis, autophagy or direct fusion. In addition, lysosomes are involved in antigen presentation, inactivation of pathogens, metal ion homeostasis, down-regulation of surface receptors and autophagy (reviewed in Mullins and Bonifacino, 2001; Eskelinen *et al*, 2003).

Biosynthesis of Lysosomal Enzymes

Complex, macromolecular substrates are catabolised by approximately 40 individual acid hydrolases comprising of proteases, glycosidases, sulphatases, phosphatases and lipases. The biosynthesis and trafficking of lysosomal enzymes is well-understood and has been reviewed in several publications and will be summarised briefly here (Griffiths *et al*, 1988; Dahms *et al*, 1989; Kornfeld and Mellman, 1989; Hopwood and Brooks, 1997).

Lysosomal acid hydrolases, secretory proteins and membrane proteins are synthesised by ribosomes within the rough endoplasmic reticulum (Dahms *et al*, 1989; Kim, 2000) (**Fig. 1.1**). Following synthesis, glycosylation at selected asparagine-linked oligosaccharides occurs and the polypeptide signal sequence is removed. The lysosomal enzymes are then transferred by vesicular transport to the endoplasmic reticulum and *trans*-Golgi compartment. It is here that the lysosomal enzymes undergo several post-translational modifications, including proteolysis, glycosylation and phosphorylation (Hopwood and Brooks, 1997). The terminal mannose residues are phosphorylated (mannose-6-phosphorylated) and these moieties have a high affinity for the mannose-6-phosphate (M6P) receptor.

Figure 1.1: Biosynthesis and trafficking of lysosomal enzymes. Lysosomal enzymes (denoted in pink) are synthesised in the rough endoplasmic reticulum by ribosomes. After posttranslational modifications, including the incorporation of a M6P moiety, the lysosomal enzymes are segregated from the secretory glycoproteins (denoted in blue) and are targeted to the lysosome via the late-endosome by the M6P receptors found in clathrin-coated pits. The acidic conditions of the late-endosome results in the dissociation of lysosomal enzymes from the M6P receptors, which can then be recycled. Exogenously-applied lysosomal enzyme can also be targeted from the plasma membrane to the lysosome ("cross-correction"). Figure taken from Kim *et al*, 2000.

Mannose-6-Phosphate Receptors

The M6P receptor is primarily localised within intracellular compartments such as the clathrin-coated pits of the *trans*-Golgi network (reviewed in Kornfeld, 1992). However, approximately 5-10% of the M6P receptor is also present on the cell surface (reviewed in Kornfeld, 1992). The interaction between the mannose-6-phosphorylated lysosomal enzyme and the M6P receptor allows the lysosomal enzymes to be segregated from other glycoproteins and selectively targeted towards the lysosome via the late endosome. Two types of the M6P receptor have been described: a 46 kDa cation-dependent receptor (Hoflack and Kornfeld, 1985) and a 300 kDa cation-independent/insulin-like growth factor II receptor (Sahagian *et al*, 1981). The cation-dependent and cation-independent M6P receptors have different structures and are differentially regulated within the rodent brain, suggesting that apart from their shared role in targeting enzymes in the *trans*-Golgi network, the receptors may have separate but complementary functions (Konishi *et al*, 2005; Romano *et al*, 2005). In addition to binding to lysosomal enzymes, the cation-independent M6P receptor can also bind to a host of other ligands, including insulin-like growth factor II, retinoic acid, plasminogen, transforming factor-β precursor, CD26 and granzyme A and B, thus enabling this receptor to be involved in many diverse cellular processes (reviewed in Hawkes and Kar, 2004).

Trafficking of Lysosomal Enzymes

The acidic environment in the late endosome dissociates the M6P receptor from the lysosomal enzyme. The M6P receptor may then be recycled from this compartment to the *trans*-Golgi network or the plasma membrane (Brown *et al*, 1986; Rohrer and Kornfeld, 2001). The majority of the newly-synthesised lysosomal enzymes are then shuttled by vesicular transport to the lysosome (biosynthetic pathway) and a small fraction is secreted into the extracellular milieu (endocytic pathway). Once in the extracellular space, neighbouring cells expressing the cation-independent M6P receptor at the cell surface can recapture phosphorylated lysosomal enzymes. This latter scenario allows exogenously applied mannose-6-phosphorylated lysosomal enzymes to be endocytosed and targeted towards the lysosome of nearby cells where it can "cross-correct" the stored material (Willingham *et al*, 1981). This concept was first demonstrated by Fratantoni *et al* (1968) when intracellular glycosaminoglycan (GAG) storage was reduced by co-culturing MPS I and MPS II fibroblasts, and also by treating MPS I fibroblasts with conditioned media collected from MPS II fibroblasts (and vice versa).

M6P-independent targeting of lysosomal enzymes to the lysosome can also occur and is mediated by sortilin (Ni and Morales, 2006), or receptors specific for mannose, galactose, fucose or *N*-acetylgalactosamine (reviewed in Hasilik, 1992). These transport mechanisms are cell-type dependent (Dittmer *et al*, 1999) and are apparent in mucolipidosis II and III (I-cell disease and pseudo-Hurler polydystrophy, respectively) patients where mannose-6-phosphorylation of lysosomal enzymes does not occur but near normal lysosomal enzyme activities are retained (Reitman *et al*, 1981; DiCioccio and Miller, 1991)

1.3. Lysosomal Storage Disorders

The aberrant expression of any one of the specific lysosomal enzymes, transporters, receptor targets or activator proteins in the degradation pathway can result in the accumulation of undegraded or partially degraded substrates within the lysosome. Collectively, these disorders are termed LSD. The resulting metabolic blockade causes a progressive build-up of undegraded substrate within the cell, causing lysosomal distension, interference in normal cellular function and a range of pathological changes.

Whilst most LSD are caused by deficiencies in an individual lysosomal enzyme, several LSD have been described where multiple enzyme activities are affected. For example, in multiple sulphatase deficiency, mutations in the *sulphatase modifying factor–1* (SUMF1) gene prevent a highly-conserved post-translational modification of a cysteine residue to a C_α-formylglycine residue in sulphatase enzymes that is essential for catalytic activity (Cosma *et al*, 2003; Dierks *et al*, 2003). Consequently, patients with multiple sulphatase deficiency do not produce active sulphatase enzymes, including those that are deficient in MPS types II, IIIA, IIID, IVA, VI and metachromatic leukodystrophy, as well as in other non-LSD sulphatases (X-linked ichthyosis from steroid sulphatase deficiency and chondrodysplasia punctata 1 from arylsulfatase E deficiency) (reviewed in Diez-Roux and Ballabio, 2005). Multiple enzyme activities are also affected in mucolipidosis II and III, where the M6P moiety is not transferred to the lysosomal enzymes due to a functional deficiency of *N*-acetylglucosamine phosphoryl transferase. Lysosomal storage can also result when the metabolite is unable to be transported out of the lysosome due to mutations in transporter genes such as *sialin* (Salla disease and infantile sialic acid storage disease; transport of sialic acid) and *cystinosin* (cystinosis; transport of cystine).

The clinical characteristics and substrate storage of many LSD were recognised long before the underlying genetic basis of the diseases had been established. All LSD are

inherited in an autosomal recessive manner with the exception of Fabry disease and MPS II, which have an X-linked recessive mode of inheritance, and glycogen storage disease IIB (Danon disease) which is X-linked dominantly-inherited. While the occurrence of each individual LSD is relatively rare, these disorders are collectively estimated to have an incidence of greater than 1:4,000 births in Portugal (Pinto *et al*, 2004), 1:7,700 in Australia (Meikle *et al*, 1999) and 1:7,100 in The Netherlands (Poorthuis *et al*, 1999). However, the prevalence of these diseases may be greatly under-estimated with two recent studies in Fabry disease (prevalence of 1:3,100; Italy) and Pompe disease (prevalence of 1:3,500; Taiwan) displaying much higher frequencies due to the detection of adult-onset varieties (Hwu *et al*, 2006; Spada *et al*, 2006).

1.4. The Mucopolysaccharidoses

The MPS are a subgroup of LSD where the functional deficiency of any 1 of 11 exoenzymes results in the storage of sulphated GAG, formerly referred to as mucopolysaccharides (**Table 1.1**). Secondary accumulation of glycosphingolipids (G_{M2} and G_{M3} gangliosides) and cholesterol are also observed in some of the MPS and will be discussed subsequently (McGlynn *et al*, 2004; Walkley, 2004).

Elevated urinary GAG can be detected in the urine of MPS patients (as well as those afflicted with multiple sulphatase deficiency and mucolipidosis II/III). Disease severity and clinical phenotype varies greatly between and within each type of MPS, with multiple organs and tissues affected. The MPS are estimated to have a prevalence between 1:22,500 in Australia to 1:52,000 births (Spranger, 1972; Nelson, 1997; Meikle *et al*, 1999; Applegarth *et al*, 2000; Baehner *et al*, 2005). Before the clinical progression and pathology of MPS IIIA is overviewed, the structure, function and degradation of HS, the GAG stored in MPS III patients, will first be discussed.

1.5. Glycosaminoglycans and Heparan Sulphate

Structure of GAG

In patients afflicted with MPS, the GAG HS, dermatan sulphate, keratan sulphate, chondroitin sulphate and/or hyaluronan accumulate in a wide variety of tissues, either singularly or in combination (Davidson and Meyer, 1954; Dorfman and Lorincz, 1957; Pedrini *et al*, 1962; Natowicz *et al*, 1996). In general, GAG exist as polyanionic proteoglycans where GAG chains of repeating disaccharide units (**Fig. 1.2**) are covalently

Table 1.1: Summary of the Mucopolysaccharidoses.

Disorder	Eponym	Enzyme Deficiency	Substrate Stored	Australian Incidence	CNS Pathology	Skeletal Pathology
MPS I	Hurler, Scheie	α-L-Iduronidase	DS, HS	1:88,000	Variable	Yes
MPS II	Hunter	Iduronate-2-sulphatase	DS, HS	1:136,000	Variable	Yes
MPS IIIA	Sanfilippo	Heparan-*N*-sulphatase	HS	1:114,000	Yes	No
MPS IIIB	Sanfilippo	α-*N*-Acetylglucosaminidase	HS	1:211,000	Yes	No
MPS IIIC	Sanfilippo	Acetyl CoA:α-glucosaminide acetyltransferase	HS	1:1,407,000	Yes	No
MPS IIID	Sanfilippo	*N*-Acetylglucosamine 6-sulphatase	HS	1:1,056,000	Yes	No
MPS IVA	Morquio	Galactose-6-sulphatase	KS, CS	1:169,000	No	Yes
MPS IVB	Morquio	β-Galactosidase	KS	-	No	Yes
MPS V	No longer used (previously Scheie syndrome; see MPS I)					
MPS VI	Maroteaux-Lamy	*N*-Acetylgalactosamine 4-sulphatase	DS	1:235,000	No	Yes
MPS VII	Sly	β-Glucuronidase	DS, HS, CS	1:2,111,000	Variable	Yes
MPS VIII	No longer used					
MPS IX	-	Hyaluronidase	Hyaluronan	-	No	No

Mucopolysaccharidosis (MPS), chondroitin sulphate (CS), dermatan sulphate (DS), heparan sulphate (HS), keratan sulphate (KS). Constructed from information in Vervoort *et al*, 1998; Meikle *et al*, 1999; Neufeld and Muenzer, 2001.
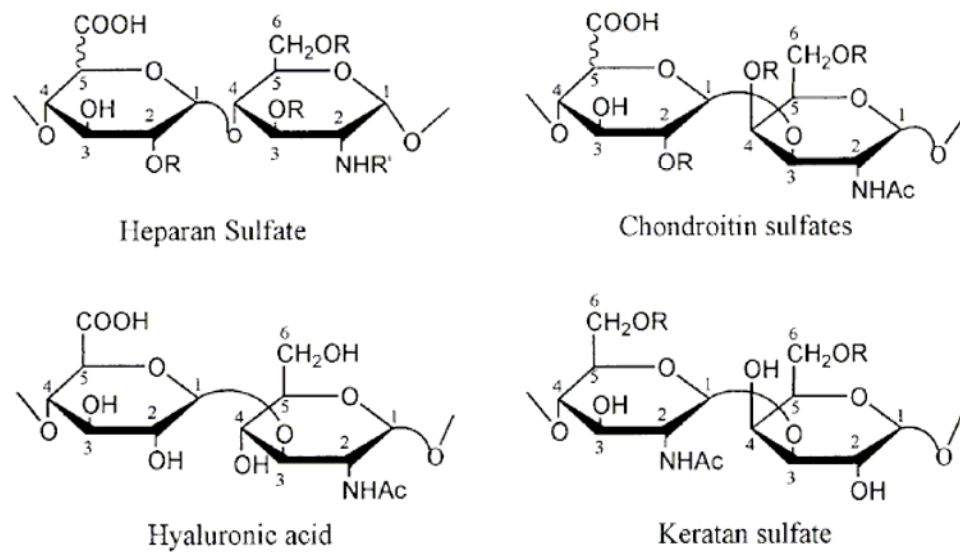
Figure 1.2: Disaccharide Unit Structures of GAG. The chemical structures of typical disaccharide repeat units that make up the GAG chains of HS, chondroitin sulphate, dermatan sulphate, keratan sulphate or hyaluronan are depicted. Chondroitin sulphates include chondroitin sulphate A, chondroitin sulphate B (dermatan sulphate) or chondroitin sulphate C. R represents H or a sulphate, and R' represents acetyl, sulphate or H. Figure taken from Liu and Thorp, 2002.

linked at specific serine residues to a protein core (Ruoslahti, 1988; Hopwood, 1989). These disaccharides are usually alternating hexosamine and hexuronic acid residues, with the exception of keratan sulphate, which has a galactose sugar substituted for the hexuronic acid. The hexuronic acid may be a glucuronic acid or an L-iduronic acid, and the hexosamine residue is a glucosamine or a galactosamine. With the exception of hyaluronan, which is unsulphated, the GAG may be *O*-sulphated and, in the case of HS, *N*-sulphated at selected residues. There is considerable diversity in the length of the GAG chains, the position and degree of sulphation and the composition of hexuronic acid and hexosamine units.

Structure of Heparan Sulphate

HS GAG are generally distributed as unbranched side-chains of proteoglycans that consist of alternating uronic acid and α-linked (1,4) glucosamine residues up to 20-200 monosaccharides in length (Hopwood, 1989; Salmivirta *et al*, 1996; Whitelock and Iozzo, 2005). The uronic acid residues are glucuronic acid or iduronic acid and are unsulphated or *O*-sulphated. The glucosamine component may be modified by *N*-sulphation, *N*-acetylation, 6-sulphation or 3-sulphation (Hopwood and Morris, 1990). HS is the only GAG containing *N*-linked sulphated residues. The linear HS GAG chains are covalently-linked to various proteoglycan core proteins that are typically classed as perlecans, agrins, syndecans, glypicans or collagen XVIII (reviewed in Bulow and Hobert, 2006). The heterogeneity in HS proteoglycan structures allows these polymers to play a role in diverse biological functions, including neurogenesis, axon guidance, synaptogenesis, neuronal migration, inflammation, and as a receptor for viral infections (reviewed in Yamaguchi, 2001; Liu and Thorp, 2002; Cavalcante *et al*, 2003; Parish, 2005).

Degradation of Heparan Sulphate

After the initial proteolysis of the proteoglycan in the early endosome, the degradation of HS GAG chains is instigated by endoglycosidases, which break down the long carbohydrate chains into smaller fragments of approximately M_r 10,000 in size (Yanagishita, 1985; Hopwood, 1989). The oligosaccharides are then transported to the lysosome and can be further degraded from the non-reducing end by the sequential action of eight lysosomal exoenzymes (Hopwood, 1989). Following the schematic representation in **Fig. 1.3**, iduronate-2-sulphatase is first required to remove a sulphate at the 2 position of the non-reducing end of iduronic acid. This allows a glycosidase, α-L-iduronidase, to cleave the non-reducing terminal
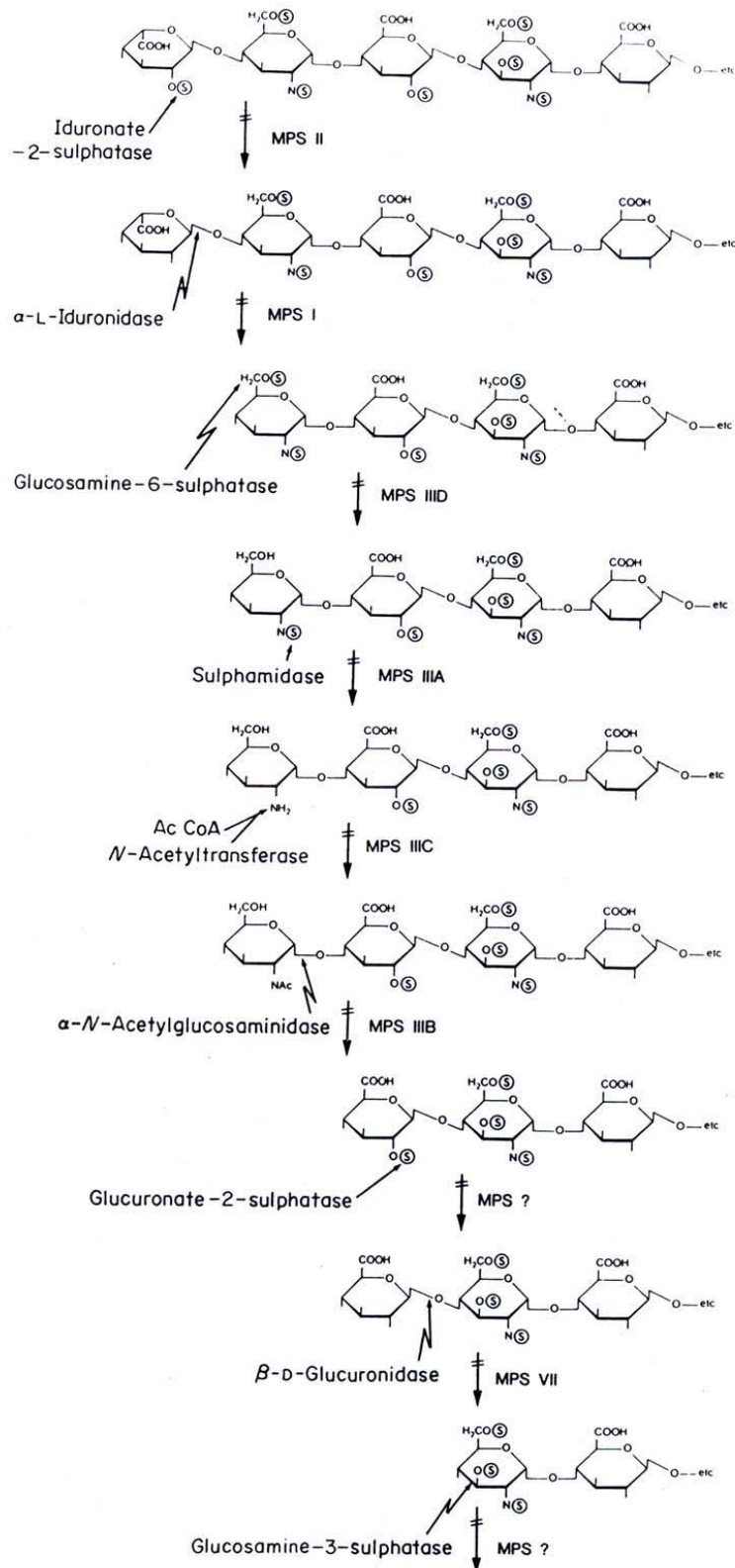
Figure 1.3: Degradation of HS. HS GAG chains are first degraded by endoglycosidases into smaller oligosaccharide fragments and are then sequentially degraded from the non-reducing end by lysosomal exohydrolases. The absence of any one of these lysosomal enzymes results in the accumulation of HS oligosaccharides. Figure taken from Hopwood and Morris, 1990.

L-iduronic acid residue from the HS chain revealing the substrate for glucosamine-6-sulphatase. The exposed terminal glucosamine residue at the non-reducing end is then desulphated by heparan-*N*-sulphatase (NS) before undergoing a biosynthetic reaction where an acetyl group is transferred from acetyl-CoA to the amino group of the glucosamine residue. α-*N*-Acetylglucosaminidase is required to remove the *N*-acetylglucosamine moiety before desulphation of glucuronate-2-sulphate by glucuronate-2-sulphatase. The terminal glucuronic acid is cleaved from the non-reducing end by β-glucuronidase. Glucosamine-3-sulphatase removes the sulphate from glucosamine before the process is repeated on the following pair of disaccharides at the non-reducing end.

Once the oligosaccharide fragments are completely hydrolysed into monosaccharides, inorganic sulphate, phosphate and amino acids, these components may then be actively transported from the lysosome and are recycled in the biosynthetic pathway or are eliminated from the cell (Hopwood, 1989). The absence of any one of these lysosomal enzymes results in the accumulation of the undegraded substrate within the lysosome and subsequent pathological changes, with the exception of glucuronate-2-sulphatase and glucosamine-3-sulphatase, where no disease state has yet been associated with these enzyme deficiencies.

1.6. Mucopolysaccharidosis type IIIA

MPS III is divided into four subtypes (A, B, C or D), and each of the disease-causing genes have been identified and cloned (Robertson *et al*, 1992; Scott *et al*, 1995; Weber *et al*, 1996; Zhao *et al*, 1996; Fan *et al*, 2006; Hrebicek *et al*, 2006) (**Table 1.1**). MPS III has a reported incidence ranging from 1:24,000 births in The Netherlands (van de Kamp *et al*, 1981), to 1:53,000 in Australia (Meikle *et al*, 1999) and 1:324,000 in British Columbia (Lowry *et al*, 1990). MPS IIIA is the most frequently observed subtype in northern European populations, whilst MPS IIIB is more common in southern Europe and Brazil (Coelho *et al*, 1997; Nelson, 1997; Poorthuis *et al*, 1999; Pinto *et al*, 2004; Baehner *et al*, 2005). The Sanfilippo disorders have identical clinical presentation and cannot be discriminated on the basis of clinical symptoms.

1.6.1. Sulphamidase

The "Sanfilippo A corrective factor" was first isolated from the urine of healthy subjects and was shown to reduce metabolically-labelled "mucopolysaccharide" storage in

MPS IIIA skin fibroblasts (Kresse and Neufeld, 1972). This factor, NS (also known as heparan-*N*-sulphatase, *N*-sulphoglucosamine sulphohydrolase and SGSH; EC 3.10.1.1), hydrolyses the *N*-sulphated bond from the non-reducing terminal glucosamine residue of HS oligosaccharides. Consequently, mutations in the NS gene cause the accumulation of HS oligosaccharide substrates within the lysosome, resulting in the Sanfilippo disease phenotype.

Human NS has been sequenced and has an open reading frame of 1506 nucleotides encoding a 502 amino acid protein (Scott *et al*, 1995). There are five potential *N*-glycosylation sites at positions 41, 142, 151, 264 and 413, and all sites are utilised as determined by Endo H and PNGase F treatment of recombinant human NS (rhNS; Scott *et al*, 1995; Perkins *et al*, 1999). One or more of these glycosylation sites are capable of carrying the M6P residue. The human NS gene has been localised to chromosome 17q25.3 by fluorescent *in situ* hybridisation (Scott *et al*, 1995) and consists of 8 exons spanning approximately 11 kb (Karageorgos *et al*, 1996). More than 85 allelic variants of the human NS gene have been described to date (Blanch *et al*, 1997; Bunge *et al*, 1997; Weber *et al*, 1997; Di Natale, 1998; Montfort *et al*, 1998; Beesley *et al*, 2000; Esposito *et al*, 2000; Yogalingam and Hopwood, 2001; Lee-Chen *et al*, 2002; Di Natale *et al*, 2003; Montfort *et al*, 2004; Muschol *et al*, 2004). Messenger RNA transcripts of sizes 3.1, 4.3 and 7.1 kb have been detected via Northern blots, potentially indicating the presence of alternative polyadenylation sites (Scott *et al*, 1995).

Human NS is synthesised as a 62 kDa precursor protein and undergoes maturational changes to a 56 kDa subunit (Perkins *et al*, 1999). NS has been predicted to exist as a 120 kDa dimer, as determined by SDS-polyacrylamide gel electrophoresis (Perkins *et al*, 1999). Whilst the crystal structure of human NS is yet to be determined, the crystal structures of three other human sulphatases (arylsulphatase A, arylsulphatase B and estrone sulphatase) have been identified and have highly similar three-dimensional structures, particularly in the core region, which conveys the catalytic ability of these enzymes (Bond *et al*, 1997; Lukatela *et al*, 1998; Hernandez-Guzman *et al*, 2003). It is likely that the conserved residues equivalent to Asp31, Asp32, Cys70, Pro72, Ser73, Arg74, Lys123, His125, Asp273 and Asn274 of NS are critical for catalytic activity (reviewed in Hopwood and Ballabio, 2001; Muschol *et al*, 2004). Similar to other sulphatases, an essential post-translation conversion of a cysteine to a C_α-formylglycine residue is required for NS enzyme activity (Cosma *et al*, 2003; Dierks *et al*, 2003). Recent studies have shown that co-expressing SUMF1 - which performs this post-translational modification - with arylsulphatase A, arylsulphatase B, arylsulphatase E, iduronate-2-sulphatase or NS can increase the specific activity of these enzymes *in vitro*

(Fraldi *et al*, 2007). Furthermore, when NS is delivered to gastrocnemius of neonatal MPS IIIA mice in the absence and presence of SUMF1, approximately 8-fold and 16-fold increases in NS specific activity (compared to untreated cells) are observed (Fraldi *et al*, 2007).

1.6.2. Diagnosis of MPS IIIA

The early diagnosis of affected individuals is essential given the severe, progressive nature of these diseases. In addition, a definitive diagnosis allows parents to make informed decisions regarding future pregnancies in consultation with genetic counsellors and can even allow the genetic screening of *in vitro* fertilised embryos prior to implantation (Thornhill and Snow, 2002). The most simple biochemical assessment for the presence of MPS is to determine whether the GAG content is elevated in urine (GAG-uria). This can be evaluated using quantitative methods, including dimethylmethylene blue-based spectrometry (de Jong *et al*, 1989) and uronic acid measurements (Bitter and Muir, 1962), or less reliable methods such as turbidity tests (high rate of false-negatives for MPS III) (Rezvani *et al*, 1973; Chih-Kuang *et al*, 2002) and qualitative spot tests (high false-positive and false-negative rates) (Berry, 1987; de Jong *et al*, 1991). Care must be taken to ensure that normal control samples are age-matched because urinary GAG excretion is higher in infants than in adults (de Jong *et al*, 1991). High-resolution electrophoresis of urinary GAG may also be used to assist in the discrimination between each MPS type – but not MPS III subtypes – by visualising the stored GAG patterns based on their electrophoretic abilities through cellulose-acetate strips in a barium acetate buffer to suggest the most appropriate follow-up enzymology for confirmation of a diagnosis (Hopwood and Harrison, 1982).

Differential diagnosis of MPS IIIA is required because all of the MPS III subtypes store HS GAG fragments. For a definitive diagnosis of MPS IIIA, reductions in NS enzyme activity can be measured in patient leucocyte or skin fibroblast samples (Hopwood and Elliott, 1981). At present two assays measuring NS activity (or lack thereof) have been described. In the first assay, the conversion of a natural, heparin-derived, tritiated, tetrasaccharide substrate to product can be measured by high-voltage electrophoresis (Hopwood and Elliott, 1982). In the second assay, NS activity can be measured using an artificial fluorogenic substrate, 4-methylumbelliferyl-α-D-*N*-sulphoglucosaminide, in a two-step digestion where the substrate is mixed with NS enzyme, followed by α-glucosaminidase digestion, thus liberating the 4-methylumelliferone fluorophore (Karpova *et al*, 1996). Prenatal diagnosis of MPS IIIA can also be performed directly on chronic villus biopsies or on cells cultured from chronic villi or

amniotic fluid (amniocentesis) from as early as 9- to 10-wks or 14- to 16-wks gestation, respectively (Kleijer *et al*, 1996; Neufeld and Muenzer, 2001; Hopwood, 2005). Direct mutational analysis may also be useful in the prenatal diagnosis of MPS IIIA, particularly in instances where an index case has been previously identified in a family (Hopwood, 2005).

More recently, methods have been developed that take advantage of high-throughput screening technologies. Urinary GAG-derived oligosaccharide accumulation can be accurately measured using electrospray ionisation tandem mass spectrometry in small volumes of approximately 100 µL urine and can discriminate between various MPS subtypes (MPS I, II, IIIA-D, IVA, VI) (Fuller *et al*, 2004; Mason *et al*, 2006). In addition, immune-quantification assays have been developed where multiple lysosomal proteins eluted from dried blood spots can be multiplexed and assessed within the same well (Meikle *et al*, 2006). Similar strategies have been employed for other LSD where the enzymatic products can be quantitated via mass spectrometry after rehydrated dried blood spots are exposed to multiplexed substrates (Li *et al*, 2004; Gelb *et al*, 2006).

1.6.3. Clinical Description of Sanfilippo Syndrome

Sanfilippo syndrome was first recognised by Dr Sylvester Sanfilippo and was described as a variant of Hunter-Hurler syndrome (Sanfilippo *et al*, 1963). The clinical presentation of Sanfilippo syndrome varies from patient to patient but most display progressive neurological abnormalities such as regression in learned behaviours, loss of social skills, sleep disturbance and profound mental deterioration (van de Kamp *et al*, 1981). A decline in cognitive function is first noted at 5.5-years of age on average, with the most common initial loss of function reported as a regression in language and memory abilities (Nidiffer and Kelly, 1983). Compared to some of the other MPS disorders, which feature pronounced skeletal involvement (**Table 1.1**), Sanfilippo patients have comparatively mild somatic pathology (Cleary and Wraith, 1993; Neufeld and Muenzer, 2001). Despite earlier suggestions that MPS IIIA patients were more clinically severe than MPS IIIB patients, it is now agreed that all MPS III subtypes have a similar clinical phenotype. Considerable variation in the age of onset and severity is observed in Sanfilippo patients with attenuated, intermediate and severe varieties described (i.e. a broad clinical spectrum exists). The severity of clinical symptoms (phenotype) may relate to the gene mutation (genotype) of the patient (Yogalingam and Hopwood, 2001).

The disease progression in Sanfilippo patients usually occurs in three phases. The initial phase is characterised by a period of seemingly normal development until the child is approximately 2- to 6-years of age (van de Kamp *et al*, 1981; Meikle *et al*, 1999). Affected children may be late to achieve developmental milestones, particularly in speech (Neufeld and Muenzer, 2001). Due to the delayed onset of noticeable symptoms and the absence of routine newborn screening, a significant period of time may lapse before a diagnosis is made. Sanfilippo children generally enter a second, more destructive phase at 3- to 4-years of age (Nidiffer and Kelly, 1983; Cleary and Wraith, 1993), which may feature temper tantrums, hyperactivity and aggressive behaviour whilst retaining good mobility, making it difficult for parents or carers to control the child (Nidiffer and Kelly, 1983; Bax and Colville, 1995; Neufeld and Muenzer, 2001). Sleep disorders and a decreased attention span are also noted (van de Kamp *et al*, 1981; Colville *et al*, 1996; Fraser *et al*, 2005). In the third, quieter phase, patients may fall frequently due to a lack of balance, experience feeding difficulties, reduced mobility and seizures (Bax and Colville, 1995; Neufeld and Muenzer, 2001). Patients are also documented as having problems with memory and anxiety (Nidiffer and Kelly, 1983).

The somatic pathology in Sanfilippo patients can result in coarse hair, hirsutism, diarrhoea, incontinence, dystosis multiplex and hearing loss (van de Kamp *et al*, 1981; Cleary and Wraith, 1993; Bax and Colville, 1995; Neufeld and Muenzer, 2001). Older patients may also present with mild skeletal pathology (Cleary and Wraith, 1993; Rigante and Caradonna, 2004), hepatosplenomegaly (van de Kamp *et al*, 1981), joint stiffness (Neufeld and Muenzer, 2001) and cardiomyopathy (Van Hove *et al*, 2003). Death commonly occurs in the late teenage years usually as a result of respiratory infections (van de Kamp *et al*, 1981). Patients with a more attenuated form of Sanfilippo syndrome may live to the third or fourth decade of life (Van Hove *et al*, 2003; Gabrielli *et al*, 2005).

1.6.4. Management of Sanfilippo Patients

At present, there is not an effective treatment available for MPS III and patient care is consequently directed at alleviating the clinical symptoms. Many Sanfilippo patients are treated for ear, nose and throat problems prior to diagnosis (Cleary and Wraith, 1993). As Sanfilippo patients suffer from bouts of insomnia, hypnotic medication is occasionally administered, and melatonin (Fraser *et al*, 2005) or benzodiazepines (chloral hydrate, imipramine, valproic acid or a combination of chloral hydrate/trimeprazine tartrate) have had some success (Nidiffer and Kelly, 1983; Cleary and Wraith, 1993). Many parents use a "bed

belt" to physically restrain the child in bed at night whilst still allowing free movement within the bed (Cleary and Wraith, 1993).

Further behavioural changes such as hyperactivity can usually be controlled using antipsychotic agents such as thioridazine, haloperidol, phenytoin and carbamazepine (Nidiffer and Kelly, 1983; Cleary and Wraith, 1993). Families often renovate their homes to include "safe rooms" containing heavily padded walls, soft furniture, reinforced glass and removal of fragile items (Cleary and Wraith, 1993). In addition, in the later stage of disease, wheelchair ramps may become necessary.

Sanfilippo patients may have difficulty swallowing and can choke on their saliva and, consequently, hyosine or benztropine mesylate may be administered to control saliva production (Cleary and Wraith, 1993). As the disease progresses, patients may ultimately require food to be vitamised and delivered via feeding tubes. The majority of patients are responsive to pharmacological management of seizures (Nidiffer and Kelly, 1983).

1.6.5. Cellular Pathology in Human MPS IIIA

HS accumulation in Sanfilippo patients results in pathological changes which can be observed at a cellular level (Ginsberg *et al*, 1999). At the ultra-structural level, human MPS IIIA cortical and cerebellar neurons feature variable amounts of storage that generally appear electron-lucent or "empty" as the water-soluble GAG material is removed during routine histological processing (Martin *et al*, 1979). Other characteristic cell morphologies include zebra bodies (multilamellar stacks), inclusion bodies, membranous cytoplasmic bodies (both transversely and concentrically lamellated) and granular storage material within vacuoles (Martin *et al*, 1979; Walkley, 1998). These types of lesions were evident in all neurons from an 11-year-old MPS IIIA boy, particularly the pyramidal cells of the cerebral cortex as well as those in the neostriatum, claustrum, pallidum, amygdaloid nucleus, Ammon's horn, hypothalamus and the substantia nigra (Martin *et al*, 1979). The brainstem and spinal cord were also affected (Martin *et al*, 1979). Gross perturbations in the neuroanatomy of MPS IIIA patients (aged 11- and 23-years) have been described with severe cortical atrophy and dilation of the lateral ventricles (Martin *et al*, 1979; Oldfors and Sourander, 1981). Vacuoles are also apparent in the visceral organs, including skin fibroblasts, chondrocytes, Kupffer cells (liver), and in the spleen, kidney and lymph nodes (Martin *et al*, 1979).

Autofluorescent material in cortical neurons and macrophages may reflect the storage of lipofuscin and other lipid material (Martin *et al*, 1979; Oldfors and Sourander, 1981;

Ginsberg *et al*, 1999). This is accompanied by the accumulation of G_{M2} and G_{M3} gangliosides (glycosphingolipids containing sialic acid residues), which are the major component of neuronal membranes (reviewed in Tettamanti, 2003). G_{M2} and G_{M3} ganglioside accumulation has been postulated to result in the formation of ectopic dendrites, meganeurites (swollen axon hillocks) and axonal spheroid formation (focal swellings of distal axons) and may co-localise with cholesterol storage (Martin *et al*, 1979; Constantopoulos *et al*, 1980; Oldfors and Sourander, 1981; Walkley, 2004). Increased amyloid β-peptides have also been reported within the neocortex and hippocampus in four human MPS IIIA brains (Ginsberg *et al*, 1999). Neuronal loss and fibrillary gliosis is seen within the central ovale and in thalamic association nuclei (Martin *et al*, 1979; Oldfors and Sourander, 1981). In addition, myelin sheaths were rarefied in two case studies (Martin *et al*, 1979; Oldfors and Sourander, 1981).

1.7. Sanfilippo Animal Models

Animal models of human disease provide a platform to gain a greater understanding of disease progression and pathogenesis. It is essential that any therapeutic approach undergoes rigorous safety and therapeutic efficacy testing in animals in order to satisfy regulatory agencies before a treatment can be administered to humans. Small animal models such as mice and rats are advantageous as they usually have a homogeneous genetic background, are easy to breed and can consequently be tested in large sample sizes to obtain statistically relevant outcomes. Large animal models are also useful as their increased lifespan and size may more accurately reflect the therapeutic efficacy and longevity of treatment. Several animal models of LSD have been identified serendipitously and others have been generated by gene disruption technologies (reviewed in Ellinwood *et al*, 2004; Haskins, 2007). For MPS III, 8 animal models and their underlying genetic mutations have been identified thus far (**Table 1.2**).

This thesis will focus on studies investigating a novel treatment for Sanfilippo syndrome (and other LSD with neurodegeneration) using the MPS IIIA mouse model. This model has been selected because it closely resembles many of the clinical features observed in the human MPS IIIA condition and has been extensively characterised at a behavioural, biochemical and histological level. Each of these factors will be discussed in more depth in the following sections (**Sections 1.7.1** to **1.7.5**).

Table 1.2: Sanfilippo Animal Models

Disorder	Species	Reference	Mutation	Reference
MPS IIIA	Dog (Huntaway)	(Jolly *et al*, 2000)	c.708-709insC	(Yogalingam *et al*, 2002)
	Dog (Dachshund)	(Fischer *et al*, 1998)	c.737-739delCCA	(Aronovich *et al*, 2000)
	Mouse	(Bhaumik *et al*, 1999)	c.91G>A (p.D31N)	(Bhattacharyya *et al*, 2001)
MPS IIIB	Cow	(Karageorgos *et al*, 2007)	c.1354G>A (p.E542K)	(Karageorgos *et al*, 2007)
	Dog (Schipperke)	(Ellinwood *et al*, 2003b)	Ins ~45A in exon 6	(Ellinwood *et al*, 2003a)
	Emu	(Giger *et al*, 1997)	1098-1099delGG	(Aronovich *et al*, 2001)
	Mouse (knock-out)	(Li *et al*, 1999)	Del Exon 6	(Li *et al*, 1999)
MPS IIIC	None identified			
MPS IIID	Nubian Goat	(Thompson *et al*, 1992)	c.322C>T (p.R102X)	(Cavanagh *et al*, 1995)

1.7.1. The MPS IIIA Mouse Model

Three naturally-occurring models of MPS IIIA have been identified, which closely parallel the human condition (**Table 1.2**). A mixed genetic background strain of MPS IIIA mice (designated the "New York" strain) consists predominantly of 129SvJ and CD1 with some C57Bl/6 and SJL strain contributions (Bhaumik *et al*, 1999). A breeding colony of these mice has been established at the Children, Youth and Women's Health Service (CYWHS, Adelaide, Australia), which has recently been back-crossed at this institution onto a pure C57Bl/6 background ("congenic strain"; B6.Cg-Sgsh[mps3a]; **Fig. 1.4**) (Crawley *et al*, 2006a). The MPS IIIA mutation has been independently back-crossed onto a C57Bl/6 strain by the Jackson Laboratory and these mice are designated B6.Cg-Sgsh[mps3a]/PstJ mice (JAX Mice Data Sheet, 2005).

The MPS IIIA mutation in "New York" mice arose when a chimera of WW6.186 embryonic stem cells with a targeted mutation in the *Mgat3* gene were injected into the blastocysts of CD1 mice (Bhaumik *et al*, 1999). A 14-month-old *Mgat3* homozygote mouse was found walking in circles and subsequent histological analyses displayed abnormal lysosomal morphology and inclusions with zebra body morphology (Bhaumik *et al*, 1999). Further analysis in additional *Mgat3* homozygous mice found severe brain lesions and
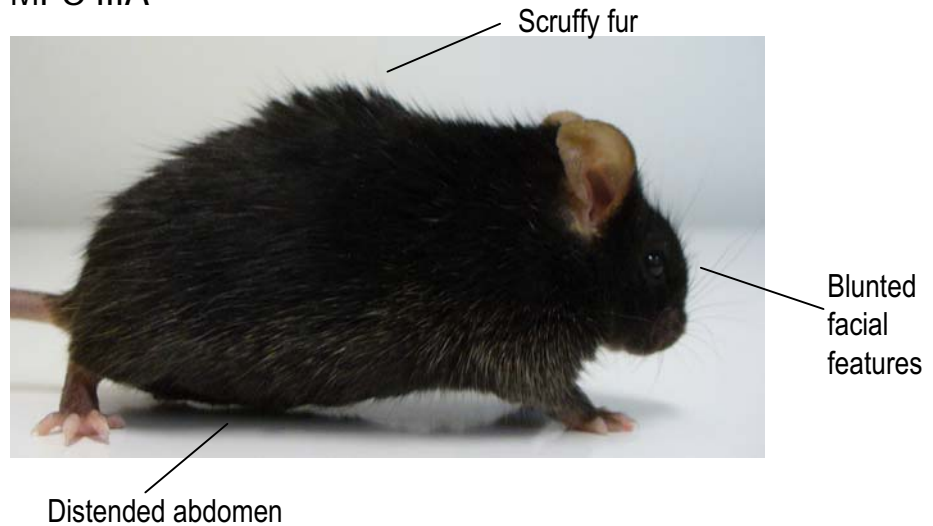
Unaffected

MPS IIIA

Scruffy fur

Blunted facial features

Distended abdomen
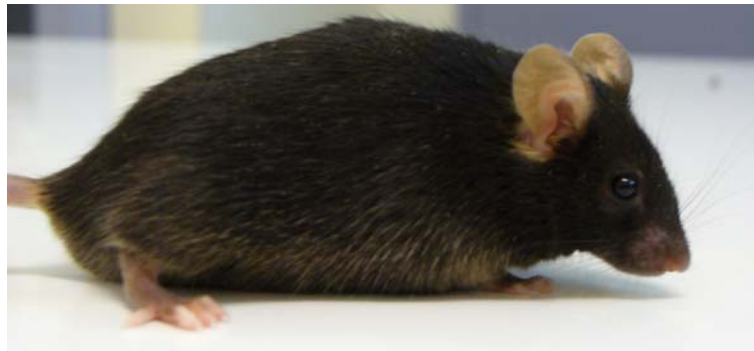
Figure 1.4: Unaffected and B6.Cg-Sgsh^{mps3a} Male Mice at 20 Weeks of Age. The MPS IIIA mouse is a naturally-occuring model containing a mutation at amino acid position 31 (p.D31N) of the NS gene. MPS IIIA mice display progressive memory and learning difficulties, increased aggression (in males) and changes in activity compared to wild-type mice. Compared to unaffected mice (top panel), MPS IIIA mice (lower panel) also present with characteristic features such as dysmorphic facial features, scruffy fur, slightly hunched posture (due to hepatosplenomegaly, enlarged abdomen and distended bladder). Lysosomal storage is evident histologically and biochemically.

vacuolation (Bhaumik *et al*, 1999). When compared with the wild-type murine NS sequence (Costanzi *et al*, 2000; 2003), a point mutation (c.91G>A) at nucleotide position 91 was eventually determined to be responsible for the MPS IIIA phenotype in mice (Bhattacharyya *et al*, 2001). This mutation results in an amino acid change from a conserved aspartic acid residue to an asparagine (p.D31N) at a location that is proposed to be involved in the coordination of a divalent metal ion required for catalytic activity in sulphatase enzymes (Bhattacharyya *et al*, 2001; Sardiello *et al*, 2005). Recombinant murine NS has been purified and characterised and has similar kinetic properties to human NS (Gliddon *et al*, 2004).

1.7.2. Behavioural Phenotype of MPS IIIA Mice

MPS IIIA mouse pups are indistinguishable from littermates at birth. At 3-wks of age MPS IIIA mice from the mixed "New York" strain are more active than wild-type mice, followed by a period of hypoactivity from approximately 6- to 15-wks of age (Hemsley and Hopwood, 2005). Congenic, unaffected mice (ages 7- to 18-wks) of both genders are also more active than age-matched MPS IIIA animals (unpublished observations, Lysosomal Diseases Research Unit, Australia (LDRU)). MPS IIIA mice begin to show gait abnormalities and a reduction in neuromuscular strength from 15-wks (mixed strain, Hemsley and Hopwood, 2005) as well as increased aggression in males and poor maternal behaviour in females (congenic strain, Crawley *et al*, 2006a). MPS IIIA mice of both strains also display memory and spatial learning deficits from approximately 20-wks of age as assessed using the Morris Water Maze (Gliddon and Hopwood, 2004; Crawley *et al*, 2006a).

1.7.3. Gross Pathology of MPS IIIA Mice

In addition to the behavioural changes, somatic pathology similar to the human Sanfilippo phenotype is also evident in the MPS IIIA mouse. Hepatosplenomegaly, distended bladders filled with turbid urine, dysmorphic facial features, a hunched posture, corneal opacities and scruffy fur are observed in affected mice (Bhaumik *et al*, 1999; Crawley *et al*, 2006a). The organomegaly may account for the heavier body weights in both female and male MPS IIIA mice when compared to age-matched, unaffected mice (Crawley *et al*, 2006a). Rectal prolapses may also be detected from 16- to 20-wks of age (Crawley *et al*, 2006a). Few mice live longer than 12- to 14-months or 9- to 12-months for the "New York" and congenic strains, respectively (Bhaumik *et al*, 1999; Crawley *et al*, 2006a).

1.7.4. Biochemical Changes in MPS IIIA Mice

Biochemical differences can also be detected between MPS IIIA and wild-type mice. The residual level of NS activity in affected mice is estimated to be 3-4% of wild-type, as measured in liver, kidney or brain homogenates using a heparin-derived tritiated substrate (Bhaumik *et al*, 1999; Crawley *et al*, 2006a). HS-uria is apparent by high resolution electrophoresis and gradient gel electrophoresis (Bhaumik *et al*, 1999). A HS-derived disaccharide marker (hexosamine-*N*-sulphate [α-1,4] hexuronic acid; HNS-UA) progressively accumulates in murine MPS IIIA brain, spleen and liver homogenates with concentrations increasing from 40-fold normal (newborn animals) to approximately 170-fold normal (10- to 15-wk-old) in the mixed strain, and approximately 110-fold (from 13-wks of age) in the congenic strain (Crawley *et al*, 2006a; King *et al*, 2006). Elevated HNS-UA is also present in MPS IIIA mouse brains *in utero* (Dr Rowani Mohd Rawi, LDRU, unpublished results).

1.7.5. MPS IIIA Mouse Histopathology

The progressive nature of substrate accumulation in the MPS IIIA mouse can also be observed histologically. Elevated HS immunoreactivity has been observed in the amygdala, septal nucleus, piriform cortex and layer V of the cerebral cortex (McGlynn *et al*, 2004). Similarly, the secondary storage of cholesterol, non-specific autofluorescent material and G_{M2} and G_{M3} gangliosides is also seen, particularly in piriform and retrosplenial cortices, hippocampus, amygdala and cerebellar Purkinje neurons (McGlynn *et al*, 2004; Crawley *et al*, 2006a). Axonal spheroid–like structures containing ubiquitin-positive lesions are prominent in the superior and inferior colliculi, brainstem and periaqueductal grey matter of MPS IIIA mice (Savas *et al*, 2004; Crawley *et al*, 2006a; Hemsley *et al*, 2007). Greater numbers of Glial Fibrillary Acidic Protein (GFAP)-positive glial cells are observed throughout the cerebral cortex (Savas *et al*, 2004).

When examined at the ultrastructural level, MPS IIIA mice have very similar CNS pathology to human MPS IIIA patients (Bhaumik *et al*, 1999; Gliddon and Hopwood, 2004; Savas *et al*, 2004; Crawley *et al*, 2006a; Hemsley *et al*, 2007). The number of neurons containing lysosomal inclusions, as well as the total number of inclusions, gradually increases as the disease progresses (Crawley *et al*, 2006a). Cortical neurons display cytoplasmic membrane-bound vacuoles filled with granular material, which appear as concentric lamellar bodies or whorl-like structures (McGlynn *et al*, 2004; Savas *et al*, 2004; Crawley *et al*, 2006a; Hemsley *et al*, 2007) (**Fig. 1.5**). Axonal spheroid formation within the cerebral cortex is
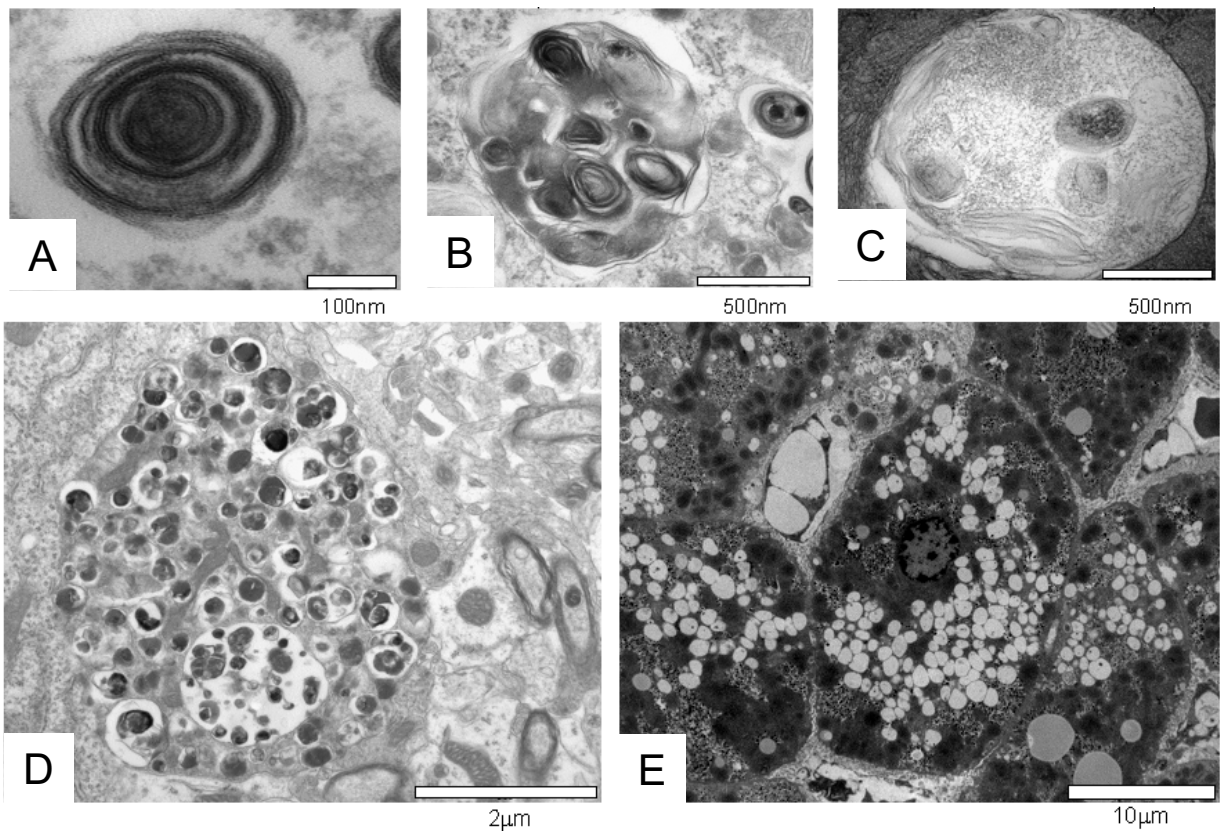
Figure 1.5: Ultrastructural features in MPS IIIA mice. (A, B, D) Cerebral cortical neurons (6-months-old MPS IIIA mouse) and **(C)** cerebellar Purkinje neurons (6-wk-old MPS IIIA mouse) display numerous electron-dense cytoplasmic inclusions, including **(A)** membraneous whorls, **(B)** multi-vesicular bodies and **(C)** granular storage material within vacuoles. Also presented is an electron micrograph of **(D)** an axonal spheroid in the cerebral cortex and **(E)** a liver hepatocyte containing electron-lucent vesicles. Figure adapted from Crawley *et al*, 2006a.

occasionally observed (Savas *et al*, 2004; Crawley *et al*, 2006a; Hemsley *et al*, 2007). In contrast, the inclusions found within cerebellar Purkinje neurons are more heterogenous, with granular, closely-packed, flocculant material observed, as well as lamellated structures such as zebra bodies, whorls and stacks (Savas *et al*, 2004; Crawley *et al*, 2006a).

1.8. Experimental Approaches for Treating Neurological LSD

ERT and BMT are the most commonly employed therapeutic approaches for ameliorating disease in LSD patients at present. However, the intravenous delivery of recombinant enzyme has not had a significant impact on the progression of CNS deficits at the doses currently employed (although recent studies in animal models suggest that high-dose ERT may have some effect on CNS storage) (Dunder *et al*, 2000; Vogler *et al*, 2005; Crawley *et al*, 2006b; Dickson *et al*, 2006). BMT is considered ineffective for Sanfilippo patients and carries a considerable risk of mortality and morbidity (Vellodi *et al*, 1992; Hoogerbrugge *et al*, 1995; Shapiro *et al*, 1995; Sivakumur and Wraith, 1999; Lange *et al*, 2006). Consequently, a concerted research effort is being directed at rectifying this situation and several of the existing and experimental therapies that are under evaluation in humans or animal models of LSD (with a particular focus on MPS IIIA) will be discussed.

1.8.1. Bone Marrow Transplantation and Cell-Mediated Therapies

Bone Marrow and Cell Transplantation - A Historical Perspective

As discussed in **Section 1.2**, the early demonstration by Fratantoni *et al* (1968; 1969) that metabolic storage in MPS I and MPS II cells could be treated by "corrective factors" secreted by neighbouring cells provided the first evidence that LSD may be amenable to treatment if normal enzyme could be supplied to the affected cells. Soon after, attempts at enzyme replacement via normal human plasma infusions in MPS I and MPS II patients mediated transitory reductions in urinary GAG but were unable to sustain metabolic correction due to insufficient concentrations of enzyme (Di Ferrante *et al*, 1971). Transplantation of normal leucocytes (Knudson *et al*, 1971) or skin fibroblasts (Dean *et al*, 1975; 1976; 1979; Gibbs *et al*, 1983) as sources of enzyme also provided temporary biochemical stabilisation or clinical improvement in MPS patients until immune responses limited the effectiveness of this mode of treatment. Enzyme replacement has been undertaken using human amnion membranes from foetal tissues in 19 MPS I, II or III patients (Muenzer *et al*, 1992). These implants were expected to be less immunogenic due to the absence of

human leucocyte-associated antigen expression. However, this strategy was not therapeutically useful due to immune reactions against the implanted tissues.

In the early 1980s, several research groups considered BMT as a method of delivering enzyme to affected cells. The rationale behind this strategy is two-fold: (1) the normal cells can repopulate the marrow compartment and secrete enzyme, thereby correcting nearby cells; and (2) metabolically-competent haematopoietic precursor stem cells can differentiate into monocyte/macrophage cells and be distributed throughout the body via the circulatory system, thus improving the spread of treatment. Dramatic improvements in the visceral pathology, enzymatic activity and GAG were observed in the first MPS patient (a Hurler patient) to undergo this procedure (Hobbs *et al*, 1981; 1982). This was followed by numerous reports of BMT in LSD patients and animal models with varying degrees of long-term clinical success (Hoogerbrugge *et al*, 1995; Neufeld and Muenzer, 2001).

Bone Marrow Transplantation

Whilst BMT is relatively effective in several LSD (e.g. MPS I, MPS VI, non-neuronopathic Gaucher disease, metachromatic leukodystrophy, Krabbe disease) (reviewed in Malatack *et al*, 2003), this procedure also carries considerable risks and drawbacks. Firstly, the mortality rate has been reported to be approximately 10% using human leucocyte-associated-identical donors or 20-25% if the marrow is mismatched (Hoogerbrugge *et al*, 1995). Secondly, patients may experience severe side-effects from the immunosuppressive agents and graft-versus-host disease (Hoogerbrugge *et al*, 1995). However, recent experiments in MPS VII mice have demonstrated that donor cells delivered in the neonatal period can successfully engraft after anti-CD40L and CTLA-4Ig costimulatory blockade in the absence of myeloablation, potentially circumventing the need for toxic, life-long, immunosuppressive regimes (Soper *et al*, 2003; Lessard *et al*, 2006). Thirdly, if a human leucocyte-associated-matched donor is unavailable, there may be potential delays in finding suitably-matched tissue which is undesirable due to the progressive nature of LSD. This is particularly emphasised in studies where improved clinical outcomes were obtained when transplanting asymptomatic Krabbe infants with umbilical cord blood cells, compared to children who received transplants when symptoms had already appeared, suggesting that treatment should be initiated as soon as possible after diagnosis (Escolar *et al*, 2005).

BMT can reduce, delay or prevent neuropathology in several animal models of neurodegenerative LSD, including α-mannosidosis cats, MPS I and fucosidosis dogs, and mice with MPS VII, Krabbe or Sandhoff diseases (Shull *et al*, 1987; Hoogerbrugge *et al*,

1988; Birkenmeier *et al*, 1991; Taylor *et al*, 1992; Bastedo *et al*, 1994; Walkley *et al*, 1994; Norflus *et al*, 1998). However, BMT is not recommended as a therapy for Sanfilippo patients due to its limited efficacy in altering the course of neurological degeneration for reasons that are, at present, unknown (Vellodi *et al*, 1992; Hoogerbrugge *et al*, 1995; Shapiro *et al*, 1995; Sivakumur and Wraith, 1999; Lange *et al*, 2006). Allogeneic cord blood transplantations have also been performed in 69 LSD patients, including 10 with Sanfilippo, with a 1-year survival rate of 72% (Martin *et al*, 2006). However, no data are available at present on the therapeutic efficacy of this treatment (Martin *et al*, 2006).

Cell Therapy

Other cell types are also being considered as vehicles for enzyme delivery. Cell-mediated therapy is directed at implanting a reservoir of cells (possibly genetically-modified to over-express lysosomal enzyme) into the affected tissue whereby the transplanted cells can engraft, migrate and act as a vehicle for enzyme production. Embryonic stem cells, which are capable of being cultured indefinitely and can potentially differentiate to any cell type due to their pluripotent nature, and adult stem cells, which are more lineage-restricted, have the potential to integrate seamlessly into the host tissue (reviewed in Singec *et al*, 2007). However, if the cell types are not terminally-differentiated, teratoma (tumour) formation may result, and continuous immunosuppression may be essential for preventing immunological responses against the transplanted cells (reviewed in Singec *et al*, 2007).

Cell-mediated therapy has been successfully employed by Snyder and colleagues (1995) to improve the amount of enzyme in newborn MPS VII mouse brains after ventricular implantation of immortalised neural progenitor cells over-expressing β-glucuronidase enzyme. More recently, histological and behavioural improvements, as measured using a novel object recognition test, were demonstrated in neonatal MPS VII mice receiving ventricular injections of green fluorescent protein (GFP)-expressing murine foetal neural stem cells (Fukuhara *et al*, 2006). Similarly, oligodendroglial progenitor cell therapy administered to neonates mediated reductions in sulphatide storage and improved motor function in metachromatic leukodystrophy mice (Givogri *et al*, 2006). In MPS IIIA, murine embryonic stem cells over-expressing rhNS have been generated for the treatment of MPS IIIA (Lau *et al*, 2004; Robinson *et al*, 2006) and are able to engraft and survive up to 6-months post-injection in unaffected and MPS IIIA mice (Robinson *et al*, 2006).

Intravenous delivery of human umbilical cord blood cells to pregnant MPS IIIB mice has also been attempted with the transplanted cells able to migrate across the placenta and

engraft in many embryonic organs at 1-wk post-delivery (Garbuzova-Davis *et al*, 2006). This prenatal treatment restored α-*N*-acetylglucosaminidase activity to heterozygote concentrations, in part due to the pluripotent nature of the haematopoietic progenitor cells within the cord blood cells (Garbuzova-Davis *et al*, 2006).

Encapsulated non-neural cells have also been explored as cellular reservoirs of lysosomal enzyme as they may better evade immunogenic responses. Urinary GAG decreased in MPS II (Friso *et al*, 2005) and MPS VII mice (Ross *et al*, 2000) after the intraperitoneal implantation of encapsulated myoblasts or fibroblasts, respectively. However, studies in a larger animal model, the MPS I dog, failed to correct neurological lesions when encapsulated Madin-Darby canine kidney (DK) cells over-expressing α-L-iduronidase were implanted in the cerebral ventricles (Barsoum *et al*, 2003).

Many other studies have also been performed where cells have been genetically-modified using various gene therapy vectors. These cells have been implanted into various brain regions and resulted in improved lysosomal enzyme activities (Wolfe *et al*, 1992; Kosuga *et al*, 2000; 2001; Serguera *et al*, 2001; Buchet *et al*, 2002; Meng *et al*, 2003; Eto *et al*, 2004; Sakurai *et al*, 2004). Gene therapy in LSD will be discussed in more detail in due course (**Section 1.8.5** and subsections therein).

1.8.2. Enzyme Replacement Therapy

Replacement of the deficient lysosomal enzyme was proposed as an effective means of correcting lysosomal storage. However, sufficient quantities of lysosomal enzymes could not be produced until the advent of recombinant DNA technology in the mid-1990s. ERT supplies the deficient enzyme by repeated intravenous infusions of enzyme produced by recombinant technologies on a weekly or fortnightly basis.

Several ERT treatments have been approved for use in LSD, where the primary disease pathology is in the peripheral organs, and phase I/II clinical trials are planned for metachromatic leukodystrophy (discussed in Sevin *et al*, 2007). The first ERT to be approved for clinical use was for the non-neuronopathic form of Gaucher disease (type I) in 1991 (β-glucosidase; Ceredase[®] and Cerezyme[®], Genzyme Corp) (Barton *et al*, 1991; Grabowski *et al*, 1995). The effect of ERT in Gaucher patients with neurological presentation (types II and III) is still uncertain. Several groups report stabilisation or improvement in cognitive function after ERT at high doses (120-480 U/kg of body weight every 4-wks) (Schiffmann *et al*, 1997;

Altarescu *et al*, 2001), whilst others have not observed any benefit on CNS function (60 U/kg every 2-wks followed by 30 U/kg each wk) (Prows *et al*, 1997).

ERT is also commercially available for Fabry disease (α-galactosidase A; Replagal[TM], Shire Human Genetic Therapies; Fabrazyme[®], Genzyme Corp) (Eng *et al*, 2001; Schiffmann *et al*, 2001), Pompe disease (α-glucosidase; Myozyme[®], Genzyme Corp) (Kishnani *et al*, 2007) and MPS VI (*N*-acetylgalactosamine-4-sulphatase; Naglazyme[®], BioMarin Pharmaceutical Inc.) (Harmatz *et al*, 2006), and for the non-neuropathic forms of MPS I (α-L-iduronidase; Aldurazyme[®], BioMarin Pharmaceutical Inc. and Genzyme Corp joint venture) (Wraith *et al*, 2004) and MPS II (iduronate-2-sulphatase; Elaprase[TM], Shire Human Genetic Therapies) (Muenzer *et al*, 2006). At present, the effect of Aldurazyme[®] administered into the cerebrospinal fluid has only been reported in one MPS I patient, with normalised cerebrospinal fluid GAG found after treatment via lumbar puncture on a monthly basis for 4 doses (Munoz *et al*, 2006). Aldurazyme[®] is also being used to pre-treat neuronopathic MPS I patients prior to undergoing BMT in an attempt to improve the general clinical condition pre-transplant and thus reduce the transplantation-related morbidity and mortality outcomes (Cox-Brinkman *et al*, 2006).

ERT for Neurological LSD, including MPS IIIA

While intravenous enzyme infusions are capable of effectively treating visceral and somatic pathology, the presence of the blood-brain barrier (BBB) is thought to hinder the efficient entry of recombinant enzyme from the blood into the CNS. In addition, infused enzyme does not readily penetrate joints and therefore cartilage tissue.

In a study by Vogler and co-workers (1999), ERT ameliorated the neurological deficits in MPS VII mice when recombinant β-glucuronidase was administered at birth, but not when therapy began after 2-wks of age. These results were confirmed in the MPS IIIA mouse model where intravenous injection of rhNS delivered weekly from birth, but not from 6-wks of age, delayed the development of CNS pathology when assessed by electron microscopy and a behavioural test of memory and learning, the Morris Water Maze (Gliddon and Hopwood, 2004). Subsequent studies with radio-labelled β-glucuronidase in MPS VII mice at various ages up to 7-wks demonstrated that neonatal mice responded to ERT due to the transport of phosphorylated lysosomal enzyme across the BBB into the brain parenchyma via a M6P/insulin-like growth factor II receptor transport mechanism, which is considerably down-regulated during development (Urayama *et al*, 2004).

However, recent studies have demonstrated that if recombinant lysosomal enzyme is delivered intravenously at very high concentrations (10 mg/kg x 8 doses in aspartylglycosaminuria mice; 4 mg/kg x 13 doses or 20 mg/kg x 4 doses in MPS VII mice; 10 mg/kg x 1 dose in α-mannosidosis guinea pigs; or 2 mg/kg x 11-13 doses in MPS I dogs), the enzyme can enter the brain parenchyma and significantly reduce stored substrate (Dunder *et al*, 2000; Vogler *et al*, 2005; Crawley *et al*, 2006b; Dickson *et al*, 2006). These results may have important implications for treating CNS pathology in neurological LSD should similar improvements be observed in long-term animal studies and in humans.

Increased lysosomal enzyme activity and reduced GAG in brain tissues can be also be achieved after delivery of recombinant lysosomal enzymes to the cerebrospinal fluid in MPS IIIA mice or MPS I and MPS IIIA dogs (Kakkis *et al*, 2004; Hemsley *et al*, 2006; Dickson *et al*, 2007; Hemsley *et al*, 2007). Given its invasive nature, intra-cerebrospinal fluid delivery of recombinant enzyme may provide an interim therapy for patients with neurological LSD.

1.8.3. Drug Therapy

Alternative treatments using small molecule drugs are also under investigation for therapeutic efficacy in neurological LSD. These compounds reduce the substrate load (referred to as substrate reduction, substrate deprivation or substrate inhibition therapy) or improve the residual enzyme activity of lysosomal enzymes. The primary advantages of these therapies are that they can be administered orally, which may improve patient compliance, are low cost in comparison to ERT, and as these compounds are small molecules they can potentially cross the BBB after peripheral delivery to treat neuropathology (Lachmann *et al*, 2004). The reduced disease burden from substrate reduction therapy, coupled with the increases in residual enzyme activity, may result in a more attenuated phenotype in affected individuals (Hopwood and Morris, 1990). However, it should be noted that whilst persistent, low concentrations of β-glucuronidase activity (<5% wild-type) are sufficient to improve several biochemical and histological changes in MPS VII mice, improvements in clinical outcomes may require higher amounts of enzyme activity (Donsante *et al*, 2007).

Substrate Reduction Therapy

In substrate reduction therapy, the substrate burden is reduced by the inhibition of substrate synthesis by chemical agents. Whereas ERT is aimed at increasing the amount of active enzyme available to metabolise accumulated substrates, the rationale behind substrate

reduction therapy is to prevent the build-up of substrate in the first instance. This treatment may have the most benefit when used in combination with a second therapy such as ERT or BMT (Jeyakumar *et al*, 2001).

Miglustat (Zavesca®, Actelion Pharmaceuticals; *N*-butyldeoxynojirimycin, *N*B-DNJ) is a glucose analogue and is commercially available as a substrate reduction therapy for Gaucher type I patients. In these patients, intravenous administration of *N*B-DNJ reduces liver and spleen sizes (Cox *et al*, 2000; Elstein *et al*, 2004) as well as improving haemoglobin and platelet counts (Giraldo *et al*, 2006). Miglustat has also been effective in reducing glycosphingolipid storage in B lymphocytes isolated from a Niemann Pick disease (type C) patient and could be detected in cerebrospinal fluid after 7-months of administration (Lachmann *et al*, 2004). Miglustat acts by inhibiting the first enzyme in glucocerebroside synthesis, glucosylceramide synthase (ceramide glucosyltransferase). Consequently, Miglustat can potentially be used to treat lysosomal glycosphingolipid disorders where glucoceramide-based components are not degraded (e.g. Gaucher, Fabry, Tay-Sachs, Sandhoff, Niemann-Pick diseases and G_{M1} gangliosidosis). In addition, Miglustat may also be beneficial in diseases such as MPS IIIA where there is secondary accumulation of glycosphingolipids, to reduce the overall disease burden. After 4- or 36-wks of administering 1200 mg/kg/day *N*B-DNJ to juvenile (4-wk-old) MPS IIIA mice, marked reductions in immunocytochemical-positive staining of G_{M2} and G_{M3} gangliosides, as well as reduced autofluorescence, were observed in treated MPS IIIA brains (Walkley, 2005).

However, side-effects, including body weight loss and gastrointestinal problems, have also been reported after *N*B-DNJ administration (Andersson *et al*, 2004; Giraldo *et al*, 2006). A more selective glycosphingolipid inhibitor, the galactose analogue *N*-butyldeoxygalactonojirimycin (*N*B-DGJ), has shown promise in Sandhoff disease mice with improvements in life expectancy, delay in the onset of disease symptoms (hind limb strength and coordination) and reduction of G_{M2} and G_{A2} storage in brain homogenates, without the side-effects observed with *N*B-DNJ administration (Andersson *et al*, 2004). *N*B-DGJ is also effective in G_{M1} gangliosidosis mice, mediating significant reductions in the total ganglioside and G_{M1} ganglioside content in brain tissues when administered in both the neonatal and postnatal periods (Kasperzyk *et al*, 2004; 2005).

Rhodamine B, a non-specific inhibitor of GAG synthesis, reduces the total GAG content in MPS II, IIIA and VI fibroblasts, and decreases urinary and liver GAG content after continuous intravenous delivery to MPS IIIA mice (Roberts *et al*, 2006). No data on the effect of rhodamine B on GAG within the brain are available at present.

Genistein (4',5,7-trihydroxyisoflavone or 5,7-dihydroxy-3-(4-hydroxyphenyl)-4H-1-benzopyran-4-one), is an isoflavone which inhibits specific GAG synthetases (Piotrowska *et al*, 2006). MPS I, II, IIIA and IIIB fibroblasts all respond to genistein treatment with near-normalisation of GAG following 6-days of treatment (Piotrowska *et al*, 2006). Ultrastructural analysis of genistein-treated MPS I fibroblasts corroborated this finding, with quantitative reductions in the number of inclusions compared to untreated MPS I control cells (Piotrowska *et al*, 2006). On the basis of these *in vitro* results, a pilot, open-label study in 20 MPS IIIA and MPS IIIB patients has been initiated (Wegrzyn *et al*, 2006).

Enzyme Enhancement Therapy

Enzyme enhancement therapy uses small molecular chaperones (e.g. DNJ, 1-deoxynojirimycin, and derivatives) to aid in the correct folding and stabilisation of unstable mutant proteins by acting as competitive inhibitors and binding to the mutant protein in the endoplasmic reticulum (where proof-reading mechanisms have been shown to degrade most mutant proteins), thus allowing greater amounts of the mutant protein with residual activity to be transported to the *trans*-Golgi network and ultimately the lysosome. Enzyme enhancement therapy is likely to be particularly beneficial in patients with small in-frame mutations and residual enzyme activity. For MPS IIIA, approximately 74% of patients have missense mutations and may be treated by this form of therapy, with the most common of these mutations (R456H, R245H and S66W) accounting for 43%, 41% and 11% of mutant alleles, respectively, in Australian populations (Yogalingam and Hopwood, 2001). The pharmacological chaperones for this form of therapy are usually monomeric substrate analogues. Other drugs may also improve the residual activity by allowing the translation or read-through of proteins with premature stop-codon mutations. The latter principle has been demonstrated with gentamicin dosing of MPS I fibroblasts (Keeling and Bedwell, 2002; Hein *et al*, 2004) and in a cystic fibrosis mouse model (Du *et al*, 2002b).

Limited success has been achieved to date with oral administration of a galactose-derivative, N-octyl-4-epi-beta-valienamine, as an enzyme enhancement therapy in G_{M1}-gangliosidosis mice (Matsuda *et al*, 2003). This transgenic knockout mouse model expresses human mutant R201C β-galactosidase protein and, after treatment, showed improved enzyme activity in peripheral organs (and to a lesser extent in the cerebrum and cerebellum) and reduced immuno-stained G_{M1} and G_{A1} substrate concentrations in the fronto-temporal cerebral cortex and brainstem (Matsuda *et al*, 2003).

In addition to their ability to inhibit substrate synthesis, DNJ and four derivative compounds have also been tested for their efficacy as chemical chaperones in Pompe fibroblasts (Okumiya *et al*, 2007). *N*B-DGJ (Miglustat) was the most effective compound at restoring α-glucosidase activity up to 15-20% of normal in two cell lines homozygous for Y445F and P545L, but was ineffective in cells containing the mutations 525del/R600C and D645E/R854X (Okumiya *et al*, 2007). *N*B-DGJ has also been used as a molecular chaperone in Gaucher disease with increases in β-glucosidase activity reported in 4 of 8 mutations assessed (Alfonso *et al*, 2005). These two examples demonstrate one of the complications of enzyme enhancement therapy, namely that the same compound can inhibit multiple lysosomal enzymes, and consequently careful dosing and toxicity studies are necessary.

1.8.5. Gene Therapy

Gene therapy is defined as the transfer of nucleic acids into cells for a therapeutic purpose. The nucleic acids are usually (a) DNA encoding a functional copy of a gene for patients whose own gene copy contains mutations, (b) anti-sense oligonucleotides for autosomal-dominant disorders or (c) genes encoding neuroprotective molecules to delay the loss of affected cells when the molecular basis of the disease has yet to be identified (reviewed in Karpati *et al*, 1996). The genes can be introduced using viral or non-viral modalities either *ex vivo*, where a patient's cells are removed, genetically-modified and then returned to the same patient, or *in vivo* where the gene transfer occurs directly within the patient. There are many classes of viral vectors, each with their own strengths and disadvantages (**Table 1.3**). It is unlikely that there will be one 'perfect' viral vector for all diseases. Rather, the most appropriate vector will be selected on criteria specific for each individual disorder.

Table 1.3: Comparison of Most Commonly Employed Viral Vectors.

NOTE: This table is included on page 29 of the print copy of the thesis held in the University of Adelaide Library.

Adapted from Thomas *et al*, 2003.

Clinical Trials - Successes and Challenges

Since the first human gene therapy trial in 1989 in patients with advanced melanoma who were treated with a retroviral vector (Rosenberg *et al*, 1990), more that 1260 clinical trials in humans have been approved world-wide (Edelstein, 2007). Of these, the majority have involved the use of a viral gene therapy vector with cancer being the primary research focus. Human adenoviral (Ad) vectors have re-emerged as a popular choice in clinical trials (26% of total trials), likely due to the use of Ad vectors in cancer research (Edelstein, 2007) and this is reflected in the first commercially approved gene therapy product, Gendicine, a recombinant Ad encoding the human p53 tumour suppressor gene for the treatment of head and neck squamous cell carcinoma (approved in China; November, 2005).

However, in addition to the successes in clinical gene therapy, there have also been many setbacks to the field. In September 1999, Jesse Gelsinger, a partial ornithine transcarbamylase deficiency patient, died after receiving the highest dose of an E1/E4-deleted (ΔE1/E4)-Ad vector encoding ornithine transcarbamylase via direct infusion to the hepatic artery. His death was attributed to an overwhelming inflammatory response leading to intravascular coagulation, acute respiratory distress and eventual multi-organ failure (Raper *et al*, 2003). This was soon followed by reports of 2 of 11 patients developing T-cell leukaemia from a retroviral insertion near the promoter of the LMO2 proto-oncogene in X-linked severe combined immune deficiency (X-SCID) patients, one of whom eventually died (Hacein-Bey-Abina *et al*, 2003a; 2003b; Bester *et al*, 2006). A third child later developed leukaemia with an insertion in the LMO2 region as well as in additional sites (Couzin and Kaiser, 2005). Whilst caution in undertaking gene therapy trials is warranted, it must be noted that of the 16 treated X-SCID patients, 15 displayed clinically significant improvements in immune function for as long as 5-years (Hacein-Bey-Abina *et al*, 2002; Fischer *et al*, 2005; Schmidt *et al*, 2005), and 4 of 4 adenosine deaminase-deficient-SCID patients showed correction of immunodeficiencies (Aiuti *et al*, 2002; Fischer *et al*, 2005).

Gene Therapy in LSD

LSD are ideal candidates for gene therapy as they are generally single gene disorders, the molecular basis of each disease is well understood, the pathophysiology has been extensively characterised and small and large animal models are available to assess safety and therapeutic efficacy of gene transfer (extensively reviewed in Ellinwood *et al*, 2004; Sands and Davidson, 2006). In addition, the ability of lysosomal enzymes to undergo anterograde (Chen *et al*, 2006) and retrograde axonal transport (Passini *et al*, 2002), trans-synaptic transfer

(Hennig *et al*, 2003), diffusion from the site of injection and to be targeted to the lysosome by M6P receptor-mediated endocytosis may indicate that only a small fraction of transduced cells may potentially distribute enzyme to widespread areas in the CNS. Small increases in lysosomal enzyme activity may be sufficient to normalise the clinical phenotype of affected individuals and this is most clearly demonstrated in a MPS IIIA patient who had approximately 50% of normal NS specific activity and exhibited an attenuated phenotype and relatively mild symptoms at 40-years of age (Perkins *et al*, 2001). It should be noted, however, that low-level, persistent expression of <5% of normal β-glucuronidase activity in MPS VII mice using an adeno-associated viral (AAV) vector has shown that whilst histopathological and biochemical deficits can be normalised, this degree of activity is insufficient to mediate significant clinical improvements in the correction of bone dysplasia, auditory function or reproductive capacity (Donsante *et al*, 2007).

Several human gene therapy clinical trials have been approved for LSD or are in progress (Edelstein, 2007). These include *ex vivo* retroviral/lentiviral gene therapy in MPS I (trial IDs FR-005, UK-011, UK-043), MPS II (US087), Gaucher disease (US-046, US-047, US-061), Fabry disease (US-377) and MPS VII (US-758) (Edelstein, 2007). Other approved human trials include the direct intracranial injection of the viral vector particles into patients with Canavan disease (Ad, US-211; AAV US-381) (McPhee *et al*, 2006) and late infantile neuronal ceroid lipofuscinosis (AAV US-619) (Crystal *et al*, 2004; Edelstein, 2007).

1.8.5.1. Non-Viral Gene Therapy

Non-viral or synthetic gene transfer technologies rely on the delivery of naked DNA, plasmid DNA complexed to polymers ("polyplexes"), lipids ("lipoplexes"), a combination of lipids and polymers ("lipopolyplexes"), or liposome-encapsulated DNA to the target cell. Synthetic vectors may be introduced into the host cell by a variety of methods including electroporation, lipofection, microinjection, biolistic particle delivery, high-frequency ultrasound, or using "pseudo-viruses" based on the simian virus 40 or the human papillomavirus as shuttle vectors (reviewed in Luo and Saltzman, 2000; Wells, 2004; Jackson *et al*, 2006).

Non-viral vectors are cost-effective to produce and, most importantly, have an increased safety profile due to reduced immunogenicity. The main limitation of synthetic vectors is the low transfection efficiency and resultant short-lived transgene expression usually caused by the episomal expression. However, recent *in vivo* studies by Ehrhardt and

colleagues (2005), using an integrase fC31 derived from a *Streptomyces* phage or the Sleeping Beauty transposase, demonstrated high transgene expression and genome persistence for greater than 150-days, even after a partial hepatectomy.

The application of non-viral agents in LSD animal models has had limited success. In MPS IIIA, small interference RNA therapy against the *EXT1* gene from the exostosin gene family is able to partially inhibit the formation of HS synthesis at the mRNA level (de Pablo *et al*, 2006). Glycosphingolipid globotriaosylceramide storage is significantly reduced in some, but not all, peripheral organs when cationic lipid-complexed plasmid DNA was administered to immunosuppressed Fabry mice pre-treated with an anti-inflammatory agent (Przybylska *et al*, 2004). Likewise, modest increases in α-L-iduronidase activity and reductions in GAG were observed in the spleens and livers of MPS I mice after intraperitoneal or hydrodynamic injection of a non-viral vector encoding α-L-iduronidase (Camassola *et al*, 2005). The greatest therapeutic benefit using synthetic vectors in a LSD model has been demonstrated by Yamaguchi *et al* (2003) where up to 35% of normal hexosaminidase activity was able to mediate a 60-70% reduction in storage in the visceral organs of Sandhoff mice receiving intravenous co-administration of plasmid DNA vectors encoding the α or β subunit of hexosaminidase.

As stated previously, synthetic vectors have historically displayed short-lived transgene expression and inefficient gene transfer and consequently many researchers have investigated various viral vector delivery systems that are highly efficient at gene transfer. The majority of gene therapy studies have been conducted with derivatives of retroviral/lentiviral, AAV or Ad vectors and these will now be reviewed.

1.8.5.2. Retroviral Gene Therapy

The *Retroviridae* family of viruses are enveloped, single-stranded RNA viruses that replicate by forming a DNA intermediate. In general, wild-type retroviruses cause relatively benign infections, although this group also includes acute transforming viruses (tumour formation) and the pathogenic human immunodeficiency virus (acquired immunodeficiency syndrome, AIDS). Retroviruses are divided into simple (e.g. murine leukaemia virus) and complex (e.g. lentivirus including human immunodeficiency virus-1) types and both forms have been employed as viral vectors (Goff, 2001). Murine leukaemia virus-based vectors exclusively transduce dividing cells, whereas lentiviral vectors can transduce both dividing and non-dividing, terminally differentiated cells (Goff, 2001).

The lack of immunogenicity and stable transgene expression due to the integrative nature of retroviral vectors makes them ideal for the treatment of monogenetic LSD where transgene expression is required for the patient's lifetime (reviewed by Biffi and Naldini, 2005). However, as previously mentioned, these integrative properties may also cause insertional leukaemia if the recombination event occurs near a proto-oncogene, as was the case in the X-SCID children treated with a retroviral vector expressing the common γ-chain of the interleukin (IL)-2 receptor (Hacein-Bey-Abina et al, 2003a; 2003b; Couzin and Kaiser, 2005; Bester et al, 2006). This is unsurprising given that many viral copies (10^7-10^{10} particles) are usually administered and random vector insertion into the host genome is expected to occur at a frequency of 1:300,000, thus increasing the likelihood that insertional events in any particular gene (including oncogenes) may occur several times (reviewed by Baum et al, 2006). A high incidence of hepatocellular carcinoma has been observed after lentiviral administration in foetal and neonatal mice (Themis et al, 2005; 2006). Additional issues that may limit the application of retroviral vectors are relatively low vector particle yields (1 x 10^6 - 1.4 x 10^7 infectious units/mL) and small transgene capacity (approximately 8 kb).

Ex $vivo$ and direct in $vivo$ transfer of retroviral vectors has been assessed in rodent models of MPS I (e.g. Zheng et al, 2003; Di Domenico et al, 2005; Jordan et al, 2005; Kobayashi et al, 2005; Liu et al, 2005b; Chung et al, 2007; Ma et al, 2007), MPS IIIA (Anson et al, 2007), MPS IIIB (e.g. Zheng et al, 2004; Di Natale et al, 2005) and MPS VII (e.g. Taylor and Wolfe, 1997; Bosch et al, 2000b; Brooks et al, 2002; Buchet et al, 2002; Xu et al, 2002; Meng et al, 2003; Hofling et al, 2004; Sakurai et al, 2004; Liu et al, 2007). A lentiviral vector encoding murine NS has been delivered intravenously to adult MPS IIIA mice after the administration of hyperosmotic mannitol in an attempt to treat CNS pathology by temporarily opening the BBB (Anson et al, 2007). Partial reductions in the urinary GAG content were observed in treated animals, however, the effect of gene therapy on CNS pathology was not discussed.

In addition, the safety and efficacy of retroviral gene transfer has been assessed in a number of large animal models including MPS I dogs (e.g. Shull et al, 1996; Lutzko et al, 1999; Meertens et al, 2002), MPS I cats (Ponder et al, 2006), MPS VI cats (Simonaro et al, 1999; Yogalingam et al, 1999) and MPS VII dogs (e.g. Ponder et al, 2002; Mango et al, 2004; Sleeper et al, 2004; Wang et al, 2006). MPS I puppies intravenously treated with an amphotropic retrovirus within 3-days of birth generate 6% of normal β-glucuronidase activity within the brain (Wang et al, 2006). In addition, retroviral administration markedly improved

the pathological manifestations of the disease, with near normalisation of sulphated GAG and reductions in lysosomal storage observed in somatic organs and the brain after 6- to 7-months of treatment (Wang *et al*, 2006). Four retroviral-treated MPS VII dogs were reported to be in good health without adverse events 5-years after treatment, indicating that this has the potential to be a long-term therapy for MPS VII patients (Ponder and Haskins, 2006).

On the other hand, in a similar study, neonatal MPS I cats intravenously treated with retroviral vectors generated a cytotoxic T lymphocyte (CTL) response against the transduced cells (Ponder *et al*, 2006). This effect was ameliorated by transient immunosuppression with CTLA4-Ig, resulting in supra-physiological α-L-iduronidase activity for at least 10-months after treatment (Ponder *et al*, 2006). In contrast, neonatal MPS I dogs receiving retroviral treatment did not generate a CTL response and displayed stable serum enzyme activity (Ponder *et al*, 2006). Whilst a species-dependent response is a possibility, whether tolerance or CTL responses are induced is potentially a function of the amount of retroviral-mediated enzyme expression, since MPS I mice expressing low α-L-iduronidase activity developed a CTL response whilst MPS I animals displaying high α-L-iduronidase activity did not exhibit CTL activity (Ponder *et al*, 2006).

1.8.5.3. Adeno-Associated Viral Gene Therapy

AAV are non-enveloped, single-stranded DNA viruses containing a 4.7 kb genome flanked by two inverted terminal repeat regions. Evidence collected to date suggests that AAV do not appear to cause pathogenic disease in humans and can only replicate in the presence of a helper virus (reviewed in Zolotukhin, 2005). At least 11 AAV serotypes have been developed as vectors (reviewed in Wu *et al*, 2006) and display serotype-dependent transduction efficiencies and cellular tropism (Burger *et al*, 2004). AAV vectors, except those in which the *rep* genes are deleted, persist episomally and are also capable of semi-random integration in the host genome at specific sites, such as in human chromosome 19, at a relatively high incidence of 0.1% per infectious genome (reviewed by Baum *et al*, 2006). This feature, combined with a low inflammatory potential due to the absence of all viral protein except the inverted terminal repeat regions (Pfeifer and Verma, 2001), results in long-term (at least 1-year post-injection) transgene expression after AAV vector delivery (reviewed in McCown, 2005). If necessary, AAV vectors may be re-administered a second time without inducing humoral immune responses in rodents (Mastakov *et al*, 2002). The greatest limitation to clinical gene therapy with AAV vectors may be the high incidence (96%) of pre-

existing AAV-specific antibodies found in humans, with 32% of the population harboring AAV-neutralising antibodies (Chirmule *et al*, 1999). In addition, hepatic tumorigenesis has been observed in long-term studies (up to approximately 18-months of age) in newborn MPS VII mice injected via the superficial temporal vein with a recombinant AAV vector (Donsante *et al*, 2001). Whether this will pose a safety risk in humans is yet to be determined.

AAV vectors have been evaluated in a host of MPS animal models in recent years with varying degrees of success. These models include MPS I (e.g. Desmaris *et al*, 2004; Hartung *et al*, 2004; Ciron *et al*, 2006; Watson *et al*, 2006), MPS II (Cardone *et al*, 2006), MPS IIIA (Fraldi *et al*, 2006), MPS IIIB (e.g. Fu, 2002; Cressant *et al*, 2004; Fu *et al*, 2007), MPS VI (Tessitore *et al*, 2006) and MPS VII (e.g. Watson *et al*, 1998; Elliger *et al*, 1999; Skorupa *et al*, 1999; Bosch *et al*, 2000a; Daly *et al*, 2001; Frisella *et al*, 2001; Elliger *et al*, 2002; Heuer *et al*, 2002; Passini *et al*, 2002; Hennig *et al*, 2003; Passini *et al*, 2003; Hennig *et al*, 2004; Sferra *et al*, 2004; Liu *et al*, 2005a; Karolewski and Wolfe, 2006; Liu *et al*, 2007).

In the majority of these studies, widely distributed transgene expression, resulting in reduction or normalisation of lysosomal storage, has been observed when conducted in small rodent models of LSD. Widespread transgene expression throughout the brain is observed for at least 9-months after intraventricular delivery of AAV-2/5 vectors in newborn MPS IIIA mice (Dr Kim Hemsley, LDRU, personal communication). Amelioration of pathological changes, such as reduced storage of G_{M2} ganglioside, a decrease in the number of immuno-reactive microglia and astrocytes, and reductions in the frequency of cells containing vacuoles, were also achieved (Fraldi *et al*, 2006). In addition, significant functional improvements were measured in the memory and spatial learning ability (Morris Water Maze), hind-limb gait and open field activity in treated mice (Fraldi *et al*, 2006).

Notably, Ciron *et al* (2006) have successfully reduced CNS pathology in MPS I dogs following four stereotaxic injections of AAV5.5-hIDUA (4.8 x 10^{11} vector genomes) performed at 3-to 5-months of age. Increased and widespread α-L-iduronidase activity, stable vector genome copy numbers and improvements in neuropathology (less severe vacuolation, reduced GAG and ganglioside storage) were observed in treated MPS I dogs when assessed between 1- and 8-months post-injection (Ciron *et al*, 2006). However, humoral responses were generated against AAV5 (but not α-L-iduronidase), or against both AAV5 and α-L-iduronidase when immunosuppressed with a cyclosporine/mycophenolate mofetil cocktail or cyclosporine, respectively (Ciron *et al*, 2006). Whilst these studies are promising and have demonstrated that widespread gene transfer can be achieved in a larger-sized brain, the humoral responses and subacute encephalitis generated by the treatment highlights some of

the safety issues that will need to be addressed prior to the administration of these vectors to humans (Ciron *et al*, 2006).

1.8.5.4. Adenoviral Gene Therapy

Adenoviral Vectors

More than 50 serotypes of human Ad have been isolated and are capable of being purified in high concentrations exceeding 10^{13} particles/mL, display strong transgene expression and infect both dividing and quiescent cells (Volpers and Kochanek, 2004; Vellinga *et al*, 2005). Ad vectors can also accommodate large sequences (>30 kb), are easy to genetically modify and are maintained as an episome (i.e. they do not integrate into the host genome), which may improve the safety profile of these vectors due to the reduced risk of insertional leukaemia. However, the episomal nature of Ad vectors may also result in short-lived transgene expression, and in several instances these vectors have displayed cytotoxicity or induced immune responses in the host due to the expression of viral genes or capsid structural proteins. The latter will be discussed in more detail with respect to the differences between human and canine Ad vectors in **Sections 1.9** and **1.10**.

First generation Ad vectors are generally based on Ad serotypes 2 or 5 and are generated by removing the E1 region from the wild-type Ad genome and replacing it with the desired transgene sequence (reviewed by Russell, 2000). As the E1 functions are essential for viral replication (discussed in **Section 1.9.1**), these vectors are unable to replicate without the assistance of a trans-complementing cell line that provides the E1 functions *in trans*. In some first-generation Ad vectors, further deletions in the E3 gene are employed to increase the transgene capacity to approximately 8 kb. As many of the other viral genes in these vectors are intact, the low amounts of viral gene transcription may result in a cellular immune response against the transduced cells, resulting in the rapid loss of transgene expression and inflammatory responses (Yang *et al*, 1994). The second-generation of Ad vectors may be additionally deleted in the E2 and/or E4 regions (reviewed in Cregan *et al*, 2000).

The latest generation of Ad vectors are the helper-dependent (HD; also known as gutless or high capacity) Ad vectors, in which all viral genes are removed except for the inverted terminal repeat regions and the packaging signal (Parks *et al*, 1996; Hardy *et al*, 1997). HD Ad vectors can only replicate with the aid of a helper virus and the trans-complementing cell line, which together provide all of the regulatory and structural viral elements *in trans*. Theoretically, these vectors can yield a total transgene capacity of

approximately 37 kb (Parks *et al*, 1996). For the production of these vectors, the helper virus contains two *loxP* recognition sites flanking the packaging signal which, when combined with a trans-complementing cell line expressing the bacteriophage Cre recombinase, is efficiently excised from the helper virus (Parks *et al*, 1996; Hardy *et al*, 1997). Consequently, the helper virus is unable to be packaged (encapsidated) whilst the desired HD Ad vector is preferentially assembled as normal (Parks *et al*, 1996; Hardy *et al*, 1997). The unpackaged, contaminating helper virus and the encapsidated HD Ad vector can then be separated on caesium chloride density gradients and purified by standard procedures (Parks *et al*, 1996).

Adenoviral Gene Therapy in LSD

In early gene transfer studies with first-generation human Ad vectors, high concentrations of lysosomal enzyme activity and concurrent reductions in lysosomal storage were achieved after peripheral administration in mouse models of Pompe (Amalfitano *et al*, 1999; Pauly *et al*, 2001; Ding *et al*, 2002; Martin-Touaux *et al*, 2002; Xu *et al*, 2004), Fabry (Ziegler *et al*, 1999), Tay Sachs (Guidotti *et al*, 1999) and Wolman diseases (Du *et al*, 2002a), as well as in aspartylglucosaminuria (Peltola *et al*, 1998), G_{M1} gangliosidosis (Takaura *et al*, 2003) and MPS VII animals (Ohashi *et al*, 1997; Stein *et al*, 1999). In many of these studies transgene expression in adult mice was transient in the absence of immunosuppressive or immunomodulatory interventions due to vector toxicity from viral gene expression and/or CTL and humoral immune responses. The advent of HD Ad vectors is likely to improve the longevity of transgene expression and reduce the inflammatory reactions associated with Ad vectors (O'Neal *et al*, 2000; Fleury *et al*, 2004; Mian *et al*, 2005).

To treat the neurodegeneration resulting from LSD, first-generation Ad vectors have been directly injected into the adult CNS of aspartylglucosaminuria and MPS VII mice (Ohashi *et al*, 1997; Ghodsi *et al*, 1998; Peltola *et al*, 1998; Stein *et al*, 1999; Virta *et al*, 2006). In MPS VII mice receiving striatal injections of Ad vectors, β-glucuronidase activity was detected for at least 84-days, peaking at 21-days post-injection (Ghodsi *et al*, 1998). In addition, Ad vectors delivered into the cerebrospinal fluid (via the lateral ventricles or the cisterna magna) can also generate elevated enzyme activity in the CNS, although the distribution of transgene is not as extensive as when delivered into the brain parenchyma (Ghodsi *et al*, 1998). The distribution of lysosomal enzyme may be improved by co-injection of the hyper-osmotic agent, mannitol, either in the periphery (Ghodsi *et al*, 1999) or as part of the vector diluent (Bourgoin *et al*, 2003). Most recently, the use of non-viral promoters has improved aspartylglucosaminidase expression, with aspartylglucosaminidase detected via

immunostaining for at least 4-months post-injection in regions connected to the striatal injection site (Virta *et al*, 2006).

Improvements in disease progression have also been observed following the delivery of Ad vectors *in utero* or during the neonatal period in murine models of Niemann Pick C, Krabbe disease, G_{M1} gangliosidosis and MPS VII (Kamata *et al*, 2001; Shen *et al*, 2001a; Kanaji *et al*, 2003; Takaura *et al*, 2003; Eto *et al*, 2004; Shen *et al*, 2004; Paul *et al*, 2005). In MPS VII pups, a single injection of Ad vector into the superficial temporal vein within 24-hrs of birth normalised CNS, skeletal and ocular abnormalities for at least 20-wks (Kamata *et al*, 2003; Kanaji *et al*, 2003). Importantly, β-glucuronidase activity was maintained in visceral organs and in the brain, with 200% and 20-30% of normal activity observed within the brain at 4- and 20-wks post-injection (Kamata *et al*, 2003). Also, if first delivered in the neonatal period, Ad vectors can be re-administered a second time (but not a third time due to the generation of a neutralising antibody response), with rapid increases in enzyme activity following the second injection (Kamata *et al*, 2003).

In an attempt to circumvent the immunogenicity of human Ad vectors in clinical gene therapy, we elected to use an E1-deleted canine adenoviral (ΔE1 CAV-2) vector expressing NS to demonstrate proof-of-concept in MPS IIIA prior to proceeding with the construction of a HD CAV-2 vector. To gain a better understanding of CAV-2 vectors, the structure and biology of wild-type human Ad will first be reviewed before a comparison with CAV-2 vectors is made.

1.9. Wild-type Human Adenovirus

Ad have been extensively characterised since they were first isolated from human adenoid tissue in 1953 (Rowe *et al*, 1953). There at least at least 51 different Ad subtypes which are grouped into 6 classes (groups A to F) and are categorised according to their ability to haemagglutinate red blood cells and the percentage of DNA homology and G+C content (Sarantis *et al*, 2004). Ad infection frequently causes respiratory and gastrointestinal tract infections but may also be associated with fevers, and ocular, urogenital, cardiovascular and CNS disease (Schmitz *et al*, 1983).

1.9.1. Adenovirus Capsid and Genomic Structures

Wild-type human Ad particles are non-enveloped viruses with an icosahedral structure measuring approximately 90 nm in diameter (Davison *et al*, 2003). Each virion consists of an outer capsid shell and an inner protein core. The Ad virion structure has been reviewed extensively using Ad serotypes 2 and 5 as representative viruses (reviewed in Cusack, 2005; Vellinga *et al*, 2005). The outer capsid coat is composed of 252 subunits (capsomers), of which 240 are hexons that form one of the 20 triangular faces of the icosahedron, and 12 are penton bases positioned at each vertex (**Fig. 1.6**) (Stewart *et al*, 1993). Hexon and penton capsomers take their name from the number of adjacent capsomers (6 or 5, respectively). Projecting from each vertex is a trimeric fibre protein consisting of a conserved N-terminal tail that interacts with the penton base, a central shaft of varying lengths depending on the viral serotype and C-terminal globular knob (Stewart *et al*, 1993; van Raaij *et al*, 1999).

Each hexon capsomer is made from three copies of polypeptide II (pII), the most abundant virion component (Stewart *et al*, 1993). Penton capsomers are composed of a pentameric ring of pIII forming the penton base "anchoring point" at each vertex, and a trimer of pIV, which forms the fibre (Stewart *et al*, 1993). As such, these polypeptides (pII, pIII and pIV) are classified as the major proteins whilst the remaining capsid proteins (pIIIa, pVI, pVIII and pIX) are considered minor capsid proteins and may function as "cement" proteins. The four remaining polypeptides - pV, pVII, μ (pX) and the terminal protein - are packaged within the inner core with the viral DNA.

The Ad genome is contained within the core of each particle and is a linear, double-stranded DNA sequence of approximately 30-38 kb in size (**Fig. 1.7**) (Roberts *et al*, 1984). Terminal proteins are covalently-linked to the 5' end of the genome. The genome consists of two inverted terminal repeat sequences that act as the origins of DNA replication and flank the coding region, a cis-acting packaging sequence and one or two virus-associated (VA) genes. The majority of Ad genes are divided into three main groups: early transcription units (E1a, E1b, E2a, E2b, E3, E4), delayed early units (IX and IVa2) and one major late unit (comprising of the L1, L2, L3, L4 and L5 families of mRNA). The early gene transcripts are mostly involved in gene transcription, DNA replication, and inhibition of the immune response and apoptosis by the host cell, whilst the proteins encoded by the late genes are associated with proteolytic trimming and virus assembly.

Figure 1.6: Ad capsid structure. Ad particles are icosahedral in structure and consist of an outer capsid shell and an inner core. The structure of the capsid and cement proteins is well-defined with the outer shell consisting of 252 capsomer subunits (hexons, penton bases and fibres) which are stabilised by the cement proteins (pVIII, pIX, pIIIa and pVI). The Ad genome is contained within the virion core and is covalently-linked to terminal proteins (TP) at the 5' end of each DNA strand. Figure taken from Russell, 2000.
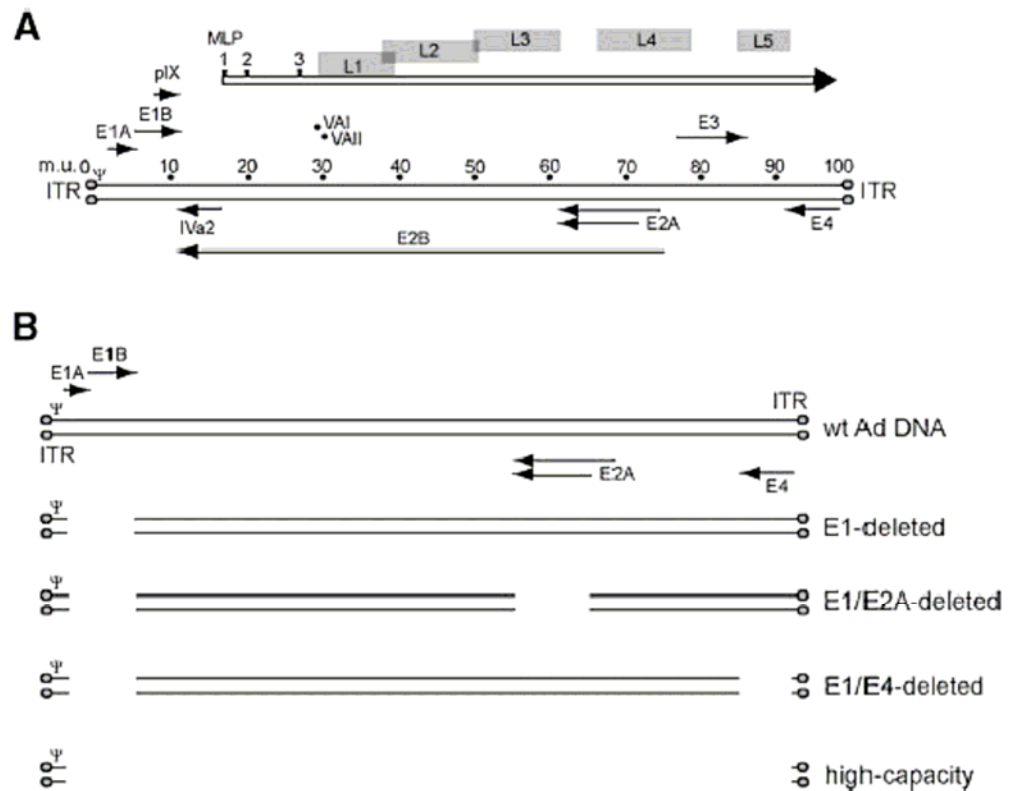
Figure 1.7: Representative genomic organisation of Ad and Ad-derived vectors. (**A**) The Ad genome is a double-stranded DNA sequence of approximately 30-38 kb depending on the Ad serotype. The genome consists of early (E) and late (L) transcription units; the mRNAs are depicted by arrows and grey boxes, respectively. The major late unit (large arrow with filled arrow head) is driven by the major late promoter (MLP). The delayed early units (pIX and IVa2) and viral-associated (VA) genes are also shown. The inverted terminal repeats (ITR) and the packaging signal are depicted by shaded circles and Ψ, respectively. Map units = m.u. (**B**) Schematic representations of the major types of Ad vectors are displayed in comparison to wild-type (wt) Ad genomic DNA. The gaps correspond to the deleted regions. For first-generation E1-deleted vectors, the E1 regions are usually replaced by the desired transgene cassette. High-capacity or HD vectors are devoid of all viral DNA except for the ITR regions and the packaging signal. Figure taken from Goncalves and de Vries, 2006.

1.9.2. The Adenovirus Life Cycle

Before viral transcripts are expressed in an infected cell, a highly regulated sequence of events occurs that can be divided into three main stages: (1) attachment of the Ad fibre to the receptors on the host cell; (2) internalisation and intracellular trafficking of the viral capsid to the nucleus; and (3) Ad replication, transcription and encapsidation. This process has been reviewed in several publications (Medina-Kauwe, 2003; Meier and Greber, 2004; Nicklin *et al*, 2005) and is depicted in **Fig. 1.8**.

Binding

The tropism of Ad infection is largely determined by cellular expression of the primary receptor. For the group B coxsackie viruses and human Ad serotype groups A, C, D, E and F, but not B, the primary receptor is the Coxsackie Adenovirus Receptor (CAR, CXADR) (Roelvink *et al*, 1998). Alternative receptors have also been shown to mediate binding and internalisation of Ad, including cell surface HS proteoglycans (which bind to Ad serotypes 2, 3 and 5) (Dechecchi *et al*, 2000; Vives *et al*, 2004), cell surface sialic acids (Ad37) (Arnberg *et al*, 2000), CD80/CD86 (B7.1/B7.2; Ad 3) (Short *et al*, 2004) and CD46 (membrane cofactor protein; group B Ad and Ad37) (Gaggar *et al*, 2003; Iacobelli-Martinez *et al*, 2005).

The initial cellular attachment is mediated by the globular knob of the Ad fibre, which binds to CAR. Three CAR molecules are required for the binding of each Ad fibre (Roelvink *et al*, 1999). CAR was first cloned in 1997 by three independent research groups (Bergelson *et al*, 1997; Carson *et al*, 1997; Tomko *et al*, 1997) and is a 46 kDa transmembrane protein (Honda *et al*, 2000). CAR is a member of the immunoglobulin superfamily and contains two extracellular domains, designated D1 and D2, which are both critical for the attachment of the Ad fibre.

Little is known about the biological function of CAR. It has been hypothesised that the CAR receptor is a potential cell adhesion molecule involved with cell-cell communication, neural migration, fasciculation and other aspects of neural network formation in the developing embryo (Honda *et al*, 2000; Hotta *et al*, 2003). Human CAR is expressed in the brain, heart, lung, liver, kidney, pancreas, prostate, testis and intestine, but not in muscle or placental tissue (Fechner *et al*, 1999; Persson *et al*, 2006).

The expression of CAR is highly regulated developmentally and regionally in rodents (Hotta *et al*, 2003). Murine CAR has been detected in a broad range of tissues, including the
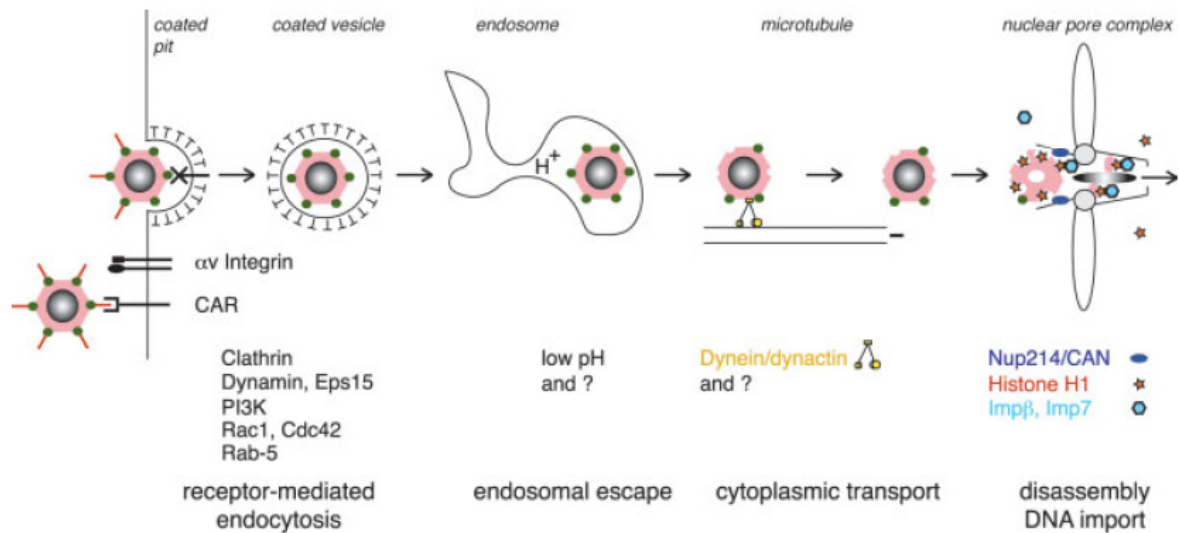
Figure 1.8: Ad endocytosis. Following the binding of the Ad fibre to CAR on the cell surface, secondary interactions with α_v integrins induce clathrin-mediated endocytosis via the activation or involvement of several factors (e.g. clathrin, dynamin). Ad capsids are partially disassembled in the acidic endosomal compartment before escaping the endosome and being transported to the cell nucleus by the dynein/dynactin motor complex via microtubules. Ad dock at the nuclear pore complex receptor, CAN/Nup214, where it recruits nuclear histone H1. The Ad genome, pVII and the terminal proteins are then imported into the nucleus via the nuclear pore complex. Figure taken from Meier and Greber, 2004.

liver, lung, kidney, heart and brain (Tomko *et al*, 1997; Bergelson *et al*, 1998). Murine CAR mRNA expression is detectable from 6.5-days post-conception in the embryonic ectoderm and peaks at birth in mice, with expression observed in the cerebral cortex, midbrain, hippocampus, various thalamic nuclei, meninges and amygdala (Hotta *et al*, 2003). No signal is observed in the corpus callosum, anterior commissure or in cerebellar white matter (Hotta *et al*, 2003). Murine CAR protein expression diminishes rapidly in the postnatal period but is still evident after postnatal day 21 in the subventricular zone of the lateral ventricle and in the rostral migratory stream (Hotta *et al*, 2003).

Following docking of the particle on the cell surface receptor, the fibre is released from the capsid and a highly conserved RGD (Arg-Gly-Asp) motif in the penton base forms a secondary interaction with cell surface integrins (including $\alpha_v\beta_1$, $\alpha_v\beta_3$, $\alpha_v\beta_5$, $\alpha_3\beta_1$ and $\alpha_5\beta_1$) (Wickham *et al*, 1993; Goncalves and de Vries, 2006).

Internalisation and Endocytosis

The binding of the penton base to integrin co-receptors induces the clustering of integrins, activating the phosphatidylinositol-3-OH kinase pathway, which in turn triggers the Rho family of GTPases and Raf/mitogen-activated protein kinase pathways to promote actin polymerisation, clathrin-mediated endocytosis of the Ad particle and uptake into the endosome (Li *et al*, 1998a; 1998b; Meier *et al*, 2002) (**Fig. 1.8**). The acidic environment destabilises the capsid proteins, resulting in a step-wise, partial disassembly of the capsid (Greber *et al*, 1993; Wiethoff *et al*, 2005). Eventually, the liberation of capsid pVI polypeptide mediates the lysis of the endosomal membrane, allowing the virus to be released into the cytosol (Wiethoff *et al*, 2005) whereby it is translocated to the cell nucleus by the dynein/dynactin motor complex via microtubules (Suomalainen *et al*, 1999). At the nucleus, the virion docks at the nuclear pore complex receptor, CAN/Nup214, where it recruits nuclear histone H1, and the Ad genome, pVII and the terminal proteins are then imported into the nucleus through the nuclear pore complex (Greber *et al*, 1997; Wisnivesky *et al*, 1999; Trotman *et al*, 2001).

Replication and Virion Assembly

After the virion is transported to the cell nucleus, Ad replication occurs rapidly with particle assembly within 8-hrs post-infection followed by cell lysis, releasing 10^5-10^6 progeny particles per cell after 30- to 40-hrs of infection (Volpers and Kochanek, 2004). Transgene expression can be observed as early as 18-hrs after infection with maximal expression at 48-

to 72-hrs. With the exception of the VA genes, which are transcribed by the host RNA polymerase III, the Ad genome is transcribed in a temporal manner by RNA polymerase II. Each transcription unit produces multiple transcripts due to alternate splicing and multiple adenylation sites (Berget *et al*, 1977).

E1a and E1b are the first viral genes to be transcribed (**Fig. 1.7**). They regulate cellular gene expression to make the host cell more susceptible to viral replication by inducing entry into the S phase of the cell cycle, stimulate apoptosis and activate or suppress other viral promoters (reviewed in Russell, 2000). The E2 regions encode DNA binding protein, DNA polymerase and the pre-terminal protein (reviewed in Goncalves and de Vries, 2006). The E3 region appears to be non-essential for viral growth and modulates the host response to Ad infection (Fessler *et al*, 2004). Products of the E4 region have many functions, including instigating the preferential translation of viral mRNA, host cell protein synthesis shut-off and virion assembly (reviewed by Leppard, 1997).

DNA replication is a two-stage process and begins from either end of the genome from the origin of replication within the inverted terminal repeat regions. One parental strand acts as a template and replication continues to the end of the strand so that a parental strand, a daughter strand and a displaced, parental single stand are present (Lechner and Kelly, 1977). The inverted terminal repeats of the displaced strand bind to each other and form a pan-handle structure that can also be duplicated by the same cellular machinery. Replication is initiated by a complex of the pre-terminal protein, DNA polymerase, and the origin of replication is stabilised by the cellular nuclear factors (NF) I and III. Virally-encoded DNA-binding protein, DNA polymerase, as well as cellular NF II and topoisomerase, are required for chain elongation (reviewed in Goncalves and de Vries, 2006).

Viral DNA synthesis activates gene expression from the delayed early unit (IX and IVa2) to induce the major late promoter (Lutz and Kedinger, 1996; Lutz *et al*, 1997) (**Fig. 1.7**). Transcription from the late gene unit (L1 to L5) encodes the viral structural capsid components, including the hexon (pII), penton base (pIII), fibre (pIV), pIIIa, pV, pVI, pVII, pVIII and μ, as well as some non-structural components (Goncalves and de Vries, 2006). After proteolytic processing of the immature polypeptides, the Ad particles are then assembled into hexon and penton capsomers in the cytoplasm and then into empty capsids and infectious particles within the nucleus (Shaw and Ziff, 1980). The mature virions then accumulate within the nucleus until the host cell eventually lyses in a process mediated by Ad death protein (Tollefson *et al*, 1996).

1.10. Canine Adenoviral Vectors

Members of the *Adenoviridae* family evolved from a common ancestor and have been isolated in many mammalian species, including cow, dog, duck, horse, fowl, frog, human, mouse, sheep, pig, possum, snake, turkey and tree shrew isolates (reviewed by Davison *et al*, 2003). In order to potentially circumvent the pre-existing immunity against human Ad whilst retaining the benefits of Ad vectors, several research groups are investigating non-human Ad as viral vectors. These include porcine (Reddy *et al*, 1999; Zakhartchouk *et al*, 2003), ovine (Hofmann *et al*, 1999; Loser *et al*, 2003), bovine (Mittal *et al*, 1995), avian (Sheppard *et al*, 1998; Michou *et al*, 1999), chimpanzee (Roy *et al*, 2004) and canine (Kremer *et al*, 2000) isolates. Two serotypes have been isolated from dogs. Wild-type canine adenovirus serotype 1 (CAV-1) is the agent of infectious canine hepatitis, affects the liver, heart and kidney and sometimes results in death (Lawler, 1989). CAV-2 is a milder, highly contagious but non-pathogenic respiratory infection commonly referred to as "kennel cough" (Buonavoglia and Martella, 2007). CAV-2-infected dogs experience a dry, hacking cough and dry retching behaviour, which usually resolves without medical intervention (Buonavoglia and Martella, 2007).

CAV-2 Vectors

The first-generation, ΔE1 CAV-2 vectors employed in this study have been generated and characterised by Dr Eric Kremer and colleagues at the Institut de Génétique Moléculaire de Montpellier (IGMM) in France. These vectors are derived from the Toronto A 26/61 strain of CAV-2, as frequent spontaneous recombination events using the Manhattan strain of CAV-2 made it difficult to obtain pure isolates (Klonjkowski *et al*, 1997). CAV-2 has been utilised as both ΔE1 and HD gene therapy vectors with successful *in vivo* gene transfer observed in several models (Soudais *et al*, 2001b; 2004; Sotak *et al*, 2005; Keriel *et al*, 2006). Both vector types are replication-defective and can only be propagated in the presence of a trans-complementing cell line containing the CAV-2 E1a and E1b regions (Klonjkowski *et al*, 1997). The generation of ΔE1 CAV-2 vectors will be discussed in more detail in **Chapter 3**.

In the case of HD CAV-2 vectors, the HD plasmid contains the inverted terminal repeat regions of viral genome, therapeutic transgene and an intact packaging sequence (ψ), which allows viral particles to be encapsidated (Soudais *et al*, 2004). An additional "helper" virus, a first-generation ΔE1 CAV-2 vector, is also required for encapsidation and contains all of CAV-2 viral genes (except E1a and E1b) and a disabled packaging signal flanked by two *loxP* sites (the target sequence for Cre). When the helper virus is propagated on E1-

transcomplementing cells expressing Cre recombinase, e.g. DK Cre cells (Soudais *et al*, 2001a), a site-specific recombination occurs between the *loxP* sites, thus excising the packaging signal and rendering the helper virus unpackagable but still able to trans-complement the replication and encapsidation of the HD CAV-2 genome. The encapsidation, or lack thereof, between the two vectors allows the HD vector to be separated from the contaminating helper vector via caesium chloride density gradient ultracentrifugation.

Receptor Binding

Similar to many human Ad serotypes, the cellular attachment of CAV-2 is via CAR (Soudais *et al*, 2000). The crystal structure of the CAV-2 fibre in complex with the CAR D1 region has determined that each CAV-2 fibre knob binds to three CAR molecules (Seiradake *et al*, 2006). In addition, the CAV-2 fibre may bind to N-acetylneuraminic acid, a sialic acid, via a lower affinity interaction (Seiradake *et al*, in preparation).

Sialiated glycoproteins are expressed on the cell surface of red blood cells and may cause haemagglutination of human red blood cells (Seiradake *et al*, in preparation). Interestingly, a point mutation in the CAV-2 fibre (R515A) at the *N*-acetyl neuraminic acid-binding motif resulted in a 1000-fold reduction in haemagglutination activity and will facilitate the generation of safer CAV-2 vectors (Seiradake *et al*, in preparation). In contrast to Ad, CAV-2 does not contain an Arg-Gly-Asp (RGD) binding motif in the penton base of CAV-2, which is usually recognised by the α_v integrins (Soudais *et al*, 2000). There is possibly a secondary interaction with $\alpha_v\beta_5$ integrins but transduction is $\alpha_M\beta_2$, major histocompatibility complex (MHC)-I and RGD-independent (Soudais *et al*, 2000).

Despite differences in receptor binding, CAV-2 vectors display comparable kinetics of trafficking and propagation to Ad5, including receptor binding (10 min), internalisation and actin filament reorganisation (10 min), endosomal escape (17 min), attachment to the nuclear membrane (30-40 min) and virion release (30-36 hr) (Chillon and Kremer, 2001).

Humoral Immunity

Until recently, it was predicted that the most advantageous aspect of CAV-2 gene therapy would be a reduction in immunogenicity (compared to human Ad) in clinical gene therapy, due to a lack of immunological memory of the CAV-2 virion. Ninety-six percent of human sera samples have antibodies (including non-neutralising) against Ad5, with the fibre, penton and hexon displaying varying degrees of immunoreactivity (92%, 87% and 55%, respectively) (Chirmule *et al*, 1999). These results were recently confirmed by Kremer and

colleagues using two types of titration assays (ELISA and surface plasmon resonance; n>50), demonstrating that 100% of normal human sera had IgG antibodies against Ad5 and the majority (>90%) harboured anti-Ad5 IgA and IgM (Perreau *et al*, submitted). Ad5-neutralising antibodies were also detected in >75% of sera (Perreau *et al*, submitted).

Surprisingly, all samples in this same cohort had anti-CAV-2 IgG antibodies recognising the external capsid proteins, with titres approximately 2-fold less than that of anti-Ad5 antibodies (Perreau *et al*, submitted). Modest reductions in the binding affinity of the antibodies for CAV-2 were measured by surface plasmon resonance (Perreau *et al*, submitted). Importantly, approximately 30% of human sera displayed CAV-2 neutralising antibodies compared to >75% Ad5-neutralising antibodies, with significantly lower anti-CAV-2 titres than that found against Ad5 (Perreau *et al*, submitted). This contrasts with previous data using a less sensitive assay, which found that 2% (1/50) of human sera samples displayed neutralising antibodies against CAV-2 (Kremer *et al*, 2000). Furthermore, purified anti-Ad5 antibodies from human sera (n=6) cross-reacted with CAV-2, porcine Ad-3 and bovine Ad-3, which would appear to limit CAV-2 gene therapy in humans (Perreau *et al*, submitted). However, *in vivo* experiments have demonstrated that similar amounts of transgene expression can be mediated by intranasal instillation of ΔE1 CAV-2 vectors after intravenous Ad5 immunisation compared to unprimed, immunologically-naïve mice (Keriel *et al*, 2006). In addition, significantly reduced inflammatory immune responses were measured in CAV-2-instilled mice (reduced tumour necrosis factor (TNF)-α secretion and less cellular infiltration) at 3- or 24-hrs post-delivery compared to mice instilled with equal titres of Ad5 (Keriel *et al*, 2006).

The presence of non-neutralising antibodies may also be problematic for effective clinical gene therapy. For example, opsonising antibodies are one of the essential links between humoral, complement and cellular immunity and thus virion-antibody immune complexes can activate the complement pathways, resulting in inflammation and antibody-dependent cellular cytotoxicity (reviewed and discussed in Perreau and Kremer, 2006). However, CAV-2 is a poor activator of the classical, alternative and mannose-binding lectin complement cascades, even in the presence of CAV-2-specific antibodies, which suggests that CAV-2 gene therapy will not be limited by immune complexes (Perreau *et al*, submitted).

Cellular Memory Immunity

Another aspect of adaptive immunity is the generation of immunological memory via memory T lymphocyte (T_M) production. Human peripheral blood mononuclear cells generate Ad2-specific CD4^{+} T_M responses in 97% of individuals exposed to Ad2 (Flomenberg *et al*, 1995). In contrast, exposure to identical titres of CAV-2 and Ad5 particles induce T_M proliferative responses in only 45% and 84%, respectively, of human blood donors (n=71) (Perreau and Kremer, 2005). Of the CAV-2 responders, the T_M activation was 3- to 10-fold less than that seen in Ad5 responders (Perreau and Kremer, 2005). The majority of the proliferating cells were memory CD4^{+} T_M lymphocytes, which differentiated into interferon (IFN)-γ-producing cells. Very few proliferating or activated CD8^{+} T_M lymphocytes were detected (Perreau and Kremer, 2005).

Dendritic Cell Interactions with CAV-2

Dendritic cells, the professional antigen-presenting cells of the body, are responsible for initiating and mobilising the cellular immune response, and can mediate immunogenic reactions against transduced cells due to antigenic presentation of capsid and viral gene products. In contrast to Ad2, CAV-2 can be internalised and targeted to the early endosome but cannot transduce immature human monocyte-derived dendritic cells, due in part to poor escape from Rab5^{+} vesicular compartments (Perreau *et al*, 2007). In addition, CAV-2 poorly induces the functional maturation of dendritic cells, upregulation of costimulatory molecules (CD40, CD80, CD86) and MHC class I/II, and induces minimal release of cytokines (TNFα, IFN-γ, IFN-α/β, interleukin (IL)-10, IL-1β and IL-12p70), all adaptive immune responses observed after Ad5 exposure (Perreau *et al*, 2007). Taken together, the differences in the humoral immunity, T_M proliferative response and the lack of dendritic cell maturation after CAV-2 exposure are encouraging for the use of CAV-2 vectors in a clinical setting when compared to human Ad vectors (but not compared with other viral vectors). It may be necessary to carefully verify the immune response to CAV-2 for each potential recipient prior to vector delivery.

Tropism and Retrograde Transport

CAV-2 primarily transduces neurons, including those present in the rat olfactory bulb, substantia nigra pars compacta (dopaminergic neurons), basal nuclei of Meynert (cholinergic neurons) and hippocampus, primary cultures of spinal cord neurons, mouse motor-neurons and, most clinically relevant, cortical neurons in *ex vivo* human brain biopsies, with little to no

transduction occurring in astrocytes and oligodendrocytes (Soudais *et al*, 2001b; Peltekian *et al*, 2002; Soudais *et al*, 2004). *In vivo*, the expression of a fluorescent marker gene can be detected in striatal neurons at least 1-year post-injection following the delivery of a HD CAV-2 vector to immunocompetent rats (Soudais *et al*, 2004). Whilst integrative vectors such as retroviruses and AAV may provide longer-term expression, the additional safety risks of insertional oncogenesis should also be considered (Pfeifer and Verma, 2001).

CAV-2 vectors can also be transported via axoplasmic retrograde transport (Soudais *et al*, 2001b; Peltekian *et al*, 2002). Consequently, CAV-2 particles may be taken up by synapses at the injection site and transported to the neuronal cell body, thus increasing the spread of treatment from each injection site. For example, retrograde transport of CAV-2 has been observed from the hippocampus to the entorhinal cortex, and from the striatum to the substantia nigra pars compacta, ventral tegmental area, cortex and thalamus in rats (Soudais *et al*, 2001b; Peltekian *et al*, 2002). Axonal retrograde transport of a GFP-expressing ΔE1 CAV-2 vector (CAV-GFP) has also been demonstrated in the contralateral hemisphere of mice receiving unilateral striatal injections of CAV-GFP, although GFP expression was approximately 10-fold less than in the ipsilateral hemisphere (Soudais *et al*, 2001b). This feature has been exploited in a mouse model of dopamine deficiency where a ΔE1 CAV-2 vector expressing tyrosine hydroxylase injected in the dorsal striatum was able to mediate clinical improvement for at least 8-months as a result of transgene expression in the afferent structure, the substantia nigra (Sotak *et al*, 2005). This is a highly desirable trait for LSD with neurological symptoms as the maximum distribution of the vector and gene product (i.e. lysosomal enzyme) within the CNS is expected to provide a more effective treatment of neuropathology.

1.11. Specific Aims

The primary objective of this PhD candidature was to evaluate the clinical efficacy and safety of CAV-2 vectors as a vehicle for delivering NS to MPS IIIA cells both *in vitro* and *in vivo*. The specific aims of this project were to:

1. Generate and purify a ΔE1 CAV-2 vector capable of co-expressing human NS and the GFP marker gene (CAV-NS).
2. Characterise this vector *in vitro* via,
    a) NS activity assays,
    b) protein processing experiments,
    c) cross-correction of deficient MPS IIIA cells.
3. Evaluate and compare the biodistribution of CAV-NS after injection into the CNS of unaffected and MPS IIIA mice, in particular to,
    a) evaluate the effect of CAV-NS administration in adult and newborn mice,
    b) determine the viral titre which provided the optimal transduction efficiency as assessed by transgene expression,
    c) develop or verify methods of tissue processing and analysis, including immunostaining of pathological and transgene markers in conjunction with biochemical markers, including NS activity and protein assays and quantitation of HS-derived markers, and
4. Evaluate the clinical efficacy of CAV-NS in MPS IIIA mice by,
    a) assessing the behavioural phenotype of CAV-NS-treated versus vehicle-treated and uninjected control mice throughout the course of disease progression, and
    b) assessing the tissues biochemically and histologically post-sacrifice using the methods detailed in Aim 3c.

CHAPTER 2:

Materials and Methods

2.1 Materials

2.1.1. Bacterial Culture

Luria Bertani (LB) Media	Tryptone 10 g, yeast extract 5 g, NaCl 10 g made to 1 L with MilliQ water. Autoclaved
LB Agar	LB Media with 15 g/L BactoAgar. Autoclaved. For antibiotic selective plates, cooled LB agar to approximately 55°C and added filter-sterilised ampicillin (100 µg/mL final concentration) or kanamycin (50 µg/mL final concentration)
SOC Media	Tryptone 20 g, yeast extract 5 g, NaCl 0.5 g, 2.5 mM KCl, 10 mM $MgCl_2$ made up to 1 L with MilliQ water. Autoclaved. Added filter-sterilised glucose to a final concentration of 20 mM before use
$CaCl_2$ Solution	60 mM $CaCl_2$, 15% (v/v) glycerol, 10 mM PIPES, pH 7.0. Autoclaved

2.1.2. Buffers and Solutions

50x TAE Buffer	Tris base 242 g, 57.1 mL glacial acetic acid, 100 mL 0.5 M EDTA (pH 8.0) made up to 1 L with MilliQ water
50x TBE Buffer	Tris base 54 g, boric acid 27.5 g, 100 mL 0.5 M EDTA (pH 8.0) made up to 1 L with MilliQ water
6x Agarose Gel Loading Buffer	1x TAE, 50% (v/v) glycerol, 1% (w/v) saturated bromophenol blue, 1% (w/v) xylene cyanol
Mini Prep Solution 1	50 mM glucose, 25 mM Tris-HCl, pH 8.0, 10 mM EDTA
Mini Prep Solution 2	0.2 M NaOH, 1% (w/v) SDS
Mini Prep Solution 3	Potassium acetate 24.9 g, 11.5 mL glacial acetic acid made up to 100 mL with MilliQ water, pH 4.8
Phenol/Chloroform	1:1 ratio, stored at 4°C in the dark
TE Buffer	10 mM Tris-HCl, 1 mM EDTA, 2 µg/mL DNase-inactivated RNase

PBS Lysis Buffer (Solubilisation Buffer)	1% (w/v) sodium deoxycholate, 0.1% (w/v) SDS, 0.5% non idet P40 (v/v) diluted in 1x PBS. Stored at 4°C
SDS-PAGE Reservoir Buffer	250 mM Tris base, 2 M glycine, 1% (w/v) SDS in MilliQ water
SDS-PAGE Gel Loading Buffer (10x)	50% (v/v) glycerol, 1% (w/v) SDS, 100 mM EDTA, 0.1% (w/v) bromophenol blue in MilliQ water, pH 8.0. Supplemented with 5% (v/v) β-mercaptoethanol immediately prior to use
Transfer Buffer (Towbin buffer)	Tris base 3 g, glycine 14.4 g, 200 mL methanol made up to 1 L with MilliQ water, pH 8.3. Stored at 4°C
Genomic DNA (Toe) Lysis Buffer	50 mM Tris (pH 8.0), 2 mM NaCl, 1 mM EDTA, 0.5% (v/v) Tween20 in MilliQ water. Supplemented with 0.4 mg/mL (final concentration) Proteinase K before use
10x PBS	NaCl 80 g, KCl 2 g, Na_2HPO_4 11.5 g, KH_2PO_4 2 g made up to 1 L with MilliQ water, pH 7.4
PBSTX	0.3% (v/v) Triton X100 in 1x PBS
10 mM Citrate Buffer for Antigen Retrieval	Citric acid 1.05 g, 2.5 mL of 5 M NaOH in 500 mL MilliQ water. Adjusted to pH 6.0
Trypsin Antigen Retrieval Working Solution	0.05% (w/v) trypsin, 0.1% (w/v) calcium chloride diluted in MilliQ water. Adjusted to pH 7.8. Prepared fresh each time
10x Tris Buffer	60.57 g Tris base, 87 g NaCl, 2.03 g $MgCl_2$, 1.11 g $CaCl_2$ made up to 1 L with MilliQ water, pH 7.6. Dilute to a 1x Tris buffer before use
1.4 g/mL Caesium Chloride	30.77 g caesium chloride in 50 mL 1x PBS
1.32 g/mL Caesium Chloride	23.88 g caesium chloride in 50 mL 1x PBS
1.25 g/mL Caesium Chloride	18.18 g caesium chloride in 50 mL 1x PBS
20x SSC buffer	NaCl 701.2 g, tri-sodium citrate 352.8 g in 4 L MilliQ water. Adjusted pH to 7.0 and autoclaved before use. Adjusted to 0.4x SSC or 2x SSC by diluting in MilliQ water
FISH Proteinase K Buffer	20 mM Tris-HCl, 2 mM calcium chloride. Adjusted pH to 7.5 and autoclaved
FISH Post-Hybridisation Wash Solution 1	0.3% (v/v) Non idet P40 in 0.4x SSC. Adjusted to pH 7.0

FISH Post-Hybridisation Wash Solution 2	0.1% (v/v) Non idet P40 in 2x SSC. Adjusted to pH 7.0
Anti-Fade DAPI Mounting Medium for FISH	Tris base 242.2 mg in 10 mL sterile distilled water. Adjust pH to 11.0 and supplemented with 0.7 ng/μL DAPI. Stored at 4°C
Kievet's Hybridisation Mix	10% (v/v) dextran sulphate (sodium salt), 2x SSC, 50% (v/v) deionised formamide, 0.1% (v/v) Tween20, adjusted pH to 7.0 and stored at -20°C
Tissue Homogenisation Buffer	20 mM Tris, 0.5 M NaCl in MilliQ water, pH 7.0-7.5
0.1 M Sodium Hydrogen Carbonate	Sodium hydrogen carbonate 8.4 g in 1 L MilliQ water. Filtered through 0.45 μm filter
DELFIA Assay Buffer	NaCl 9 g, bovine serum albumin 5 g, sodium azide 0.5 g, bovine γ globulin 0.5 g, Tween40 0.1 g, Tris base 6.06 g, diethylene triamine penta acetic acid 7.85 mg in 1 L MilliQ water, pH 7.75. Stored at 4°C
DELFIA Wash Buffer	NaCl 225 g, Tris base 15.2 g, thimerosal 0.5 g, Tween20 1.25 g in 1 L MilliQ water. Filtered through 0.2 μm filter prior to adding Tween20 and stored at 4°C
DELFIA Enhancement Solution	Triton X100 2 g, potassium hydrogen phthalate 2.78 g, 11.44 mL acetic acid, 4 mL tri-n-octylphosphine oxide (TOPO; 50 μM final concentration), 4 mL 2-naphthoyltrifluoroacetone (β-NTA, 15 μM final concentration) in 2 L MilliQ water using a siliconised measuring cylinder. Stored in the dark at 4°C
1x ELISA Wash Buffer	20 mM Tris, 25 mM NaCl, pH 7.0-7.2
ELISA Blocking Solution	Heated 100 mL ELISA wash buffer in microwave for 30 sec. Added gelatine 0.5 g and 200 μL Tween20. Prepared fresh each time
ELISA Citrate Buffer	Citric acid 5.25 g in 500 mL MilliQ water. Stored at –20°C in aliquots
ABTS Substrate for ELISA	ABTS 3.33 mg, 10 μL of 30% (v/v) H_2O_2 in a total volume of 10 mL citrate buffer. Prepared fresh each time

2.1.3. Enzymes and Purified Proteins

*Aci*I (10 U/μL)	New England Biolabs, USA
Calf intestinal phosphatase	New England Biolabs, USA
DNA polymerase I (Klenow) fragment	New England Biolabs, USA
HotStart Taq polymerase	Qiagen, Germany
Proteinase K	Roche, Switzerland
Recombinant human sulphamidase (rhNS1)	Dr Peter Clements, LDRU, Australia
Recombinant human sulphamidase (rhNS2)	Shire Human Genetic Therapies, USA
Restriction enzymes (miscellaneous)	Invitrogen, USA; New England Biolabs, USA
T4 DNA ligase	Invitrogen, USA
Taq DNA polymerase	Roche, Switzerland

2.1.4. Cell Culture

Albumin	Sigma, USA
Basal Medium Eagle (BME)	JRH Biosciences, USA
Cellstar® flasks (25 cm^2 & 75 cm^2)	Greiner Bio-One, Germany
Costar® cell lifters, plates, trays	Corning, USA
Cysteine	Sigma, USA
Dimethylsulphoxide (DMSO)	Sigma, USA
DNase I	Roche, Switzerland
Dulbecco's Modified Eagle's Media (DMEM)	JRH Biosciences, USA
Foetal Calf Serum (FCS)	JRH Biosciences, USA
Glucose	Sigma, USA
Ham's nutrient F12 media	JRH Biosciences, USA
Horse serum	Institute of Medical and Veterinary Science, Australia
Lipofectamine™ 2000	Invitrogen, USA
Opti-MEM® I Reduced Serum Media	Invitrogen, USA
Papain	Sigma, USA
Penicillin G (5000 U/mL), Streptomycin sulphate (5000 mg/mL)	JRH Biosciences, USA
Phosphate Buffered Saline (PBS) (without Ca^{2+} & Mg^{2+})	JRH Biosciences, USA
Poly-L-lysine	Sigma, USA
Poly-L-ornithine	Sigma, USA
Sodium pyruvate	Sigma, USA

2.1.5. Histological Reagents

APES (3-aminopropyletriethoxysilane)	Sigma, USA
Bovine Serum Albumin (BSA)	Sigma, USA
Cold water fish skin gelatin	Sigma, USA
Coverslips, thickness #1	Tissue-Tek, USA
Cryomolds®	Tissue-Tek, USA
Electron Microscopy (EM) fixative	Adelaide Microscopy, Australia
Fluorescein Avidin DCS (A2011)	Vector Laboratories, USA
Haematoxlin (Mayer's)	Amber Scientific, Australia

Hydrogen Peroxidase, 30%	Ajax Fine Chem, Australia
Lectin from *Bandeiraea simplicifolia* (Isolectin B_4, peroxidase conjugate)	Sigma, USA
Lithium carbonate	Sigma, USA
Microscope slides (uncoated)	Mensel-Glaser, Germany
Normal Donkey Serum (NDS)	Jackson Immunoresearch Lab, USA
Optimal Cutting Temperature (OCT) compound	Tissue-Tek, USA
PapPen (DakoCytomation Pen)	DakoCytomation, Denmark
Paraformaldehyde	Sigma, USA
Permount mounting media	ProSciTech, Australia
Target Retrieval Solution (TRS) for Antigen Retrieval	DakoCytomation, Denmark
Vectashield mounting media with DAPI	Vector Laboratories, USA
Vectastain universal elite ABC	Vector Laboratories, USA
Vectastain VIP substrate kit	Vector Laboratories, USA

2.1.5. Antibodies

Rabbit α-rhNS (polyclonal); 8 mg/mL	Kelly Perkins, LDRU, Australia
Sheep α-rhNS (polyclonal); 2.785mg/mL	Alison Whittle, LDRU, Australia
Mouse α-rhNS (monoclonal clone 23B2); 0.57 mg/mL	Briony Gliddon, LDRU, Australia
Sheep α-rhNS (polyclonal), europium-labelled; 139 μg/mL (DL) or 103 μg/mL (TR)	Debbie Lang, Tina Rozaklis, LDRU, Australia
Sheep α-mouse IgG, europium labelled; 100 μg/mL	Alison Whittle, LDRU, Australia
Biotinylated goat α-avidin D (BA-0300)	Vector Laboratories, USA
Sheep α-mouse IgG, horse-radish peroxidase (NA931V)	Amersham Biosciences, Australia
Rabbit α-GFAP (polyclonal, Z0334)	DakoCytomation, Denmark
Rabbit α-GFP (polyclonal, A6455)	Molecular Probes, USA
Mouse α-GFP (monoclonal, A11120)	Invitrogen, USA
Donkey α-rabbit-Cy3 IgG (711-165-152)	Jackson Immunoresearch, USA
Donkey α-rabbit-biotinylated IgG (AP182B)	Chemicon, USA
Donkey α-rat-biotinylated IgG (AP189B)	Chemicon, USA

2.1.6. Animal Handling and Surgical Apparatus

Dental needles, 27G (0.4 x 41 mm)	Nipro Medical, Japan
Dextrose (20% aqueous solution)	Abbott Australasia, Australia
Drill bit (0.5 or 1 mm) and hand-drill	Flintware, Australia
Dymadon (Panadol)	Glaxo Smith Kline, Australia
Finadyne® solution	Schering-Plough Animal Health, Australia
Gloves, sterile, surgical	Ansell, Australia
Glucose (25% aqueous solution)	Baxter, Australia
Glycopyrrolate (Robinul®)	Wyeth Ayerst, USA
Hamilton Syringes, 25 μL	SGE Incorporated, USA

Insulin syringes (1 or 0.5 mL)	Beckton Dickson, USA
Isofluorane (Forthane®)	Abbott Australasia, Australia
Ketamine	Parnell Laboratories, Australia
Lacrilube	Allergan, Australia
Micro-injector pump (model SP200iz)	World Precision Instruments, USA
Microlight 150	Fibreoptic Light Guides, Australia
Plastic tubing (inside diameter 0.35 mm)	Tyco Electronics, USA
Saline for injection, sterile	AstraZeneca, Australia
Stereotaxic frame	David Kopf Instruments, USA
Sutures, surgical	Dynek, Australia
Thermometer (electronic)	Becton Dickson , USA
Water for injection, sterile	AstraZeneca, Australia
Wheatbags	Hand-made
Xylazine (Xylazil-20)	Ilium-Troy Laboratories, Australia

2.1.7. Cell Lines, Bacterial Strains and Viral Vectors

BJ5183 *E. coli*   Stratagene, USA
endA1 sbcBC recBC galK met thi-1 bioT hsdR (Str$_r$)

DH5α *E. coli*   Invitrogen, USA
F′/endA1 hsdR17 (rK–mK+) glnV44 thi-1 recA1 gyrA (Nalr) relA1
Δ(lacIZYA-argF)U169 deoR (φ80dlacΔ(lacZ)M15)

Top10 *E. coli*   Invitrogen, USA
F-mcrA Δ(mrr - hsdRMS-mcrBC) φ80lacZΔM15 ΔlacX74 recA1 ara Δ139
Δ(ara-leu)7697 galU galK rpsL (Strr) endA1 nupG

XL1Blue *E. coli*   Stratagene, USA
recA1 endA1 gyrA96 thi-1 hsdR17 supE44 relA1 lac [F′ proAB lacIqZ ΔM15
Tn10 (Tetr)]

Human 293 cells (CRL-1573)	ATCC, USA
Madin-Darby canine kidney cells (DK; CRL6247)	ATCC, USA
DKCre and DKZeo cells	Eric Kremer, IGMM, France
Human MPS IIIA (SF4636) and normal (SF5435) skin fibroblasts	National Referral Laboratory, CYWHS, Australia
Murine primary neural cells	Leanne Sutherland, LDRU, Australia
CAV-GFP ("SA4", 3 x 10^{12} physical particles/mL)	Eric Kremer, IGMM, France
CAV-NS (3.2 x 10^{12} physical particles/mL)	Adeline Lau, LDRU, Australia

2.1.8. Miscellaneous Materials, Chemicals and Kits

1 kb DNA ladder	Invitrogen, USA
3MM Whatmann paper	Invitrogen, USA
Agarose, DNA grade	Quantam Scientific, Australia
BenchMark prestained protein ladder	GibcoBRL, USA
Blocking solution (for Western Blotting)	Amersham Biosciences, Sweden
Caesium Chloride, MB grade	Ambion, USA
Centricon™ concentrator, YM-10	Millipore, USA
Chondroitin sulphate disaccharide (ΔUA-GalNAc4S) (4-deoxy-L-threo-hex-4-enopyranosyluronic (133) *N*-acetylgalactosamine-4-sulphate)	Sigma, USA
CytoTox-One™ Membrane Integrity Assay Kit	Promega, USA
ECL Western blotting analysis system	Amersham Biosciences, Sweden

Ethidium bromide	Geneworks, Australia
Evan's Blue dye	Sigma, USA
Food colouring	Queens Fine Foods, Australia
GFP protein, recombinant, MB-0752	Vector Laboratories, USA
Hybond ™ ECL nitrocellulose membrane	Amersham Biosciences, Sweden
Immunolon® 4 HBX wells	Thermo Labsystems, USA
Mannose-6-phosphate	Sigma, USA
MicroBCA kit	Pierce, USA
Nick translation kit	Vysis, USA
Nitrocellulose Membrane (Immuno-Lite™)	Bio-rad, USA
Non-protein binding plates (96-well)	Greiner Bio-one, Germany
Paint (BreatheEasy low sheen acrylic in white, cat. no. 642-61030)	Berger Paints, Australia
PD10 columns (with Sephadex™ G-25, P10)	Amersham Biosciences, Sweden
1-Phenyl-3-methyl-5-pyrazolone (PMP)	Tokyo Kasei Kogyo, Japan
5 mL polystyrene tubes for FACS	Evergreen Scientific, USA
Primers for PCR, custom-designed	Invitrogen, Australia
pUC19 DNA/*Hpa* II DNA ladder	Geneworks, Australia
Qiagen plasmid or Qiafilter midi kit	Qiagen, Germany
Qiaquick gel extraction kits	Qiagen, Germany
Salmon sperm DNA	Eppendorf, USA
Sodium sulphate ($Na_2{}^{35}SO_4$); specific activity 391.9 mC/mM	Dupont NEN Research Products, USA
Solid phase extraction columns, C18	United Chemical Technologies, USA
Slide-A-Lyzer® dialysis cassette, MWCO10,000	Pierce, USA
Spectrum green or orange labelled dUTP	Vysis, USA
SPP1 Phage DNA/*Eco*RI DNA ladder	Geneworks, Australia
Tert-amyl alcohol (isopentane)	Sigma, USA
Tris-glycine iGels, pre-cast polyacrylamide gels	Gradipore, USA
Tritium–labelled tetrasaccharide substrate for NS activity assays	Dr Peter Clements and Mrs Tina Rozaklis, LDRU, Australia
Tween20	Sigma, USA
Ultra-clear ™ tubes for SW41 rotor	Beckman, USA
Ultrafiltration membranes (XM300), MWCO300,000	Amicon, USA
X-ray film	Kodak, USA
XY18 FISH Probe	Department of Genetic Medicine, CYWHS, Australia

All other chemicals used within this study were analytical grade and purchased from Ajax Finechem (Australia), BDH Chemicals (USA), Boehringer Mannheim (Germany), Sigma-Aldrich (USA) or AnalaR (UK).

2.2. Methods

2.2.1. Molecular Biology

2.2.1.1. DNA Extraction

Large-scale DNA Midi Preparations

High quality DNA was prepared using Plasmid Midi Kits according to the manufacturer's instructions. In general, 100 mL of selective LB media was inoculated with 1 mL of starter culture and incubated overnight at 37°C, with agitation. Cells were lysed by standard alkaline lysis and the lysate cleared by column filtration or centrifugation. Plasmid DNA was loaded onto the columns by gravity-flow, washed in 20 mL wash buffer and eluted in 5 mL total volume. The DNA was desalted, precipitated and washed with isopropanol, 100% ethanol and 70% (v/v) ethanol before being air-dried. Pellets were resuspended in 100 µL MilliQ water and stored at -20°C.

The concentration of DNA was estimated by measuring the absorbance at 260 nm using a Shimadzu spectrophotometer (UV-1201) and a conversion factor of 50 µg/mL for double-stranded DNA.

Glycerol stocks were prepared from each large-scale culture by mixing 500 µL bacterial broth and 500 µL 80% (v/v) sterile glycerol per tube and stored at -70°C. To revive bacteria, the frozen glycerol stock was scraped with a heat-sterilised loop and streaked onto selective LB plates.

Small-scale DNA Mini Preparations ("1-2-3" Method)

Starter cultures were prepared by inoculating 5 mL selective LB with a single bacterial colony using a heat-sterilised loop or an autoclaved toothpick and incubating at 37°C for 8- to 16-hrs. The bacterial suspension was aliquoted into 2 mL Eppendorf tubes and microfuged (1 min, 17900 x *g*). The pellet was thoroughly resuspended in 100 µL Solution 1. Cells were lysed by adding 200 µL Solution 2, mixed by gently inverting the tube 5 times and incubated on ice for 5 min. Solution 3 (150 µL) was then added to neutralise the reaction, mixed by inverting 5 times and incubated on ice for a further 5 min. The tubes were clarified by centrifugation (17900 x *g*, 5 min, room temperature) and the supernatant transferred to a fresh Eppendorf.

An equal volume of phenol/chloroform was added, vortex-mixed and aqueous and phenol layers separated by centrifugation (17900 x *g*, 5 min, room temperature). The upper,

aqueous layer was removed and then mixed with 2x vol 100% ethanol and 0.1x vol 3 M sodium acetate, pH 5.2. The precipitate was collected by centrifugation (17900 x *g*, 20-30 min, room temperature), washed in 250 µL 70% (v/v) ethanol (17900 x *g*, 10 min, 4°C) and air-dried for 15 min. DNA was resuspended in 50 µL TE buffer and stored at -20°C.

Genomic DNA Extraction from Paraformaldehyde-Fixed, Frozen Tissue

Paraformaldehyde (PFA)-fixed, optimal cutting temperature (OCT)-embedded brain tissues were cryo-sectioned at 12 µM and transferred into autoclaved 1.5 mL tubes. For retrospectively analysed tissues, sections were detached with the sharp edge of a coverslip and transferred to an Eppendorf.

Sagittal mouse (35-50 µM) or guinea pig (10-25 µM) sections were incubated overnight at 37°C in 75 µL genomic DNA toe lysis buffer supplemented with a final concentration of 400 µg/mL proteinase K. After solubilisation, the proteinase K was deactivated at 95°C for 10 min before DNA was extracted by adding an equal volume (75 µL) of phenol:chloroform (1:1 ratio) in a fume hood and mixing with a vortex. The mixture was centrifuged at 17900 x *g* at room temperature for 5 min and the upper aqueous layer (approximately 100 µL) transferred to a fresh Eppendorf.

Genomic DNA was precipitated by vortex-mixing 2x vol 100% ethanol and 0.1x vol 3 M sodium acetate, pH 5.0, and then pelleting the DNA at 17900 x *g* for 20 min at room temperature. The DNA pellet was washed with 250 µL of 70% (v/v) ethanol and centrifuged at 17900 x *g* for 10 min at 4°C. The DNA pellet was briefly air-dried and then resuspended in 20 µL of water. One µL of genomic DNA was used to detect the presence of vector DNA using the conditions and primer sequences detailed in **Section 3.2.1.2.** The expected PCR product size was 845 bp.

Genomic DNA Extraction from Paraformaldehyde-Fixed, Paraffin-Embedded Tissue

Tissue shavings (20 µm) from paraffin blocks were collected into individual, autoclaved 1.5 mL screw-cap Eppendorfs and stored at room temperature. Uninjected and saline-treated tissue blocks were sectioned prior to CAV-2 vector-injected animals to prevent cross-contamination.

Genomic DNA was extracted according to the method of Schulze and Baumgartner (1998). In brief, the tissue was digested without de-waxing in 200 µL of buffer containing 50 mM Tris-HCl, 5 mM EDTA, 0.5 % (v/v) Tween20 supplemented with 200 µg/mL proteinase

K for 5-days at 37°C. The proteinase K was inactivated at 95°C for 10 min and 1 µL genomic DNA was either directly used for PCR or stored at -20°C. If the yield of DNA was poor, an additional 200 µg/mL proteinase K digestion was performed overnight at 37°C.

For mouse tissue, the MPS IIIA genotyping PCR (**Section 2.2.4.2**) was conducted to verify that genomic DNA had successfully been extracted, followed by the CAV recombination PCR (**Section 3.2.1.2**) to verify that vector DNA was present in the tissue section.

2.2.1.2. Restriction Enzyme Digestions

All restriction digests were prepared on ice in 1x recommended restriction enzyme buffer ± 100 µg/mL BSA according to the manufacturer's instructions.

For cloning, high quality plasmid DNA (5 µg) was digested with 5-10 U of the desired restriction enzyme/s overnight to obtain the transgene cassettes or vector backbone in a total reaction volume of 50 µL. To screen bacterial colonies for correct transgene orientation or positive recombination, 10 µL of Mini Prep DNA or 200-500 ng Midi Prep DNA was digested with 1 U of restriction enzyme in a reaction volume of 20 µL for 2- to 16-hrs at the recommended temperature.

Digested DNA and 500 ng of the appropriate DNA ladder marker were mixed with loading buffer (at a 1x final concentration) and loaded onto 0.7-5% (w/v) agarose in 1x TAE or 1x TBE gels. After electrophoresis in the corresponding buffer (1x TAE or 1x TBE), gels were stained with 50 µg/mL ethidium bromide for 30 min and imaged under ultraviolet light. Expected fragment sizes were determined using DNA Strider (http://www.cellbiol.com/soft.htm) or pDraw (http://www.acaclone.com).

2.2.1.3. DNA-modifying Enzyme Reactions
End-filling of Digested DNA for Blunt Ligations

To form blunt-ended DNA by filling in the 5' overhang and removing the 3' overhang, 5 µg DNA was digested with the appropriate restriction enzymes and 500 ng was electrophoresed on a check gel to ensure complete digestion. The remaining digested DNA was supplemented with 33 µM of each dNTP before adding 1 U of Klenow fragment per µg of DNA. Tubes were incubated for 25 min at 25°C and the reaction stopped by heating at 75°C for 20 min.

Dephosphorylation of DNA with Calf Intestinal Phosphorylase

To prevent re-circularisation of complementary sticky-end digests, DNA was dephosphorylated with calf intestinal phosphatase (CIP) by mixing 1 µg digested DNA, 1x CIP buffer and 5 U CIP in a total volume of 49 µL. Tubes were incubated at 37°C for 15 min and then CIP deactivated at 56°C for 15 min. Tubes were supplemented with an additional unit of CIP and the incubation and deactivation repeated as before.

2.2.1.4. Gel-Purification of DNA Fragments

Digested DNA for ligation was electrophoresed through 0.7% (w/v) agarose in 1x TAE gel, stained briefly with 50 µg/mL ethidium bromide and visualised under UV light. The desired band was excised with a clean scalpel blade and transferred to a pre-weighed Eppendorf tube.

DNA was purified using Qiaquick Gel Extraction columns as per the manufacturer's directions. In brief, each mg of gel weight was estimated to be 100 µL volume. The gels were melted in 3x vol of BufferQG at 50°C, with vigorous shaking for 10 min. After the gel had complete dissolved, 1x vol isopropanol was added, vortex-mixed and loaded onto a spin column. After binding the DNA onto the filter by centrifugation (17900 x g, 1 min) the filter was washed with 750 µL wash buffer (17900 x g, 1 min), the flow-through discarded and the DNA dried by an additional spin cycle. The filter was transferred to a fresh collection tube and the DNA eluted with 50 µL Buffer EB. To estimate the DNA concentration, 1 µL of purified DNA was electrophoresed on an agarose gel and compared to the staining intensity of DNA marker bands with known concentrations of DNA.

2.2.1.5. Ligations

After gel purification of DNA, insert and vector DNA were ligated in as small a volume as possible using the following equation to calculate the number of ng of insert DNA required for a 3:1 to 10:1 insert to vector ratio.

$$\text{Insert DNA (ng)} = \frac{(50\text{ng Vector DNA}) \times (\text{Size of Insert in kb}) \times (\text{Insert : Vector Ratio})}{(\text{Size of Vector in kb})}$$

The appropriate volumes of insert and vector DNA were mixed with 1x ligation buffer and 1 U ligase, and incubated overnight at 4°C for blunt ligations or 37°C for 2 hr for sticky ligations.

2.2.1.6. Electrocompetent Cell Preparation and Transformation by Electroporation

All manipulations were performed with sterile reagents using aseptic techniques. A single colony was used to inoculate a 5 mL starter culture without antibiotics and grown overnight at 37°C, with agitation. Two hundred mL of 2x LB media was inoculated with 2 mL of starter culture and cultured until the OD_{600} was 0.5-0.8. The cells were chilled on ice for 30 min and then pelleted at 4000 x g, 15 min, 4°C. Cells were desalted by serial washes in 200 mL ice-cold water, 100 mL ice-cold water, 4 mL 10% (v/v) glycerol and 0.5 mL 10% (v/v) glycerol. The bacteria were aliquoted (50 µL/tube), snap-frozen in liquid nitrogen and stored at -70°C.

Electrocompetent cells were quickly thawed on ice and 1-20 ng of DNA (in a volume of 1-5 µL) added per tube. Cells and DNA were transferred to pre-chilled cuvettes and electroporated at 0.5 kV, capacitance 25 µF, pulse 200 Ω. One mL of SOC media was immediately added to the cells, transferred to 10 mL tubes and then incubated for 1 hr at 37°C, with agitation. Cells were plated onto selective LB plates and grown overnight at 37°C.

2.2.1.7. Preparation of Chemically-Competent Cells and Heat-Shock Transformation

A 5 mL starter culture was prepared and grown overnight at 37°C, with shaking. Four mL of starter culture was used to inoculate 400 mL of LB media and cultured until the OD_{590} was 0.375. Cells were chilled on ice for 10 min, aliquoted into 50 mL tubes and then pelleted at 1600 x g, 7 min, 4°C. The cell pellets were resuspended in 10 mL ice-cold $CaCl_2$ solution and then collected at 1100 x g, 5 min, 4°C. Cells were resuspended in 10 mL of ice-cold $CaCl_2$ solution and incubated on ice for 30 min. The cells were centrifuged (1100 x g, 5 min, 4°C), resuspended in 16 mL of $CaCl_2$ solution, aliquoted and snap-frozen in liquid nitrogen.

For transformations, 10 ng DNA (in 5 µL) was aliquoted into a 10 mL tube and chilled on ice. Competent cells were thawed rapidly and 50 µL cells added to each tube. The cells and DNA were mixed, briefly incubated on ice and then heat-shocked at 42°C for 2 min. Cells were returned to ice, 1 mL SOC media added per tube and grown for 1 hr, 37°C. Cells were then plated onto selective LB plates overnight at 37°C.

2.2.2. Cell Culture

Tissue culture was performed using aseptic techniques in a biohazard hood, which was sterilised with 70% (v/v) ethanol before and after use and UV-irradiated at the end of each session. All cell lines were cultured in a humidified environment at 37°C with 5% carbon dioxide. Viable cells were counted using trypan blue exclusion and a haemocytometer. Liquid waste was inactivated with 5% (v/v) sodium hypochlorite. Within the tissue culture hood, untreated cells were always manipulated prior to CAV-treated cells to prevent the likelihood of cross-contamination. Plastic-ware from transduced cultures was disposed of according to the Guidelines of the Office of the Gene Technology Regulator.

2.2.2.1. General Cell Culture Methods
DK Cells

DKCre and DKZeo cells were cultured in the same manner. Both cell lines contained the CAV-2 E1A and E1B regions and were the trans-complementing cell line for CAV-2 vector preparation (Kremer *et al*, 2000). DKCre cells also expressed Cre recombinase (Kremer *et al*, 2000).

For routine culture, 10 cm plates were fed every 3- to 4-days with DMEM supplemented with 10% (v/v) FCS. Confluent plates were passaged by washing twice in 1x PBS, 2 mM EDTA, pH 8.0 and incubating with 3 mL 50% (v/v) trypsin, 2 mM EDTA, pH 8.0 diluted in PBS at 37°C for 10 min as cells were strongly adherent. Cells were encouraged to detach with a 1 mL pipette tip before neutralising trypsin activity with 7 mL normal media. Cells were pelleted at 250 x g for 3 min, counted and plated at 1-3 x 10^6 cells per 10 cm plate.

Human Skin Fibroblasts

Skin biopsies were obtained from referrals for diagnosis to the National Referral Laboratory (CYWHS, Australia). For this study, de-identified MPS IIIA and unaffected control skin fibroblasts were cultured in 75 cm^2 flasks in BME supplemented with 10% (v/v) FCS. Confluent flasks were divided 1:3 by washing twice in PBS, detaching with 33% (v/v) trypsin in 1x PBS and cultured at 37°C with 5% carbon dioxide.

Primary Murine Mixed Neural Cultures

Primary neural cultures were harvested and plated by Dr Leanne Sutherland (Sutherland *et al*, submitted by LDRU). Cerebellar tissue from newborn to 3-day-old pups

was preferentially selected to improve yields of neurons in the mixed cultures. Neural cells were plated for a minimum of 7-days after harvesting from fresh tissue or thawing from frozen stocks before being used experimentally.

Neural tissue was harvested by decapitating newborn pups with sterile scissors in a laminar flow-hood. Tissue was stored in ice-cold 50% (v/v) PBS, 50% (v/v) base DMEM whilst processing litter-mates. Debris was rinsed through a 70 μm nylon filter (BD Falcon) with cold complete media (5% (v/v) FCS, 5% (v/v) horse serum, 4.5 g/L glucose, 0.11 mg/mL sodium pyruvate in DMEM) before mincing the retained brain portions to a fine slurry in 5 mL complete media. Cells were pelleted at 250 x g (5 min, 4°C) and then digested for 1 min at 32°C in 5 mL digestion solution (1.5 U papain, 0.25 mg/mL DNase I, 0.06 mg/mL cysteine, 0.2 mg/mL albumin in 10 mL PBS). Cells were gently triturated to a single cell suspension with a P1000 followed by a P100 pipette tip. After three washes by centrifugation/resuspension in complete media at room temperature for 5 min at 250 x g, cells were counted and plated at a density of 2.5 x 10^5 cells per cm^2 onto 0.1 mg/mL poly-L-lysine and 0.1 mg/mL poly-L-ornithine-coated plates.

2.2.2.2. Transduction

Cells were detached as detailed in **Section 2.2.2.1,** and counted with trypan blue dye and a haemocytometer. Cells were plated at the desired density and incubated overnight at 37°C. The following day, cells were transduced by adding fresh media containing the desired concentration of vector stock to each plate. For DK cell transductions, cells were continuously rocked on "The Bellydancer" (Stovall Life Science) at the lowest rpm setting in a 37°C room to maximise the transduction efficiency of the cells. For transductions performed in Adelaide, Australia, cells were inoculated with vector, rocked on "The Bellydancer" for 30-60 min at room temperature and then returned to the 37°C incubator in a PC2 facility.

2.2.2.3. Harvesting

Unless stated otherwise, cells were harvested as follows. After viewing under fluorescent or light microscopy to check the condition of the cells, conditioned media was collected, clarified of cell debris by centrifugation and stored at 4°C. Cells were washed twice in 1x PBS and harvested in one of two ways. Cells were solubilised in PBS lysis buffer (10 mL for 10 cm plates, 2 mL per well for 6-well trays) overnight at 4°C. Alternatively, cells were detached with trypsin, pelleted and resuspended in 20 mM Tris/0.5 M NaCl (pH 7.0) and lysed by 6 alternate cycles of freezing in a dry ice/100% ethanol slurry, followed by thawing

in a 37°C water bath. Membranes were removed by centrifuging at 17900 x g for 5 min and the supernatant was stored at -20°C.

2.2.2.4. Freezing and Thawing Cell Lines

Low passage stocks of cell lines were stored in dewars containing liquid nitrogen. Cells were revived by quickly thawing in a 37°C water bath, liberally swabbing the outside of the cryo-vial in 70% (v/v) ethanol and transferring the cells to a 10 mL tube. Ten mL of the appropriate media containing FCS was added to the thawed cells to dilute the DMSO present, before the cells were pelleted at 250 x g for 5 min and resuspended in 1 mL of media. The viability and cell numbers were determined with trypan blue dye exclusion and the cells were seeded at usual plating densities. If the cell densities were low, smaller vessels were used at the proportional cell-to-area ratio. Media was changed the following day to remove unattached cells and any remaining DMSO, and then cells were cultured as normal.

To freeze cells, confluent plates or flasks were detached and pelleted. Cells were resuspended in 1 mL of cold 10% (v/v) DMSO in routine media containing 10% (v/v) FCS per confluent plate or flask and aliquoted into pre-labelled cryo-vials. Vials were placed in a Nalgene^{TM} Cryo 1°C freezing container filled with isopropanol and frozen overnight at -70°C. Cells were then transferred to liquid nitrogen for long-term storage.

2.2.3. Vector Preparation from Purified Stock

2.2.3.1. Transduction

Five 15 cm plates were seeded with 8 x 10^6 DK cells in a total volume of 20 mL per plate. The next day, cells were inoculated with 100 physical particles/cell (8 x 10^8 total particles per plate), followed by continuous rocking for 30- to 36-hrs at 37°C. Cells were scraped into the media using a cell lifter and were then pelleted at 250 x g for 5 min. The cell pellets were resuspended in a total volume of 45 mL, evenly divided into four 50 mL tubes and freeze/thawed. Vector was then purified as described in **Section 2.2.3.2**.

2.2.3.2. Purification of E1-deleted CAV

Caesium chloride at a density of 1.25 g/mL was added to six SW41 ultra-clear centrifuge tubes. Using a transfer pipette, 2 mL of 1.4 g/mL caesium chloride was gently underlaid in each tube, taking care to maintain the phases. Clarified vector supernatant was

then added drop-wise to each tube until ~0.5 cm from the top of the tube. The tubes were then 'capped' with 0.5 mL mineral oil to prevent aerosol formation.

The tubes were weighed and balanced in a Beckman L8-70 ultracentrifuge and centrifuged at 35,000 rpm for 90 min under vacuum at 18°C. The tubes were gently removed from the centrifuge and placed in a custom-made tube holder held in place by a retort stand. Both opaque viral bands were collected in a volume of ~1 mL by piercing the tube with an 18G needle attached to a 2 mL syringe 1 cm below the bottom band. The remaining media was allowed to drain in a waste bottle containing bleach.

The vector bands were pooled in a fresh ultra-clear tube and the tube filled with 1.34 g/mL caesium chloride and capped with mineral oil, as before. An isopynic gradient was formed by centrifuging at 35,000 rpm for 18-hrs at 18°C without the centrifuge brake. The lower band containing CAV-NS vector was removed in a 1 mL total volume with an 18G syringe, taking care to not disturb the top band containing the empty viral capsids.

The vector was desalted in one of two ways: (1) pre-packed PD-10 Sephadex^{TM} columns were washed with at least 50 mL sterile, tissue culture-grade PBS by gravity flow, taking care to not let the column dry out. The vector was loaded onto the column and the flow-through collected into transparent tubes. Successive 0.5 mL aliquots of PBS were used to elute the vector and each fraction was collected in a FACS tube. The two most opaque fractions (i.e. those with the highest concentration of vector) were pooled and 100 μL of sterile glycerol added to give a final concentration of 10% (v/v) glycerol. The purified vector stock was quickly aliquoted into pre-labelled 0.5 mL tubes and stored at -70°C. (2) If the concentration of vector particles appeared low, as observed by the thickness of the vector band, the vector band was harvested in 1 mL total volume with 100 μL neat glycerol added. The vector was then desalted by dialysing in a Slide-A-Lyzer® Dialysis Cassette (MWCO 10,000) following the manufacturer's instructions in four changes of 500 mL of PBS/10% (v/v) glycerol for 45 min each. The vector was then aliquoted and stored at –70°C.

2.2.3.3. Physical Particle Determination in Vector Stock

Purified vector DNA was diluted 1:5 and 1:10 in 10 mM Tris, 1 mM EDTA, 0.1% (w/v) SDS, 10% (v/v) glycerol in duplicate. Tubes were heated at 56°C for 10 min to free vector DNA from the capsid and centrifuged for 10 sec on a Capsulefuge (TOMY). The absorbance at 260 nm was determined on a spectrophotometer using a conversion of 1 OD$_{260}$ correlating to 1.1×10^{12} physical particles per mL according to Mittereder *et al* (1996).

2.2.3.4. Titration of Infectious Units

DK cells were plated at 2×10^5 cells per well in 12-well trays and cultured overnight at 37°C. After determining the particle concentration of vector stock, serial 1:2 dilutions starting at 200 physical particles per cell were prepared in duplicate in a total volume of 500 µL/well. Two wells per plate were not transduced as negative controls. Vector stock and dilutions were kept on ice until inoculation.

Cells were transduced, rocked for 30 min and then incubated for 24 hrs at 37°C. Cells were prepared for flow cytometry (FACS) by washing twice in PBS, detaching in trypsin (200 µL per well) and triturating thoroughly to a single cell suspension with a P200 yellow pipette tip. Cells were neutralised with 200 µL DMEM with 10% (v/v) FCS, transferred to FACS tubes, and more than 10,000 gated (live) cells were counted using a FACScan equipped with CellQuest software (version 3.2.1f1, Becton Dickson). Total cell numbers were determined in both of the untransduced wells using trypan blue dye and the particle-to-transduction ratio determined using the following equation:

$$\text{Physical Particle-to-Transduction ratio} = \frac{(\text{Number of input physical particles}) \times 100}{(\%GFP_{transduced} - \%GFP_{untransduced}) \times (\text{total number of cells per well})}$$

2.2.4. Animal Maintenance and Care

2.2.4.1. Breeding

Mice were bred as required from breeding colonies established in the CYWHS Animal House. All procedures were performed with the approval of the CYWHS and University of Adelaide Animal Ethics Committees. Mice were housed at a constant humidity and temperature with a 12 hr light-dark cycle. Cages were cleaned on a weekly basis and mice were allowed access to dried food pellets and water *ad libitum*. Mice were group-housed where possible, however MPS IIIA males were separated from 10- to 12-wks of age due to fighting.

Mice were generally maintained in monogamous pairs and were placed in a freshly prepared cage with ample shredded paper and yoghurt containers to encourage nesting. Where possible, heterozygous females were paired with litter-mate MPS IIIA males because of suspected reduced fertility in homozygous MPS IIIA matings and because of poor maternal behaviour in the older MPS IIIA females, e.g. cannibalism or reduced feeding of the pups (Crawley *et al*, 2006a). MPS IIIA x MPS IIIA homozygous or wild-type x wild-type homozygous matings were performed in mice from the "New York" colony (Bhaumik *et al*, 1999). Pups were weaned from dams at 19- to 21-days of age.

2.2.4.2. Genotyping MPS IIIA Mice

This method has previously been described in detail (Bhattacharyya *et al*, 2001). The G to A mutation in the MPS IIIA mouse colony is in exon 2 and abolishes the *Aci*I restriction enzyme site.

Genomic DNA Extraction

Mice toes or tail tips were clipped at 5- to 7-days after birth using ethanol-swabbed scissors and collected into Eppendorf tubes stored on ice during tagging. Fifty μL of toe lysis buffer containing 0.4 mg/mL proteinase K was added to each tube and incubated at 37°C overnight. Proteinase K was deactivated by heating at 60°C for 10 min and genomic DNA was stored at -20°C.

Polymerase Chain Reaction (PCR) Amplification of the MPS IIIA Mutation

The 5' MSI2 primer (5' GGTCTGTCTTCCTCAGCG 3') and 3' MS4 primer (5' GATAAGGCTGTGGCGGGACAGGG 3') flank the point mutation producing a 105 bp PCR product. Each PCR reaction was prepared on ice in a PCR hood and contained the following:

10x PCR buffer (with 15 mM MgCl$_2$)	5 μL
10 mM dNTP (Roche)	1 μL
5' MSI2 primer (100 ng/μL)	2 μL
3' MS4 primer (100 ng/μL)	2 μL
Taq polymerase (5 U/μL)	0.2 μL
Sterile water for injection	37.8 μL
TOTAL VOLUME (after addition of 2 μL DNA)	50 μL

Two μL of genomic DNA lysate was aliquoted in each tube to bring the total reaction volume to 50 μL. A negative control of 2 μL water instead of genomic DNA was always included. The PCR cycling conditions had an initial denaturation step at 94°C for 3 min, followed by 35 cycles of 94°C for 45 sec, 55°C for 45 sec and 72°C for 40 sec, with a final extension at 72°C for 4 min.

After confirmation of successful PCR reactions by electrophoresis through a 3.5% (w/v) agarose gel using 5 μL of PCR product, the PCR product was digested overnight at 37°C with 5 U *Aci*I in 1x New England Biolabs Buffer 3 in a total volume of 20 μL. The *Aci*I restriction enzyme cuts between the CC in the sequence 5' CCGC 3'. Digested DNA was electrophoresed through a 4.5% (w/v) agarose gel and the genotype of each animal identified. Homozygote unaffected and MPS IIIA mice displayed bands at 73 or 87 bp, respectively, and a heterozygous mouse had bands at both 73 and 87 bp.

2.2.5. Surgical Procedures

2.2.5.1. Cryo-anaesthesia and Injection into the Lateral Ventricles of Newborn Mice

A 25 µL Hamilton syringe was filled with sterile water and then connected via plastic tubing (inside diameter 0.35 mm) filled with sterile saline to a 27G dental needle (**Fig. 2.1A**). After ensuring that no air bubbles were present in the lines, the appropriate volume of fluid was expelled, the needle was ethanol-swabbed and the CAV-2 vector particles were then loaded by gentle back-suction. The needle was then ethanol-sterilised a second time prior to intraventricular injection.

Using gloves to prevent scent transfer, half of the litter was removed from the dam and identified with a permanent marker. A newborn pup (day 0) was buried approximately 5 cm deep in freshly retrieved ice to induce hypothermia, cessation of respiration and a reduction in neural conduction. Each pup was monitored every 30 sec for a maximum of 2 min until the pup had changed from red/purple to blue/purple and no withdrawal response was observed from a toe pinch. Excess ice was quickly removed and the skull illuminated with a cold light source from below the jaw (**Fig. 2.1B, C**). The bevel of the needle was orientated in the rostral-caudal plane, and was lowered using the stereotaxic frame to target the lateral ventricle (halfway between bregma and lambda, approximately 1 mm bilaterally from the midline, and approximately 1 mm deep) and infused at a rate of 2.5 µL/min using a micro-injector pump. The needle was left within the brain parenchyma for a further 15-20 sec to allow for the dispersal of treatment and then slowly withdrawn from the skull.

Pups were warmed under a heat lamp until the injections of the remaining littermates were completed. The pup was allowed to completely recover before re-anaesthetising and injecting the contralateral hemisphere of the pups in the same order as before. Once the pups were responsive to toe pinches, they were rolled in home cage bedding material and returned to the dam simultaneously to reduce the likelihood of cannibalism. Mice were monitored and weighed daily post-surgery for complications for at least 2-wks post-injection.

2.2.5.2. Perfusion Fixation

Reagent grade 4% PFA (w/v) in PBS (pH 7.4) was prepared fresh each session by stirring overnight at room temperature. Mice were euthanased by carbon dioxide asphyxiation, transferred to a biohazard hood and each limb pinned to a foam board. The abdominal cavity was opened along the midline to expose the heart and a 23G butterfly needle connected to the perfusion apparatus was inserted into the left ventricle.

Figure 2.1: Layout of cryo-anesthesia and newborn injection apparatus. (A) A 25 mL Hamilton syringe fixed in a micro-injector infusion pump was connected via plastic tubing to a 27G dental needle which was secured vertically in the stereotaxic frame. The flexible light guide of the cold light source was positioned beneath the lower jaw to illuminate the skull during the injection procedure. Pups were allowed to recover under a heat lamp on soft toweling material. For the injection of viral vector particles, the equipment was assembled as displayed within a biohazard hood. **(B, C)** The infusion of 0.025% (v/v) Evan's Blue dye diluted in sterile PBS into the lateral ventricle of a newborn pup is shown. The midline, bregma and lambda (arrow) skull sutures are clearly illuminated by the cold light source. Evan's Blue dye is evident in the lateral ventricle of the left hemisphere of the brain. **(D)** Recovery of injected pups under a heat lamp next to a 1 mm scale bar. Texta markings on the right side of the upper pup indicate that this was the fifth pup injected from the litter.

(A)

Cold light source

Heat lamp

Stereotaxic frame

Microinjector pump

(B)

(C)

(D)

30   20   10   0
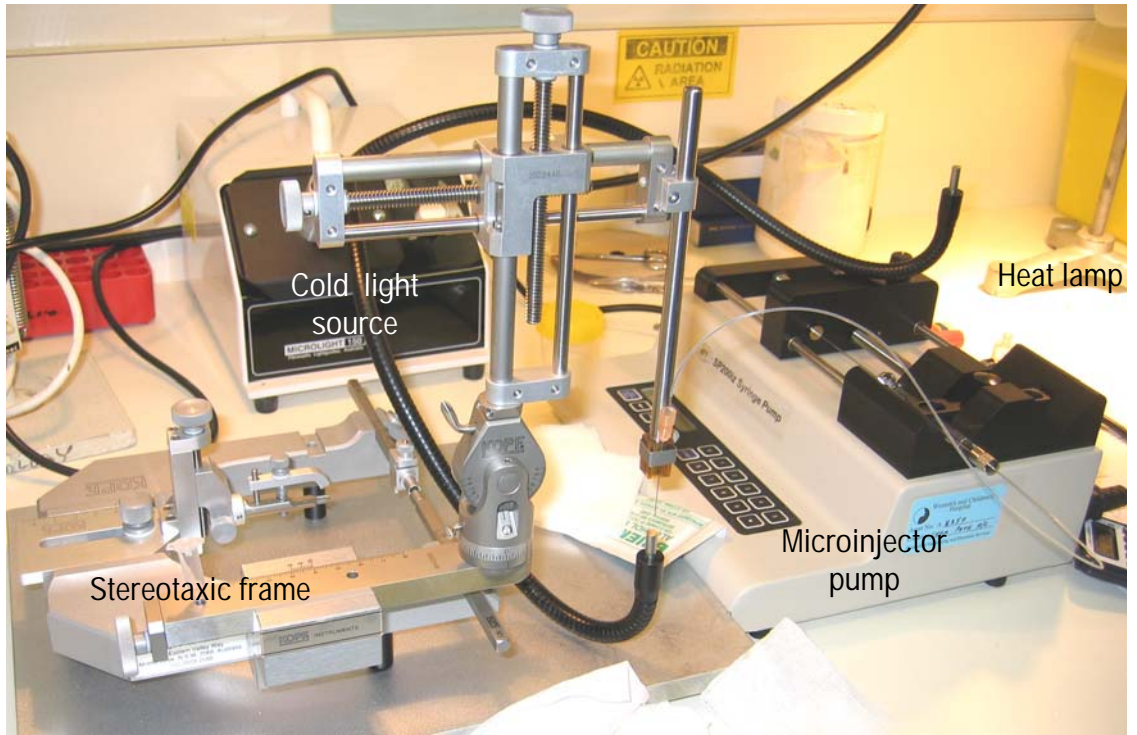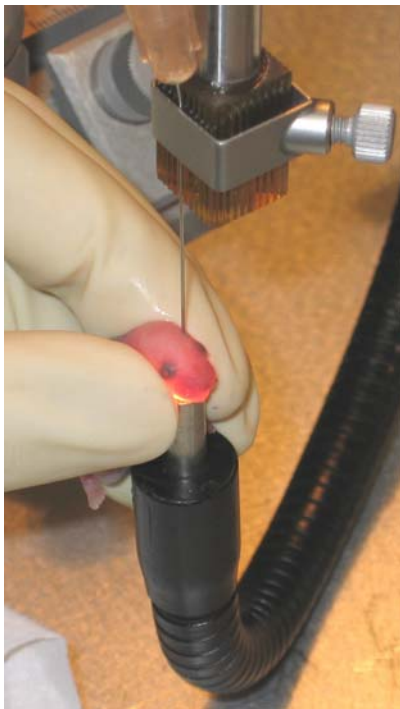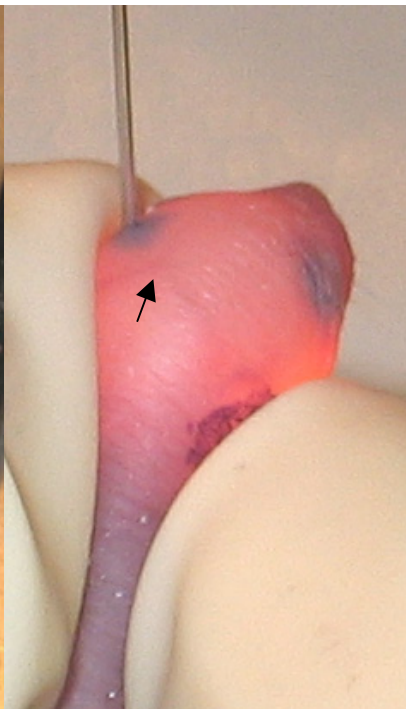
The right auricle was snipped with scissors and whole blood collected for neutralising antibody analysis with a 1 mL syringe. Mice were then perfused with approximately 15 mL ice-cold PBS by gravity flow before switching to cold 4% (w/v) PFA (20-50 mL). The success of the perfusion was monitored by observing stiffening in the torso and tail of the mouse and by twitching of the limbs. After fixation, the brain and peripheral organs (liver, spleen, kidney, lung, heart) were removed and post-fixed in 4% (w/v) PFA overnight at 4°C.

2.2.5.3. Fresh Tissue Collection

Mice were euthanased by carbon dioxide overdose and the brain quickly removed from the skull and chilled in ice-cold saline whilst the peripheral organs were harvested and transferred to 1.5 mL screw-cap Eppendorfs. All tissues were stored on ice. The brain was retrieved, positioned level in a plastic mouse brain matrix (Braintree Scientific) and sectioned in the coronal plane with a flat blade into five 2 mm portions for adult mice (or three 4 mm portions for weanling mice), so that portions 1 and 5 contained the entire olfactory bulb and cerebellum, respectively (**Fig. 2.2**). Each portion was divided along the midline and all tissues were stored at -20°C until ready for further processing.

2.2.6. Histology

2.2.6.1. APES-Coating of Microscope Slides

3-Aminopropyletriethoxysilane (APES)-coated slides were prepared by dipping slides through the following series for 10 sec each: 100% ethanol to remove greasy residues; 2% (v/v) APES; 100% ethanol wash; distilled water. Slides were inspected for a lack of white precipitate and then dried overnight at 37°C.

2.2.6.2. Frozen Sections

Tissue Preparation and Sectioning

Mice were euthanased and perfused as described in **Section 2.2.5.2**. After post-fixing for 24-hrs in 4% (w/v) PFA at 4°C, the tissues were transferred to 30% (w/v) sucrose in PBS and cryo-protected for 24- to 72-hrs at 4°C in the dark. Following this, tissues were embedded in OCT compound and snap frozen in isopentane (*tert*-amyl alcohol)-quenched liquid nitrogen. Blocks were wrapped in alfoil and stored at -70°C.
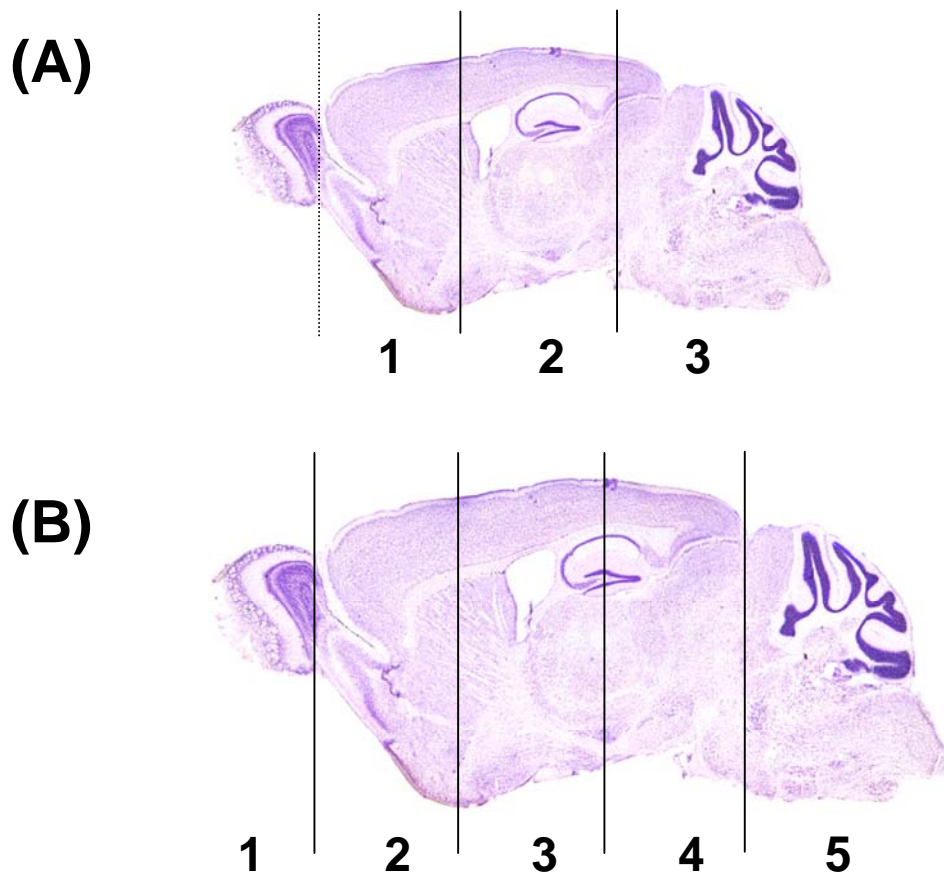
Figure 2.2: Schematic representation of freshly-collected brain tissue. **(A)** Mice were euthanased by decapitation (1-wk) or carbon dioxide asphyxiation (3-wks) and the brains were removed and positioned in the brain matrix so that the olfactory bulb/cerebrum aligned with the first division in the matrix (dotted line). The brain was divided into 3 portions at 4 mm and 8 mm from the first division (solid lines) and along the midline. **(B)** After carbon dioxide asphyxiation, the brains of 6-, 10- or 20-wk-old mice were removed and positioned in the brain matrix so that the olfactory bulb/cerebrum aligned with the first division in the matrix. The entire olfactory bulb of each hemisphere was designated as portion 1 and the subsequent divisions were spaced 2 mm apart and along the midline to divide the brain into 10 portions in total.

For sectioning, cryo-blocks were warmed to $-10°C$ to $-12°C$ prior to cutting and sectioned at 12 μm in the sagittal plane. Sections were collected on to APES-coated slides and air-dried. Sections were stored in slide boxes at -70°C.

Immunofluorescent GFP Staining in Paraformaldehyde-Fixed, Frozen Tissue

All incubations were conducted in a humid chamber at room temperature. Sections were washed in 0.3% (v/v) Triton X100 in 1x PBS (PBSTX) for 5 min to remove OCT and then blocked in 10% (v/v) normal donkey serum (NDS) in PBSTX for 1 hr. The sections were then incubated overnight in polyclonal rabbit anti-GFP (1:10,000) diluted in 10% (v/v) NDS diluted in PBSTX.

After 3 washes in PBSTX (5 min each), tissues were incubated in dark conditions for 1 hr with donkey anti-rabbit-Cy3 IgG (1:600). After an additional three washes in PBSTX (10 min each), excess fluid was drained and the sections mounted in Vectashield mounting media containing the nuclear stain 4',6-diamidino-2-phenylindole (DAPI). Stained sections were stored at 4°C in the dark until ready for analysis. Immunopositive brain regions were visualised on an Olympus BX40 microscope fitted with Cy3, FITC and DAPI filters (excitation/emission wavelengths 510/550 nm, 470/490 nm and 330/385 nm, respectively) and compared to a Mouse Brain Atlas (Paxinos and Franklin, 2001) to determine the location of GFP-expressing cells.

2.2.6.2. Paraffin Sections
Tissue Preparation and Sectioning

Animals were euthanased and perfusion-fixed with 4% (w/v) PFA by cardiac puncture (**Section 2.2.5.2**). An incision was made along the midline of the brain and tissues were embedded in paraffin wax by staff in the Department of Histopathology, CYWHS. Tissues were sectioned at 4-6 μm on a Leitz rotary microtome (model 1512; Germany) by members of the Department of Histopathology or by Mrs Helen Beard (LDRU), collected onto APES-coated slides and stored at room temperature.

Immunohistochemical Staining of EM-Fixed, Paraffin-Embedded Tissues

All methods described under this subheading were developed and optimised by Mrs Helen Beard (LDRU). Mrs Hanan Elmassih (LDRU) performed the immunohistochemical staining.

Prior to immunostaining, sections were dried for 15 min at 60°C. Brain sections from MPS IIIA mice (~13-wks-old) were employed as positive immunostaining controls. The same tissue sections were used as a negative staining controls, with the primary antibody omitted and blocking solution used in its place. The slides were then de-waxed in xylene twice and cleared in absolute ethanol 3 times (2 min each). The endogenous peroxidase activity was inhibited for 30 min by incubating in 0.5% (v/v) hydrogen peroxidase diluted in methanol. Tissue sections were washed/rinsed by incubating in 3 changes of the appropriate wash buffer for 5 min each. All incubations were conducted at room temperature unless otherwise stated.

Glial Fibrillary Associated Protein (GFAP)

Paraffin-embedded tissues were dried, de-waxed and cleared as described above. After inhibiting endogenous peroxidase activity and washing in 1x PBS, the tissues were subjected to antigen retrieval in citrate buffer by boiling for 2-3 min on high power using a Panasonic microwave oven (model no. NN-5676WA, input 1600 W) followed by medium/low power for a further 10 min. After cooling to less than 50°C, the tissues were washed in 1x PBS and blocked for 2 hrs in 5% (v/v) NDS, 1% (w/v) BSA, 0.1% (v/v) cold water fish skin gelatin in 1x PBS (block solution). The tissues were then incubated overnight with polyclonal anti-GFAP (1:13,000) diluted in the block solution.

After rinsing in 1x PBS, the sections were incubated with biotinylated donkey anti-rabbit IgG (1:800 diluted in 1x PBS) for 2 hrs, washed in 1x PBS and incubated with Vector ABC Reagent for 1 hr. The slides were rinsed in 1 x PBS and detected with Vector VIP reagent for 2-10 min before the reaction was stopped by immersion in water. The tissues were then dehydrated/cleared through 3 changes of absolute ethanol and 2 changes of xylene before cover-slipping with Permount mounting media.

Isolectin B₄

Tissue sections were dried, de-waxed, cleared and blocked for endogenous peroxidase activity. After rinsing in 1x Tris buffer, the antigens were retrieved by incubating the sections in trypsin working solution at 37°C for 15 min followed by cooling for 10 min at room

temperature. Following 3 rinses in 1x Tris buffer, the sections were incubated in peroxidase-conjugated isolectin B_4 (1:80 diluted in 1x Tris buffer) from 3 hrs to overnight.

The excess isolectin B_4 was removed by washing in 1x Tris buffer and rinsing once in 1x PBS. The sections were then incubated in Vector VIP substrate (prepared according to the manufacturer's instructions) for 2-10 min. After immersing the slides in water, the sections were dehydrated, cleared and mounted using Permount mounting media.

2.2.6.3. Epoxy resin embedding

All tissues were processed, embedded and sectioned by Ms Lyn Waterhouse from Adelaide Microscopy, Adelaide, Australia.

Mice were perfused with EM fixative (4% (w/v) PFA, 1.25% (v/v) glutaraldehyde, 4% (w/v) sucrose, pH 7.2; Adelaide Microscopy) at 20-wks post-injection. Brains were divided along the mid-line and one hemisphere was coronally-sliced at 3 and 4 mm from the olfactory bulb using a brain matrix. The hemi-coronal brain slice was further trimmed into approximately 1 mm x 2 mm x 2 mm portions containing the intact lateral ventricle, parts of the corpus callosum, striatum and cortex. The tissues were post-fixed in 1% (w/v) osmium tetroxide, dehydrated through a graded ethanol series and embedded in epoxy resin (100% Epon–Araldite). Semi-thin sections (1 μm) were stained with toluidine blue in 1% (w/v) borax and were assessed via light microscopy by an operator blinded to the treatment and genotype of each mouse.

For semi-quantitative analysis of storage inclusions in 20-wk-old MPS IIIA mice treated with PBS or CAV-NS (n=2/group; n=12 in total), 5-7 random fields of view were captured at 100x magnification from layers II-III ("surface") or layers V-VI ("deep"). Pale neurons, dark neurons (possibly a processing artefact indicating dying neurons) and glial cells (a mixed population of microglia and oligodendrocytes identified by a dark, punctate nucleus and their small cell size) were scored for the presence or absence of inclusions (> 2 white "bubbles" per cell as described in Chung *et al*, 2007) and the statistical significance of the data assessed using unpaired t-tests.

2.2.6.4. Metamorph® Quantification of Immunohistochemical Staining

Paraffin-embedded tissue sections were immunohistochemically batch-stained (n=2 sections/mouse; n=2 mice/group) as detailed in **Section 2.2.6.2**. Representative images were captured of the ependymal layer of the lateral ventricle (adjacent to the cortex; magnification

20x) or the granular (isolectin B_4-staining) or glomerular layer (GFAP-staining) of the olfactory bulb (magnification 40x) using identical microscope settings (exposure of $^1/_{10,000}$ sec).

Due to the fibrillar nature of the astrocytes, the percentage of immunopositive GFAP-staining area (in μm^2) was calculated with Metamorph® software (from the Meta Imaging Series® software series; Molecular Devices, USA). In brief, images were converted from pixels to μm^2 areas, made flat to adjust for illumination differences and changed to monochrome using automated programs in the software by an operator who was blind to the treatment and genotype of the tissues. Immunostained areas were selected ("thresholded") before being converted to binary format. After removing single pixels, the images were converted to 8-bit formats and the brain tissue (i.e. the "region of interest") was selected, excluding 2-3 cell widths from the edge of the tissue to eliminate edge-staining artefacts. The percentage of immunostained area was calculated automatically by the software.

For the estimation of isolectin B_4-expressing cells per tissue area, an examiner blind to the genotype and treatment status of the sections counted individual isolectin B_4-positive cells manually. The surface area of the tissue was calculated using Metamorph® software and data were expressed as isolectin B_4-expressing cells/area in mm^2.

2.2.7. Fluorescent In Situ Hybridisation

All methods in this section were developed, optimised and conducted in conjunction with Ms Helen Eyre (Department of Genetic Medicine, CYWHS, Australia).

2.2.7.1. Cell Smear Preparation

Human 293 kidney cells were transduced with CAV-GFP at 1000 particles/cell and incubated at 37°C with 5% carbon dioxide for 2-days. After verification that cells were GFP-positive using an inverted fluorescent microscope, cells were detached with 10% (v/v) trypsin, pelleted and then washed once in 1x PBS. The cell pellet was then fixed in 3 parts methanol : 1 part acetic acid (500 µL) and two drops of the cell suspension were applied to microscope slides which had been de-greased in methanol. The cell smears were then subjected to staining by FISH.

2.2.7.2. Fluorochrome-labelling of Probe

Midi Prep-quality plasmid DNA of the pCAV-NS vector was prepared as described in **Section 2.2.1.1.** For fluorophore-labelled probe, 1 μg of plasmid DNA was incubated at 15°C for 16 hrs according to the instructions provided in the Vysis nick translation kit, in a total volume of 50 μL.

After Spectrum Green or Spectrum Orange-labelled dUTP was incorporated, the DNA was precipitated with 25 μL of 10 mg/mL salmon sperm DNA, 7.5 μL of 3 M sodium acetate (pH 5.5) and 207.5 μL 100% ice-cold ethanol for 3 hrs at -70°C. The DNA was then centrifuged at 17900 x g for 15 min in a refrigerated centrifuge, and the pellet washed in 900 μL 70% (v/v) ethanol for 2 min. The supernatant was then carefully removed and the DNA pellet desiccated for 30 min before resuspension in 45 μL of Tris-EDTA buffer (pH 7.0) to give a final probe concentration of 20 ng/mL. Labelled probe was stored at -20°C and kept in the dark at all times to prevent photo-bleaching.

Prior to hybridisation, the appropriate volume of labelled probe (6 μL/section) was desiccated in a SpeediVac for approximately 10 min before resuspension in 3 μL of Kievet's hybridisation mix. The probe was then heated at 60°C for 20 min and then directly added to the tissue sections as detailed below.

2.2.7.3. Hybridisation and Direct Detection of DNA Probe in Paraffin Sections

FISH was performed according to modified protocols from standard methods used in the Department of Genetic Medicine, CYWHS, Australia, and the Krause Laboratory (http://info.med.yale.edu/labmed/faculty/labs/krauselab/ychrom_frozen.html). All incubations were performed at room temperature in a humidified chamber unless stated otherwise.

PFA-fixed, paraffin-embedded mouse tissue was de-waxed by agitating sections for 2 min each in coplin jars through the following series: xylene; xylene; 100% ethanol; 100% ethanol; 70% (v/v) ethanol; water. The tissue was then pre-treated in 100 μL FISH proteinase K buffer supplemented with 10 μL of 10 mg/mL proteinase K, cover-slipped and incubated in a humid chamber for 1 hr at 37°C to increase the accessibility of the DNA probe to the nucleus.

Tissue sections were washed in 2x SSC (3 min) prior to and between each pre-treatment. Sections were immersed in 0.2 M HCl for 20 min, washed and treated with 1 M sodium thiocyanate at 75-80°C in a humid chamber for 20 min. After further rinsing, the labelled probe (or negative control containing only Kievet's hybridisation mix without DNA)

was added to the tissue, cover-slipped and sealed with rubber cement (Maruni Earth). The DNA probe was hybridised at 78°C on a flat-bed PCR machine for 30 min before the slides were transferred to a humid chamber for overnight incubation at 37°C.

Coverslips were removed and the slides rinsed in Post-hybridisation Wash 1 for 2 min at 73°C, and then a 1 min wash in Post-hybridisation Wash 2 at room temperature. Sections were mounted in anti-fade medium containing a DAPI counterstain, and slides were stored in the dark at room temperature until ready for image analysis.

2.2.7.4. Detection of Biotin-labelled Probe

For sections that had been hybridised with a biotinylated probe, the first day of the protocol was performed as described in the previous section. Following the post-hybridisation washes, the slides underwent a wash in 4x SSC with 0.05% (v/v) Tween20 before non-specific binding in the tissue sections was blocked by a 10 min incubation in 4x SSC with 1% (w/v) BSA (100 µL per slide).

The tissues were then treated with Avidin FITC (1:400 diluted in block solution; 100 µL per slide) for 20 min and washed in 4x SSC with 0.05% (v/v) Tween20. If amplification of signal was required, slides were incubated for 20 min with biotinylated goat anti-Avidin (1:500 diluted in block solution) and washed in 4x SSC with 0.05% (v/v) Tween20 for 5 min before repeating the Avidin FITC treatment. After a final rinse in 2x SSC for 1 min, the sections were mounted with anti-fade medium containing DAPI and stored at room temperature in the dark.

2.2.8. Mass Spectrometry

Tissues were collected as described in **Section 2.2.5.3** and stored at -20°C. The wet weight of each tissue portion was determined before the tissue was transferred to a 10 mL tube containing 1 mL of ice-cold tissue homogenisation buffer. Brain tissue was homogenised using an UltraTurrax T25 IKA-Labortechnik homogeniser (Janke and Kunkel, Germany) at 8000 rpm for 30 sec, and then rinsed with an additional 0.5 mL of buffer.

Homogenates were sonicated twice at output control 2 for 15 sec each, transferred to 1.5 mL tubes and then centrifuged at 17900 x g for 5 min at 4°C. The total protein content of the supernatant was assessed (**Section 2.2.13**). One hundred µg of total protein was then lyophilised overnight and stored at -20°C.

Oligosaccharides were derivatised with 1-phenyl-3-methyl-5-pyrazolone (PMP) by Mrs Barbara King (LDRU) according to the method of King *et al.* (2006). The concentration of the disaccharide HNS-UA was determined using a PE Sciex API 3000 triple–quadrupole mass spectrometer by Dr Maria Fuller (LDRU). The relative amounts of HNS-UA were determined by relating the peak height to a chondroitin sulphate disaccharide internal standard (ΔUA-GalNAc4S).

2.2.9. Detection of Neutralising Antibodies Against CAV-2

This method was based on the conditions described by Perreau and colleagues (submitted). The CellQuest software settings were optimised by Dr Greg Hodge, and technical advice was provided by Mr Vaughn Williams and Mr Adrian Griffiths (Department of Haematology, CYWHS, Australia).

Whole blood samples were collected into 1.5 mL screw-capped Eppendorfs using a 1 mL syringe and stored on ice during tissue processing. Sera were separated by centrifugation at 17900 x g for 5 min at room temperature and the complement inactivated by heating at 56°C for 30 min.

DKCre cells were seeded into 24-well plates at 1 x 10^5 cells/well and cultured overnight. Sequential 1:2 dilutions of sera in media were performed in a volume of 10 µL. Each dilution was then mixed with $TCID_{20}$ of CAV-GFP (10 particles/cell) in 10 µL for 10 min at 37°C so that the final concentration ranged from 1:2 to 1:512. The pre-absorbed vector particle mix was then applied to DK cells, mixed on "The Bellydancer" for 30 min and then cultured at 37°C. A CAV-2-immunised, normal dog serum was used as a positive control, and quadruplicate CAV-GFP vector without sera and untransduced samples were also included.

The following day, cells were detached in 150 µL trypsin per well, triturated to a single cell suspension and neutralised with an equal volume of DMEM containing 10% (v/v) FCS. Greater than 10,000 gated DK cells were acquired on a FACScalibur (Beckton Dickson) and analysed using CellQuest software (version 3.1). Forward and side scatters were adjusted to gate viable, unaggregated DKCre cells. The M1 level was set so that the untransduced DK cell control was set at 0.1% GFP-positive events in the gated population. Data were plotted as dot plots of forward scatter (FSC) versus log GFP intensity, and as a histogram of counts versus log GFP intensity. The percentage of gated, GFP-positive cells was measured and the inverse of the highest dilution, where there was a 50% reduction of GFP-positive cells, was

reported as the neutralising antibody titre. Significant neutralising antibody titres were classified as ≥ 16.

2.2.10. ELISA Detection of Anti-rhNS Antibodies

This method was established and optimised by Drs Dyane Auclair and Kim Hemsley (LDRU).

Immulon® 4 HBX wells were coated overnight at 4°C with 5 µg/mL rhNS protein diluted in 100 mM NaHCO$_3$ in a volume of 100 µL/well. Wells were washed 4 times with wash buffer using a microtitration plate washer (ADL Instruments, France). Non-specific binding was inhibited by incubating for 2 hrs at room temperature in freshly prepared blocking solution.

The blocking solution was drained and dilutions of sera serially diluted in blocking solution (total volume 200 µL/well) were allowed to bind at room temperature for 2 hrs. Buffer-only negative control wells and a positive sera sample from a mouse receiving rhNS ERT therapy (MPS 34) were included in each assay. Wells were washed as before (Program 7) and captured antibodies were detected by incubation for 1 hr at room temperature with horse-radish peroxidase-conjugated sheep anti-mouse antibody (1:1000). After washing 4 times, the chromogen was developed using 100 µL/well of freshly prepared ABTS substrate. The optical density at 405 nm was measured after 20 min.

Significant titres were classified as being the inverse of the highest dilution that was >2 standard deviations above mean background absorbance values.

2.2.11. DELFIA Detection of Human Sulphamidase Protein

Dr Caroline Dean, Ms Debbie Lang and Dr Peter Meikle (LDRU) were very generous in providing helpful discussions and reagents in the optimisation of this method.

Immulon 4 HBX wells were coated with 5 µg/mL polyclonal sheep anti-rhNS antibody diluted in 100 mM NaHCO$_3$ (filter-sterilised, pH 8.5) in a volume of 100 µL/well. Plates were incubated overnight at 4°C.

Excess capture antibody was removed by washing twice with DELFIA wash buffer (Perkin-Elmer Life Sciences, USA; Program 3) using a DELFIA plate washer (model 1296-026, Perkin-Elmer Life Sciences, USA). Duplicate brain homogenates diluted in DELFIA

assay buffer were assayed at two concentrations (1:2, 1:4) in a total volume of 50 µL/well. Normal mouse brain homogenate (total protein 1 mg/mL) spiked with 2 ng or 4 ng purified rhNS served as a positive control. A row of negative controls (n=12) was included on each plate. Purified rhNS diluted in assay buffer (0 to 5 ng in duplicate) was used as a standard curve. Fifty µL/well of the detection antibody, europium-labelled sheep anti-rhNS antibody (0.4 µg/mL diluted in DELFIA assay buffer), was added and mixed for 15 min in the dark on a Milenia plate shaker (Micromix 4, Diagnostic Products Corporation, The Netherlands). The plates were then incubated overnight in the dark at 4°C.

Wells were washed 6 times with DELFIA wash buffer (Program 2) before 200 µL of enhancement solution was added to each well. After shaking the wells at setting 5 for 10 min in the dark, the europium counts were detected on a DELFIA 1234 Research Fluorometer (Program 116) and the concentration determined using a Spline fit program. Readings were considered significant if they were more than 2 standard deviations above the mean of the blank wells.

2.2.12. Sulphamidase Activity

NS activity was measured using a tritated, heparin-derived tetrasaccharide substrate, as described in Hopwood and Elliott (1982). This substrate, glucosamine-N-sulphate-(1,4)-iduronic or glucuronic acid-(1,4)-glucosamine-*N*-sulphate-(1,4)-[1-^{3}H]idonic, gulonic or anhydro idonic acid is converted to glucosamine-(1,4)-iduronic or glucuronic acid-(1,4)-glucosamine-*N*-sulphate-(1,4)-[1-3H]idonic, gulonic or anhydro idonic acid in the presence of NS activity.

For cell samples, conditioned media and cell lysates were harvested as described in **Section 2.2.2.3**. In general, 100-200 µL of conditioned media was dialysed in more than 2 L of 0.9% (w/v) NaCl through a 10 kDa membrane at 4°C overnight. For brain homogenates, 50 µL of sample was dialysed in 2 L of sodium acetate, pH 5.2, overnight at 4°C.

A master-mix consisting of 1 µL of tetrasaccharide substrate (350-450 pmol/µL), 3 µL of 0.2 M sodium acetate, pH 5.2, and 7 µL water was prepared on ice. One µL of sample was added, and tubes were incubated at 60°C for 4 hrs. For tissue homogenates where NS activity was very low, 11 µL of dialysed sample was mixed with 1 µL of tetrasaccharide substrate and incubated for 16 hrs at 60°C.

Reactions were halted by the addition of 100 µL of 100 mM ammonium hydroxide and the samples were then analysed using HPLC-GINA Star^{TM} software (version 2.18;

Raytest, Staubenhardt, Germany) on a Hewlett Packard Series 1100 HPLC with Packard 150 TR Flow Through Scintillation Analyser. NS activity was determined using the following equation and normalised to total protein content (**Section 2.2.13**).

$$\text{NS activity (pmol/min/mg)}=$$

$$\frac{[(\text{product cpm}_{test} / \text{total cpm}_{test})-(\text{product cpm}_{blank} / \text{total cpm}_{blank})] \times [\text{pmol of substrate per reaction}]}{[\text{time in min}] \times [\text{sample volume in mL}] \times [\text{total protein concentration in mg/mL}]}$$

2.2.13. Total Protein Determination

Cell extracts, lysates or tissue homogenates were assessed for total protein content using a commercial MicroBCA kit according to the manufacturer's instructions. In brief, duplicate samples (5-10 μL for cell samples; 5-15 μL for brain homogenates) were made up to a total volume of 100 μL with water for injection in non-protein-binding 96-well plates. A standard curve ranging from 1 to 20 μg of bovine serum albumin per well was also included on each plate. One hundred μL of MicroBCA working reagent was added to each well, covered and incubated at 37°C for 2 hrs. The absorbance was determined at 560 nm on a Multilabel Counter Victor3 (Perkin Elmer 1420, USA), transformed using a cubic Spline fit and the protein concentration of each well was determined. Samples were repeated if the duplicate values had a coefficient of variation greater than 10%, or if the protein concentration at the selected dilution factor did not fall between 2 and 16 μg on the standard curve.

CHAPTER 3:

Construction, Purification and *In Vitro* Characterisation of CAV-NS

3.1. INTRODUCTION

As described in detail in **Chapter 1**, the potency of gene therapy for LSD lies in the ability of transduced cells to continuously produce and secrete recombinant enzyme into the extracellular milieu. M6P-mediated delivery of the lysosomal enzyme to neighbouring cells has the potential to enhance the spread of treatment, which is a highly desirable trait in diseases displaying global pathology.

To begin the assessment of CAV-2 vectors as a therapy for MPS IIIA, it was necessary to generate a vector encoding NS, the enzyme deficient in this disorder. Because of the difficulty in producing HD CAV-2 vectors, a technically less-demanding, first-generation ΔE1 CAV-2 vector capable of expressing NS was first generated to provide preliminary proof-of-concept data before proceeding with the construction of HD CAV-2 vectors.

Murine and human NS share 88% identity and 93% similarity (Costanzi *et al*, 2000), and the recombinant proteins have been purified and characterised (Bielicki *et al*, 1998; Gliddon *et al*, 2004). Previous studies undertaken within the LDRU have assessed the therapeutic efficacy of rhNS in MPS IIIA mice (Gliddon and Hopwood, 2004; Savas *et al*, 2004; Hemsley *et al*, 2007), and given that the two NS homologues displayed similar properties, we selected the rhNS transgene over the murine NS to allow comparisons with these experiments. Additionally, the rhNS gene was preferred in view of the fact that the long-term objective of this project was to utilise CAV-2 vectors as a gene transfer strategy in the MPS IIIA dog model and, eventually, in human patients. In addition to rhNS, the GFP transgene was included to provide a valuable fluorescent marker gene to improve the monitoring of transduction efficiency and to allow the real time observation of transgene expression.

The major aims of the experiments conducted within this chapter were to construct, purify and titrate a ΔE1 CAV-2 vector that expressed rhNS, and to characterise and evaluate the therapeutic efficacy of this vector *in vitro* by assessing NS activity, sulphated GAG concentrations, processing pathways and transduction efficiencies in a variety of cell types.

3.2. SPECIFIC METHODS

3.2.1. Preparation and Verification of CAV-NS Vector DNA

The preparation of the ΔE1 CAV-NS vector was the continuation of a PhD project by Dr Nadia Skander from the IGMM, France, under the supervision of Dr Eric Kremer. Consequently, the sub-cloning of the rhNS-IRES-EGFP insert into the pTCAV-12VK vector and the transformation of the pTCAV-NS and pTG5412 plasmids into BJ5183 E. coli *were conducted by Dr Skander. All other methods described in this chapter were performed by Ms Adeline Lau.*

3.2.1.1. Recombination in BJ5183 and DH5α *E. coli* Strains

A defined nomenclature exists for plasmids used in the generation of ΔE1 CAV-2 vectors. All items containing the prefix "p" are plasmid DNA. The two plasmids that are required for recombination are denoted either with the prefix "pTG" (plasmid encoding the CAV-2 viral genome obtained from <u>T</u>rans<u>G</u>ene SA) or "pT" (indicating a transfer plasmid containing the expression cassette of interest). When recombined into a single plasmid ready for amplification, the plasmid has the prefix "pCAV" and after being amplified in trans-complementing cells the CAV-2 vector particles are denoted by the prefix "CAV".

Two plasmids are required to generate ΔE1 CAV-2 vectors. The first vector, pTG5412, was constructed by TransGene SA (France) and contains the entire CAV-2 genome (Genbank accession no. J04368) flanked by *Not*I linkers, cloned into a pPolyII backbone (**Appendix**). This 33375 bp plasmid contains a unique *Swa*I site within the E1 region at position 1027 and is ampicillin-resistant.

The second plasmid, pTCAV-12VK, is a transfer plasmid derived from the pTCAV-12a plasmid, modified to contain the kanamycin/neomycin gene in the *Fsp*I site of the ampicillin gene to reduce the level of background transformation during the recombination (**Appendix**). This plasmid was 5155 bp in length and also contained a CAV-2-inverted terminal repeat (ITR) sequence, poly A signal, multiple cloning site (MCS), intervening sequence (IVS), cytomegalovirus (CMV) early region enhancer/promoter, simian virus 40 (SV40) intron with a splice donor and acceptor sites and the CAV-2 E2B region (bp 2898 to 5298). The desired transgene expression cassette can then be subcloned into the MCS of the pTCAV-12VK vector and, when combined with the pTG5412 vector, undergoes homologous recombination in the CAV-2 E2B region and either the pPolyII backbone or the ITR to replace the E1 region, thus rendering the vector replication-defective.

In vivo homologous recombination was employed as previously described to produce the recombined plasmid, pCAV-NS (Chartier *et al*, 1996; Kremer *et al*, 2000). The rhNS transgene (GenBank accession no. U30894) was excised from the pcDNA3.1- vector with *Eco*RI and sub-cloned into the *Eco*RI site in the multiple cloning site of the pIRES2-EGFP vector (Clontech, cat. no. 6029-1) forming pNS-IRES using standard molecular biology methods (**Sections 2.2.1.2** to **2.2.1.6, 2.2.1.1**, in sequence). The rhNS-IRES-EGFP insert sequence was removed by digesting pNS-IRES with *Not*I, blunting with Klenow fragment and then digesting with *Nhe*I. This fragment was then ligated into the multiple cloning site of the pTCAV-12VK transfer vector by digesting with *Nhe*I and *Eco*RV (a restriction enzyme forming blunt ends) to form pTCAV-NS.

One hundred ng of pTCAV-NS was linearised with *Ssp*I, mixed with approximately 100 ng of *Swa*I-linearised pTG5412 vector, transformed into rec$^+$ BJ5183 *E. coli* by heat-shock or electroporation (**Sections 2.2.1.6** and **2.2.1.7**) and plated on ampicillin-selective plates. Control transformations included pTG5412 (*Swa*I), pTCAV-NS (*Ssp*I) and transformations containing no DNA. When the background level of transformation was low (as determined by the growth of few bacterial colonies on the *Swa*I-linearised pTG5412 control plate), small-sized colonies were selected and screened by PCR (**Section 3.2.1.2**). Small-sized colonies were likely to have a reduced growth rate because of successful transformation with the large recombined plasmid.

Stab cultures of positive recombinants were used to streak LB plates and to prepare 5 mL starter cultures. Mini Prep DNA extractions were performed and the DNA digested with *Eco*RI to confirm that the recombinants had the expected DNA fragment pattern. Following this, high-quality DNA was extracted by Midi Prep and used to transform the rec$^-$ *E. coli* strains, XL1Blue, Top10 or DH5α, to obtain stable bacterial cell lines. Glycerol stocks were prepared and stored at -20°C.

3.2.1.2. PCR Screening of Recombinant Colonies

The forward 5'CMV primer (5' GAAAGTCCCTATTGGCGTTAC 3') binds to the CMV promoter of the transgene on the shuttle plasmid pTCAV-NS, and the reverse 3'E2B primer (5' TCAAGCTAAAGTGTACCAAG 3') binds to the CAV-2 E2B region of pTG5412. Consequently, an 845 bp PCR product will only be generated in recombinant clones. A master-mix was prepared on ice, as described below, and 20 μL aliquoted per tube. Sterile toothpicks were used to scrape small, well-isolated, bacterial colonies under aseptic conditions and used to prepare a stab culture in LB plates containing ampicillin and then

placed into the PCR tubes for approximately 2 min. A positive control (1 ng of recombinant DNA or a bacterial colony from a ΔE1 CAV-2 vector encoding β-glucuronidase) and a negative control were included with each PCR. After an initial denaturation step at 95°C for 5 min, the DNA was amplified by 35 cycles of 95°C for 30 sec, 55°C for 40 sec and 72°C for 90 sec, with a final extension cycle at 72°C for 5 min.

10x PCR buffer (Invitrogen)	2 μL
20 mM MgCl$_2$	0.6 μL
2.5 mM dNTPs	1.6 μL
5' CMV primer (10 μM)	1 μL
3' E2B primer (10 μM)	1 μL
Taq polymerase (5U/μL)	0.2 μL
Water	<u>13.6 μL</u>
MASTER-MIX VOLUME	20 μL

Ten μL of PCR product was electrophoresed through a 1% (w/v) agarose gel and visualised by ethidium bromide staining.

3.2.2. Transfection of DK Cells with Recombinant Plasmid DNA

3.2.2.1. Preparation of DNA

High quality pCAV-NS DNA was digested overnight with *Asc*I and *Not*I to excise the pPolyII backbone and free the ITR regions, and complete digestion was confirmed by electrophoresis. The digested recombinant pCAV-NS DNA or control circular plasmids (pIRES2-EGFP, pTCAV-NS, pCAV-NS) were sterilised by ethanol precipitation by gently mixing with 2x vol 100% ice-cold ethanol and 0.1x vol 3 M sodium acetate, pH 5.0. The DNA was pelleted at 17900 x *g* for 10 min at room temperature and sterilised with 250 μL 70% (v/v) ethanol (17900 x *g* for 5 min). DNA was air-dried in sterile conditions and then resuspended in OptiMEM media at a final concentration of 5 μg in 250 μL.

3.2.2.2. Transfection

DKZeo and DKCre cells were utilised interchangeably in some of the experiments described in this chapter and are referred to DK cells. DK cells were passaged the day before transfection and seeded at 1 x 10^6 cells/well in 6-well trays. Two wells were required for each treatment (A and B). For pCAV-NS, three sets of wells (i.e. 6 wells in total) were required due to the large plasmid size and low transfection efficiency of DK cells. Lipofectamine 2000 (22.5 μL) was diluted in 227.5 μL OptiMEM Reduced Serum Medium per treatment and

incubated at room temperature for 5 min. For each treatment, 5 μg of sterile DNA in 250 μL OptiMEM media was mixed with the diluted Lipofectamine, giving a final concentration of 4.5 μL Lipofectamine per μg of DNA, and allowed to complex at room temperature for 20 min.

Meanwhile, DK cells were washed once with OptiMEM and the media replaced with 1.5 mL OptiMEM. The Lipofectamine-DNA complexes were added to Well A for each treatment, bringing the total volume to 2 mL. Cells were incubated for 5 hrs at 37°C before the Lipofectamine-DNA media ("complex media") was transferred from Well A to Well B, bringing the total volume to 4 mL in Well B (2 mL original media plus 2 mL "complex" media). Transfected cells in Well A were fed with 2 mL DMEM/10% (v/v) FCS media/well and cultured overnight at 37°C. After 24 hrs, the media was changed in all wells to DMEM/10% (v/v) FCS containing penicillin/streptomycin. The transfection efficacy was monitored by daily viewing of GFP-positive cells in control treatments using an inverted fluorescent microscope.

3.2.3. Amplification of E1-Deleted CAV-2 Vectors from Plasmid DNA

DK cells, which are E1-trans-complementing, were transfected as detailed in **Section 3.2.2.2**. Four- to 5-days post-transfection, the cells transfected with linearised, recombined plasmid DNA were harvested by scraping into the conditioned media using a rubber policeman and pooled into a 50-mL Falcon tube. The lid of the tube was sealed with parafilm to prevent ethanol leaks from potentially inactivating the viral capsid. The vector particles were liberated by three alternate cycles of freezing in a dry ice/100% ethanol slurry and heating in a 37°C water bath, with vortex mixing after each thaw step.

Membrane debris was removed by centrifuging at 2770 x *g* for 10 min and 90% of the supernatant containing viral particles was added to 3×10^6 DK cells plated the previous day. Cells were incubated at 37°C with continuous rocking overnight and the cells were fed with DMEM containing 10% (v/v) FCS and penicillin/streptomycin the following morning. Cells were monitored for GFP expression at regular intervals using an inverted fluorescent microscope. Ten percent of the vector-supernatant was stored at -20°C in case of contamination in the cell culture at each stage.

Thirty to 36 hrs post-inoculation, cells were harvested and freeze/thawed as detailed in the previous paragraph, and seeded on successive rounds of DK cells plated at densities of 3×10^6 cells in a 10 cm plate (rounds 2 and 3). When high numbers of GFP-positive cells were

evident, a "pre-stock" was prepared by inoculating 10 plates (10 cm each) seeded at 5 x 10^6 cells. After verifying that all plates were GFP-positive, a large-scale vector preparation was performed by inoculating 30 plates (15 cm each) seeded at 8 x 10^6 DK cells with vector-supernatant from the pre-stock. Cells were viewed under a light microscope to determine whether a cytopathic effect was evident, as seen by a dark 'halo' effect around the nuclei due to the accumulation of vector particles (**Fig. 3.1**).

The cells/conditioned media suspension from all plates were pelleted in 4 x 50 mL tubes at 250 x g for 5 min and the final pellets resuspended in a total volume of 45 mL. Cells were freeze/thawed and clarified as before and then purified on a caesium chloride gradient (**Section 2.2.3.2**). The CAV-NS vector preparation was shipped from France to the CYWHS (Australia) on dry ice.

At the CYWHS, 5 μL of neat viral stock used in the large-scale *in vivo* study (in duplicate, **Chapter 6**) or in the *in vitro* studies (this chapter) were diluted 1:20 with endotoxin-free water and assessed according to the method of Mürer and colleagues (1975) for the presence of contaminating endotoxin.

3.2.4. Adenoviral DNA Extraction

Viral DNA was extracted from purified CAV-2 vector band fractions (He, 2004). CAV-NS vector (250 μL) was gently mixed by inversion with 4x vol proteinase K solution (1 mg/mL proteinase K, 50 mM Tris-HCl, 1 mM EDTA, 0.5% (w/v) SDS) and incubated at 37°C for 1 hr without agitation to prevent the shearing of DNA.

DNA was extracted twice with 2x vol phenol:chloroform (1:1), and the aqueous and phenol layers separated by centrifugation at 17900 x g for 5 min at room temperature. The upper, aqueous layer was then extracted with 1x vol chloroform and centrifuged at 17900 x g for 5 min at room temperature. Viral DNA was precipitated with 0.1x vol 3 M sodium acetate and 2x vol ice-cold 100% ethanol and microfuged at maximum speed for 20 min at 4°C. The resulting DNA pellet was washed with 250 μL 70% (v/v) ethanol, briefly air-dried and resuspended in 50 μL water.

(A)
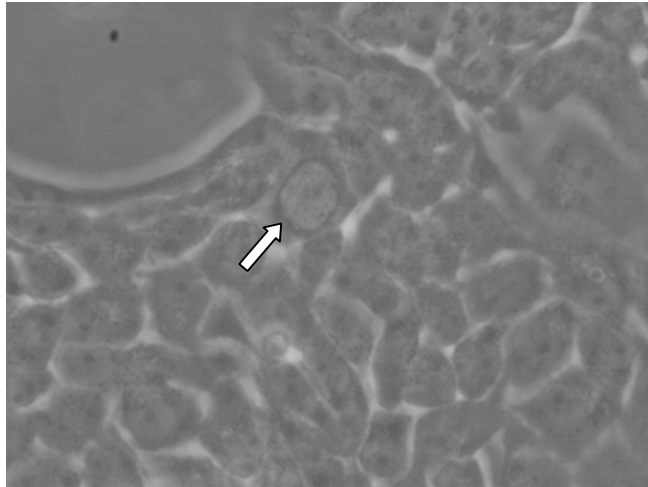
(B)
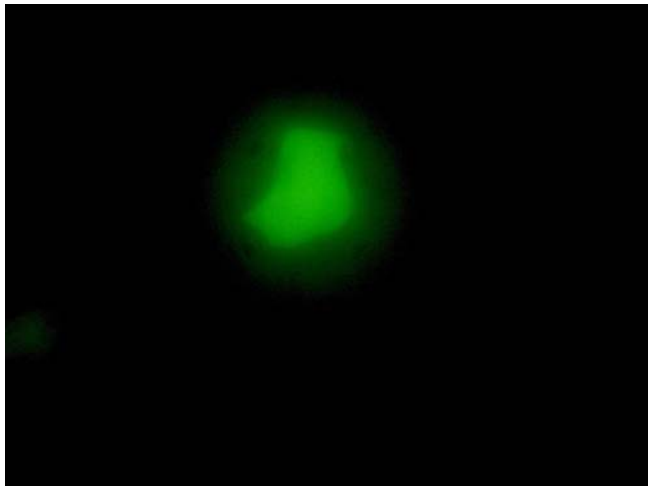
Figure 3.1: Induction of a cytopathic effect by CAV-NS transduction. (A) Phase contrast or **(B)** GFP expression in the same field of view of DKCre trans-complementing cells incubated with 100 particles/cell of CAV-NS vector, cultured for 3 days at 37°C and imaged on an inverted fluorescent microscope. The arrow indicates where a cytopathic effect is evident, as seen by a dark 'halo' around the nucleus of the transduced cell due to the high levels of replicating viral particles within the nucleus.

3.2.5. PCR Amplification of the E1-Region of CAV-2 Vectors

Forward and reverse primers were designed to amplify the E1A region of the Toronto strain of the CAV-2 genome (GenBank accession no. U77082) to give a PCR product of 685 bp. The sequences for the forward and reverse primers were F5-CAVE1A 5' AATATACTATTGTGCCGGCG 3' and R690-CAVE1A 5' GCGTGGCTTCAAAGACAAAT 3'. DNA was extracted from purified viral particles as described in **Section 3.2.4,** and mixed in the following master-mix:

10x PCR buffer	2 μL
10 mM dNTP	0.4 μL
5' F5-CAVE1A primer (10 μM)	1 μL
3' R690-CAVE1A primer (10 μM)	1 μL
Taq polymerase (5 U/μL)	0.2 μL
Sterile water for injection	14.4 μL
TOTAL VOLUME (after addition of 1 μL DNA)	20 μL

One μL of viral or plasmid DNA was added to each tube. The tubes were then denatured at 95°C for 5 min, followed by 35 cycles of 95°C for 30 sec, 55°C for 40 sec and 72°C for 90 sec, with a final extension at 72°C for 5 min. One ng of pTG5412 plasmid DNA was included as a positive control. PCR products were electrophoresed though a 1% (w/v) agarose gel and visualised by ethidium bromide staining.

3.2.6. Western Blotting

3.2.6.1. Sample Preparation

DKCre cells in 6-well trays were incubated with 100 particles/cell and cultured for 48 hrs. Conditioned media (2 mL/well) was collected and concentrated through Centricon YM10 columns at 4685 x g at 4°C until 1 mL of retentate remained in the columns. Cells were scraped into 2 mL of 20 mM Tris/500 mM NaCl, pH 7.0, and subjected to 6 rounds of freezing/thawing. Total cell protein was determined, and 3 μg of cell extract was diluted in 1x SDS-PAGE loading buffer supplemented with 5% (v/v) β-mercaptoethanol for reducing conditions. Samples were boiled for 5 min at 100°C to cleave sulphide bonds, and clarified by centrifugation at 17900 x g for 5 min at room temperature.

3.2.6.2. SDS-PAGE Gel Electrophoresis

Mini gel apparatus was assembled and filled with 1x Reservoir Buffer. Samples (50 µL) and Benchmark pre-stained protein ladders (10 µL) were electrophoresed through pre-poured Tris-glycine iGels (4% (v/v) polyacrylamide stacking gel, 12% (v/v) polyacrylamide resolving gel) at 150 V for 90 min.

3.2.6.3. Transfer and Detection

The gels were removed from the plastic cassette and equilibrated for 10 min in cold Transfer Buffer. The transfer sandwich was prepared by soaking each component in Transfer Buffer, and assembled in the following order without air bubbles: cathode (-); Scotch-Brite™ pad; 3 pieces of 3MM Whatmann filter paper (10 x 8 cm); gel; nitrocellulose membrane (10 x 8 cm); 3 pieces of Whatmann filter paper; Scotch-Brite™ pad; anode (+). Proteins were transferred to the nitrocellulose membrane at 40 V for 4 hr with the Transfer Buffer temperature maintained at 4°C by placing the transfer apparatus in a container of ice, with slow stirring.

The expression of rhNS was determined using the ECL western blotting detection system following the manufacturer's instructions. In brief, membranes were blocked for 1 hr at room temperature in 5% (w/v) non-fat dried milk in wash solution (0.1% (v/v) Tween20 in PBS), with gentle rocking. After washing three times, membranes were probed overnight at 4°C with rabbit anti-rhNS polyclonal antibody (1:1000) (Perkins *et al*, 2001). Membranes were again washed extensively before incubation with horse-radish peroxidase-conjugated sheep anti-rabbit IgG (1:1000) for 1 hr at room temperature. After washing, membranes were developed in detection reagent for 1 min, promptly rinsed in distilled water and placed between two sheets of plastic-wrap. Air bubbles were removed and the wrapped membrane was exposed to X-ray film for up to 90 sec in a darkroom and developed in the Department of Radiology (CYWHS).

3.2.7. Cross-Correction of Human MPS IIIA Fibroblasts

3.2.7.1. Conditioned Media Preparation and Filtration

Five 10 cm plates seeded at 5 x 10^6 DKCre cells/plate were incubated with 100 particles/cell CAV-NS and the conditioned media was collected after 6-days without feeding between inoculation and harvest. The media was filtered through a 300 kDa membrane in stir-cell apparatus to remove CAV-NS viral particles from the rhNS enzyme produced from

transduced cells (Nicolino *et al*, 1998). To prevent contamination during the subsequent cell culture, the membrane was rinsed in 70% (v/v) ethanol and sterile Baxter water for injection, and the assembled stir cell apparatus was sterilised with 70% (v/v) ethanol, sterile PBS and then filled with the conditioned media. The filtrate containing rhNS was then assayed for NS activity.

3.2.7.2. Metabolic Labelling and Harvest

Confluent 25 cm^2 flasks of normal (SF5435) and MPS IIIA (SF4636) human skin fibroblasts were depleted in sulphate-free media (F12) containing 10% (v/v) dialysed FCS for 3-days (Bielicki *et al*, 1998). Following this, the cells were metabolically-labelled in the same medium containing 7 μCi/mL $Na_2^{35}SO_4$ for 48 hrs. The radio-labelled media was replaced with BME media containing 10% (v/v) FCS, penicillin/streptomycin, and conditioned media containing filtered rhNS (or an equal volume of control media) in the presence or absence of 5 mM M6P. Flasks were incubated for 72 hrs at 37°C.

To harvest cells, the media was discarded and the cell layer washed twice with PBS. Cells were detached with 1 mL trypsin for 5 min, neutralised in 0.5 mL F12/10% (v/v) FCS and collected in 1.5 mL Eppendorf tubes. After centrifugation at 17900 x *g* for 5 min, the cell pellet was washed three times by resuspension in 500 μL of 150 mM NaCl and centrifuged as before. After the final wash, the cells were resuspended in 100 μL of 20 mM Tris-HCl/250 mM NaCl (pH 7.0) and lysed by 6 alternate cycles of freezing in dry ice/ethanol and thawing at 37°C. After clarification at 17900 x *g* for 5 min, the cell supernatants were dialysed against 5 mM sodium acetate (pH 4.0) and analysed for NS activity and radioactivity (^{35}S counts per minute in 10 μL of lysate diluted in 5 mL of scintillation fluid) and values were normalised to total protein content.

3.2.8. Transduction of Primary Murine Neural Cultures

Primary, mixed neural cells derived from newborn C57Bl/6 or "New York" mice of both unaffected or MPS IIIA genotypes were plated in 12-well trays (**Section 2.2.2.1**). One well from each of the four groups was transduced with 1000 particles/cell CAV-GFP, CAV-NS or an equal volume of saline and cultured for 10-days. Media was replaced 6-days post-inoculation. GFP expression of the cells was monitored daily with an inverted fluorescent microscope.

3.3. RESULTS

3.3.1. Homologous Recombination and Generation of a Stable Clone

In vivo homologous recombination of pTG5412 and pTCAV-12VK plasmids was performed in BJ5183 rec^+ *E. coli* and positive recombinants identified by PCR. Selected recombinant colonies from the stab plate were grown in LB supplemented with ampicillin, and Mini Prep DNA was extracted using commercial kits and used to transform DH5α *E. coli* cells. Recombinant Mini Prep DNA could not be extracted from DH5α recombinant clones when using commercially-purchased Mini Prep kits.

The original BJ5183 *E. coli*-positive recombinant clones were re-screened to determine which clones still contained intact DNA and a total of 4 positive recombinants were confirmed by PCR amplification (clones 21_{BJ5183}, 26_{BJ5183}, 27_{BJ5183} and 29_{BJ5183}). Bacterial clones were cultured overnight in 15 mL LB broth containing ampicillin and Mini Prep DNA extracted by the alkaline lysis "1-2-3" method (**Section 2.2.1.1**). This method provided a more crude preparation with increased yields of DNA compared to commercial kits. Mini Prep DNA was electroporated into Top10 and XL1Blue rec^- *E. coli* strains to generate stable clones and 5 of 40 (12.5%) positive recombinants were detected by PCR (**Fig. 3.2A**). These 5 positive clones were derived from clone 21_{BJ5183}. Mini Prep DNA was extracted and the identity of the DNA confirmed by digestion with *Eco*RI.

Following this, three clones (clone numbers 1_{Top10}, 3_{Top10} and $14_{XL1Blue}$) were randomly selected for further characterisation and cultured overnight as large-scale Midi Prep cultures. The Midi Prep DNA yielded incorrect restriction enzyme digestion patterns when cut with *Asc*I/*Not*I. Consequently, Top10 cells were re-transformed with Mini Prep DNA from clones 1_{Top10}, 3_{Top10} and $14_{XL1Blue}$ and, as before, several clones containing the correct pattern for recombined pCAV-NS DNA were identified by *Eco*RI digestion.

One starter colony (clone $3A_{Top10}$), derived from clone 3_{Top10}, was used to inoculate small- and large-scale cultures for 7 hrs or overnight (16 hrs), respectively. DNA was extracted from the cultures using the Mini Prep alkaline lysis method. Spontaneous recombination was observed in the large-scale cultures, as before, while the 7 hrs small-scale cultures generated the expected digestion pattern (**Fig. 3.2B**).

To establish a stable clonal line containing the pCAV-NS plasmid, Mini Prep DNA from clones 1_{Top10}, 3_{Top10} and $14_{XL1Blue}$ was electroporated into DH5α *E. coli* and 5 of the 8 colonies tested displayed the correct digestion pattern. A randomly selected clone (clone
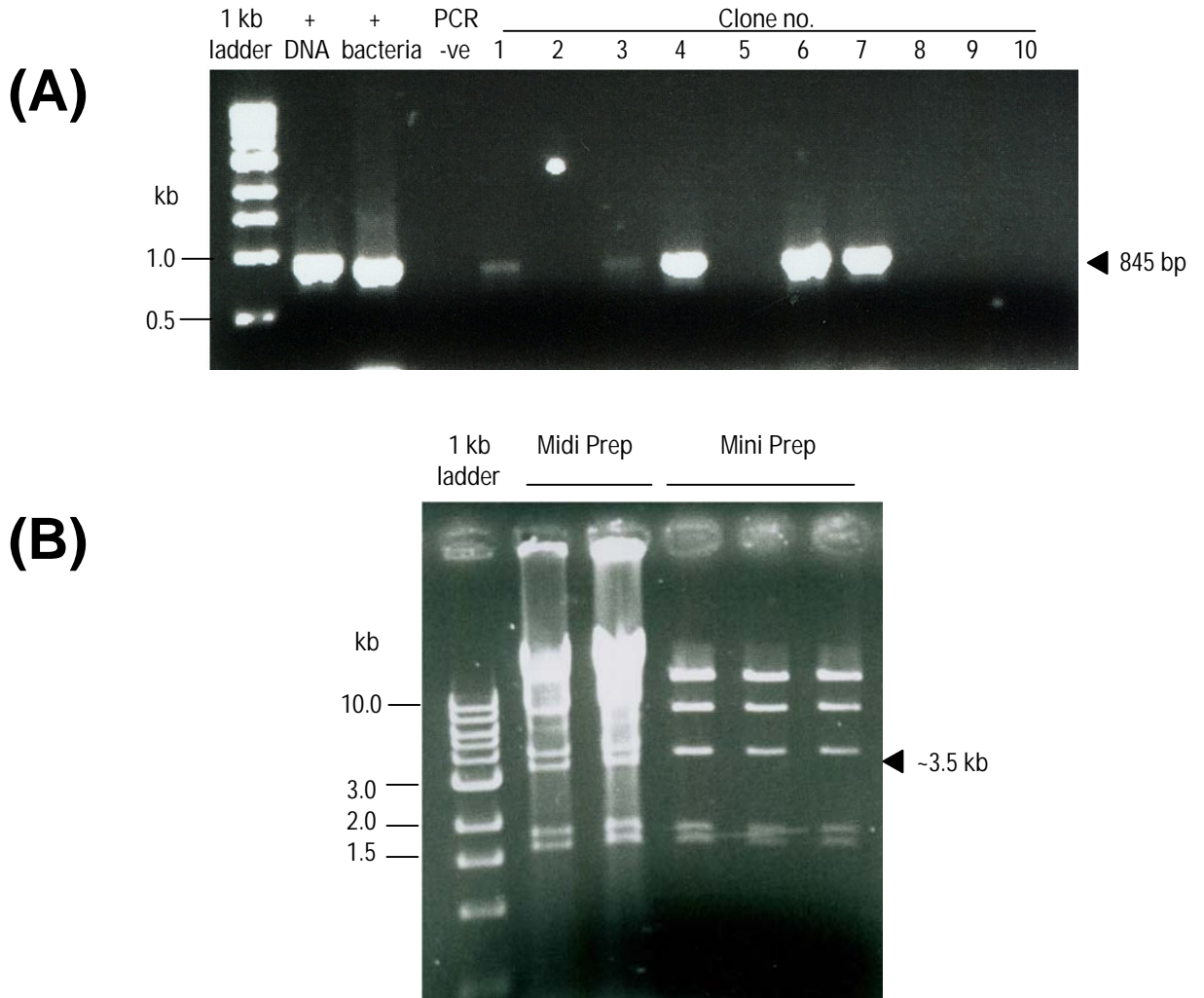
Figure 3.2: PCR screening and restriction enzyme digestion of bacterial recombinant clones. (A) Bacterial colonies were screened for homologous recombination using primers designed against the CMV promoter and the CAV-2 E2B region. PCR-positive controls included 5 ng of plasmid DNA and a bacterial colony from a ΔE1 CAV-2 vector encoding β-glucuronidase. Clones derived from 21_{BJ5183} were transformed into Top10 *E. coli* (clone no. 1-5) or XL1Blue *E. coli* (clone no. 6-10). Recombination-positive clones are numbered 1, 3, 4, 6 and 7, as seen by the 845 bp PCR product. **(B)** Large- and small-scale Top10 bacterial cultures were inoculated with the same starter colony (clone 3) and cultured for 16 or 7 hrs, respectively. DNA was extracted, digested with *Eco*RI and analysed by agarose gel electrophoresis. The arrowhead indicates an extra band from spontaneous recombination at approximately 3.5 kb in the Midi Prep samples. pCAV-NS digested with *Eco*RI was predicted to give bands of size 19567, 8189, 3991, 1796, 1616 bp.

$3_{DH5\alpha}$) could be cultured stably overnight and was consequently used to generate large-scale Midi DNA preparations. The schematic diagram of the pCAV-NS vector is displayed in **Fig. 3.3**.

3.3.2. Transfection and Amplification of CAV-NS

As recombination occurred in the CAV-2 E2B and the pPolyII sequences, *Asc*I/*Not*I double-digestion was used to free the ITR ends and excise the pPolyII backbone (**Fig. 3.4**). If the recombination had occurred in the ITR and E2B regions, only *Not*I single digestion would be required.

DKCre cells were transfected with linear, sterile pCAV-NS DNA and control plasmids using Lipofectamine 2000 (**Section 3.2.2.2**). Within 24 hrs post-transfection, a high transfection efficiency was observed in pIRES2-EGFP and pTCAV-NS controls with greater than 50% GFP-positive cells detected, as viewed on an inverted fluorescent microscope. No GFP expression was observed in *Asc*I/*Not*I-digested pCAV-NS wells at this time point. Strong GFP expression was not seen in pCAV-NS-transfected cells until just prior to harvest in round 3, with an estimated 5% of cells displaying some level of GFP expression. All subsequent rounds during the CAV-NS vector amplification were observed to have GFP expression in excess of 90% of DKCre cells and a cytopathic effect was observed under bright field light microscopy (**Fig. 3.1**).

3.3.3. Titration and Purification of CAV-NS

The CAV-NS vector was purified by vector banding on consecutive caesium chloride gradients and displayed thick, opaque bands of CAV-NS particles and empty capsid vectors (**Fig. 3.5**). The vector was desalted over a PD-10 Sephadex™ column and eluted in 0.5 mL aliquots with sterile PBS. The vector was most concentrated in fractions 6 and 7, as determined by the degree of opacity. Consequently, these were pooled, adjusted to 10% (v/v) glycerol and frozen in aliquots at -70°C. This CAV-NS vector stock was 3.2×10^{12} physical particles/mL and had a particle-to-transduction ratio of 4.5 to 1. (**Sections 2.2.3.3** and **2.2.3.4**). This vector stock was utilised in all experiments described in this thesis.

Selected aliquots of CAV-NS were analysed for the presence of endotoxin, which were determined to be 0.11, 0.12 and 0.03 endotoxin units/mL. The Media Production Unit (Institute of Medical and Veterinary Science, Australia) considers samples with endotoxin
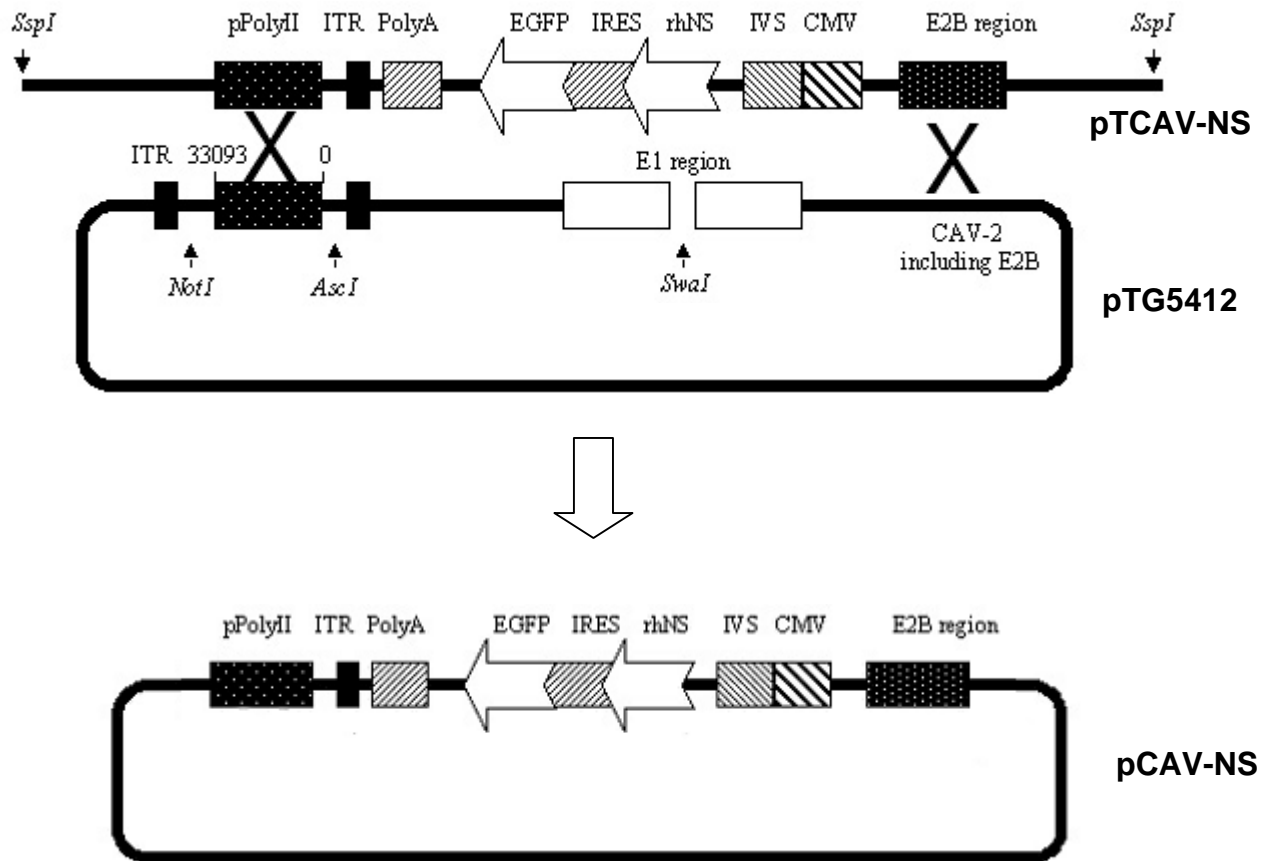
Figure 3.3: Schematic representation of the pCAV-NS plasmid. The upper line indicates *Ssp*I-linearised pTCAV-NS transfer vector containing a single ITR region, the pPolyII backbone and a CAV-2 E2B region, as well as the transgene expression cassette containing rhNS under the control of the CMV promoter and the enhanced GFP transgene following an IRES sequence. The central circular plasmid is pTG5412, which contains two ITR regions flanking the pPolyII backbone and the entire CAV-2 genome. The bold '**X**' indicates the position of the recombination events required to produce pCAV-NS. The pCAV-NS recombined plasmid (bottom panel) is predicted to be 35179 bp.
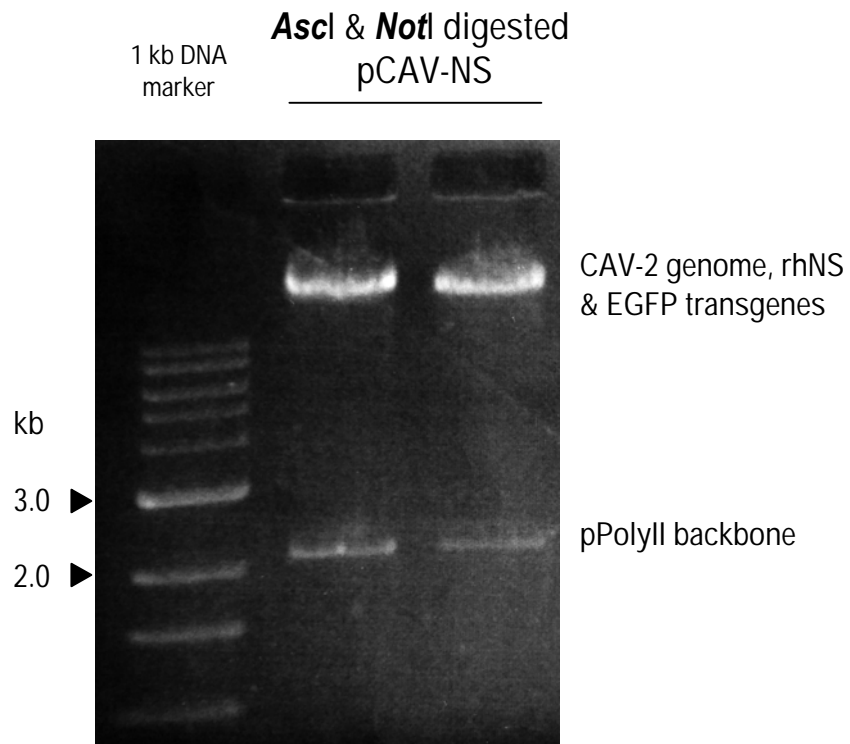
Figure 3.4: Confirmation of complete digestion of pCAV-NS to remove the pPolyII backbone. Prior to transfection into E1-trans-complementing DK cells, replicate samples of the pCAV-NS plasmid DNA were linearised with the restriction enzymes *Asc*I and *Not*I to free the CAV-2 ITR (approximately 33 kb) from the pPolyII plasmid vector backbone (approximately 2 kb). The digested DNA was electrophoresed though a 1% (w/v) agarose gel and visualised by ethidium bromide staining.
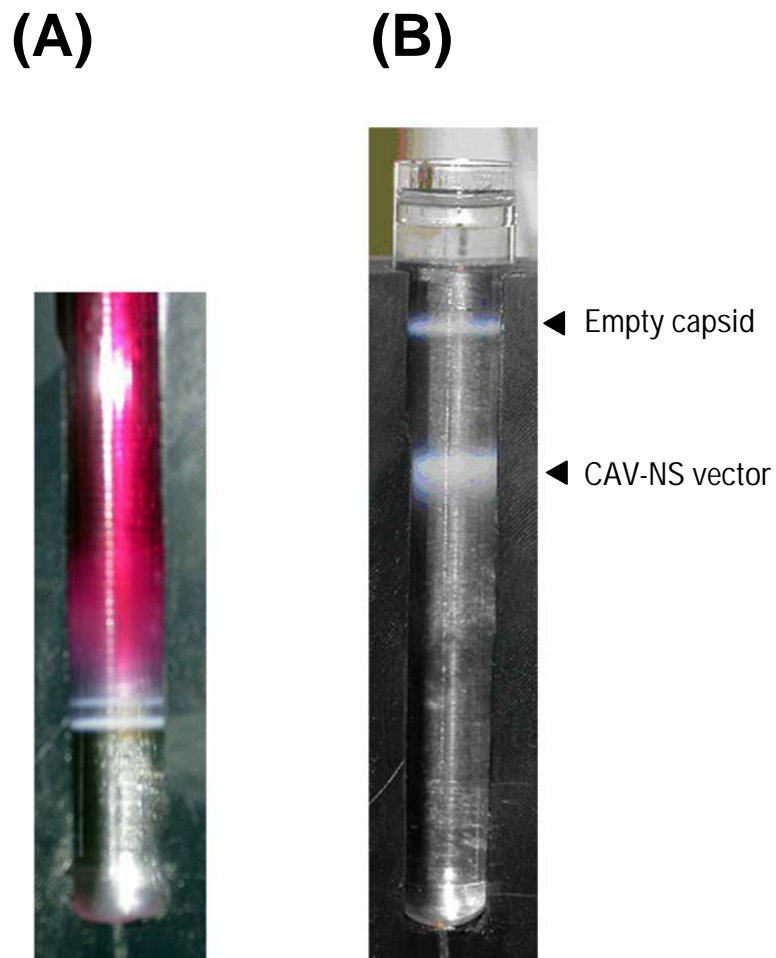
Figure 3.5: CAV-NS vector preparation. (A) Representative example of banding of CAV-NS vector particles from clarified supernatant on the initial caesium chloride step gradient after centrifugation at 35,000 rpm for 90 min. **(B)** After the second isopynic caesium chloride gradient, the empty capsid (upper band) and thicker, white, opaque CAV-NS band (lower band) is clearly observed. The CAV-NS vector particles were collected by piercing the tube 1 cm below the lower band with an 18G needle before being desalted, adjusted to 10% (v/v) glycerol, aliquoted and frozen at –70°C.

values less than 0.15 endotoxin units/mL to be endotoxin-free (Dr Tom Pryor, personal communication).

3.3.4. Verification of Plasmid Identity and Replication-Defective Particles

The homologous recombination of the pTG5412 and pTCAV-NS plasmids in *E. coli* is expected to remove the E1-region, thus rendering the vector particles replication-defective. To evaluate whether replication-competent (i.e. E1A-positive) particles were present in the purified CAV-NS vector stock, PCR amplification of DNA extracted from CAV-NS virions was performed (**Section 3.2.4; Fig. 3.6**). PCR amplification of the CAV-NS viral DNA using the CMV and E2B primers verified that the DNA extraction had been successful (data not shown). The E1-region was not detected in the equivalent of 3.5×10^8 physical particles of vector DNA.

3.3.5. Western Blotting

DKCre cells were selected for the initial assessment of transduction efficiency as this cell line has been documented as expressing CAR, the primary receptor of CAV-2 vectors, and is amenable to transduction by CAV-2 vectors (Soudais *et al*, 2000). Cell extracts from CAV-NS-treated DKCre cells were electrophoresed under reducing conditions on a 12% SDS-PAGE gel, transferred to nitrocellulose membrane, and rhNS detected with a polyclonal rabbit anti-rhNS antibody (1:1000). As anticipated, two specific bands at approximately 62-64 kDa and 56-58 kDa were evident in CAV-NS-transduced samples but not the corresponding untreated DKCre control cells (**Fig. 3.7**). The major band is likely to be the immature, unprocessed polypeptide (62 kDa), and the minor band the mature, cleaved protein (56 kDa), as has been previously reported (Perkins *et al*, 1999). A non-specific band was also observed at approximately 49 kDa in all samples.

3.3.6. Over-Expression of rhNS in DKCre Cells

Triplicate wells of DKCre cells seeded at 10^6 cells per well in 6-well trays were transduced with 100 particles/cell CAV-NS or with an equal volume of PBS and cultured for 48 hrs. Conditioned media and the attached cells were harvested as described in **Section 2.2.2.3** using PBS lysis buffer and analysed for NS activity and total protein content.

NS activity was significantly increased in CAV-NS-treated samples in both cell lysates and in dialysed conditioned media compared to untransduced controls (unpaired t-test,
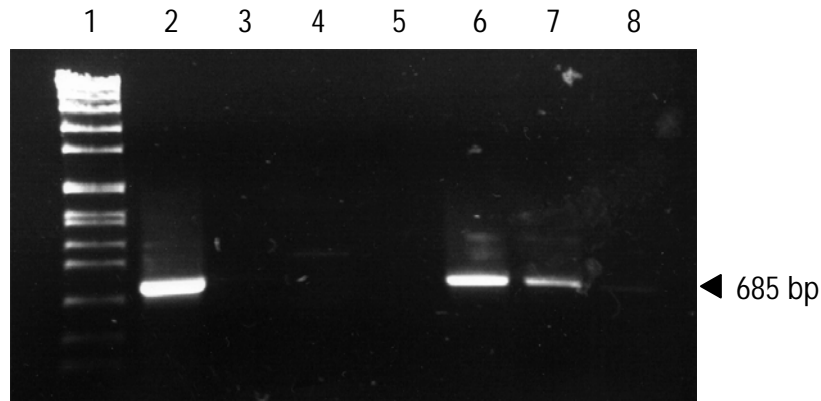
Figure 3.6: PCR amplification of the E1A region of CAV-NS. Viral DNA was obtained from 1.4 x 10^{10} purified CAV-NS vector particles and the CAV-2 E1A region amplified by PCR amplification. Twenty μL of PCR product was separated on a 1% (w/v) agarose gel and stained with ethidium bromide. The E1A region was not detected in CAV-NS viral DNA, indicating the absence of replication-competent particles. The sensitivity of the assay was sufficient to detect 0.001 ng of spiked pTG5412 plasmid DNA (Lane 8).

Lane 1:   SPP1 DNA ladder
Lane 2:   PCR positive control (pTG5412 plasmid DNA; 1 ng)
Lane 3:   PCR negative control
Lane 4:   CAV-NS viral DNA
Lane 5:   pCAV-NS plasmid DNA
Lane 6:   CAV-NS viral DNA spiked with 0.1 ng pTG5412
Lane 7:   CAV-NS viral DNA spiked with 0.01 ng pTG5412
Lane 8:   CAV-NS viral DNA spiked with 0.001 ng pTG5412

Figure 3.7: Western blot analysis of CAV-NS-transduced DKCre cell extracts.

Three μg of total protein isolated from DK cell extracts were separated on a 12% SDS-PAGE gel, transferred onto nitrocellulose membrane and subjected to western blotting analysis using a polyclonal rabbit anti-rhNS antibody. The molecular weights of pre-stained standards are indicated. The molecular weights of precursor and mature forms of rhNS are predicted to be 62 and 56 kDa, respectively (Perkins *et al*, 1999).

p=0.001; **Fig. 3.8**). In CAV-NS-transduced lysates, a 50-fold increase in NS activity was detected compared to untreated cells (299 ± 18.3 and 6 ± 4.8 pmol/min/mg total protein, respectively). The corresponding dialysed conditioned media samples also saw 6-fold improvements in NS activity, from barely detectable activity in untreated media (13.8 ± 20.6 pmol/min/mg) to 82 ± 7.7 pmol/min/mg in media collected from CAV-NS-treated cells.

3.3.7. Cross-Correction of MPS IIIA Human Fibroblasts

Duplicate samples of MPS IIIA and unaffected human skin fibroblasts were incubated with 0, 100 or 1000 particles/cell of CAV-NS and incubated at 37°C for 48 hrs. No GFP-positive cells were observed by fluorescent microscopy and NS activity was not significantly increased in the CAV-treated flasks over the untreated controls, indicating negligible transduction of human fibroblasts.

Consequently, conditioned media was collected from CAV-NS-transduced DKCre cells and used as a source of rhNS enzyme. The conditioned media was filtered through a 300 kDa membrane to remove viral particles and incubated with MPS IIIA fibroblasts for 72 hrs to determine the degree of sulphated GAG correction. Untreated MPS IIIA fibroblast cells had undetectable NS activity, however, the addition of 280 pmol/min/flask restored the NS activity to 41% of normal (unpaired t-test, p=0.037; **Fig. 3.9A**). The addition of 5 mM M6P to the media inhibited uptake of rhNS into the cells, as shown by NS activity within the cell extracts. This demonstrated that endocytosis of exogenously applied rhNS is mediated by a M6P receptor-dependent mechanism.

Concurrently, the amount of ^{35}S-sulphated GAG storage in CAV-NS-treated MPS IIIA fibroblasts was reduced by 82% compared to untreated MPS IIIA controls (unpaired t-test, p=0.068; **Fig. 3.9B**). However, GAG storage in treated MPS IIIA cells was 2.5-fold higher than wild-type concentrations, indicating that the amount of NS added to the culture media was insufficient to completely reduce GAG storage to normal.

3.3.8. CAV-NS Transduction of Newborn Murine Neural Cells

Transduction of primary neural cells from adult mice

In preliminary experiments, mixed neural primary cells derived from adult mouse brains were selected, as the yield of viable cells per animal is much greater than that in newborn mice (Sutherland *et al*, submitted by LDRU). Adult neural cultures were incubated

NS activity in transduced DKCre cells
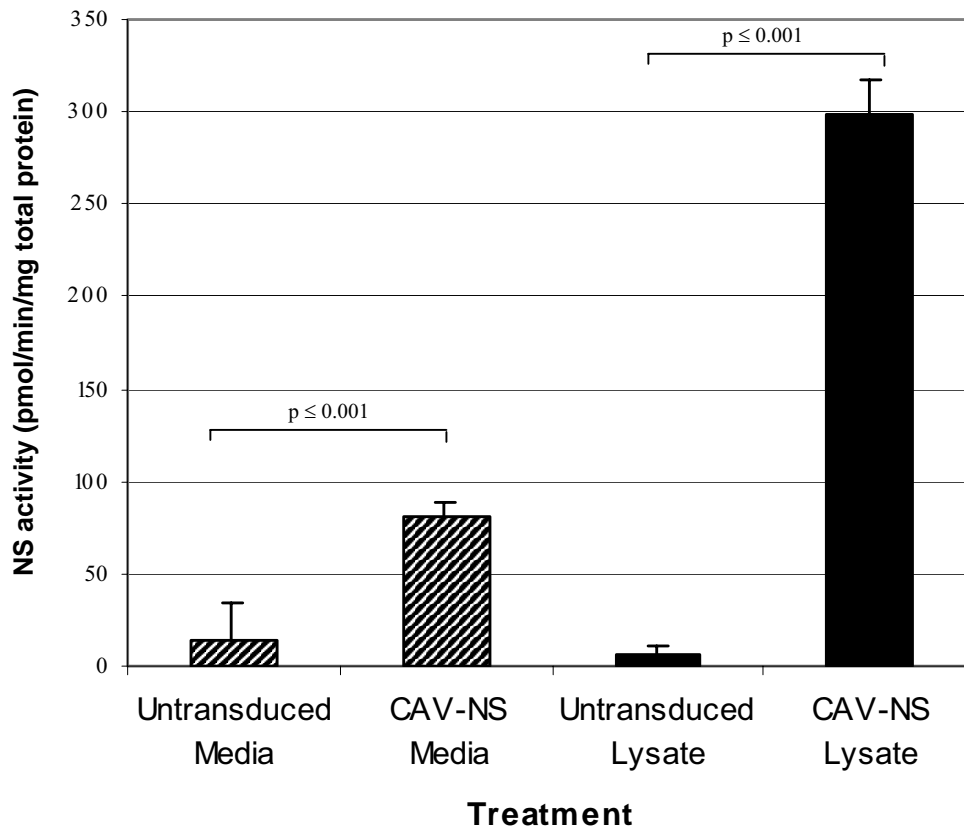
Figure 3.8: NS activity in CAV-NS-transduced DKCre cells. Triplicate wells of DKCre cells were incubated with 100 particles/cell CAV-NS and cultured for 48 hrs. CAV-NS treatment increased NS activity 6-fold in dialysed conditioned cell media samples (grey bars) and 50-fold in cell lysates (black bars) compared to untreated samples. Results are displayed as the mean of three experiments + 1 SEM.

Figure 3.9: Cross-correction of human MPS IIIA fibroblasts. Conditioned media from CAV-NS-transduced DKCre cells was filtered to remove viral particles and assayed for NS activity. Human MPS IIIA or normal fibroblasts were metabolically-labeled with $^{35}SO_4$, and then treated for 3-days with 280 pmol/min/flask of rhNS-containing filtered media, or an equal volume of untransduced control media, in the presence or absence of 5 mM M6P. Cell extracts were assayed for **(A)** NS activity and **(B)** ^{35}S GAG, and the results normalised to total protein content. Results are displayed as the mean of duplicate experiments + 1 SEM.

(A)

NS activity in human fibroblasts
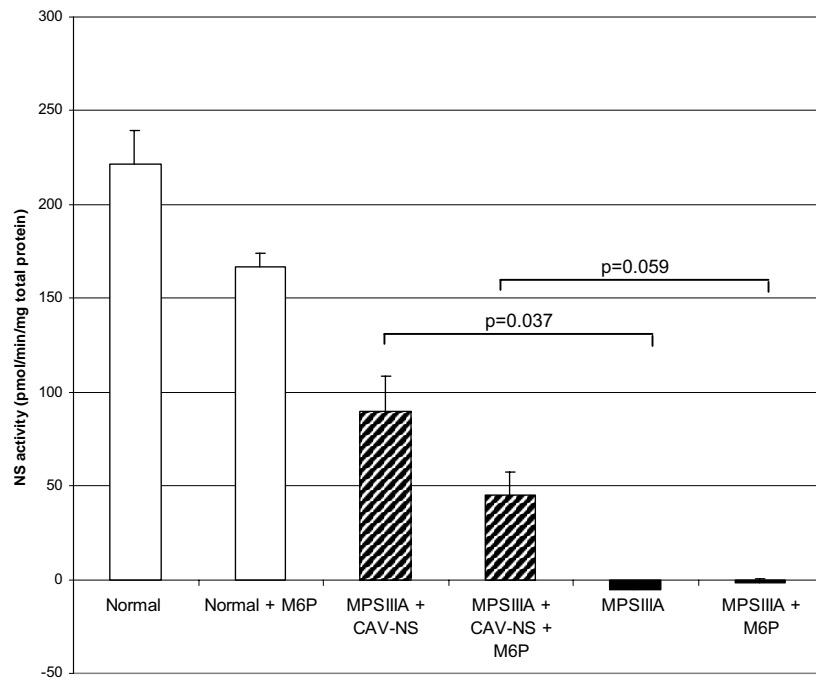
(B)

GAG in human fibroblasts
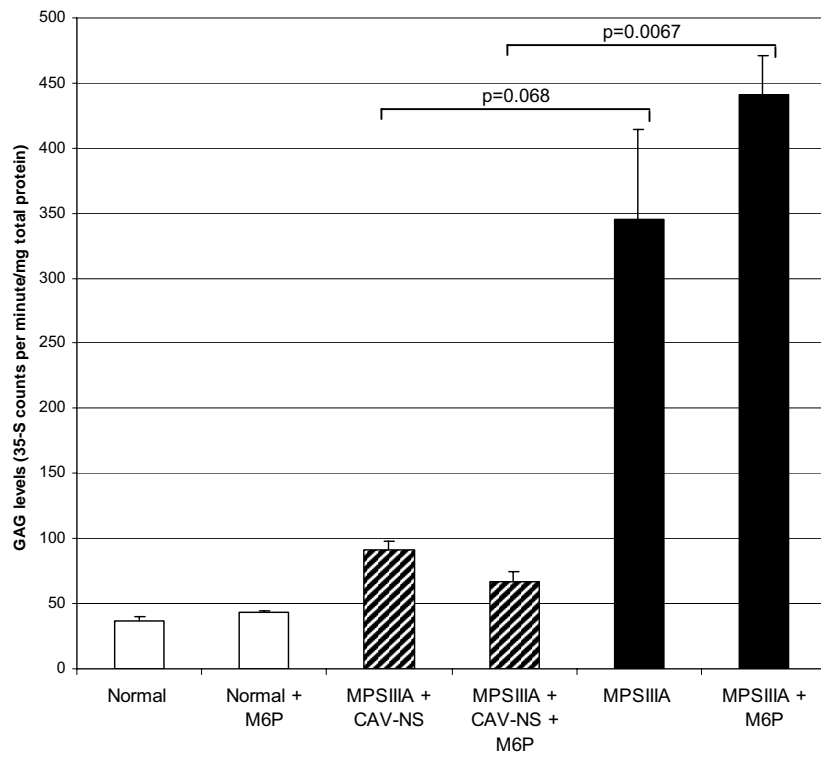
with 100 particles/cell CAV-NS (n=10) or saline (n=2) to compare the transduction efficiency with the other mammalian cell lines tested to date. However, no GFP expression was observed up to 3-days post-inoculation using an inverted fluorescent microscope.

Transduction of primary neural cells from newborn mice

Primary neural cells derived from newborn congenic (C57Bl/6) or "New York" mice were treated with CAV-NS, CAV-GFP (1000 particles/cell) or PBS to assess the transduction efficiencies in the different strains. MPS IIIA or normal cells of each mouse strain were transduced and cultured for 10-days. GFP expression was monitored daily with an inverted fluorescent microscope.

Strong and widespread expression of GFP was observed within 24 hrs post-transduction in the CAV-GFP-treated cells (**Fig. 3.10**). GFP was expressed both within the nucleus and cytoplasmically, and was also seen throughout axonal processes extending from the neuronal cell bodies. From 2-days post-transduction, the CAV-GFP-transduced C57Bl/6 cells appeared to have slightly higher GFP expression than the "New York"-derived cells, but these observations were not quantitated. A cytotoxic effect (i.e. cell death and blebbing) was evident after 48 hrs in all CAV-GFP-treated wells (for both congenic and "New York" cells) and this progressed until more than 95% of cells had detached from the wells at 10-days post-transduction.

In comparison, the CAV-NS-transduced cells displayed minimal expression of GFP transgene with long photographic exposures (>5 secs) required to capture GFP expression. After 3-days, low to moderate expression of GFP was observed in >80% CAV-NS-treated cells and this was the peak expression observed for CAV-NS-transduced cells. Gross cytotoxic effects, as determined by cell death and the presence of blebbing following CAV-NS transduction, were not apparent.

GFP expression was not detected in any of the untransduced cells. However, autofluorescent debris was occasionally observed in isolated MPS IIIA cells of both strains.

Days post-transduction
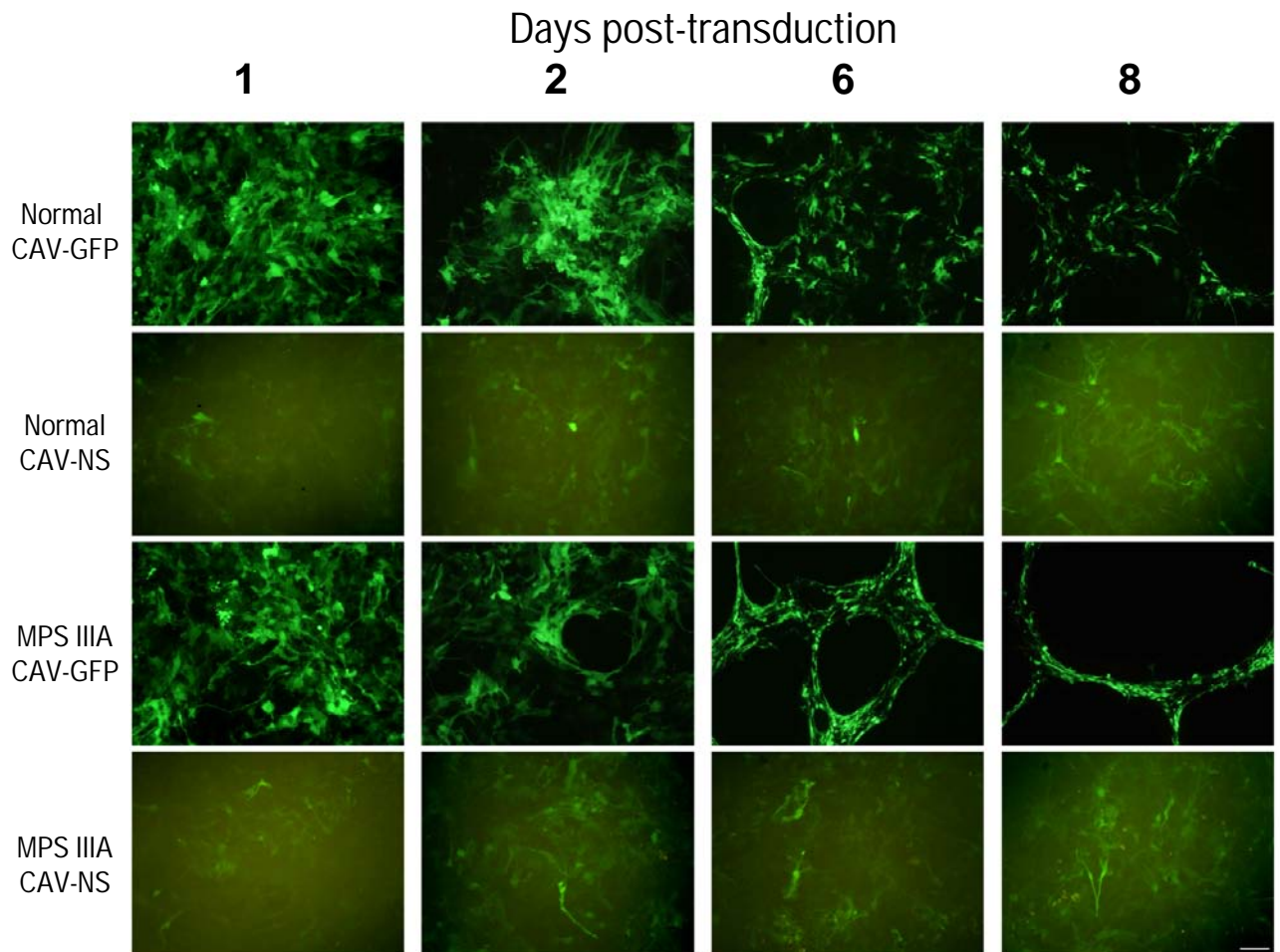
Figure 3.10: Transduction of "New York" primary murine neural cultures from newborn mice. Primary neural cells were harvested from newborn MPS IIIA or normal mice and grown to confluence. Cells were transduced with 1000 particles per cell of CAV-GFP or CAV-NS and cultured for 10 days. GFP expression was monitored daily on an inverted microscope. GFP-positive cells were not detected in untreated cells (not shown). Representative images of GFP expression in transduced "New York" newborn cells are displayed. Scale bar is 100 μm

3.4. DISCUSSION

To assess the therapeutic efficacy of CAV-2 gene therapy in MPS IIIA mice, it was necessary to construct a vector capable of expressing rhNS and to verify that this vector was functional in mammalian cells. A first generation ΔE1 CAV-2 vector encoding the enhanced GFP marker gene, the humanised red-shift variant of the wild-type GFP, has been described in detail (Kremer *et al*, 2000). The cloning strategy used to generate this plasmid, pCAV-GFP, exploits the high efficiency of recombination-positive (rec$^+$) *E. coli* bacterial strains to undergo homologous recombination *in vivo* (Chartier *et al*, 1996) and has consequently been used to generate other ΔE1 CAV-2 vectors expressing an assortment of transgenes such as β-galactosidase (Klonjkowski *et al*, 1997), tyrosine hydroxylase (Sotak *et al*, 2005), the lysosomal enzyme β-glucuronidase and the cystine transporter, cystinosin (Dr Eric Kremer, personal communication).

CAV-NS particles were purified by caesium chloride banding to high concentrations from crude DKCre cell extracts with a physical particle titre of 3.2 x 10^{12} particles/mL or 7.1 x 10^{11} infectious particles/mL. The low particle-to-transduction ratio yielded by the CAV-NS vector (< 5:1) was comparable with other ΔE1 CAV-2 vectors, with physical particle titres ranging from 0.3 – 6 x 10^{12} particles/mL and reported particle-to-transduction ratios between 3:1-10:1 (Kremer *et al*, 2000; Perreau and Kremer, 2005; Sotak *et al*, 2005). Large-scale human Ad vector production techniques have been optimised to reach titres exceeding 1 x 10^{13} plaque forming units/preparation via active gassing of a 10-tray cell factory system (Okada *et al*, 2005), or 2 x 10^{15} particles/preparation by use of a 14 L Celligen Plus bioreactor with a packed bed basket (Peng, 2004). It is feasible that these culture systems may be adapted for large-scale purification of CAV-2 vectors in future studies.

Whilst verification of plasmid DNA by molecular biological methods indicated that the DNA sequences were in the desired order, it was necessary to verify that the CAV-NS vector correctly processed and expressed active and mannose-6-phosphorylated rhNS. In CAV-NS-transduced DKCre cell extracts, two polypeptide bands at 62 kDa and 56 kDa were detected by Western blotting, indicating that the predicted post-translational modifications of rhNS occur within 48 hrs. At this time-point, the major polypeptide species detected in transduced DKCre cells was expressed in the precursor form. The predicted size of the human NS monomer is 54,679 Da (Scott *et al*, 1995). rhNS protein synthesised by treated DKCre cells had a comparable molecular mass to the rhNS produced in expression studies using

CHO cells where the mature human and precursor proteins were detected at 56-58 kDa and 62-64 kDa, respectively (Bielicki *et al*, 1998; Perkins *et al*, 1999).

Elevations in NS activity were measured in cell extracts and in conditioned media samples of transduced DKCre cells (50- and 6-fold normal, respectively), indicating that the rhNS produced by CAV-NS transduction was secreted into the media within 48 hrs after treatment. In principle, even greater amounts of NS activity may have been achieved if higher titres or longer time-points post-injection were assessed. However, as DKCre cells contain the CAV-2 E1 regions, vector transduction results in the active production of viral particles that eventually cause cell death due to a cytopathic effect. Taken together with the Western blots, these results provided the first verification that the CAV-NS vector generated in this chapter was able to successfully transfer vector DNA to the cell nucleus with the necessary transcriptional and translational events occurring to produce both functional NS and GFP protein.

To demonstrate that rhNS produced by cells transduced with CAV-NS was able to have a therapeutic effect *in vitro*, human MPS IIIA skin fibroblasts were treated with culture supernatant containing rhNS produced by DKCre cells. Direct transduction of human skin fibroblast cells with CAV-NS was unsuccessful even at high multiplicities of infection (1000 particles/cell). This was surprising given that Soudais *et al* (2000) were able to transduce 32% of transformed human skin fibroblast cells with the CAV-GFP vector at an identical titre. MPS IIIA cells treated with 280 pmol/min of rhNS increased intracellular NS activity, however, the addition of M6P resulted in a 25% or 50% decrease in NS activity in normal or CAV-NS-treated MPS IIIA fibroblasts, respectively. This demonstrated that rhNS uptake was partially mediated by M6P endocytosis. However, in M6P-treated flasks, intracellular NS activity was not reduced to undetectable amounts, potentially due to rhNS out-competing M6P for its receptor at this concentration as a result of differences in the binding co-efficient of the two agents.

This amount of NS activity was sufficient to reduce ^{35}S-sulphated GAG by 82% in CAV-NS-treated MPS IIIA fibroblasts to near normal. The amount of GAG storage was unaffected by the addition of M6P, with a 94% decrease observed in MPS IIIA cells treated with both rhNS and M6P compared to MPS IIIA cells treated with M6P alone. Similar observations have been described using rhNS produced by CHO cells where increased concentrations of rhNS (320 or 3200 nmol/min rhNS, i.e. >1000-fold and 10,000-fold, respectively) were able to normalise intracellular sulphated GAG (Bielicki *et al*, 1998). These

results demonstrate that rhNS produced by cells transduced by the CAV-NS vector was able to "cross-correct" human MPS IIIA cells and reduce sulphated oligosaccharide storage.

To determine whether the CAV-NS vector was able to transduce murine neural cells prior to *in vivo* injections, primary neural mixed cell cultures from newborn mice were incubated with CAV-NS at 1000 particles/cell. Newborn cultures were selected for two reasons: (a) the yield of neurons was expected to be greater in newborn mice than adults (Sutherland *et al*, submitted by LDRU) and CAV-2 vectors efficiently transduce neuronal cells (Soudais *et al*, 2001b); and (b) the expression of the CAR receptor is down-regulated in the adult rodent brain compared to that observed in newborns and *in utero* (Hotta *et al*, 2003). MPS IIIA and unaffected neural cells from newborn mice of either the C57Bl/6 (Crawley *et al*, 2006a) or the "New York" mixed strain (Bhaumik *et al*, 1999) were transduced with equal titres of CAV-NS, CAV-GFP or saline as a control. Widespread and intense GFP fluorescence was observed in CAV-GFP-treated cells within 24 hrs post-transduction. This correlates with data obtained using Ad vectors where enhanced GFP driven by the human CMV promoter can be observed as early as 7 hrs in cultured rat brain slices (Stokes *et al*, 2003).

For CAV-NS-transduced cells, reduced GFP expression was observed compared to CAV-GFP-treated cells. This is likely to be due to the GFP transgene sequence following the IRES element, as the encephalomyocarditis virus IRES sequence employed in the pIRES2-EGFP plasmid has been partially disabled leading to a reduced rate of GFP translation to maximise the expression of the first transgene (Rees *et al*, 1996). Mizuguchi and colleagues (2000) reported similar observations, where the expression of the second transgene following the IRES ranged from 6-100% (generally 20-50%) relative to the first transgene expression in a variety of cell lines and in mouse liver. Furthermore, it has been demonstrated via the simultaneous flow cytometric detection of various combinations of bi- or tri-cistronic expression of GFP (green), YFP (yellow) and BFP (blue), that the placement of a gene after the IRES linkage resulted in reduced protein translation as measured by intensity of fluorescing cells (Zhu *et al*, 1999). For example, GFP following a single IRES element resulted in 10% (for IRES-GFP) or 44% (for BFP-IRES-GFP) GFP expression relative to GFP in the first position (100%) (Zhu *et al*, 1999).

CAV-GFP-treated cells exhibited evidence of cytotoxicity and patches of cell death were observed within 48 hrs post-transduction. GFP cytotoxicity has been described in rat brain slice cultures (Stokes *et al*, 2003) as well as in several non-neural cell lines (NIH/3T3, BHK-21, HepG2, Huh-7) and the cytotoxicity in the latter were determined to be due to the

induction of apoptosis in transduced cells (Liu *et al*, 1999). Similarly, high expression of GFP mediated by a herpes simplex virus-packaged amplicon in primary cortical neurons from embryonic mice has induced apoptosis and neurotoxicity in a dose-dependent manner (Detrait *et al*, 2002). These observations have been confirmed *in vivo* with AAV-mediated GFP expression inducing neurotoxicity in dopaminergic neurons of the substantia pars nigra compacta (Klein *et al*, 2006). The absence of overt cytotoxic effects in CAV-NS-transduced cells, where GFP is not as strongly expressed, further supports the findings that cytotoxicity in the CAV-GFP-transduced cultures was likely to be induced by the extremely strong expression of GFP.

3.5 SUMMARY AND CONCLUSIONS

This chapter described the generation of a ΔE1 CAV-2 vector expressing rhNS and GFP, which was purified at high titres and infectivity. The CAV-NS vector transduced DKCre cells, resulting in greatly increased NS activity in an *in vitro* setting. Conditioned media collected from CAV-NS-transduced cells reduced sulphated GAG storage in human MPS IIIA fibroblasts and this process was mediated in part by the M6P pathway. This vector was also shown to be capable of transducing murine neural cells.

To evaluate whether CAV-mediated gene transfer had a similar therapeutic benefit in an *in vivo* scenario, gene transfer studies were conducted in the MPS IIIA mouse model, which will be described in the subsequent chapters.

CHAPTER 4:

In Vivo Gene Transfer into Adult Animals

4.1. INTRODUCTION

The similarities between disease progression in the MPS IIIA mouse and the human condition, as described in the literature overview in **Chapter 1**, demonstrates the potential of the MPS IIIA mouse model to examine novel treatment modalities and determine their therapeutic efficacy. The findings from the previous chapter demonstrated that the CAV-NS vector mediated efficient gene transfer in mammalian cells and the recombinant product was able to correct disease pathology in human MPS IIIA fibroblasts, which permitted the investigation of whether similar benefits could be obtained in the MPS IIIA mouse model.

The objectives of the experiments described in this chapter were to determine the optimal conditions for efficient gene transfer *in vivo* by establishing or verifying the parameters for vector administration. CAV-GFP vector was first delivered to unaffected guinea pigs to assess the transgene distribution in a species which had not previously been evaluated, and to become familiar with the stereotaxic surgery techniques. In addition, supporting biochemical and histological assays were developed to assess the biodistribution and gene transfer efficiency. These preliminary experiments were essential to gain a basic understanding of the vector kinetics prior to initiating a large-scale study.

4.2. SPECIFIC METHODS

4.2.1. Genotyping and Maintenance of α-Mannosidosis Guinea Pigs

4.2.1.1. Breeding

The α-mannosidosis guinea pig colony was maintained by Dr Dyane Auclair (LDRU) under PC1 conditions in the CYWHS Animal House. All procedures were performed with the approval of CYWHS and University of Adelaide Animal Ethics Committees.

4.2.1.2. Genotyping of α-Mannosidosis Guinea Pigs

Identification of α-mannosidosis guinea pigs was performed as previously described (Berg and Hopwood, 2002). In brief, the 679C > T mutation abolishes the *Aci*I restriction enzyme site. The 5'mpgimutF primer (5' ATGGGCTTTGATGGTGTCT 3') and 3'mpgmutR primer (5' AGTGAAGAGGTCGGCCGCAG 3') amplify a 241 bp PCR product which flanks the mutation.

Blood was collected onto Guthrie cards by superficially scratching the guinea pig along an ear vein with a needle after cleansing with ethanol-impregnated swabs. Blood spots were dried and stored at room temperature. A 3 mm punched blood spot was vigorously vortexed in 90 µL of 1x PCR buffer (9 µL of 10x HotStart PCR buffer and 81 µL sterile water for injection), and soaked from 30 min to overnight at 4°C to allow blood to elute from the filter paper. After heating at 99°C for 15 min, tubes were placed on ice and 10 µL of master-mix was added.

HotStart Taq polymerase (5 U/µL)	1 µL
20 mM dNTP	1 µL
5' mpgimutF primer (50 µM)	2 µL
3' mpgmutR primer (50 µM)	2 µL
10x HotStart PCR buffer	1 µL
Sterile water for injection	3 µL
MASTER-MIX VOLUME	10 µL

The PCR cycling conditions had an initial denaturation step at 95°C for 15 min, followed by 40 cycles of 94°C for 30 sec, 55°C for 45 sec and 72°C for 40 sec, with a final extension at 72°C for 4 min.

PCR products (10 µL) were electrophoresed through a 2% (w/v) agarose gel prior to overnight digestion with 5 U *Aci*I at 37°C. The *Aci*I restriction enzyme cuts between the CC in the sequence 5' CCGC 3'. Digested DNA was electrophoresed through a 3.5% (w/v) agarose gel and the genotype of each animal identified. Wild-type guinea pigs displayed a band at 226 bp, α-mannosidosis guinea pigs at 165 bp and carrier heterozygotes presented with both bands.

4.2.2. Bilateral Hippocampal Injections in Adult Guinea Pigs

The CAV-GFP vector (batch "SA4"; 3 x 10^{12} particles/mL) used in the guinea pig studies was prepared by Dr Eric Kremer and colleagues (IGMM, France) and shipped to Australia on dry ice. CAV-2 vector injections were performed in a PC2 biohazard hood. Two 25 µL Hamilton syringes containing sterile water for injection were connected to 27G dental

needles with saline-filled polyethylene tubing. Glycopyrrolate (Robinul, 0.02 mg/kg) was administered subcutaneously 10 min prior to anaesthesia to reduce respiratory secretions. Anaesthesia was induced with 5% (v/v) isofluorane in 8-wk-old guinea pigs and then maintained between 1-3% (v/v) isofluorane mixed with 2 L/min oxygen throughout surgery.

Once unresponsive to a toe pinch, the scalp was shaved and the guinea pig was placed on a warm wheat bag to aid heat retention. Lacrilube was applied to the eyes and the skull was securely fastened in a stereotaxic frame. An incision was made along the midline to expose bregma and lambda and the skull was adjusted so that it was level in the horizontal plane. After determining the hippocampal co-ordinate sites in reference to bregma, an indent into the skull was made with a 0.5 mm drill bit and then enlarged to 1 mm. Meningeal membranes were punctured with a 25G needle. Co-ordinates for the dentate gyrus were adapted from newborn guinea pig co-ordinates (Robinson *et al*, 2005) and were determined to be posterior –2.8 mm, lateral ± 1.2 mm, ventral –5.5 mm.

Dental needles were ethanol-sterilised and 3×10^9 particles/µL of CAV-GFP viral vector (or saline as a vehicle control) were loaded into the injection lines immediately prior to injections. Two µL per hemisphere was infused bilaterally at a constant rate of 0.5 µL/min using an automated micro-injector pump and the needles were left in place for 3 min to allow the fluid to disperse. The needles were slowly withdrawn to prevent back-suction of virus and the needle checked for blockages by expelling 0.2 µL. After surgically closing the incision with sutures, each guinea pig received a subcutaneous injection of warm 4% (v/v) dextrose in 0.18% (v/v) saline (30 mL/kg) to replenish lost fluids. In addition, animals were also injected intramuscularly with the analgesic flunixin (2.5 mg/kg) to relieve pain. Guinea pigs were warmed in a 30°C recovery chamber until they regained consciousness and were then returned to their pen.

The diet of the guinea pigs was supplemented with lucerne hay and fresh, leafy vegetables in addition to dried food pellets. Body weights and rectal temperatures were measured daily to monitor post-operative recovery. Flunixin was administered each time the rectal temperature exceeded 40°C.

4.2.3. Bilateral Thalamic Injections in Adult Mice

Adult mice were given paracetamol (Dymaddon; 0.16 mg/mL) orally for 3-days prior to and post-surgery to ensure that therapeutic concentrations of the analgesic were present. This concentration was based on the assumption that mice drank 5 mL of water per day to

administer a daily dose of 0.8 mg. Each mouse was pre-treated intramuscularly with 50 μL Robinul (10 μg per mouse) at least 10 min before anaesthesia to reduce respiratory secretions.

Mice were anaesthetised for approximately 1 hr with a ketamine/xylazine cocktail, administered intraperitoneally at previously determined optimal doses (Savas *et al*, 2004). Unaffected mice received 170 mg/kg ketamine and 10 mg/kg xylazine, while MPS IIIA mice required 170 mg/kg ketamine and 20 mg/kg xylazine. When no response was observed to toe pinching as a measure of surgical depth, the mouse was placed on a warm wheat-bag to aid in heat retention and the head was secured into a stereotaxic frame. The eyes were kept moist with Lacrilube.

A midline incision was made to expose the skull and the skull adjusted until bregma and lambda were level in the horizontal plane. The skull was kept moist with sterile saline throughout surgery. Once level, the appropriate co-ordinates were measured in reference to bregma and marked on the skull with a fine-tip pen. The co-ordinates for the adult mouse thalamus were confirmed to be posterior –1.5 mm, lateral ± 1.5 mm, ventral –3.25 mm (Paxinos and Franklin, 2001).

Holes were drilled with a hand-drill fitted with a 0.5 mm drill bit and meningeal membranes were perforated with a 25G needle. The stereotaxic frame was transferred to the biohazard hood and two Hamilton syringes (25 μL) filled with sterile water were connected to plastic tubing joined to a pre-cut dental needle (27G) containing sterile saline. The vector (or saline as a vehicle control) was loaded into ethanol-swabbed dental needles by expelling the appropriate volume of saline and back-filling with vector stock. The vector concentration ranged from 4.5×10^8 to 6×10^9 particles per hemisphere in a volume of 1-2 μL per injection. The needles were again ethanol-sterilised and slowly lowered into the brain parenchyma to the appropriate depth and fluid was expelled at a constant rate of 0.33 μL/min using a micro-injector pump. The treatment was allowed to disperse for 3 min before the needle was slowly withdrawn. After the needle was completely removed, 0.2 μL was expelled to check for blockages. The incision was sutured and mice were left to recover on a second warm wheat-bag. Each mouse received warmed 4% (v/v) dextrose in 0.18% (v/v) saline subcutaneously (30 μL/g) to replenish fluid loss.

Mice were monitored and weighed daily for 2-wks or until body weights had stabilised. If mice were observed to be in pain (e.g. hunched posture, dull and ungroomed coat) or had a rapid loss in weight (>5% reduction in 24 hr), they were administered with 2.5 mg/kg flunixin intramuscularly and subsequently euthanased.

4.2.4. Vector Genome Detection by PCR in Frozen Tissues

The extraction of genomic DNA from PFA-fixed, frozen tissues and the subsequent amplification of viral genome by PCR was established (Nadia Skander, unpublished results) (Nadon and Draeger, 1996; Hurtado-Lorenzo *et al*, 2003). Two lysis buffers were compared to determine the efficacy of genomic DNA extraction from a guinea pig expressing GFP-positive cells or an uninjected guinea pig as a control. Buffer A consisted of 10 mM Tris-HCl, 10 mM NaCl, 25 mM EDTA, 1% (w/v) SDS, 4 mg/mL proteinase K, pH 8.0 (Hurtado-Lorenzo *et al*, 2003). Buffer B was identical to the MPS IIIA genotyping genomic DNA toe lysis buffer (50 mM Tris, 2 mM NaCl, 1 mM EDTA, 0.5% (v/v) Tween20, 0.4 mg/mL proteinase K, pH 8.0; **Section 2.1.2**). Tissue sections were processed, with or without phenol/chloroform extraction, as described in **Section 2.2.1.1,** and the genomic DNA amplified by PCR using the primers and conditions for the detection of CAV-2 recombination (**Section 3.2.1.2**).

4.3. RESULTS

4.3.1. *In Vivo* GFP Expression in Guinea Pigs

Six unaffected 8-wk-old guinea pigs were bilaterally injected with 2 µL per hemisphere of either CAV-GFP (6 x 10^9 particles/hemisphere; n=4) or saline as a vehicle control (n=2) into the dentate gyrus of the hippocampus (**Table 4.1**). Two uninjected guinea pigs served as additional controls. Intracerebral injection of the CAV-GFP vector allowed assessment of the CAV-2 vector biodistribution in a species that has not previously been analysed and provided the opportunity to become familiar with stereotaxic surgery in a larger animal model.

4.3.1.1. Overall Health Indicators

The guinea pig colony was reared in PC1 conditions in the CYWHS Animal House. All guinea pigs listed in **Table 4.1** were transferred into the PC2 holding room prior to or following surgery. Two uninjected guinea pigs were also transferred to the same room to serve as controls for the change in weight and temperature as a result of stress associated with moving rooms (**Figs. 4.1** and **4.2**).

Table 4.1: Identification and surgical summary of 8-wk-old guinea pigs injected with CAV-GFP in the dentate gyrus of the hippocampus.

Name & Sex	Genotype	Treatment	Acclimatisation	Sacrifice (days post-injection)	Flunixin administration	GFP expression
Sandra ♀	+/-	CAV-GFP	No	8 days	Days 0, 2	Strong
Rose ♀	+/+	CAV-GFP	Yes	14 days	Days 0, 1, 6	Strong-moderate
Pirate ♀	+/-	CAV-GFP	Yes	8 days	Days 0, 1, 6, 8	Moderate
Mawi ♂	+/+	CAV-GFP	Yes	14 days	Day 0	Not detected
Pringle ♂	+/-	PBS	Yes	14 days	Day 0	Not detected
Chicago ♀	+/-	PBS	Yes	8 days	Day 0	Not detected
Pepper ♀	+/+	Uninjected	Yes	0*	-	Not detected
Kranski ♀	+/-	Uninjected	Yes	0*	-	Not detected

+/+ and +/- indicate that the guinea pigs were normal or heterozygote, respectively.

* These animals were age-matched with the guinea pigs sacrificed at 8-days post-injection.

The first guinea pig to undergo surgery, Sandra, was not pre-acclimatised to the PC2 holding room prior to surgery and was singly-housed post-operatively. She lost 13% of body-weight over 2 consecutive days (compared to the day of surgery; **Fig. 4.1**). For subsequent stereotaxic procedures, animals were pre-acclimatised in the new room and group-housed for at least 2-days prior to surgery.

The rectal temperature was measured in Sandra 2-days post-surgery and was found to be 40.5°C (**Fig. 4.2**; normal range for a healthy guinea pig is 37.2-39.5°C) (Harkness and Wagner, 1995). A reduction in body weight and a measurable fever was observed in 3 of 4 CAV-GFP-treated guinea pigs. Losses in body weight were also measured in guinea pigs prior to surgery and in uninjected animals, indicating that the anaesthesia and surgical procedures were not the only factors affecting weight loss. Although there was considerable variation in the rectal temperatures, temperatures exceeding 40°C were only detected in animals receiving CAV-GFP treatment, although some animals had rectal temperatures higher than the reported normal range even before receiving surgical manipulations. The administration of flunixin reduced the temperature to within the normal range within 24 hrs.
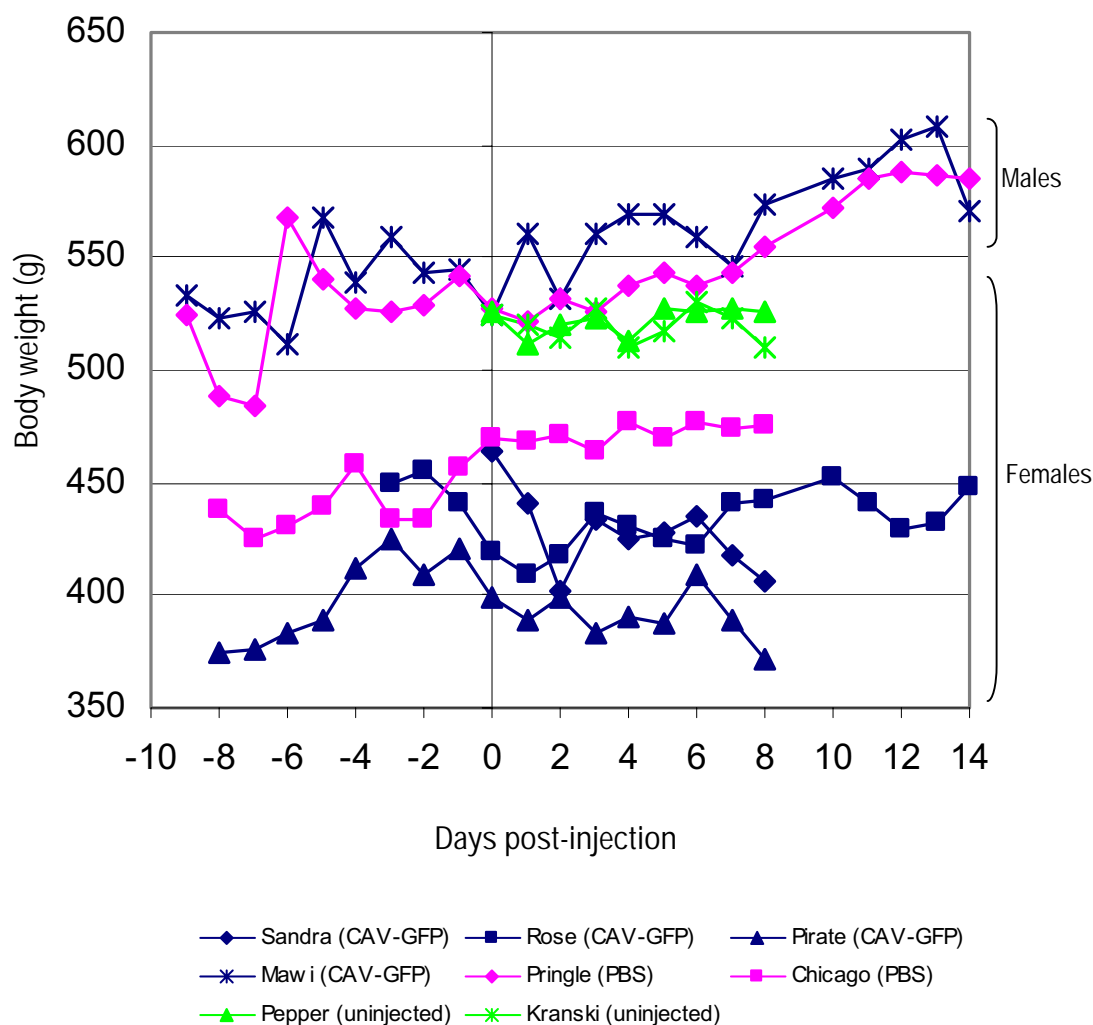
Figure 4.1: Body weights of young adult guinea pigs after stereotaxic surgery. Guinea pigs were weighed daily to monitor recovery after surgery (day 0). CAV-GFP-injected animals are coded blue, sham-injected are coded pink and uninjected control animals are coded green. The uninjected animals were weighed after transfer from the PC1 to PC2 holding rooms to serve as controls for body weight.

Figure 4.2: Rectal temperatures of young adult guinea pigs after stereotaxic surgery. The rectal temperature of each guinea pig was measured daily with a digital thermometer (Beckton Dickson). Flunixin (2.5 mg/kg) was administered intramuscularly on the day of surgery and each time the rectal temperature exceeded 40°C. The reported minimum and maximum rectal temperatures of a healthy guinea pig are indicated by a dashed line (Harkness and Wagner, 1995).
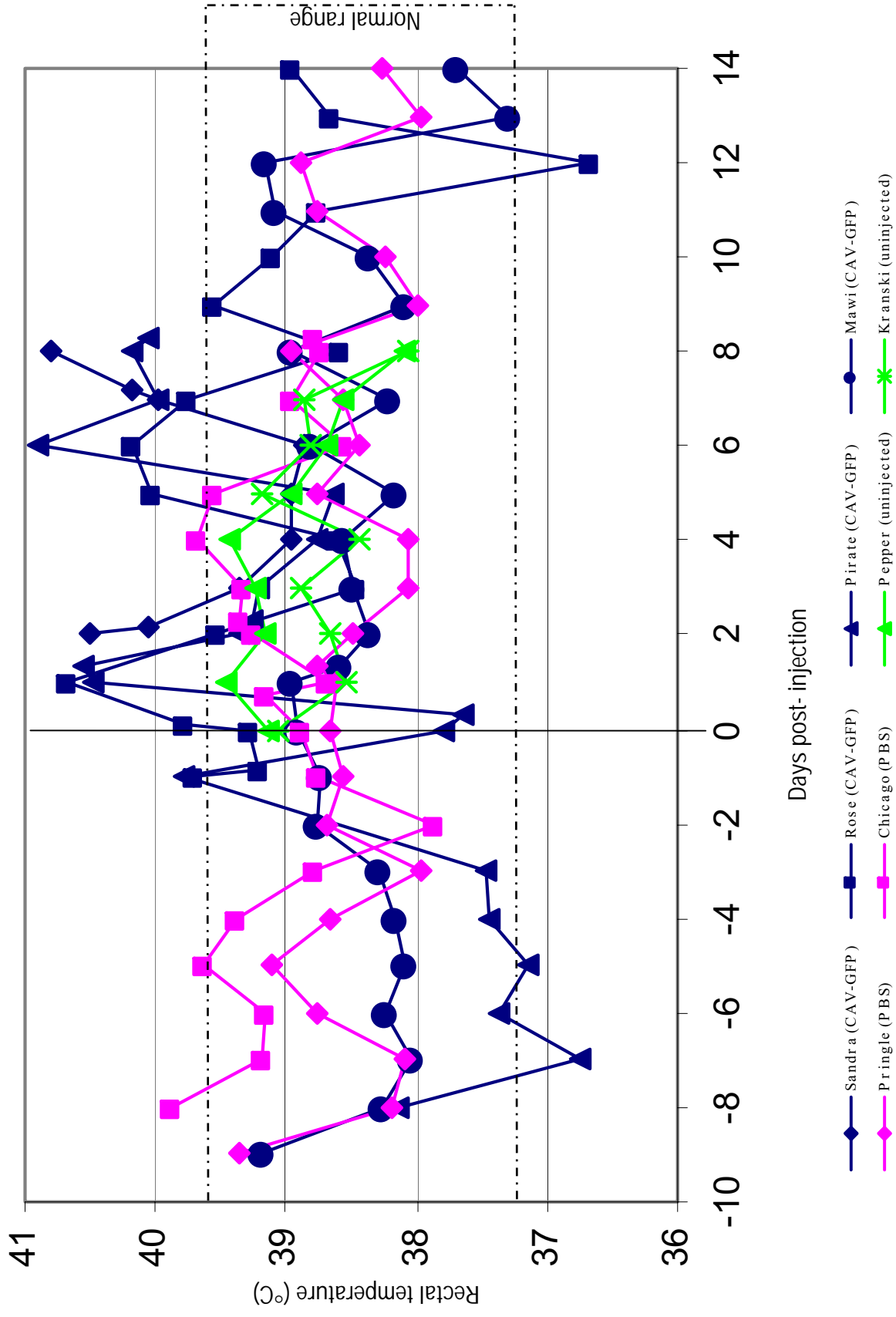
4.3.1.2. GFP Biodistribution and Immunostaining

GFP expression was able to be visualised in PFA-fixed, frozen sagittal brain sections in three out of four CAV-GFP-treated guinea pigs with transgene expression correlating with the order of injection, i.e. Sandra had the highest level of GFP expression and best transgene distribution within the brain, followed by Rose and Pirate, whilst no transgene expression was observed in Mawi. GFP transgene expression was not detected in vehicle controls or in uninjected animals, even with immunofluorescent staining against GFP, at any time point throughout this study.

Intense GFP expression and a large number of transgene-positive cells were observed in the cortex, septum and in the corpus callosum, while more moderate expression was detected in the choroid plexus of the fourth ventricle, olfactory bulb, supraoptic nucleus, lateral parabrachial nucleus, cerebellum and the polymorph layer of the hippocampus. GFP staining was observed within the cytoplasm and/or nucleus of transduced cells and strong staining was evident along the axonal processes of neurons, particularly within the hippocampus.

An immunofluorescent method of detecting GFP was established to improve the limit of detection of GFP protein in PFA-fixed, frozen guinea pig tissue. A polyclonal rabbit anti-GFP antibody at dilutions ranging from 1:250 to 1:20,000 was assessed and visualised with a Cy3-conjugated donkey anti-rabbit IgG secondary antibody (**Section 2.2.6.2**). The optimal dilution was determined to be 1:10,000, with strong, specific staining observed throughout the cytoplasm, nucleus and neurite extensions (**Fig. 4.3**). As anticipated, immunofluorescent detection of GFP correlated with unstained GFP expression in positive control tissue. However, immunostaining was also able to identify additional GFP-positive cells and axonal or dendritic processes which were not apparent without staining, thus greatly increasing the sensitivity of detection.

Immunostaining of brain tissues from CAV-injected guinea pigs showed extremely high GFP expression in the pyramidal neurons of the cerebral cortex (layer V), the granular neurons of the olfactory bulb and molecular layer of the hippocampus, in addition to the regions listed previously (**Fig. 4.4**). GFP-positive cells with moderate expression were also observed in the striatum. The widespread distribution of GFP in regions distant from the injection site suggests that the CAV-GFP vector is capable of undergoing retrograde axonal transport and that highly efficient gene transfer was attainable in young adult guinea pigs.

Figure 4.3: Immunofluorescent detection of GFP. PFA-fixed, frozen sections from CAV-GFP-injected guinea pigs underwent immunofluorescent staining with a rabbit polyclonal anti-GFP antibody (1:10,000; Molecular Probes) followed by detection with a Cy3-conjugated donkey anti-rabbit IgG secondary antibody (1:600; Jackson Immunoresearch). Compared to endogenous GFP expression without immunostaining (green cells, **A**, **C**, **E**), the sensitivity of GFP detection was greatly improved with indirect visualisation using immunostaining (red cells, **B**, **D**, **F**). All images were captured at an exposure of ¼ seconds. Brains from Sandra **(A, B)**, Rose **(C, D)** and Pirate **(E, F)** are displayed. Scale bar is 100 μm.
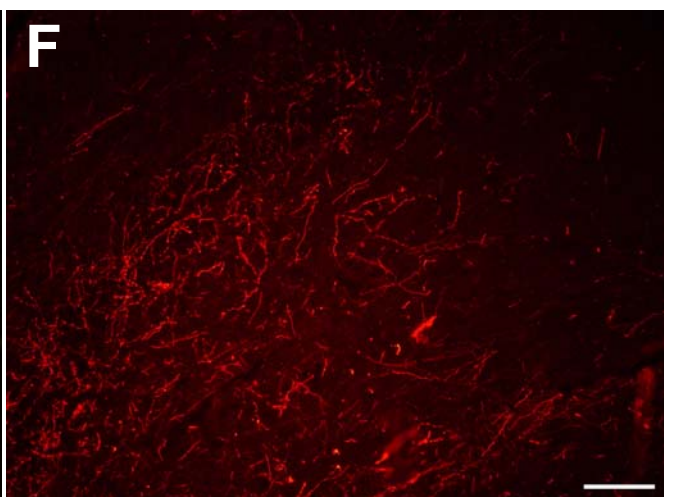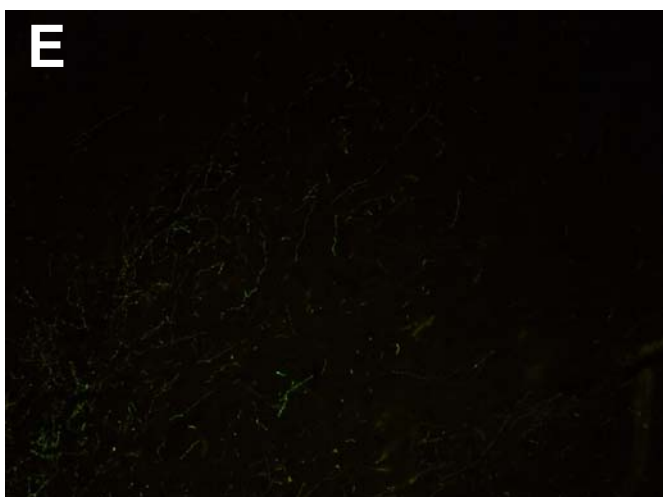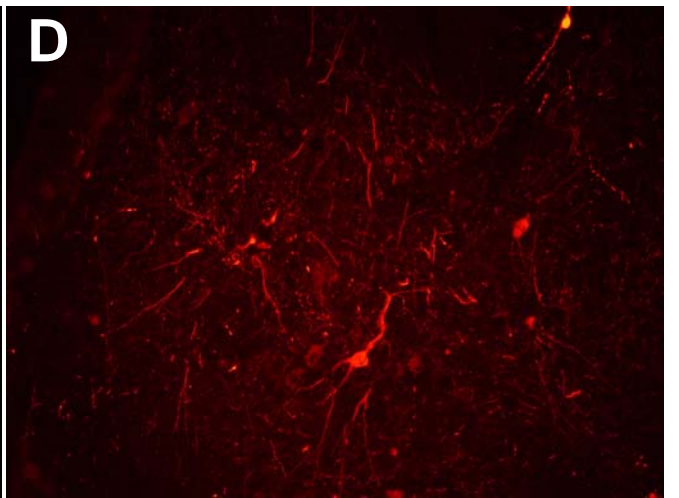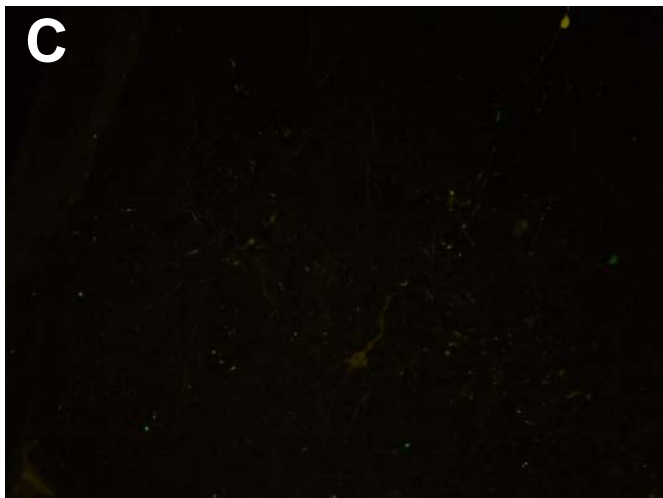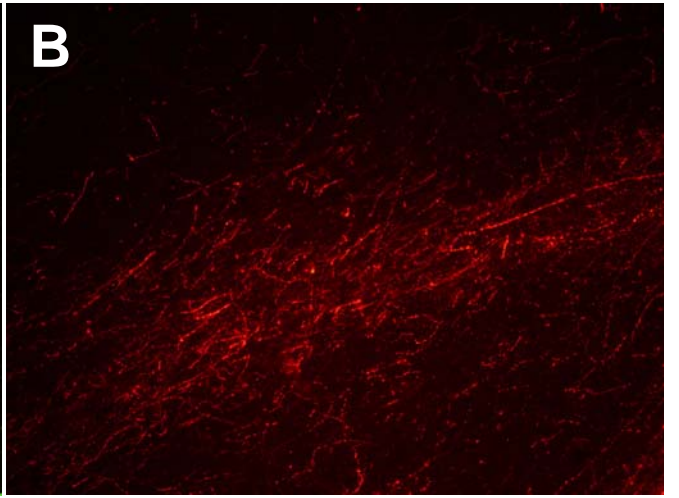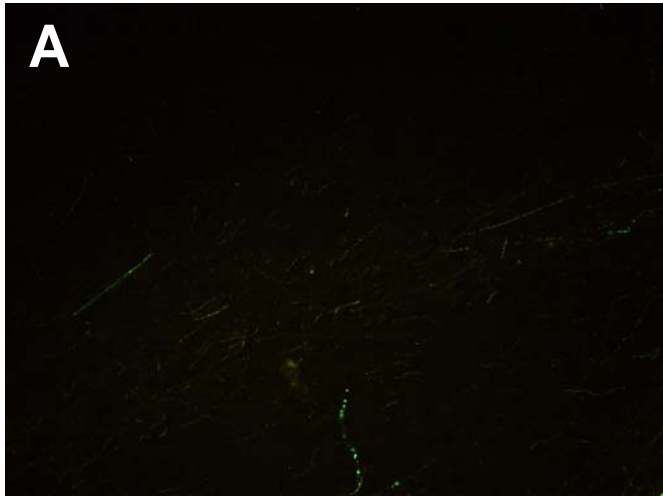
Figure 4.4: GFP biodistribution in CAV-GFP-injected guinea pigs. GFP expression was detected with immunostaining in PFA-fixed, frozen brain sections at 8-days post-injection. GFP fluorescence was observed in regions, including **(A)** the forceps minor of the corpus callosum and **(B)** layer V of the cortex (indicated by white arrowheads). **(C)** The polymorph layer of the hippocampus also displayed transduced cells (the boundary of the granular (GR) and polymorph (PM) layer of the hippocampus is indicated by arrowheads). **(D)** Granular neurons of the olfactory bulb were also GFP-positive, as was the **(E)** ependymal layer of the lateral ventricle (ventricle wall marked by arrowheads) and **(F)** the choroid plexus of the fourth ventricle (ventricle wall marked by arrowheads). All images were captured at an exposure of ¼ seconds. GFP-positive cells are represented in the schematic diagram below as red clusters, and the injection site is marked by a yellow triangle. Scale bar is 100 µm. Images are from Pirate.
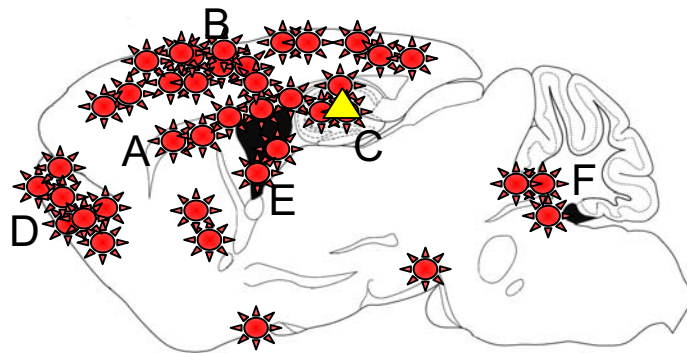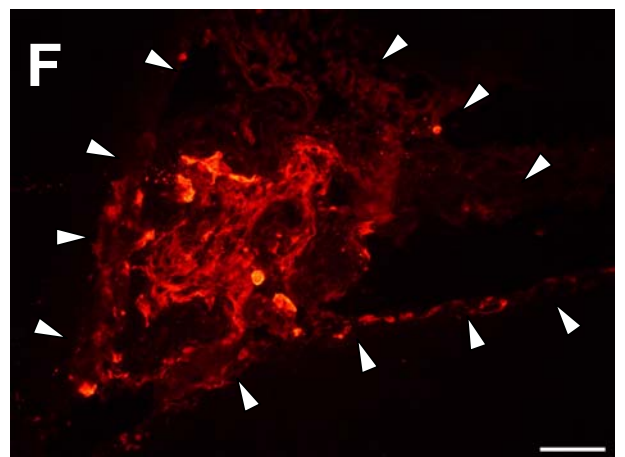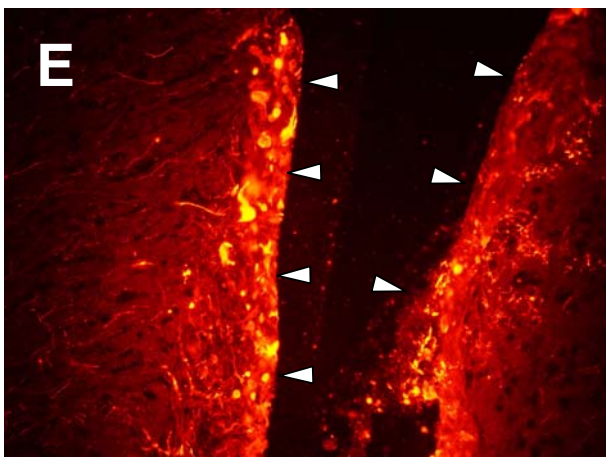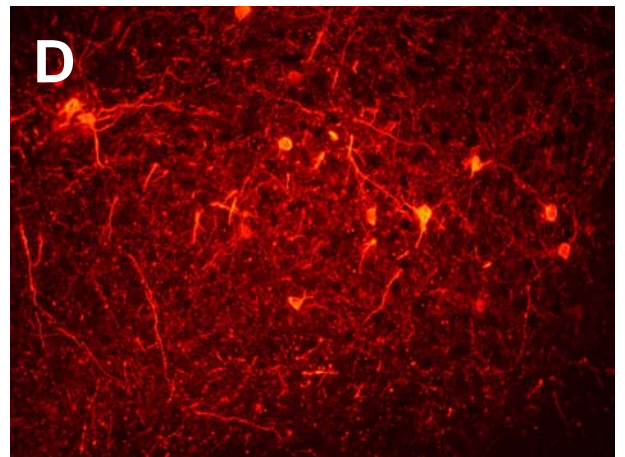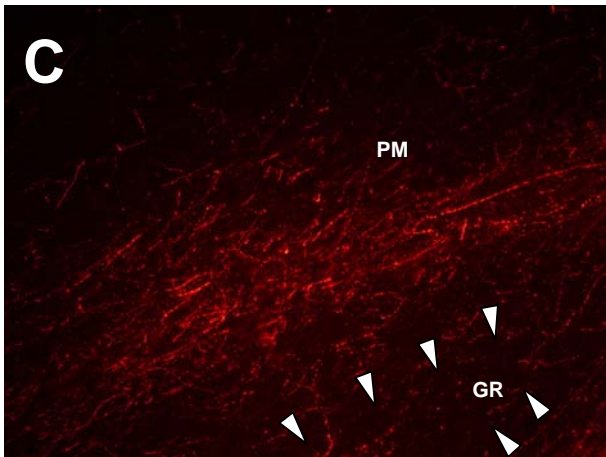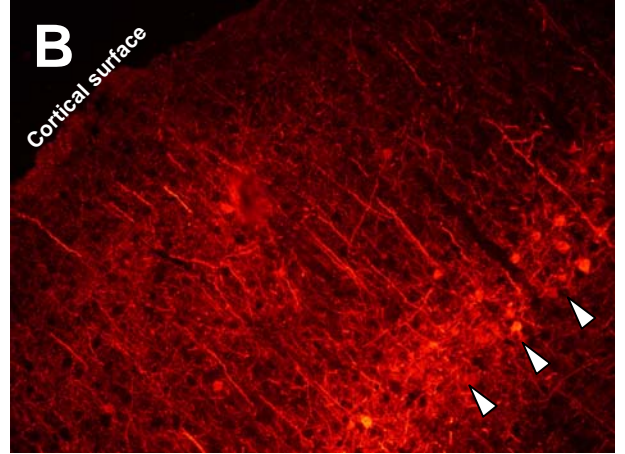
4.3.1.3. Humoral Immune Response

Heparinsed plasma and sera samples were collected prior to surgery and at sacrifice from all guinea pigs. The samples were sent to the Kremer laboratory (France) to determine whether neutralising antibodies had formed against the CAV-2 capsid proteins (**Section 2.2.9**). No neutralising antibodies were detected in CAV-GFP, saline or untreated guinea pigs.

4.3.2. Injection of CAV-2 Vectors into the Adult Mouse Thalamus

The stereotaxic co-ordinates used for targeting the adult mouse thalamus were (with respect to Bregma) posterior –1.5 mm, lateral ± 1.5 mm, ventral –3.25 mm (Paxinos and Franklin, 2001). Three surplus mice from the breeding colony were euthanased, injected with 1 μL/hemisphere toluidine blue into the thalamus and the brains removed and cryo-embedded. The listed co-ordinates were confirmed to be suitable by identification of autofluorescent cells in the needle tract damaged during the injection procedure and by the detection of toluidine blue-stained cells within the thalamus.

4.3.2.1. Preliminary Thalamic Injections of CAV-2 Vectors in Adult Mice

A small *in vivo* study was conducted with the CAV-2 vectors in adult mice. The initial experiments were performed on unaffected mice from the mixed "New York" strain, as the MPS IIIA congenic C57Bl/6 strain was not yet available. In total, 15 adult mice ranging in age from 6- to 30-wks received bilateral intra-thalamic injections of 3×10^9 particles/hemisphere of CAV-NS (n=9), CAV-GFP (n=2) or the same volume of saline (n=4; **Section 4.2.2**). Of these mice, 4 animals died from hyperthermia after inadvertent over-heating during surgery/recovery (n=3 CAV-NS; n=1 saline). One saline-injected mouse was euthanased the day following surgery after presumed damage to the eardrums from securing the ear bars too tightly, resulting in a "head tilt". An additional CAV-NS-injected mouse was euthanased 8-days post-surgery due to a urinary tract infection believed to be unrelated to any of the procedures. The majority of the adult mice undergoing surgery, regardless of the treatment administered, lost weight the day following surgery and then stabilised or gained weight for the remaining days of monitoring (data not shown).

Of the remaining 9 mice, 7 had been treated with a GFP-expressing CAV-2 vector. Frozen brain sections from CAV-injected mice were viewed under a fluorescent microscope fitted with a FITC filter. Twelve sections per mouse (4 taken at each of 3 lateral levels) were examined and no GFP-positive cells were observed, even when these sections were examined

using the more sensitive immunofluorescent method (**Section 4.3.1.2**). It is possible that the absence of transgene expression was the result of damage to the vector capsid during the injection process (discussed in **Section 4.3.2.2**). However, it is more likely that the vector particles within the Eppendorf were inactivated by the freshly ethanol-sterilised injection needles prior to loading and delivery of the vector. In subsequent injections, the ethanol-sterilised needles were thoroughly air-dried prior to loading the vector particles.

4.3.2.2. Mechanical Damage to Vector Particles

The structural integrity of the CAV-2 fibre is critical to internalisation and subsequent transgene expression. The transduction efficiency of CAV-2 vectors was therefore assessed after infusion to determine whether mechanical damage had occurred. CAV-NS (1 x 10^7 particles/µL) was loaded into a dental needle and duplicate samples expelled from the injection apparatus at either 0.33 µL/min or 2 µL/min into Eppendorfs, i.e. the infusion rate for adult and newborn mice, respectively. Two unloaded/uninjected positive control samples were also processed. The viral particle suspensions were applied to DKCre cells at 400 particles/cell and incubated for 3-days at 37°C. No difference in transduction efficiency was observed between the loaded/injected and unloaded samples, with all CAV-NS-treated cells expressing >90% GFP-positive cells as visualised on an epifluorescent microscope. This suggested that absence of GFP expression *in vivo* was not caused by mechanical damage to the vector particles during the stereotaxic injection process.

4.3.2.3. Vector Genome Detection in Adult Mice after CAV-2 Vector Injection

Injections of biologically-active CAV-2 vectors (or saline vehicle control) were administered to a further 14 adult mice from both the mixed "New York" and the congenic C57Bl/6 strains (a summary of all adult mice injected with viable CAV-2 vectors is displayed in **Table 4.2**). Care was taken to ensure that the injection needle was completely dry after ethanol sterilisation prior to loading the CAV-NS vector particles. Doses between 4.5 x 10^8 to 6 x 10^9 particles/hemisphere (in a volume of 1 or 2 µL) of CAV-NS (n=8) or CAV-GFP (n=3) were assessed. Three mice received the same volume of vehicle. Mice were weighed daily for at least 2-wks post-injection (**Fig. 4.5**).

Two unaffected mice (Mouse IDs 1 and 2; **Table 4.2**) were injected at 10-wks of age with 3 x 10^9 particles of CAV-NS per hemisphere and sacrificed 3-days after treatment. Autofluorescent cell clusters were observed in the cerebral cortex adjacent to the needle tract in both mice. Brain tissues were screened with anti-GFP immunostaining at several lateral

Table 4.2: Summary of adult mice injected with CAV-2 vectors. The identification numbers in column 1 refer to the data presented in **Fig. 4.4.** Adult mice were bilaterally injected into the thalamus. GFP expression within the CNS of injected mice was detected via immunostaining. In Mouse IDs 3, 4 and 8, sera were either not collected or insufficient sera was obtained for antibody titre analyses. The GFP-positive brain structures included the ependymal layer of the lateral ventricle (LV), striatum (STR), corpus callosum (CC), paramedian raphe nucleus (PRN), thalamus (THAL) and the choroid plexus of the fourth ventricle (CP4). -, not assessed.

ID	Strain	Genotype	Treatment	CAV dose (particles per injection)	Age at Injection	Sacrifice (days post-injection)	GFP Expression, Location & Quantity (cells/section)	Autofluorescent Cellular Infiltration	Vector Genome Detected	rhNS Antibody Titre	Neutralising Antibody Titre
1	Mixed (New York)	Unaffected	CAV-NS	3×10^9	10 wk	3 days	LV (1)	Yes	Yes	25	512
2			CAV-NS				No	Yes	Yes	25	512
3			PBS			14 days	fresh sacrifice	fresh sacrifice	-	-	-
4			CAV-NS			14 days	fresh sacrifice	fresh sacrifice	-	-	-
5	Mixed (New York)	MPS IIIA	CAV-NS	6×10^9	13 wk	14 days	LV, STR, CC, PRN (~50)	No	-	25	512
6			CAV-GFP			14 days	LV (~70)	No	-	25	256
7			CAV-NS			19 days	fresh sacrifice	fresh sacrifice	-	50	256
8			CAV-NS			Found dead (day 20)	-	-	-	-	-
9			PBS	0			No	No	No	-	<2
10			PBS				No	No	No	-	<2
11	C57Bl/6	Unaffected	CAV-NS	4.5×10^8	18 wk	14 days	THAL, (~50)	Yes	Yes	-	128
12			CAV-NS				LV, CP4, STR (~120)	Yes	Yes	-	512
13			CAV-GFP	4.5×10^8			No	Yes	No	-	16
14			CAV-GFP				No	Yes	No	-	128

Figure 4.5: Percentage change in body weight of adult mice post-injection. Adult mice were weighed daily to monitor recovery after bilateral stereotaxic injection of saline (crosses), CAV-GFP (hollow squares) or CAV-NS (filled diamonds) into the thalamus. Doses of CAV-2 vectors ranged from 4.5 x 10^8 to 6 x 10^9 particles/hemisphere in volumes of 1 or 2 µL/injection. Data are expressed as a percentage of body weight compared to the day of surgery (day 0). The mouse identification numbers correspond to the data presented in **Table 4.2**.

Body weight (as a % of day of surgery)

Days post-injection

Legend: 1, 2, 3, 4, 5, 6, 7, 8, 9, 10, 11, 12, 13, 14

planes from the midline. One GFP-expressing cell was detected in the lateral ventricle wall of Mouse ID 1. None were seen in tissues from Mouse ID 2.

In an attempt to establish whether the absence of GFP expression in these 2 mice was caused by the unsuccessful delivery of CAV-2 vectors to the CNS, or down-stream transcriptional and/or translational problems, genomic DNA was extracted from CAV-treated, cryo-embedded brains and viral DNA amplified by PCR (as described in **Section 4.2.4**). Two different tissue lysis buffer compositions were assessed. As seen in **Fig. 4.6**, similar PCR band intensities were observed with both lysis buffers when extracted with phenol/chloroform suggesting comparable efficiencies of genomic DNA extraction. However, in samples that were precipitated, but not phenol/chloroform-extracted, superior amplification and detection of viral genome was obtained with lysis Buffer B. Consequently, genomic DNA extracted in subsequent tissues was processed using Buffer B with a phenol/chloroform clean-up precipitation (optimised method described in **Section 2.2.1.1**).

CAV-NS viral genomic DNA was detected in frozen brain tissues from both (indeed all) of the CAV-NS-treated mice that were assessed (detailed in **Table 4.2**) indicating that CAV-NS vector particles were successfully delivered to the CNS. The CAV-NS vector genome was also amplified in the mice described in **Section 4.3.2.1,** which had received ethanol-inactivated vector. However, not every lateral plane from the midline was positive for viral genome. No viral genome was observed in saline or uninjected control samples. PCR product was amplified in all samples when the primers and conditions for the MPS IIIA genotyping PCR method were used, indicating that the absence of viral genome was not due to a failed genomic DNA extraction.

4.3.2.4. Effect of Increased CAV-NS Titre

A higher dose of CAV-NS was assessed to determine whether the amount of CAV-2 vector administered in the previous experiments resulted in GFP expression below the limit of detection. MPS IIIA mice were used in an attempt to measure increases in NS activity over background to establish whether the poor transgene expression observed in Mouse IDs 1 and 2 involved one or both of the transgenes included in the CAV-NS vector (i.e. rhNS and/or GFP genes). In addition, one mouse received CAV-GFP to determine whether the undetectable GFP expression was from positional effects of the GFP gene sequence following
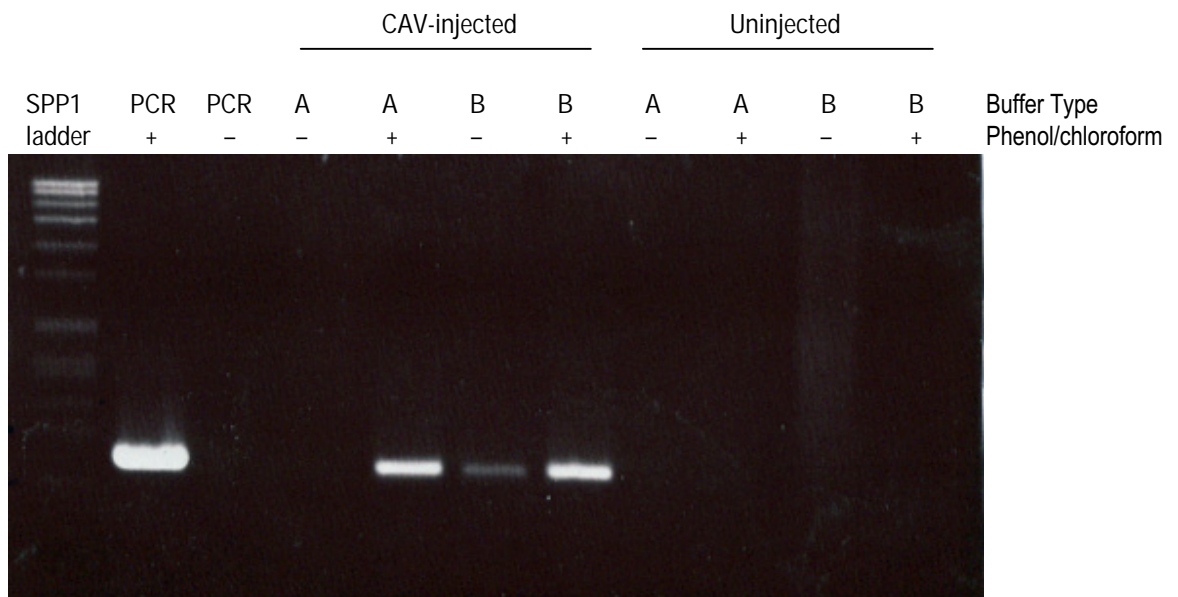
	CAV-injected				Uninjected			
SPP1 ladder	PCR +	PCR −	A −	A +	B −	B +	A −	A +	B −	B +	Buffer Type Phenol/chloroform

Figure 4.6: PCR amplification of CAV-2 viral genome. Genomic DNA was extracted from PFA-fixed, cryo-embedded brain sections from a guinea pig expressing GFP transgene or an uninjected control. Two genomic DNA lysis buffers were assessed (A, B) with and without phenol/chloroform clean-up (+/-). The lysis buffer compositions are described in **Section 4.2.4.** The best genomic DNA extraction was obtained when Buffer B was utilised for the tissue lysis and digestion with a phenol/chloroform clean-up, as seen by the strongest band intensity on the gel photo. The CAV-2 recombination PCR amplifies a product of 845 bp. pCAV-NS plasmid DNA was used as a PCR positive control.

an IRES element in the CAV-NS vector (batch SA4, biologically-active aliquot) (Zhu *et al*, 1999).

Adult MPS IIIA mice were injected bilaterally with 6 x 10^9 particles/hemisphere in a volume of 2 μL with CAV-NS, CAV-GFP or vehicle (Mouse IDs 3-8, **Table 4.2**). CAV-NS- and saline-treated mice (n=1 each) were euthanased 2-wks after surgery, the brain portioned and homogenised and the intracellular contents liberated by freeze/thawing (**Section 2.2.5.3**). No detectable increase in NS activity was observed in brain homogenates with CAV-NS treatment.

In addition, one CAV-NS- and one CAV-GFP-treated mouse were perfused to determine whether higher doses of CAV-2 vector resulted in improved GFP expression. At 14-days post-injection, a small cluster of GFP-expressing cells was identified in the ependymal layer of the lateral ventricle of both animals. In Mouse ID 6, an additional collection of GFP-expressing cells were detected within the striatum, corpus callosum and within an unknown structure, potentially the paramedian raphe nucleus (refer to **Table 4.2**). No obvious cellular infiltration was observed and the needle tract could not be located.

The two remaining mice treated with CAV-NS were designated for sacrifice at 6-wks post-injection. However, one of these mice (Mouse ID 8; **Table 4.2**) was found dead at 20-days post-injection, and the second mouse (Mouse ID 7), which was injected 24 hrs after the first mouse, required euthanasia at 19-days post-injection. Mouse ID 7 had lost approximately 30% of its body weight compared to the day of injection, had scruffy fur, a hunched posture and appeared dehydrated.

4.3.2.5. Humoral Response

Following the unexpected adverse events described in the previous section, a method for detecting neutralising antibodies against the CAV-2 capsid was established to determine whether a humoral response had developed in any of the mice injected to date (**Section 2.2.9**). This method was conducted according to the conditions employed in the Kremer laboratory (Perreau *et al*, submitted). The neutralising antibody detection assay was optimised using complement-inactivated sera from a normal dog immunised with CAV-2. This sample was included as a positive control in every batch of sera tested and the neutralising antibody titre was >98% inhibition at a 1:512 dilution. Neutralising antibody titres of 256, 256 and 512 were detected in the sera of all MPS IIIA mice injected with CAV-GFP or CAV-NS vectors (Mouse IDs 5-7; **Table 4.2**). Elevated titres were detected in the unaffected mice that had received 3 x 10^9 particles/hemisphere CAV-NS (titres 512, 512; Mouse IDs 1 and 2). CAV-2

neutralising antibodies were not found in uninjected or saline-treated mice at titres greater than 16. A larger cohort of uninjected control mice will be discussed in **Chapter 7**. The mice which received ethanol-inactivated CAV-NS vector (3 x 10^9 particles/hemisphere) also displayed low neutralising antibody titres of 4, 32 and 32.

Concurrently, antibodies against the rhNS protein were measured to see whether rhNS transgene expression resulted in a humoral response (**Section 2.2.10**). The highest rhNS titre measured in the adult CAV-NS-injected mice was 50 (**Table 4.2**), which was very low compared to the positive control mouse sera (a mouse receiving ongoing ERT; titre >800). Saline-injected (n=1) and uninjected mice (n=3) did not display absorbance values over the negative control sample without sera.

In addition, live unaffected mice of the "New York" strain (n=2; 20-wks) and the congenic C57Bl/6 strain (n=2; 30-wks) were sent to the Murine Virus Monitoring Service (Institute of Medical and Veterinary Science, Australia) to determine whether mouse adenovirus type I antibodies were present using an ELISA assay (Stevenson and Nicolson, 2002). These mice were determined to be pathogen-free, eliminating the possibility of mouse adenoviral antibodies potentially cross-reacting and neutralising the CAV-2 viral vector.

4.3.2.6. Effect of Mouse Strain on GFP Expression

Congenic MPS IIIA and within-colony unaffected control C57Bl/6 mice became available for experimental use during the course of these experiments. To determine whether improved transgene expression could be obtained in mice with a pure genetic background, congenic unaffected mice (n=2 per treatment) were bilaterally injected with 4.5 x 10^8 particles/hemisphere of CAV-GFP, CAV-NS or saline as a control (Mouse IDs 9-14, **Table 4.2**).

A small number of GFP-positive cells were detected by immunofluorescence in the thalamus of one CAV-NS-treated mouse (Mouse ID 11), whilst limited transgene expression was evident in the ependymal cells of the lateral ventricle, choroid plexus of the fourth ventricle and in the striatum of the other CAV-NS-injected mouse (Mouse ID 12). All of the CAV-2 vector-treated mice displayed autofluorescent cellular infiltration below the cortical surface at the site of the injection tract. No GFP-expressing cells were observed in the mice injected with CAV-GFP or the saline vehicle controls.

High neutralising antibody titres against the CAV-2 capsid were detected in one CAV-GFP and both CAV-NS-treated mice (Mouse IDs 11, 12 and 14; titres 128, 128 and 512,

respectively; **Table 4.2**), but the neutralising antibody titre in the other CAV-injected mouse was insignificant (Mouse ID 13, titre 16).

4.4. DISCUSSION

4.4.1. Adult Guinea Pig Injections

GFP Expression

One of the major aims of the experiments described in this section was to establish the procedures for *in vivo* CAV-2-mediated gene transfer. The preliminary experiments were undertaken in guinea pigs. Widespread and strong GFP transgene expression was detected throughout the brain of three guinea pigs, indicating that the viral vector and/or transgene were transported throughout the brain. This is the first report of CAV-mediated gene transfer and expression in guinea pigs (**Fig. 4.4**). The majority of the GFP-expressing regions were in close proximity to the injection site, the dentate gyrus of the hippocampus. For example, CAV-GFP particles may have transduced the cortical layer as the injection needle passed directly through this structure. The olfactory bulb and the choroid plexus were the only transgene-expressing regions that were not directly adjacent to the hippocampal injection site. For the olfactory bulb, CAV-GFP likely transduced cells within the subventricular zone of the lateral ventricle and these cells were able to migrate to the olfactory bulb within 8-days post-injection via the rostral migratory stream. Labelled cells implanted in the same region of adult mice have been shown to migrate to the olfactory bulb within 2-days (Lois and Alvarez-Buylla, 1994). In addition, the choroid plexus of the fourth ventricle expressed GFP transgene. It is possible that some CAV-GFP vector particles entered the lateral ventricle and were transported to the 4th lateral ventricle by cerebrospinal fluid flow (Ghersi-Egea *et al*, 1996).

The hippocampus was selected as the injection site based on this region being implicated in memory and learning processes (as reviewed in Squire, 1992; McClelland *et al*, 1995). This is a potential injection site in adult affected guinea pigs and mice given that α-mannosidosis and MPS IIIA disease progression results in memory and learning deficits (Gliddon and Hopwood, 2004; Crawley *et al*, 2006a; Robinson *et al*, submitted by LDRU). In addition, previous studies conducted in 7- to 10-day-old guinea pigs utilising embryonic stem cell-derived implants exhibited survival and migration from this injection site (Robinson *et al*, 2005).

Variable GFP expression was observed in the CAV-GFP-injected guinea pigs, with the strongest and most widespread GFP expression observed in the first animal to undergo surgery. We hypothesise that the variability in GFP expression may be due to ethanol-inactivation of the CAV-GFP vector stock prior to stereotaxic delivery.

Body Weight and Rectal Temperatures

With one exception, weight loss was observed in all guinea pigs used in the study when they were moved from PC1 to PC2 holding rooms (**Fig. 4.1**). This may partially be attributed to the stress of moving from group- to single-housing (for the first guinea pig injected, Sandra) and alterations in housing conditions (e.g. different holding rooms, changing from a pen to a rabbit cage, first exposure to mice and rats in the holding room), as weight loss was observed in untreated animals and guinea pigs who were yet to undergo surgical procedures.

The rapid weight loss in the first injected guinea pig prompted the inclusion of rectal temperature measurements as part of the post-surgery monitoring of recovery. Similar to the weight loss in uninjected/pre-surgery guinea pigs, elevated rectal temperatures were observed in three animals prior to injection, indicating that the surgical procedures are unlikely to be the sole reason for the occurrence of fever (**Fig. 4.2**). All animals received 2.5 mg/kg of the analgesic flunixin intramuscularly immediately following surgery for pain relief. No uninjected or sham-injected guinea pigs required supplementary flunixin injections. However, 3 CAV-GFP-injected animals required additional flunixin doses due to rectal temperatures exceeding 40°C. CNS tissues taken from these guinea pigs were shown to have GFP transgene expression. The fourth CAV-GFP-injected guinea pig, Mawi, was not feverish and did not display GFP-positive cells in the cerebrum. Fevers have also been observed following the injection of an ΔE1/E3 Ad vector into the lateral ventricle, but not the striatum, of adult rats (Cartmell *et al*, 1999). Interestingly, fevers in these rats were induced by two different transgenes and by an Ad vector encoding no transgene, but not with vehicle, caesium chloride or with a heat-inactivated Ad encoding no transgene (i.e. biologically-inactive particles), suggesting that the fever response was induced due to the Ad particles being biologically-active and not transgene expression (Cartmell *et al*, 1999). Likewise, psoralen-treated, UV-inactivated Ad vector particles administered peripherally in adult mice induced a cellular inflammation, including the infiltration of $CD4^+$ and $CD8^+$ T lymphocytes and a CTL response (Kafri *et al*, 1998). It is likely that fevers observed in the first 3 CAV-GFP guinea pigs were linked to the translation of the remaining viral proteins in the ΔE1 CAV-GFP vector

and that the fourth guinea pig did not display a fever or transgene expression as it may have received ethanol-inactivated CAV-GFP vector.

Neutralising Antibody Detection

No neutralising antibodies were detected in sera or plasma from CAV-GFP or sham-injected unaffected guinea pigs, indicating the absence of a humoral response. ERT studies conducted with the α-mannosidosis guinea pig model have demonstrated that a humoral response can be mounted after 2 or 3 weekly intravenous injections of recombinant α-mannosidase from birth or from 30-days of age (Crawley *et al*, 2006b). In the CAV-GFP-treated guinea pigs, a humoral response may have developed if longer times post-injection were assessed. However, the route of administration of the viral vector directly into the cerebrum, compared to the intravenous administration of recombinant enzyme in the ERT study, possibly influenced the development of a humoral immune response.

4.4.2. Adult Mouse Injections

After demonstrating that ΔE1 CAV-GFP was capable of widespread distribution and gene transfer within the CNS of young adult guinea pigs, intracerebral injections were performed in adult mice to obtain a comparison of the efficacy and biodistribution of gene transfer in another species. The CAV-NS vector was used in preference to the CAV-GFP vector because of the cytotoxicity observed with the latter during the *in vitro* transduction of primary murine neural cells (**Chapter 3**).

We anticipated that one of the major advantages of using CAV-2 would be an improvement in vector distribution via retrograde axonal transport (Soudais *et al*, 2001b; 2004; Sotak *et al*, 2005). Consequently, the thalamus was selected as the initial injection site, as this region is a processing station for sensory information and is highly inter-connected with other brain regions (McKenna and Vertes, 2004). Various thalamic nuclei are inter-connected and involved with spatial learning and memory. The thalamus has reciprocal connections with the cerebral cortex (including visual, somatosensory and auditory regions). It also sends afferents to regions including the hippocampus (memory and learning), septum (reward centre), basal forebrain nuclei, amygdala (anxiety and emotion), striatum (movement), hypothalamus (endocrine, metabolic and emotional function), substantia nigra (voluntary movement and influences mood) and the brain stem (reviewed in McKenna and Vertes, 2004; Smith *et al*, 2004; Nagaeva and Akhmadeev, 2006).

Absence of GFP Expression in Adult Mice

In preliminary experiments, reduced or no transgene expression was observed in CAV-2 vector-injected adult mice. We hypothesised that the absence of transgene expression *in vivo* was caused by mechanical damage to the viral vector, the vector not being successfully delivered to the CNS of adult mice or inactivation of the viral particles by freshly ethanol-sterilised injection needles. It was demonstrated that the first two scenarios were not the reason for the absence of GFP expression and that it was likely due to ethanol-inactivated vector particles.

Based on the *in vitro* findings utilising the CAV-NS vector in murine primary neural cells described in **Chapter 3**, GFP expression may have been insufficient to visualise endogenous GFP fluorescence, akin to the long exposures required to capture GFP fluorescence in CAV-NS-transduced murine neural primary cultures *in vitro*. It is estimated that at least 1 μM of GFP is required to double the GFP fluorescence over autofluorescent background and thus approximately 10^6 copies would be required to achieve this degree of fluorescence for a typically-sized mammalian cell (Niswender *et al*, 1995; Tsien, 1998). Consequently, an immunofluorescent detection method was developed to amplify the GFP signal in tissue sections. In addition to endogenous GFP fluorescence, immunofluorescent staining would also detect GFP protein that did not fluoresce due to changes in pH, denaturation of the protein by high temperatures or alcohols, or because of photo-bleaching (reviewed in Tsien, 1998).

Humoral Response in Adult Mice

Adult mice receiving intra-thalamic delivery of biologically-active CAV-2 vectors mounted a strong humoral response with elevated neutralising antibody titres against the CAV-2 capsid (**Section 2.2.9**). This response was generated against the vector in the CNS within 3-days and lasted for at least 19-days post-injection (**Table 4.2**). In contrast, a limited neutralising antibody response against the CAV-2 capsid was elicited in mice which received inactive, ethanol-fixed CAV-2 vectors. The kinetics of the humoral response compare with a study by Kajiwara and colleagues (2000) where intra-striatal delivery of 6 x 10^6 plaque forming units of an ΔE1-deleted Ad5 vector expressing β-galactosidase to adult mice induced a humoral response against Ad within 2-days post-injection, with the level of anti-Ad antibodies peaking at 30-days post-injection. The anti-Ad response was dose-dependent and was also mounted against UV-inactivated Ad vector, but not to the same degree as the

functional Ad-βgal vector (Kajiwara *et al*, 2000). Surprisingly, neutralising antibodies were not detected in the mice from the Kajiwara (2000) study, with the exception of one mouse, and this was attributed to the low titres employed. These results are in stark contrast to the high neutralising antibody titres observed with CAV-2 vectors in the present study. The absence of mouse adenovirus (MAV) type I antibodies in untreated mice from the "New York" and C57Bl/6 congenic strains (**Section 4.3.2.5**) suggests that that the humoral response observed in the CAV-injected mice was unlikely to be caused by cross-reactivity between the MAV and CAV epitopes.

Transgene-specific antibodies against β-galactosidase transgene can also be formed after 30-days post-injection (Kajiwara *et al*, 2000). Similarly, repeated intrathecal injection of rhNS protein into the cerebrospinal fluid of adult mice generates strong rhNS-specific antibody titres (Hemsley *et al*, 2007). Weekly injection of rhNS into the cerebrospinal fluid of adult MPS IIIA dogs also induces an anti-rhNS antibody response within 3-wks after the first administration (Hemsley *et al*, 2006). The absence of anti-rhNS antibodies in adult mice receiving CAV-NS may indicate that there was insufficient rhNS expression from CAV-NS-transduced cells to generate a humoral response against rhNS.

The limited GFP transgene expression observed in the CAV-NS- and CAV-GFP-injected mice may have been the result of infiltrating B-lymphocytes eliminating transduced cells within the CNS. A recent study by Zirger and colleagues (2006b) demonstrated that CD19^{+} B cells play a pivotal role in the early elimination of Ad viral genomes from transduced brain cells after adult C57Bl/6 mice receiving intra-striatal injections were re-challenged by systemic administration of a second Ad vector encoding a mismatched transgene. However, Igh-6 mice, which lack mature B cell populations, were unable to eliminate transduced cells within the CNS at early time points. In addition, inflammatory responses are also well documented as playing a role in the elimination of transduced cells within the CNS. The inflammatory response to CAV-2 vector particles was not examined. Ad transduction can result in the activation of the mitogen-activated protein kinase pathways, which facilitate the activation of microglial cells, the primary immune mediators within the brain (Byrnes *et al*, 1996; Bhat and Fan, 2002; Stone *et al*, 2003). Injection of Ad into the CNS of naïve rodents also increases the level of pro-inflammatory cytokines (TNF-α, IL-1β, IL-6 and IFN-regulated proteins), chemokines (RANTES, IFN-γ-inducible protein 10, and monocyte chemoattractant protein 1) as well as MHC I within the brain (Byrnes *et al*, 1996; Cartmell *et al*, 1999; Thomas *et al*, 2000; Zirger *et al*, 2006a). The transduction of CNS cells by Ad vectors can also induce the rapid infiltration of CD4^{+} and CD8^{+} T lymphocyte cells,

brain macrophages and leukocytes (Byrnes *et al*, 1995; Thomas *et al*, 2000; 2001a; Stone *et al*, 2003). It is thought that much of this inflammation is a result of the virion particles rather than the *de novo* expression of viral proteins, as cellular inflammatory responses have also been detected in rats treated with Ad vectors not encoding a transgene or with UV-inactivated Ad vector (Byrnes *et al*, 1995).

The detection of GFP-positive cells in the ependymal layer of the lateral ventricle in mice injected with 6 x 10^9 particles of CAV-NS indicates that the vector was present in the ventricular system. It has been established that antigens delivered intra-ventricularly are more immunogenic than when delivered directly into the brain parenchyma (Stevenson *et al*, 1997). Similarly, higher β-glucuronidase activity was measured after intra-striatal injection of a ΔE1 Ad vector in adult mice compared to cerebrospinal fluid delivery of an identical titre to the cisterna magna (Ghodsi *et al*, 1998).

Other Factors Potentially Affecting GFP Expression

Several reports have documented that the genetic background of the mouse influences the immunological response (Guida *et al*, 1995; Christenson *et al*, 1998; Charles *et al*, 1999a; 1999b; Ohmoto *et al*, 1999; Mazzolini *et al*, 2001; Peng *et al*, 2001; Zhang *et al*, 2004). After demonstrating that a humoral response was generated at 3 x 10^9 and 6 x 10^9 particles of CAV-2 vectors in the mixed "New York" strain (containing contributions from 129SvJ, CD1, C57Bl/6 and SJL strains, Bhaumik *et al*, 1999), it was postulated that the simpler genetic background of the congenic C57Bl/6 MPS IIIA strain may alter the experimental outcome.

To further improve the chances of success, the titre was lowered to 4.5 x 10^8 particles/hemisphere (equivalent to 1 x 10^8 infectious units per injection) based on the findings of Thomas *et al* (2001a), where doses exceeding 10^8 infectious units induced chronic inflammation and acute vector-mediated cytotoxicity after intra-striatal delivery in immunocompetent adult rats. This threshold effect has subsequently been characterised in C57Bl/6 mice and has been shown to be caused by the upregulation of IFN-regulated and chemokine messenger RNA transcripts at doses greater than 10^8 infectious units of a first-generation Ad vector (Zirger *et al*, 2006a). However, similar to the results observed in the mixed "New York" strain, comparable neutralising antibodies were elicited against the CAV-2 capsid in adult mice of the congenic C57Bl/6 strain after CAV-NS and CAV-GFP injection.

Future Directions to Circumvent Vector Immunogenicity

Low transduction efficiency was observed in adult-injected animals due to immune responses against the ΔE1 CAV-2 vector. Several strategies could be implemented to circumvent vector immunity and improve transgene expression in adult MPS IIIA mice without reconstructing the CAV-NS vector. Firstly, adult mice could be pre-treated with immunosuppressive or immunomodulatory agents prior to CAV-2 injection. The use of immunosuppressive agents such as cyclosporine (Fang *et al*, 1995; Shen *et al*, 2001b) or tacrolimus (FK-506) (Lochmuller *et al*, 1995; Vilquin *et al*, 1995; Durham *et al*, 1997) can greatly improve the duration of transgene expression in systemic and CNS-delivered first-generation Ad vectors. However, the effect of cyclosporine immunosuppression does not always improve Ad-mediated transgene expression (Dai *et al*, 1995; Petrof *et al*, 1995) and both of these immunosuppressants require daily administration to maintain therapeutic concentrations from just prior to injection to terminal sacrifice and are neurotoxic (reviewed in Gijtenbeek *et al*, 1999).

Similarly, immunomodulatory procedures such as transient depletion or blockade of CD4$^+$ T lymphocytes (Kolls *et al*, 1996; Ye *et al*, 2000; Thomas *et al*, 2001a) or macrophages (Kuzmin *et al*, 1997; Stein *et al*, 1998; 2001) have been shown to abrogate the immune response when Ad was administered peripherally. Likewise, the injection of antibodies directed against CD40 ligand to inhibit CD40-CD40 ligand costimulatory interactions has been demonstrated to prolong Ad-mediated lysosomal enzyme expression in MPS VII and Fabry mice (Stein *et al*, 1999; Ziegler *et al*, 1999). Comparable improvements in transgene duration after Ad administration have been observed by blockade of the B7-CD28 interaction using CTLA4Ig within the CNS (Uchida *et al*, 2001) or systemically (Schowalter *et al*, 1997). Several of these strategies have allowed the successful re-administration of recombinant Ad vectors (Stein *et al*, 1998; Ye *et al*, 2000; Kuzmin *et al*, 2001; Ziller *et al*, 2002).

Secondly, an immune response in adult mice injected with the CAV-NS vector may have been avoided if pups were tolerised at birth to the CAV-2 capsid proteins. Direct intrathymic (but not intravenous) inoculation of recombinant Ad vectors into neonatal mice induced tolerance and these mice failed to mount an effective CTL response when rechallenged with Ad at 4- to 8-wks post-injection (DeMatteo *et al*, 1997). This enabled prolonged β-galactosidase expression in the liver lasting up to 260-days. Tolerisation and long-term transgene expression has also been achieved in Gunn rats by oral administration of Ad proteins (Ilan *et al*, 1997; 1998) or by direct intrathymic injection (Ilan *et al*, 1996).

A third strategy to evade the immune response to ΔE1 CAV-2 vectors in adult mice could potentially involve the covalent binding of the capsid proteins to molecules such as polyethylene glycol (PEG) to mask the structural epitopes of the vector (O'Riordan *et al*, 1999; Eto *et al*, 2005; Mok *et al*, 2005). In studies conducted by Croyle and colleagues (2001; 2002), reductions in the CTL response and neutralising antibodies against the first-generation Ad capsid proteins were observed when using PEGylated vectors. In addition, considerable transgene expression was observed when native Ad or PEGylated Ad was re-administered in the lung (Croyle *et al*, 2001) or liver (Croyle *et al*, 2002) when inoculated with the opposite Ad vector (i.e. native then PEGylated Ad or vice versa) but not when PEGylated Ad was delivered twice.

A fourth approach to avoid a ΔE1 CAV-2 vector-initiated immune response is to alter the age at which the vector is administered (i.e. inject younger mice). The neonatal immune system is less likely to develop immunogenic responses against transgenic proteins because there are fewer immune cells and those that are present in neonates are developmentally immature (Adkins and Du, 1998; reviewed in Waddington *et al*, 2004). Additionally, newborn mice are more likely to develop Th2 secondary responses when challenged and the kinetics of cytokine production are altered compared to the profiles observed in developmentally mature mice (Adkins and Du, 1998). This strategy also takes advantage of the higher expression of the primary receptor, CAR, within the CNS *in utero* and in neonates (compared to adult mice; Honda *et al*, 2000; Hotta *et al*, 2003). Additionally, for disorders such as MPS IIIA, it is desirable to treat as early as possible to prevent disease progression (Gliddon and Hopwood, 2004; Savas *et al*, 2004). Ad vectors have successfully been administered at birth to LSD mouse models via the superficial temporal vein (Kamata *et al*, 2003; Kanaji *et al*, 2003; Takaura *et al*, 2003) or by direct injection within the CNS (Shen *et al*, 2001a; Eto *et al*, 2004). *In utero* delivery of Ad vectors is also feasible (Jerebtsova *et al*, 2002; Shen *et al*, 2002; Bouchard *et al*, 2003; Shen *et al*, 2004; Bilbao *et al*, 2005) but the survival rate of pups has been reported to be less than 40% at weaning (Bouchard *et al*, 2003). Given that early treatment is best for LSD patients, this strategy was selected for further evaluation of CAV-mediated gene expression in newborn MPS IIIA mice.

4.5. SUMMARY AND CONCLUSIONS

CAV-GFP mediated strong and widespread distribution of the GFP transgene after bilateral injection into the hippocampus of young adult guinea pigs without inducing a humoral response. This suggests that gene therapy studies assessing the therapeutic benefit of a CAV-2 vector expressing recombinant α-mannosidase could be conducted in the naturally-occurring α-mannosidase guinea pig model (Crawley *et al*, 1999). Alpha-mannosidase guinea pigs have been documented to have severe neuropathological (Crawley *et al*, 1999; Crawley and Walkley, in press) and behavioural disturbances (Robinson *et al*, submitted by LDRU). However, before the clinical effect of gene transfer in this animal model can be assessed, the longevity of CAV-mediated gene expression needs to be determined.

In contrast, delivery of CAV-NS or CAV-GFP into the thalamus of adult mice resulted in the induction of a humoral immune response against the CAV-2 capsid, thus greatly limiting the efficacy of gene transfer in adult mice. These data suggest that immunocompetent adult mice are unsuitable for ΔE1 CAV-2-mediated gene therapy using the delivery strategy employed in this chapter.

CHAPTER 5:

Preliminary *In Vivo* Gene Transfer in Newborn Mice

5.1. INTRODUCTION

For ΔE1 CAV-2 viral vectors to mediate improvements in MPS IIIA pathology, widespread and efficient NS gene transfer is required within the CNS of affected individuals. However, as described in the previous chapter, stereotaxic delivery of ΔE1 CAV-2 viral vectors into the brains of immunocompetent, adult mice resulted in a rapid induction of a humoral immune response against the CAV-2 capsid proteins, thus greatly limiting transgene expression.

The primary objectives of the experiments outlined in this chapter were to determine whether CAV-NS vector delivery into the newborn mouse brain could successfully generate sufficient transgene expression and, if so, to determine the dose that provided the optimal distribution and longevity of GFP marker gene expression. In addition, a sandwich ELISA method for rhNS protein quantification was developed to monitor rhNS protein production in brain homogenates after injection.

5.3. RESULTS

5.3.1. Dose-Dependent GFP Expression Following CAV-NS Delivery to Newborn Mice

To examine whether CAV-NS was able to mediate transgene expression in newborn mice (and, if so, to determine the optimal dose of the CAV-NS vector as assessed by GFP staining), newborn mice received intraventricular injections at four different CAV-NS titres (bilateral injections of 5 x 10^6, 1 x 10^7, 1 x 10^8, 1 x 10^9 particles in 1 μL/hemisphere; **Section 2.2.5.1**) and were sacrificed at three times post-injection (2-, 7- or 14-days post-injection). Heterozygous x MPS IIIA pairings were performed and two pups were randomly assigned to each of the above groups prior to identifying the pup's genotype, as genomic DNA from a toe clip could only be obtained after 5-days of age. MPS IIIA x MPS IIIA homozygous pairings

were avoided due to a suspicion of reduced fertility and increased cannibalism of pups by affected mice (Crawley *et al*, 2006a). All mice regained colour and were responsive within minutes of the cryo-anaesthesia/injections. Once returned to the cage, pups were quickly recovered to the nest and nurtured by the dam.
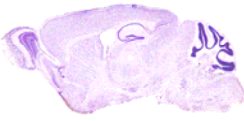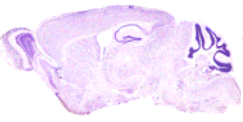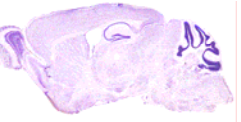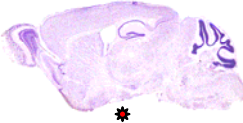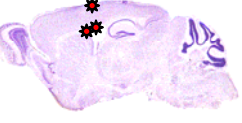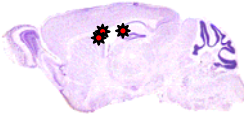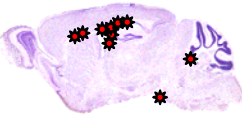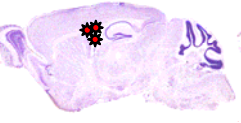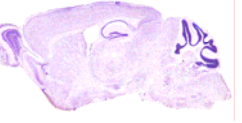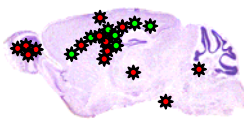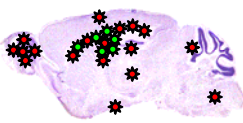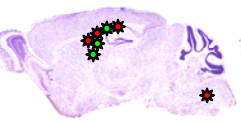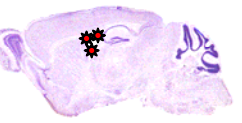
The expression and distribution of GFP fluorescence after bilateral injections at each of the doses of CAV-NS vector was assessed at three different lateral levels with 4 sections viewed at each lateral plane. For animals euthanased at 2-, 7- and 14-days post-injection, the lateral planes assessed were approximately 0.4 to 1.5 mm, 1.0 to 2.1 mm or 0.6 to 2.0 mm lateral from the midline, respectively. The findings of these experiments are summarised in **Table 5.1.**

GFP-positive cells were not detected in the brains of mice receiving 5×10^6 particles/µL CAV-NS at any time-point post-injection, even with immunostaining.

Two pups receiving a dose of 1×10^7 particles/µL were not cared for by the dam (no milk in stomachs of pups, pups rejected from the nest) and were found dead at 2-days post-injection. Consequently, no tissues were analysed at this time-point and dose. At 7-days post-injection, one pup injected with 1×10^7 particles of CAV-NS displayed limited GFP expression in cell processes in an unidentified region, while another treated identically displayed no transgene expression. GFP transgene expression had improved at 14-days post-injection with GFP-positive cells found in the ependymal layer of the lateral ventricle, layer I of the cortex and the corpus callosum (adjacent to the lateral ventricle) in both mice. However, the expression was very limited, with no more than 30 GFP-expressing cells detected in a single 12 µm sagittal section at each of the lateral planes assessed.

Improved GFP expression was observed in pups injected with 1×10^8 particles/µL CAV-NS. At 2-days post-injection, the intensity and amount of GFP expression in the corpus callosum, hippocampus and lateral ventricle of one pup was similar to that observed at 7-days post-injection in mice treated with 1×10^7 particles/µL CAV-NS. The other pup assessed at 2-days post-injection was GFP-negative. By 7-days post-injection, the number of GFP-positive cells had greatly increased, as had the distribution of transgene with GFP immunoreactivity found in the corpus callosum (minor), choroid plexus and pontine nucleus in one of the pups (listed in descending order of GFP expression). However, by 14-days post-injection, GFP expression was restricted to the lateral ventricle and choroid plexus of mice and in one of these pups it appeared that a proportion of GFP-positive cells were necrotic (shrunken cytoplasm, loss of membrane integrity and autofluorescent).

Table 5.1: GFP biodistribution in newborn mice injected with CAV-NS. Mice were cryo-anaesthetised and bilaterally injected on the day of birth with 5 x 10^6 to 1 x 10^9 particles of CAV-NS per hemisphere in a volume of 1 µL/injection. At 2-days or 1-, 2- or 6-wks post-injection, the mice were euthanased, the brain tissues fixed with 4% (w/v) PFA and cryo-embedded. GFP-positive cells were determined via immunostaining using a polyclonal rabbit anti-GFP antibody and detected with a Cy3-conjugated donkey anti-rabbit IgG antibody. The brain regions displaying GFP immunoreactivity are listed below, from 2 or 4 injected mice from both genotypes at each dose and time-point (>4 sections from 3 lateral planes from the midline). Bold regions indicate that GFP could also be visualised without immunostaining. In the schematic representations, the areas marked with red clusters indicate that GFP-expressing cells were visualised with immunostaining, whilst green clusters indicate that GFP-positive cells were observed with and without immunostaining (i.e. stronger transgene expression).

| CAV-NS Dose | Time post-injection | | | |
(particles/hemisphere)	**2 days** (n=2/group)	**1 wk** (n=2/group)	**2 wk** (n=2/group)	**6 wk** (n=4/group)
5×10^6	No GFP- positive cells (n=2)	No GFP- positive cells (n=2)	No GFP- positive cells (n=2)	Not assessed
1×10^7	Not assessed (pups found dead)	unknown structure (n=1) No GFP-positive cells (n=1)	lateral ventricle (n=2) cortex (n=2) corpus callosum (n=2)	Not assessed
1×10^8	lateral ventricle (n=1) hippocampus (n=1) corpus callosum (n=1) No GFP-positive cells (n=1)	corpus callosum (n=1) choroid plexus (n=1) pontine nucleus (n=1) No GFP- positive cells (n=1)	lateral ventricle (n=2) choroid plexus (n=2)	No GFP-positive cells (n=4)
1×10^9	lateral ventricle (n=2) corpus callosum (n=2) choroid plexus (n=2) olfactory bulb (n=1) thalamus (n=1) pontine nucleus (n=1)	lateral ventricle (n=2) corpus callosum (n=2) olfactory bulb (n=2) cortex (n=2) choroid plexus (n=2) thalamus (n=1) hippocampus (n=1) hippocampal fissure (n=1) brainstem (n=1) lateral parabrachial nucleus (n=1) cerebellum (n=1)	lateral ventricle (n=2) corpus callosum (n=2) brainstem (n=1) choroid plexus (n=1)	lateral ventricle (n=4) choroid plexus (n=4)

The highest dose tested (1 x 10^9 particles/µL CAV-NS) provided the best transgene expression, distribution and longevity. It was only at this dose that GFP was detected in transduced cells without immunostaining. At 2-, 7- and 14-days post-injection, CAV-NS-treated mice displayed the highest GFP expression in the lateral ventricle and corpus callosum. Other strongly GFP-expressing regions included the olfactory bulb, choroid plexus and thalamus, while GFP-positive cells were occasionally seen in the cerebellum, brainstem, lateral parabrachial nucleus and cortex (**Table 5.1; Fig. 5.1**). The highest GFP expression (i.e. the most intense fluorescence, most transduced regions and highest number of GFP-expressing cells) was observed in the mice sacrificed at 7-days post-injection.

5.3.2. Weights and Survival Rates

After successfully detecting GFP expression within the CNS of newborn mice, a supplementary study was conducted with the two highest doses (1 x 10^8 or 1 x 10^9 particles/hemisphere) in both unaffected and MPS IIIA mice. The maintenance of transgene expression was assessed in PFA-fixed, frozen tissue sections at 6-wks (n=2/genotype and dose) via GFP immunostaining (**Section 2.2.6.2**). In addition, brain homogenates (n=4/genotype and dose) were analysed at 1- and 6-wks post-injection to determine whether CAV-NS treatment increased the amount of measurable rhNS protein in the brain (**Sections 2.2.5.3** and **5.3.6**) and whether this could mediate a reduction in HS-derived HNS-UA oligosaccharide storage compared to saline-injected controls (**Section 5.3.7**). Mice were injected with CAV-NS particles from different aliquots (prepared in **Chapter 3**).

Mice were weighed daily from approximately 12-days post-injection to monitor the effect of the cryo-anaesthesia and injections over a longer time period (**Fig. 5.2**). A comparison was made with untreated colony mice (Crawley *et al*, 2006a). In general, the mean body weights of the cryo-anaesthetised mice were comparable to those of gender-matched, untreated mice, with the exception of three MPS IIIA mice receiving CAV-NS at 1 x 10^8 particles/hemisphere (1 male, 2 female). These mice were nurtured by the same dam but failed to gain weight at a similar rate to other pups, potentially due to lactation/feeding difficulties. Consequently, these pups were left with the dam whilst she delivered and nursed her next litter (approximately 21-days after the first litter had undergone surgery) from which point all pups from both litters steadily gained weight.
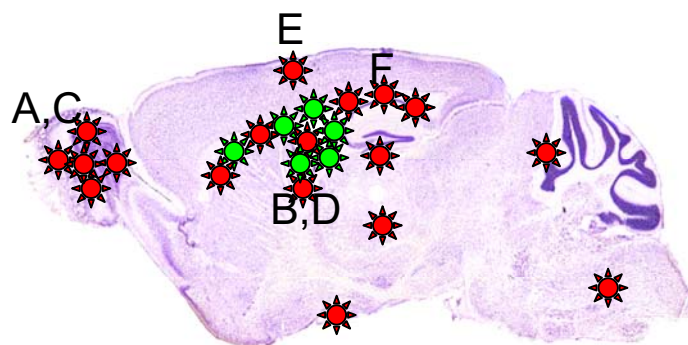
In total, 100 newborn mice were injected in the experiments detailed in this chapter. Higher losses of pups were noted post-injection compared to the initial dose assessment

Figure 5.1: Biodistribution of GFP in mice injected with CAV-NS at birth. Mice were bilaterally injected with 10^9 particles/µL CAV-NS vector on the day of birth. Two- or 7-days post-injection, mice were sacrificed, brain tissues fixed in 4% (w/v) PFA, cryo-embedded and frozen sections were immunostained with a rabbit polyclonal anti-GFP antibody and detected with a Cy3-conjugated donkey anti-rabbit IgG secondary antibody.

GFP was observed in **(A)** the granular neurons of the olfactory bulb and **(B)** the ependymal cells of the lateral ventricle (LV) at 2-days post-injection (corpus callosum, indicated by arrow heads; hippocampus, HP). At 7-days post-injection, immunostained GFP-expressing cells (red) were detected in the **(C)** olfactory bulb (granular and external plexiform layers), **(D)** ependymal lining of the lateral ventricle, **(E)** cortex (layer III) and **(F)** corpus callosum. The same field of view in DAPI-stained nuclei (blue) of regions shown in **A-F** are provided for structural definition. Solid lines indicate the edge of the tissue section. Scale bar is 100 µm.

A schematic representation of GFP expression at 7-days after injection of 10^9 particles/µL CAV-NS is shown below to indicate the position of the captured images. Areas marked with red clusters indicate that GFP-expressing cells were visualised with immunostaining whilst green clusters indicate that GFP-positive cells were observed with and without immunostaining.
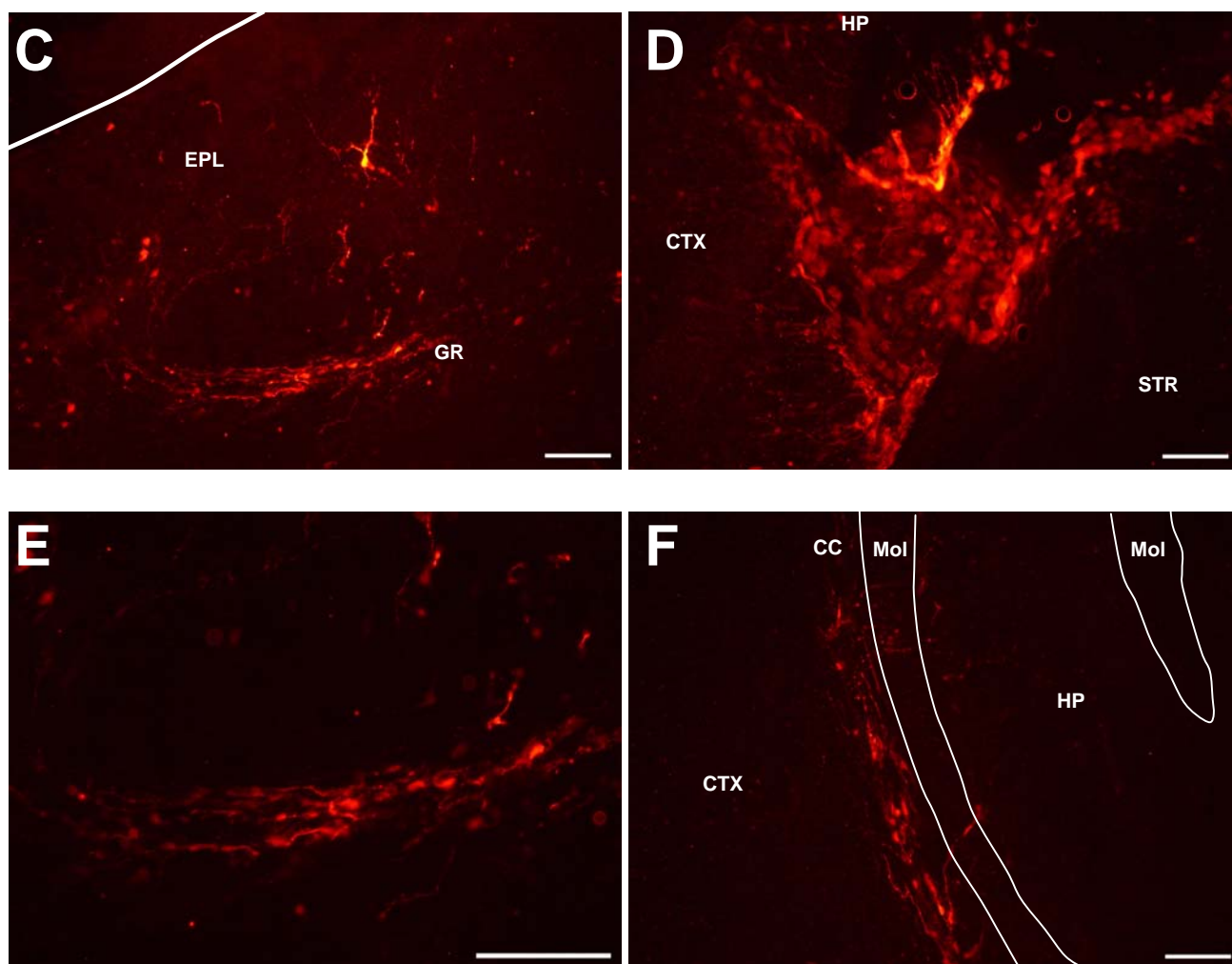
GL, glomerular layer; EPL, external plexiform layer; GR, granular layer; LV, lateral ventricle; CTX, cortex; HP, hippocampus; STR, striatum; Mol, molecular layer of the hippocampus.
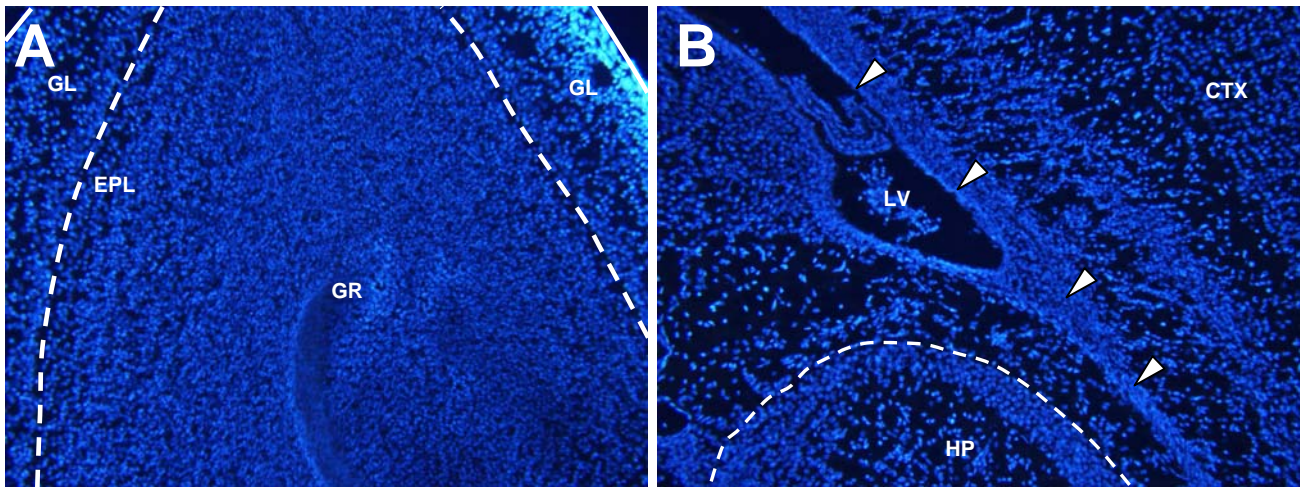
2 DAYS POST-INJECTION

A GL EPL GR GL

B CTX LV HP

7 DAYS POST-INJECTION

C EPL GR

D HP CTX STR

E

F CC Mol Mol CTX HP
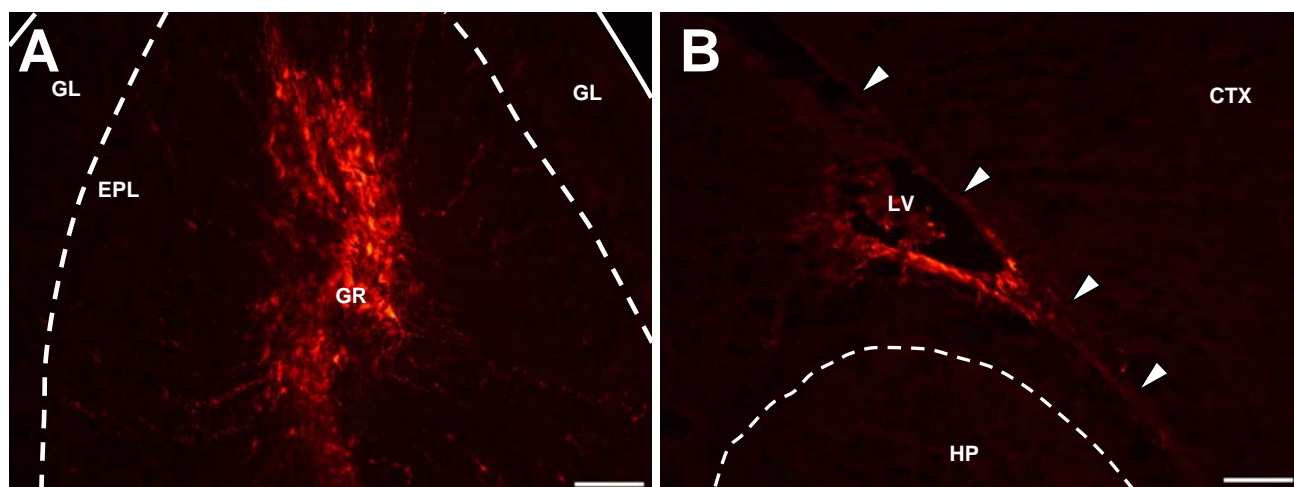
2 DAYS POST-INJECTION
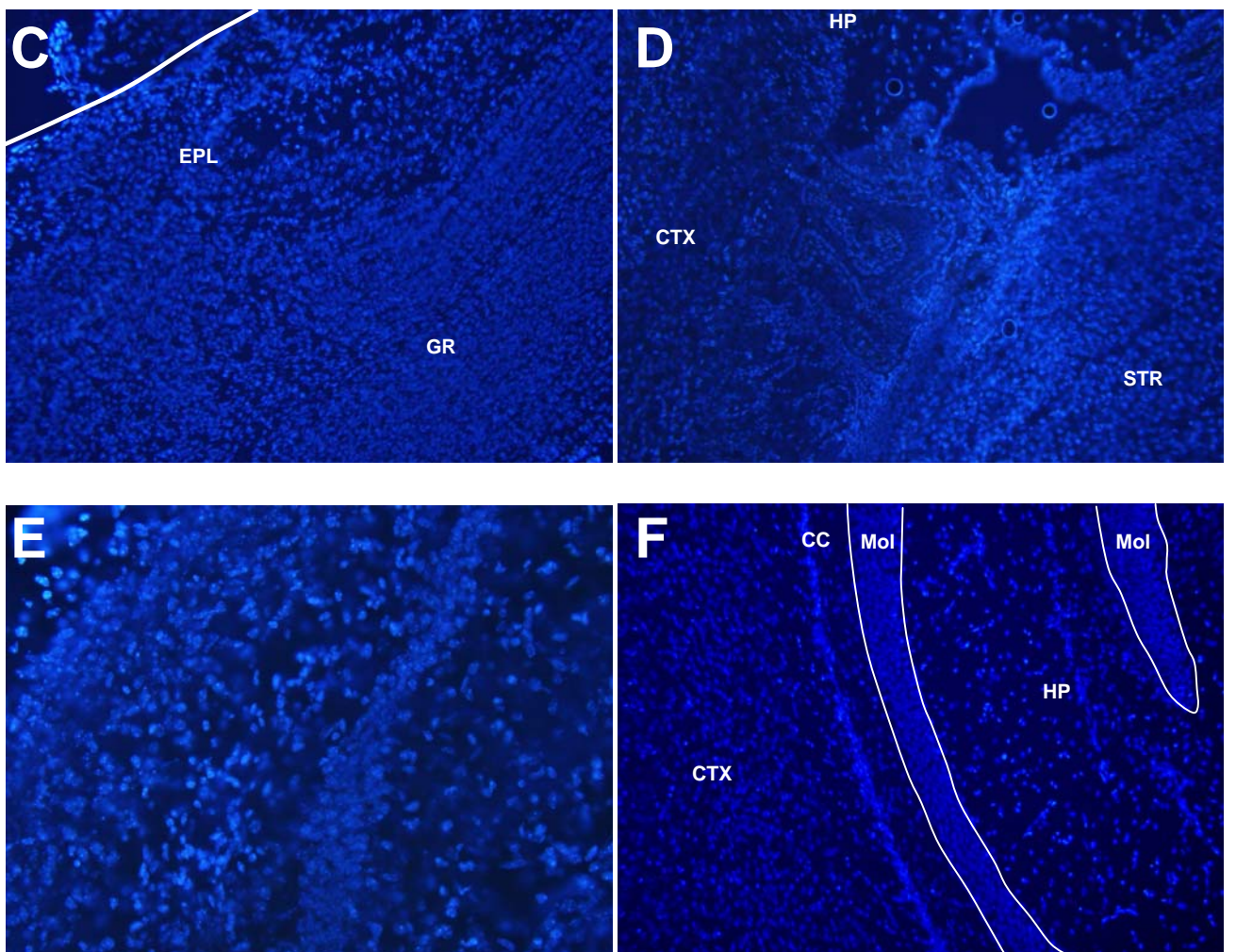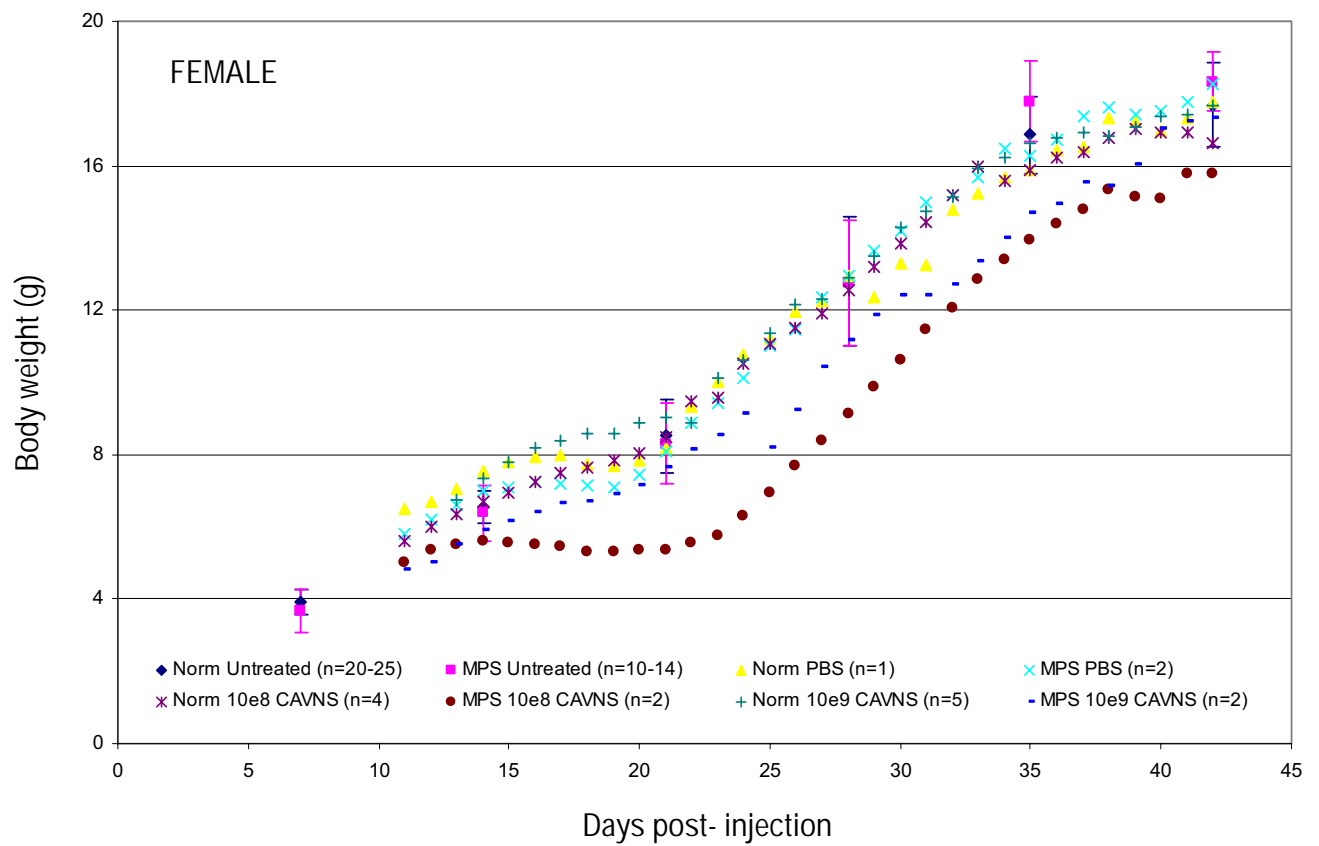

7 DAYS POST-INJECTION

Figure 5.2: Body weights of mice injected at birth. Mouse pups were cryo-anaesthetised and injected with saline or 10^8 or 10^9 particles CAV-NS into each lateral ventricle on the day of birth. Mice were weighed daily from 11-days of age until sacrifice. Data represents the mean of each treatment group. The weekly weights of untreated normal/heterozygous (blue diamonds) and MPS IIIA (pink squares) C57Bl/6 colony mice published in Crawley *et al*, 2006a are also shown. The error bars are ± 1 SEM of the untreated mice.

MALE

Body weight (g)

Days post- injection

◆ Norm Untreated (n=20-25) ■ MPS Untreated (n=10-22) ▲ Norm PBS (n=3) ✕ MPS PBS (n=2)
✳ Norm 10e8 CAVNS (n=2) ● MPS 10e8 CAVNS (n=4) + Norm 10e9 CAVNS (n=1) - MPS 10e9 CAVNS (n=4)

FEMALE

Body weight (g)

Days post- injection

◆ Norm Untreated (n=20-25) ■ MPS Untreated (n=10-14) ▲ Norm PBS (n=1) ✕ MPS PBS (n=2)
✳ Norm 10e8 CAVNS (n=4) ● MPS 10e8 CAVNS (n=2) + Norm 10e9 CAVNS (n=5) - MPS 10e9 CAVNS (n=2)
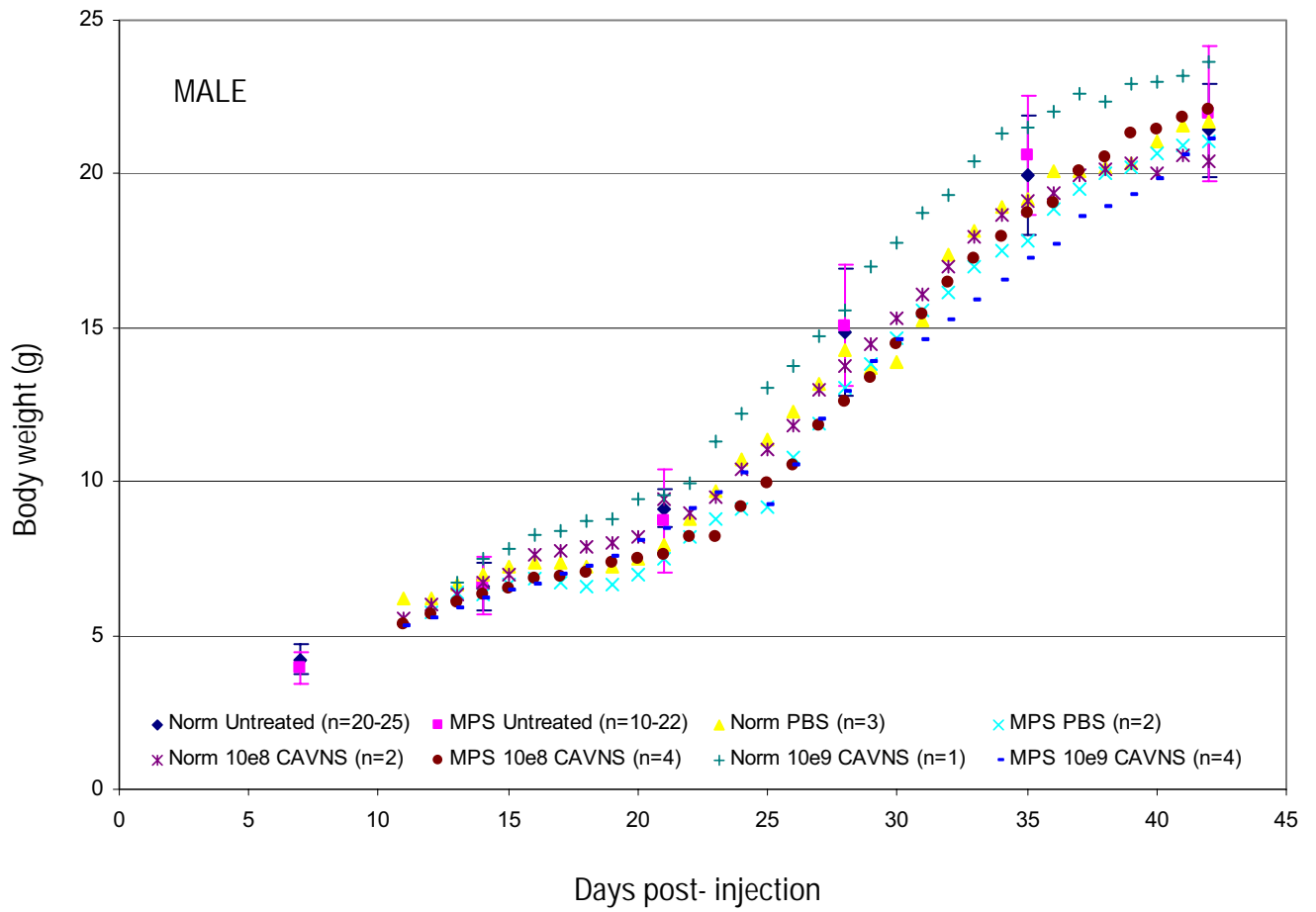
experiment (**Section 5.3.1**) where four titres were compared (19% or 7%, respectively; **Table 5.2**). The survival rate of pups born to an experienced dam (>1 litter delivered) was 92.6% compared to 73.9% for dams delivering their first litter. The overall survival rate post-injection was 84% for newborn mice. The data are also presented in **Table 5.2**.

5.3.3. Immune Response

Four mice, including one treated with PBS, were considered "responders" based on titres $\geq$ 16, as reported in Perreau *et al* (submitted). The responding mice included a PBS-treated mouse sacrificed at 6-wks (titre 16), two CAV-NS-treated mice receiving 10^8 particles/hemisphere (2-wks post-injection, titre 64; 6-wks post-injection, titre 16) and one CAV-NS-treated mouse injected with 10^9 particles/hemisphere (6-wks post-injection, titre 64). Obvious signs of autofluorescent cellular infiltration were not detected in the cortical layers above or adjacent to the lateral ventricle injection site in frozen tissue sections. In addition, May Grunwald-giemsa-stained brain impression smears made of the cortical surface of the brain revealed an absence of lymphocyte infiltration in saline- or CAV-injected mice. Cell smears were analysed by Dr Dyane Auclair (LDRU) in a blinded fashion.

5.3.4. GFP Expression at 6-Weeks Post-Injection

At 6-wks post-injection, the biodistribution of GFP expression was greatly reduced, with GFP-positive cells only detected in the ependymal layer of the lateral ventricle and the choroid plexus in all mice injected with 1 x 10^9 particles/μL of CAV-NS. No transgene expression was observed in MPS IIIA or unaffected mice treated with 1 x 10^8 particles/μL at 6-wks after CAV-NS delivery in mice (**Table 5.1**).

5.3.5. Validation of Sandwich ELISA Detection of rhNS Protein (DELFIA)

To correlate the expression of the rhNS and GFP transgenes, a sandwich ELISA (DELFIA) assay was adapted to quantitate the amount of rhNS protein in brain homogenates (optimised method described in **Section 2.2.11**). Immunohistochemical detection of rhNS was not performed as the rabbit polyclonal antibody against rhNS cross-reacts with murine NS (Savas, 2003) and positive staining could not be obtained using the monoclonal mouse anti-rhNS antibody (Perkins *et al*, 1999) on human paraffin or frozen tissue (data not shown). Three capture/detection combinations of anti-rhNS antibodies were assessed using purified

Table 5.2: Survival rates in newborn mice after cryo-anaesthesia and bilateral injections. Newborn mice were cryo-anaesthetised and bilaterally injected with 1 μL of CAV-NS vector (5 x 10^6 to 1 x 10^9 particles CAV-NS per hemisphere) or saline vehicle control. The injected mice were returned to the dam until weaning and monitored daily. Mice were weighed daily from approximately 11-days post-injection until sacrifice. Mice were euthanased at 2-days or 1-, 2-, or 6-wks post-injection. The percentage of surviving pups was recorded and comparisons were made between experienced dams (>1 litter) and first-time dams, the genotypes of the dams (MPS IIIA versus unaffected) and between the study trials (Study 1, **Section 5.3.1**; Study 2, **Section 5.3.2;** and Crawley *et al*, 2006a). All losses of pups appeared to be due to maternal neglect or cannibalism. No hydrocephalus was observed in any pups.

	Present study:	Crawley *et al*, 2006a:
	Cryo-anaesthesia and injections	*No surgical manipulations*
% Survival		
Study 1	92.8% (26/28 pups)	
Study 2	80.6% (58/72 pups)	
Overall	84.0% (84/100 pups)	65 - 94%, Average: 81.7% (including entire litters lost before counting)
% Survival		
First time dam	73.9% (34/46 pups)	
Experienced dam	92.6% (50/54 pups)	
% Survival		94.9 – 95 % (not including 3.8% loss of entire litters before counting)
Unaffected dam	87.2% (41/47 pups)	
MPS IIIA dam	81.1% (43/53 pups)	85.3 - 89.5% (not including 18.2% loss of entire litters before counting)
% First time dams		
Study 1	32% (9/28 pups)	
Study 2	50% (36/72 pups)	

rhNS protein produced in the LDRU (rhNS1) using a method modified from Perkins *et al* (1999) and Gliddon (2002). The combinations were (capture antibody/detection antibody):

- 5 μg/mL rabbit anti-rhNS polyclonal/0.4 μg/mL mouse anti-rhNS monoclonal and 0.1 μg/mL europium-labelled sheep anti-mouse IgG
- 5 μg/mL sheep anti-rhNS polyclonal/0.4 μg/mL mouse anti-rhNS monoclonal and 0.1 μg/mL europium-labelled sheep anti-mouse IgG
- 5 μg/mL sheep anti-rhNS polyclonal/0.4 μg/mL europium-labelled sheep anti-rhNS polyclonal.

All stock concentrations of the antibodies are listed in **Chapter 2**. Coating and detection antibodies were used at identical volumes and final concentrations for all combinations tested. Each antibody was allowed to bind overnight so that the combinations utilising the mouse anti-rhNS monoclonal as the detection antibody were 4-day assays, whilst the assay with the europium-labelled sheep anti-rhNS polyclonal as the detection antibody was a 3-day assay. Data were expressed as europium counts per well (including background counts).

The sensitivity of the DELFIA-based assay was improved with the use of the polyclonal europium-labelled sheep anti-rhNS as the detection antibody (i.e. sheep/sheep combination) compared to the monoclonal mouse anti-rhNS antibody (**Fig. 5.3A**). For the sheep/sheep combination, the working range of the assay was 0.15 ng rhNS protein to at least 20 ng rhNS per well. The linearity of this assay was also excellent with a fitted linear trendline displaying an R^2 value of 0.993.

Using the most sensitive conditions (i.e. sheep/sheep combination; **Section 2.2.11**), untreated normal and MPS IIIA mouse whole brain homogenates were assessed to quantify the cross-reactivity between human and mouse epitopes with the sheep anti-rhNS polyclonal antibody (**Fig. 5.3B**). Serial dilutions of low (1 mg/mL) or high (5 mg/mL) total protein stocks in a volume of 50 μL/well were analysed to see whether a dose-dependent effect was present. The average background of the assay was 3546 ± 320 counts per well. Mutant D31N murine NS protein was barely detected above the background level of the assay, even when using high total protein concentrations (5 mg/mL). Similarly, minimal cross-reactivity was observed in the 1 mg/mL normal brain homogenate with the europium counts displaying similar values to background assay counts. However, in normal mouse brain homogenates at a concentration of 5 mg/mL, the sheep anti-rhNS polyclonal antibody was able to cross-react and bind to murine NS.
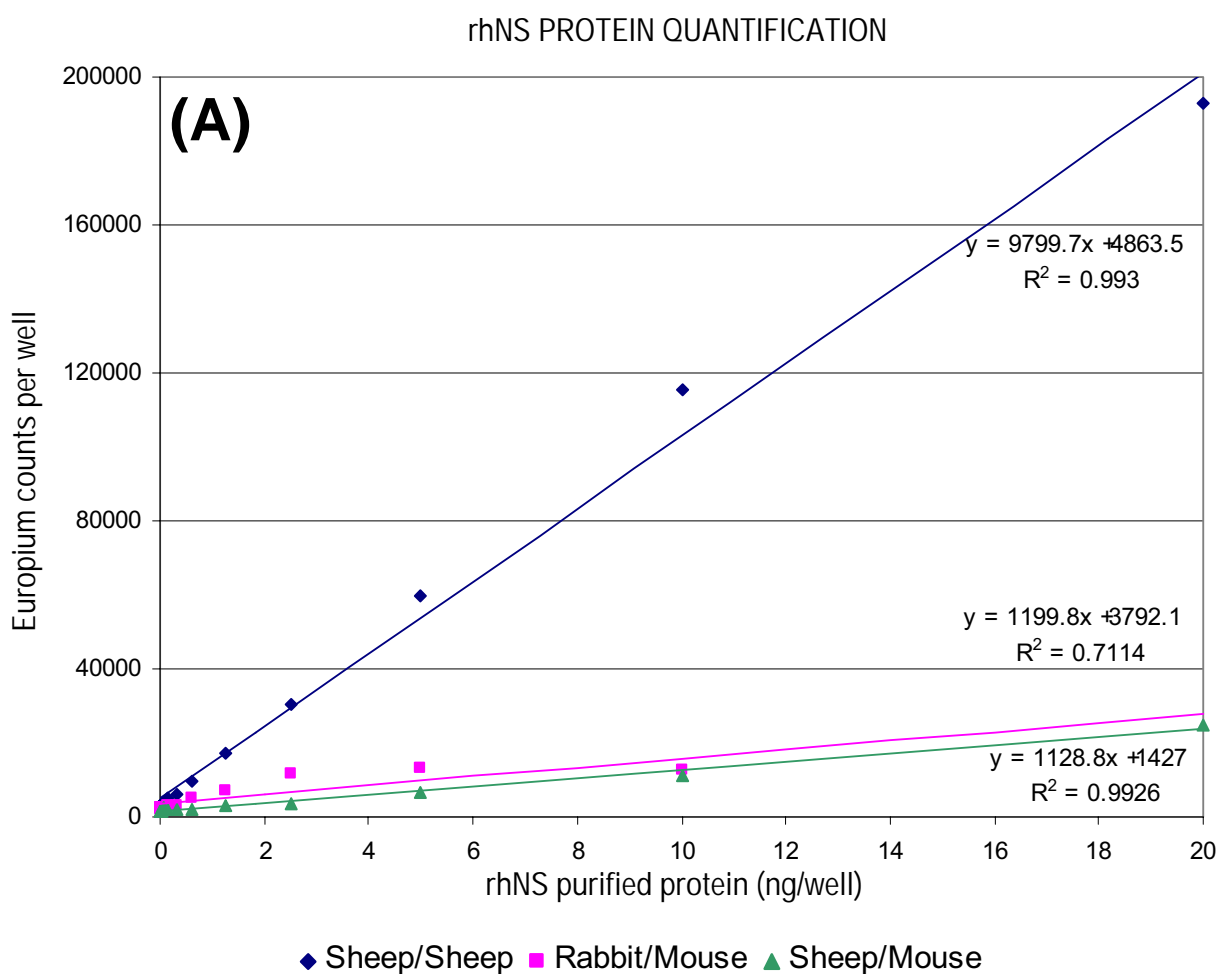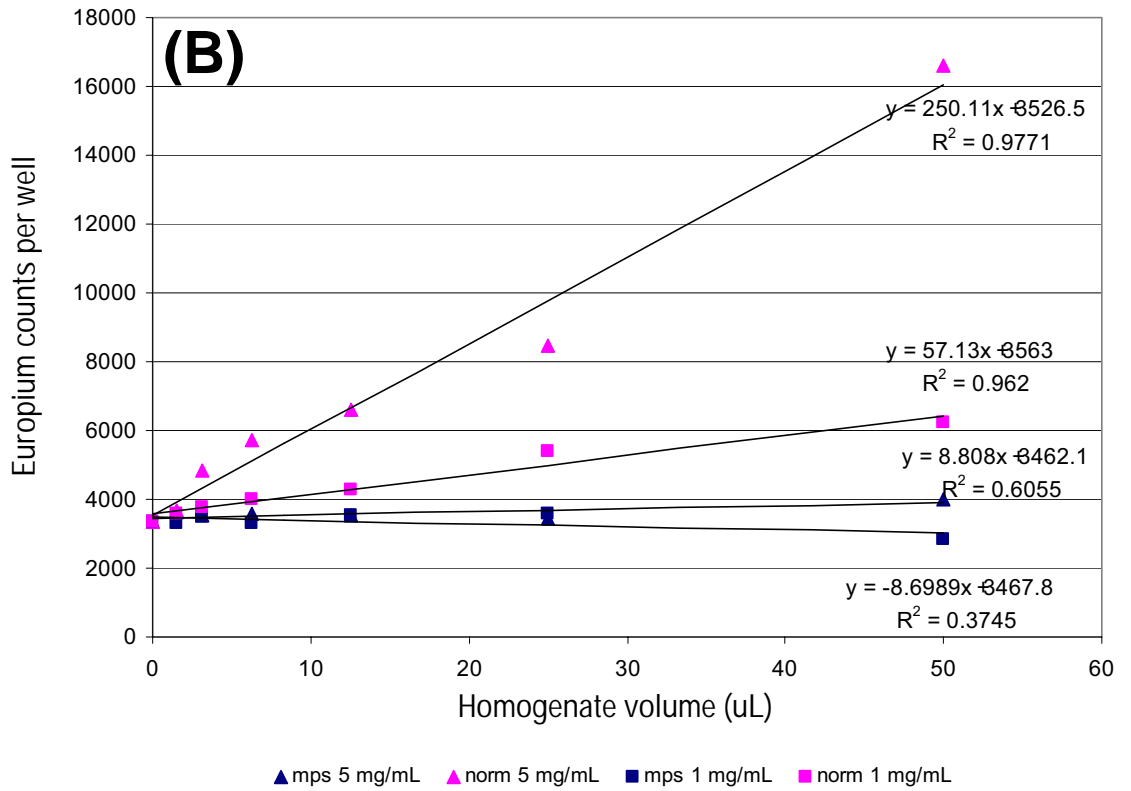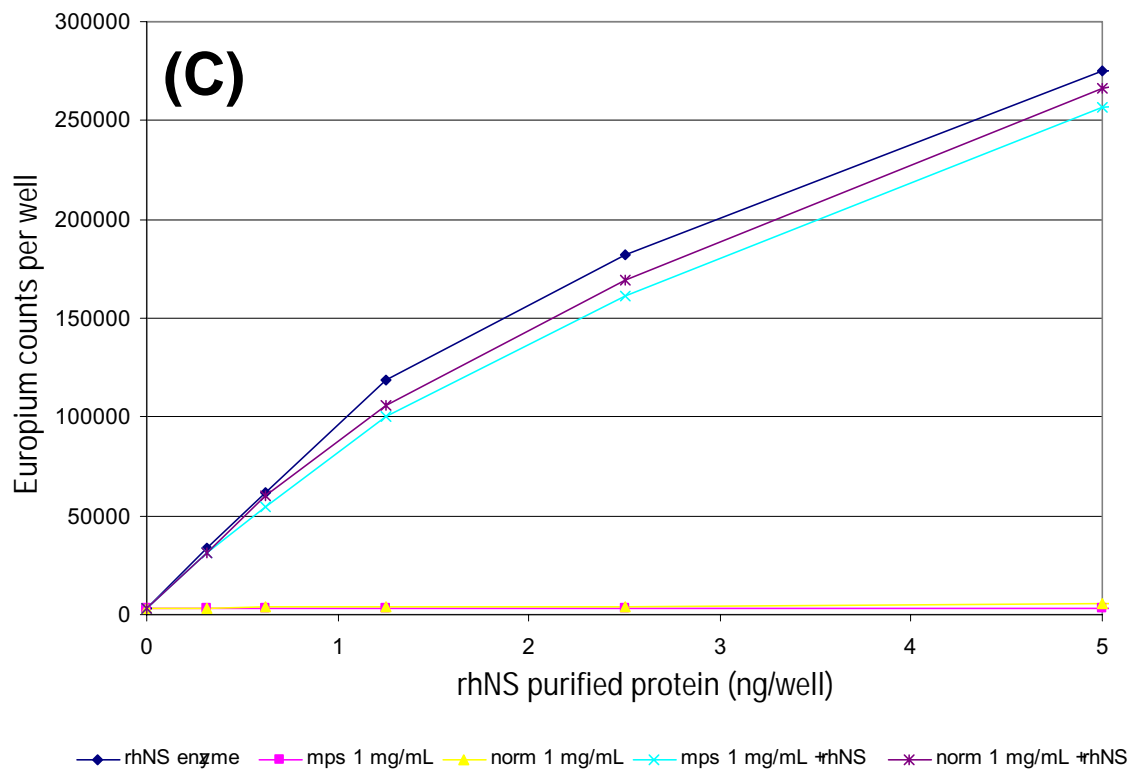
rhNS PROTEIN QUANTIFICATION

(A)

$y = 9799.7x + 4863.5$
$R^2 = 0.993$

$y = 1199.8x + 3792.1$
$R^2 = 0.7114$

$y = 1128.8x + 1427$
$R^2 = 0.9926$

Europium counts per well

rhNS purified protein (ng/well)

◆ Sheep/Sheep ■ Rabbit/Mouse ▲ Sheep/Mouse

Figure 5.3: Sandwich ELISA (DELFIA) detection of rhNS protein. (A) Three standard curves of rhNS1 protein were assessed using different combinations of antibodies against rhNS (polyclonal sheep anti-rhNS, polyclonal rabbit anti-rhNS or monoclonal mouse anti-rhNS) in a sandwich ELISA. The sheep/sheep combination provided the greatest level of sensitivity. Background levels are 2170 ± 203 counts/well. **(B)** The cross-reactivity between the sheep anti-rhNS polyclonal antibody with the normal and mutant D31N murine NS in brain homogenate supernatants was determined at two total protein concentrations. Background levels are 3366 ± 67 counts/well. Note the different scale on the y-axis. **(C)** The signal intensity of purified rhNS in the presence or absence of brain homogenates was measured. The europium counts were suppressed in the homogenates spiked with purified rhNS1 protein compared to the purified rhNS1-only control. Background levels are 3366 ± 67 counts/well.

MURINE NS CROSS-REACTIVITY

(B)

$y = 250.11x + 3526.5$
$R^2 = 0.9771$

$y = 57.13x + 3563$
$R^2 = 0.962$

$y = 8.808x + 3462.1$
$R^2 = 0.6055$

$y = -8.6989x + 3467.8$
$R^2 = 0.3745$

Europium counts per well

Homogenate volume (uL)

▲ mps 5 mg/mL   ▲ norm 5 mg/mL   ■ mps 1 mg/mL   ■ norm 1 mg/mL

EFFECT OF HOMOGENATE ON SIGNAL

(C)

Europium counts per well

rhNS purified protein (ng/well)

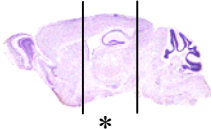◆ rhNS enzyme   ■ mps 1 mg/mL   ▲ norm 1 mg/mL   ✕ mps 1 mg/mL +rhNS   ✳ norm 1 mg/mL +rhNS
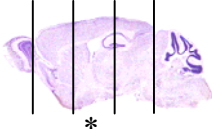
When the 1 mg/mL MPS IIIA and normal brain homogenates were spiked with known concentrations of purified rhNS protein (0.3 to 5 ng, rhNS1) and compared to a standard curve of rhNS protein diluted in assay buffer, a slight inhibition (ranging from 5-10%) was observed in the amount of rhNS detected (**Fig. 5.3C;** background 3546 ± 320 counts per well). This inhibition appeared to be consistent across the standard curve. In addition, the rhNS1-spiked normal control displayed slightly higher rhNS protein concentrations than the rhNS1-spiked MPS IIIA control, presumably because of cross-reactivity with the murine NS protein in the homogenates.

A second batch of rhNS protein (rhNS2) was used for subsequent analyses (i.e. for standard curves and in spiked homogenate control samples for comparison against CAV-NS treated mouse brain homogenates), as there were insufficient amounts of rhNS1 protein available to conduct all the planned experiments with one batch of enzyme. The intra-assay coefficient of variation of 5 ng purified rhNS2 protein without brain homogenate (n=22 well in one plate) was 6.18%. The inter-assay coefficients of variation for whole brain homogenates from control mice spiked with either 4 ng or 2 ng purified rhNS2 protein were 6.78% and 7.30%, respectively (n=4 for each sample repeated on 6 occasions over a 2-wk period).

5.3.6. Detection of rhNS Protein in Brain Homogenates

The amount of rhNS protein in the brain slice containing the lateral ventricle injection site was measured using the assay developed in **Section 5.3.5**. Highly variable amounts of rhNS protein were detected within each treatment group (with the exception of the MPS IIIA saline-treated mice), which may represent biological variation, in addition to differences in gene transfer efficiency (**Table 5.3**). The background level of cross-reactivity of unaffected mice injected with saline was 0.25 ± 0.14 ng rhNS/mg total protein. A dose-dependent increase in rhNS protein was seen in mice injected with 1×10^8 or 1×10^9 particles/µL CAV-NS at birth, with average NS protein concentrations determined to be 1.11 ± 0.3 and 4.72 ± 1.1 ng rhNS/mg total protein, respectively, at 1-wk post-injection. However, the amount of rhNS protein detected in CAV-NS-injected and saline-injected unaffected mice at 6-wks post-injection was comparable (0.60 ± 0.01 versus 0.47 ± 0.03 and 0.06 ± 0.06 ng).

Table 5.3: Measurement of rhNS protein in the lateral ventricle slice of mice. Newborn mice were bilaterally injected with saline or with 10^8 or 10^9 particles/hemisphere CAV-NS into the lateral ventricles. Mice were sacrificed and the brain portioned along the midline and then into three (for 1-wk post-injection) or five (for 6-wks post-injection) coronal slices. Homogenates from the slice containing the injection site (indicated with an asterisk) were assessed for rhNS protein using a sandwich ELISA assay. The amount of rhNS protein of 4 individual mice per group is displayed. The mean value of rhNS per group $\pm$ 1 SEM is in brackets. nd, not detected.

Genotype	Treatment	rhNS protein (ng/mg total protein) (Mean ± SEM)	
		1 week	6 weeks
Unaffected	PBS	0.51, 0.47, nd, nd (0.25 ± 0.14 ng)	0.61, 0.61, 0.60, 0.56 (0.60 ± 0.01 ng)
Unaffected	CAV-NS (10^8 particles)	1.04, 1.41, 1.63, 0.36 (1.11 ± 0.28 ng)	0.53, 0.51, 0.44, 0.38 (0.47 ± 0.03 ng)
Unaffected	CAV-NS (10^9 particles)	6.96, 6.32, 3.33, 2.28 (4.72 ± 1.13 ng)	0.24, nd, nd, nd (0.06 ± 0.06 ng)
MPS IIIA	PBS	nd, nd, nd, nd (0 ± 0 ng)	nd, nd, nd, nd (0 ± 0 ng)
MPS IIIA	CAV-NS (10^8 particles)	3.70, 0.29, nd, nd (1.0 ± 0.9 ng)	nd, nd, nd, nd (0 ± 0 ng)
MPS IIIA	CAV-NS (10^9 particles)	0.97, nd, nd, nd (0.24 ± 0.24 ng)	0.25, nd, nd, nd (0.06 ± 0.06 ng)

In MPS IIIA mice, no protein was detectable in saline-treated animals at any time-point. CAV-NS injection (10^8 particles/μL) slightly increased the amount of rhNS protein detected to 1.0 ± 0.9 ng rhNS/mg total protein at 1-wk post-injection. Unexpectedly, MPS IIIA mice injected with a higher dose of CAV-NS (10^9 particles/μL) expressed less rhNS protein in lateral ventricle portions at the same time-point (0.24 ± 0.24 ng rhNS/mg). In all MPS IIIA injected mice, undetectable or very low (up to 0.25 ng/mg) amounts of rhNS protein were measured at 6-wks post-injection.

5.3.7. Measurement of HNS-UA Disaccharide by Tandem Mass Spectrometry

In an attempt to determine whether the rhNS protein in brain homogenates (**Section 5.3.6**) was able have a therapeutic effect and decrease HS storage, the amount of a HS-derived disaccharide, HNS-UA, was measured in brain homogenates (**Section 2.2.8**). The intra-batch coefficient of variation was 7.9% (n=10) when using an untreated MPS IIIA brain quality control sample at an equivalent protein concentration. Elevated HNS-UA was observed in PBS-treated MPS IIIA mice compared to the PBS-injected unaffected mice at both time-points (undetectable; **Fig. 5.4**). In the lateral ventricle portion of the brain (slice 2 or 3), HNS-UA was elevated in PBS-treated MPS IIIA mice compared to PBS-treated unaffected mice at 1-wk post-injection and this amount increased by 6-wks post-injection. Similarly, HNS-UA storage in the olfactory bulb (slice 1) was greater in PBS-treated MPS IIIA mice at 1-wk post-injection compared to unaffected mice injected with PBS. However, the rate of HNS-UA accumulation was more rapid in the olfactory bulb than in the lateral ventricle slice and by 6-wks post-injection more HNS-UA was measured between the PBS-treated MPS IIIA and unaffected mice.

At 1-wk post-injection, no difference was observed in the HNS-UA concentration detected in the lateral ventricle portions between the PBS- and CAV-NS-treated groups of MPS IIIA mice. However, treatment with 10^9 particles/μL CAV-NS reduced the mean concentration of oligosaccharide storage in the lateral ventricle portion of MPS IIIA mice by 16% at 6-wks post-injection compared with PBS-injected MPS IIIA mice, but not to the extent where it was statistically significant (unpaired t-test p=0.125). No difference was measured in HNS-UA in the lateral ventricle portions of MPS IIIA mice treated with PBS and 10^8 particles/μL CAV-NS at 6-wks post-injection (p=0.45).
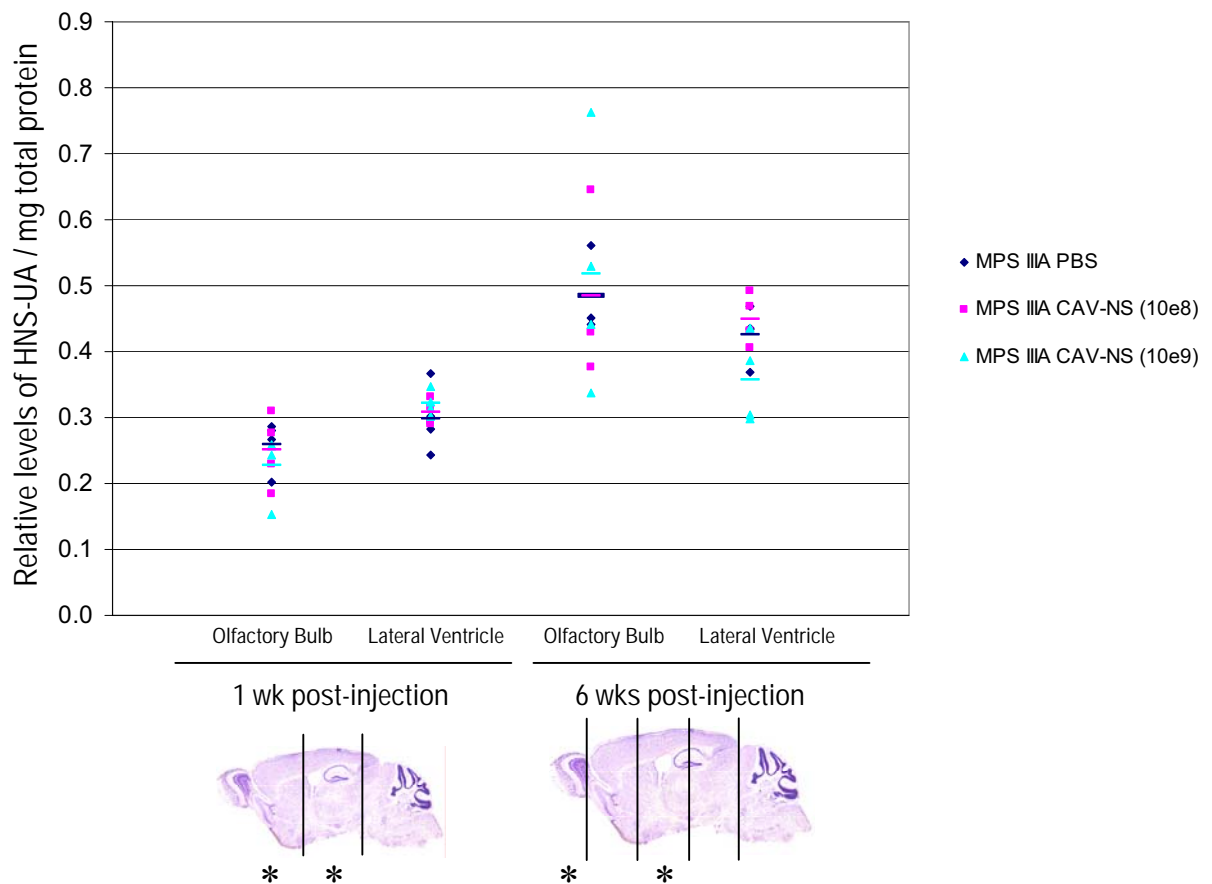
Figure 5.4: HNS-UA in mice injected with CAV-NS at birth. Newborn mice were bilaterally injected with 1 μL of saline or CAV-NS at 10^8 or 10^9 particles into each lateral ventricle and were sacrificed at 1- or 6-wks post-injection. The brain was divided along the midline and into coronal slices, and the olfactory bulb and the slice containing the injection site were processed for tandem mass spectrometry (slices assessed are indicated with an asterisk). Unaffected mice injected with CAV-NS or PBS did not have detectable HNS-UA in either brain region (not depicted on graph). Each point represents the relative HNS-UA concentrations normalised per mg of total protein in an individual mouse (n=2-4 per group). The mean of the group is indicated by a horizontal bar.

Injection of 10^8 or 10^9 particles/µL CAV-NS at birth slightly reduced the concentration of HNS-UA detected in the olfactory bulb of some of the treated mice at both 1- and 6-wks post-injection. However, given the variation in the PBS-treated MPS IIIA group at these time-points, no significant differences were measured at either titre (p=0.80, p=0.30).

5.4. DISCUSSION

Following the generation of a humoral response in adult mice stereotaxically-injected in the CNS with CAV-2 vectors, we assessed whether transgene expression could be obtained when delivering CAV-2 vectors to newborn mice and, if so, which dose provided the most widespread distribution and duration of transgene expression. In order to do this, CAV-NS was injected at 4 different titres (5 x 10^6, 1 x 10^7, 1 x 10^8, 1 x 10^9 CAV-NS particles per hemisphere) and sacrificed the mice at 3 time points (2-, 7- or 14-days post-injection). These doses were selected on the basis of results published by Tada *et al* (2005), where the optimal dose of ΔE1/E3 Ad encoding β-galactosidase unilaterally injected into the lateral ventricle of newborn C57Bl/6 mice was determined to be 1 x 10^7 particles (2.6 x 10^5 plaque forming units) delivered in 10 µL. Titres above 1 x 10^8 Ad particles resulted in reduced transgene expression, demyelination, lymphocyte infiltration and astrocyte activation (Tada *et al*, 2005).

Limited GFP expression was evident at 1 x 10^7 particles of CAV-NS, the recommended titre in the Tada *et al* (2005) study. Apart from utilising Ad vectors from different species, the variations in transgene expression may be attributed to the vastly different volumes of fluid infused into the ventricular space (10 µL unilaterally versus 1 µL bilaterally). It has previously been shown that intramuscular injection of the same dose of the same Ad vector had improved β-galactosidase expression (more widespread distribution and quantitatively higher transgene expression) when the particles were delivered in a larger volume (5 µL versus 2 µL; Bilbao *et al*, 2005).

A dose-dependent correlation between the number of GFP-positive cells and the CAV-NS titre was observed, with the most widespread distribution and greatest transgene expression detected at the highest titre assessed (10^9 particles/hemisphere). Peak transgene expression was observed at 7-days post-injection. Dose-dependent β-galactosidase expression has also been documented after intramuscular injection of a first-generation Ad vector in foetal mouse pups (Bilbao *et al*, 2005). However, it was hypothesised that the highest titre assessed was not necessarily the most therapeutically beneficial, as there was also a dose-dependent inflammatory response (activation of microglia/macrophages, upregulation of

MHC I, cellular infiltration of CD43$^+$ T lymphocytes, monocytes and granulocytes) within the CNS of adult rats receiving intra-striatal delivery of ΔE1/E3 Ad vectors (Stone *et al*, 2003). Accordingly, a moderate dose of CAV-NS (e.g. 1 x 10^8 particles of CAV-NS), with less inflammation, may provide reduced transgene expression for longer periods of time.

Consequently, neonatal pups were injected at 1 x 10^8 or 1 x 10^9 CAV-NS particles per hemisphere and assessed at 6-wks to determine which titre provided the greatest reduction of oligosaccharide storage in brain homogenates at longer time-points. Sterile PBS was used rather than CAV-GFP vector as the vehicle control for these experiments, as the CAV-GFP particles were cytotoxic to primary murine mixed neural cell cultures derived from newborn mice (**Chapter 3**). All pups recovered from the cryo-anaesthesia and the delivery of PBS vehicle or vector particles. However, only 84% mice survived until terminal sacrifice, with losses mainly attributed to maternal neglect or cannibalism. The survival rate post-injection was comparable to that recently reported in our congenic C57Bl/6 colony with survival rates ranging from 65-94%, depending on the genotypes of the parents, and an overall average of 81.7% (Crawley *et al*, 2006a). This survival rate is better than that reported following the *in utero* delivery of recombinant Ad vectors (Bouchard *et al*, 2003), where only 42.8% of pups were born alive (218/509 pups) and 37.7% of pups (192/509) survived to weaning age.

CAV-NS injection at 10^9 particles/hemisphere mediated slight reductions in HNS-UA in some of the treated MPS IIIA mice when compared to their PBS-treated counterparts. The most likely explanation as to why a consistent reduction in HNS-UA was not observed is that a local reduction (close to the injection site) in HNS-UA may have occurred but this effect may have been diluted by the many untransduced cells not receiving treatment when assessed as a brain slice, as demonstrated by regional GFP expression (**Fig. 5.1**). Consequently, in the succeeding experiments (**Chapter 7**), additional mice were included to try and visualise storage vacuoles (or a reduction thereof) in brain regions close to the injection site using toluidine blue-stained resin-embedded sections.

Additionally, different aliquots of CAV-NS vector were utilised in this experiment. Whilst they all originated from the same original vector preparation, there were potential inconsistencies in the biological activity of the vector particles pre-injection due to different numbers of freeze/thawing cycles, thus increasing the variation in transduction efficacy. Although a difference in GFP transgene expression was not grossly obvious by histological analysis, the DELFIA quantification assay of rhNS protein tends to support this hypothesis. For example, at 7-days post-injection in unaffected and MPS IIIA mice injected with 1 x 10^8 CAV-NS particles, the mice with the highest rhNS protein received an aliquot of CAV-NS

that had undergone 1-2 freeze/thaw cycles (MPS IIIA 3.70, 0.29 ng; unaffected 1.04, 1.41, 1.63 ng), whilst the remaining mice were injected with the same aliquot after 3-4 freeze/thaw cycles. These mice had a marked reduction in the amount of rhNS produced (MPS IIIA nd, nd; unaffected 0.36 ng). Similarly, unaffected mice injected with 1×10^9 particles of CAV-NS from 2 different aliquots displayed variable transgene expression (6.96, 6.32 ng rhNS versus 3.33, 2.28 ng rhNS) when the same titre was delivered. The aliquot generating lower amounts of rhNS protein in the unaffected mice at 1×10^9 particles of CAV-NS (3.33, 2.28 ng) underwent an additional freeze/thaw cycle before being delivered at 1×10^9 particles to MPS IIIA mice. After 7-days post-injection, undetectable rhNS protein was observed in 3 out of 4 of these treated MPS IIIA mice. Consequently, the difference in rhNS observed at 7-days post-injection between the two genotypes is likely to have been caused by variations in vector quality rather than by potential differences in the immunological state or transduction efficiencies between the different genotypes.

GFP expression mediated by the CAV-NS vector was still detectable at 6-wks post-injection via immunofluorescent staining. rhNS is the first transgene in the CAV-NS vector and it is therefore highly likely that rhNS was also being expressed at 6-wks post-injection, but not to the degree where rhNS protein was quantifiably elevated compared to saline controls in the immunoquantification assay.

It has previously been reported that when rhNS is administered weekly from birth by intravenous injection, cellular pathology and behavioural outcomes are improved in treated MPS IIIA mice (Gliddon and Hopwood, 2004). It is likely that these mice only received 2-3 doses of rhNS before developmental changes prevented the transport of rhNS across the blood-brain barrier into the CNS (Urayama et al, 2004). Therefore, it is possible that the generation of continued, low amounts of rhNS by CAV-NS could potentially mediate clinical improvements in CAV-NS-treated mice. However, as previously discussed, recent studies conducted in MPS VII mice revealed that low, persistent β-glucuronidase activity (1-5% of normal) mediated by an AAV2 vector administered 2- to 3-days after birth revealed limited improvement on clinical measures, even though biochemical and histological pathology had been ameliorated (Donsante et al, 2007). This suggests that greater than 2.5% of circulating enzyme activity may be required for a clinically effective therapy.

5.5. SUMMARY AND CONCLUSIONS

Newborn mice were bilaterally injected into the lateral ventricles, and dose-dependent transgene expression was observed with the greatest biodistribution and highest GFP expression observed at 10^9 particles of CAV-NS per hemisphere, the highest dose assessed. Transgene expression was observed for at least 6-wks after administration. This mediated a small reduction in a HS-derived storage marker in some, but not all, CAV-NS-treated brain homogenates. The preliminary experiments described in this chapter form the foundation for a larger-scale study assessing whether CAV-NS-mediated gene transfer is able to improve clinical signs and symptoms and reduce neuropathology in CAV-NS-treated MPS IIIA mice.